Schweizerische Eidgenossenschaft
Confédération suisse
Confederazione Svizzera
Confederaziun svizra

Eidgenössisches Departement für Umwelt, Verkehr, Energie und Kommunikation UVEK
Département fédéral de l'environnement, des transports, de l'énergie et de la communication DETEC
Dipartimento federale dell'ambiente, dei trasporti, dell'energia e delle comunicazioni DATEC

Bundesamt für Strassen
Office fédéral des routes
Ufficio federale delle Strade

PM10-Emissionsfaktoren von Abriebspartikeln des Strassenverkehrs (APART)

PM10 emission factors of abrasion particles from road traffic

Facteurs d'émission des particules d'abrasion dues au trafic routier

Empa: Eidgenössische Materialprüfungs- und Forschungsanstalt
Nicolas Bukowiecki
Robert Gehrig
Peter Lienemann
Matthias Hill
Renato Figi
Brigitte Buchmann

PSI: Paul Scherrer Institut, Labor für Atmosphärenchemie
Markus Furger
Agnes Richard
Claudia Mohr
Silke Weimer
André Prévôt
Urs Baltensperger

Forschungsauftrag ASTRA 2005/007 auf Antrag des Bundesamtes für Strassen (ASTRA)

August 2009 **1268**

Schweizerische Eidgenossenschaft
Confédération suisse
Confederazione Svizzera
Confederaziun svizra

Eidgenössisches Departement für Umwelt, Verkehr, Energie und Kommunikation UVEK
Département fédéral de l'environnement, des transports, de l'énergie et de la communication DETEC
Dipartimento federale dell'ambiente, dei trasporti, dell'energia e delle comunicazioni DATEC

Bundesamt für Strassen
Office fédéral des routes
Ufficio federale delle Strade

PM10-Emissionsfaktoren von Abriebspartikeln des Strassenverkehrs (APART)

PM10 emission factors of abrasion particles from road traffic

Facteurs d'émission des particules d'abrasion dues au trafic routier

Empa: Eidgenössische Materialprüfungs- und Forschungsanstalt
Nicolas Bukowiecki
Robert Gehrig
Peter Lienemann
Matthias Hill
Renato Figi
Brigitte Buchmann

PSI: Paul Scherrer Institut, Labor für Atmosphärenchemie
Markus Furger
Agnes Richard
Claudia Mohr
Silke Weimer
André Prévôt
Urs Baltensperger

Forschungsauftrag ASTRA 2005/007 auf Antrag des Bundesamtes für Strassen (ASTRA)

August 2009 **1268**

Impressum

Forschungsstelle und Projektteam

Projektleitung
Nicolas Bukowiecki, Empa
Robert Gehrig, Empa

Mitglieder
Nicolas Bukowiecki, Empa
Robert Gehrig, Empa
Peter Lienemann, Empa
Matthias Hill, Empa
Renato Figi, Empa
Brigitte Buchmann, Empa
Markus Furger, PSI
Agnes Richard, PSI
Claudia Mohr, PSI
Silke Weimer, PSI
André Prévôt, PSI
Urs Baltensperger, PSI

Begleitkommission

Präsidentin
B. Gälli Purghart (BAFU)

Mitglieder
D. Fux, Kt SO
T. Gasser, ASTRA
M. Jung, ASTAG
S. Krähenbühl, BAFU
A. Porchet, TCS
H. Sommer, Kt ZH
E. Strozzi, VCS
U. Zihlmann, Kt LU

Antragsteller

Robert Gehrig, Empa
Urs Baltensperger, PSI

Bezugsquelle

Das Dokument kann kostenlos von http://partnershop.vss.ch herunter geladen werden.

Table of Contents

Der Hauptbericht ist in englischer Sprache verfasst.

Die folgende Liste benennt die Autoren der einzelnen Teilkapitel dieses Projekts.
The following list indicates the authors of the individual sections of this report:

5.1: Brake Wear
Author: Nicolas Bukowiecki (Empa)

5.2: Road Wear and Resuspension
Author: Robert Gehrig (Empa)

5.3: Road Dust Analysis
Authors: Markus Furger (PSI),
Fulvio Amato (Institute of Environmental Assessment and Water Research (IDAEA) in Barcelona, Spain)

5.4: Distance Measurements
Author: Markus Furger (PSI)

5.5: Mobile Measurements
Author: Markus Furger (PSI)

5.6: Mass Balance and Emission Factors
Author: Nicolas Bukowiecki (Empa)

1 Zusammenfassung

1.1 Ausgangslage

Oft werden mit den Feinstaubemissionen des Strassenverkehrs nur die Auspuffemissionen (Russ) in Verbindung gebracht. Im Gegensatz dazu wurden durch mechanische Abriebsprozesse erzeugte Partikel lange Zeit weitgehend vernachlässigt. Im Forschungsprojekt ASTRA2000/415 und in einigen neueren Studien konnte jedoch gezeigt werden, dass Abriebspartikel quantitativ bedeutend zur PM10-Belastung beitragen. Diese setzen sich aus dem Abrieb von Strassenbelägen, Bremsen, Reifen sowie aus der Aufwirbelung von auf der Strasse deponiertem Staub zusammen. Allerdings ist noch kaum bekannt, wie viel diese Prozesse im Einzelnen zur PM10-Belastung beitragen. Quantitative Informationen sind für effiziente PM10-Minderungsmassnahmen aber unerlässlich. Vor allem interessiert, ob die Abriebpartikel vorwiegend vom Strassenbelag oder den Fahrzeugen stammen, und wie viel die Aufwirbelung zu den Emissionen beiträgt.

1.2 Projektziele, Forschungskonzept und Experimente

1.2.1 Projektziele

Das Hauptziel des Projekts APART (Abriebspartikel das Strassenverkehrs) war es, nicht auspuffbedingte PM10-Emissionen des Strassenverkehrs für typische Verkehrssituationen zu identifizieren und zu quantifizieren.

Spezifische Ziele:

- Erarbeiten einer Faktengrundlage im Hinblick auf künftige Minderungsmassnahmen.
- Bestimmung von Emissionsfaktoren (mg/km/Fz) für Spurenelemente, welche typischerweise vom Strassenverkehr emittiert werden.
- Berechnung von Emissionsfaktoren (mg/km/Fz) für nicht auspuffbedingte PM10-Emissionsquellen des Strassenverkehrs.
- Betrachtung unterschiedlicher Verkehrssituationen.
- Aufteilung der Emissionsfaktoren auf leichte und schwere Motorfahrzeuge.
- Standortspezifische Beurteilung des Beitrags einzelner verkehrsbedingter PM10-Quellen.

Nicht Gegenstand des Projekts war:

- Die quantitative Untersuchung nicht verkehrsbedingter PM10-Quellen.
- Auspuffbedingtes PM10 wurde zwar aus Gründen der Gesamtmassenbilanzierung ebenfalls gemessen. Eine detaillierte Interpretation dieser Emissionen ist aber nicht Gegenstand dieser Untersuchung.

1.2.2 Forschungskonzept

Die in diesem Projekt untersuchten Standorte wurden primär aufgrund ihrer Verkehrsregimes und ihrer lokalen Umgebung ausgewählt, welche typisch für viele schweizerische Verkehrssituationen waren. Zusätzlich mussten die Standorte eine geeignete Infrastruktur für die Messungen aufweisen und allen methodischen Anforderungen des Messkonzepts genügen. Um den lokalen PM10-Verkehrsbeitrag von der meist dominierenden PM10-Hintergrundsbelastung an den Messorten unterscheiden zu können, wurden entweder Konzentrationsdifferenzen aus Lee-Luv-Messungen oder aus zeitgleichen Messungen direkt am Strassenrand und einer nahe gelegenen Hintergrundstation verwendet (Figur 1.1). Die Identifizierung der einzelnen verkehrsbedingten Feinstaubquellen basierte auf der Messung quellenspezifischer Elementsignaturen (sogenannte Fingerprints). Dazu wurde mit einem 'Rotating Drum Impactor' (RDI) Feinstaub in Stundenauflösung und 3 Grössenklassen (2.5-10, 1-2.5 und 0.1-1 µm) gesammelt. Die darin enthaltenen Spurenelemente wurden anschliessend mit Synchrotron-Röntgenfluoreszenzspektrometrie (SR-XRF) bestimmt. Ergänzt wurden diese Messungen durch weitere Messungen einer breiten Palette zusätzlicher Aerosol- und Gasphaseneigenschaften, meteorologischer Parameter, sowie durch fahrzeugspezifische Verkehrszählungen. Die eigentliche Identifikation der einzelnen Emissionsquellen aus den Messdaten erfolgte mittels 'Positive Matrix Factorization' (PMF), einer für diesen Zweck häufig eingesetzten Methode. Die lokale atmosphärische Verdünnung der Emissionen zwischen dem Emissionspunkt und der Messstelle (10-20 m) wurde aus hintergrundkorrigierten Messungen der NO_x-Konzentrationen und den für die entsprechende Verkehrssituation bekannten NO_x-Emissionsfaktoren berechnet. Unter Berücksichtigung dieser Verdünnung sowie der gemessenen Verkehrsfrequenzen und –zusammensetzung konnten mit statistischen Modellen Fahrzeug-Emissionsfaktoren für die einzelnen Emissionsquellen berechnet werden. Da die atmosphärische Verdünnung als wesentlicher Parameter in die Berechnungen einfloss, waren nur Zeitperioden mit markanten lokalen Beiträgen von NOx zur Auswertung geeignet (ΔNO_x > 20 µg m^{-3}). Die berechneten Emissionsfaktoren waren grundsätzlich weder von der exakten Position der Messstelle entlang der Strasse noch von der Probenahmehöhe signifikant abhängig, da die atmosphärische Verdünnung orts- und zeitspezifisch berücksichtigt wurde.

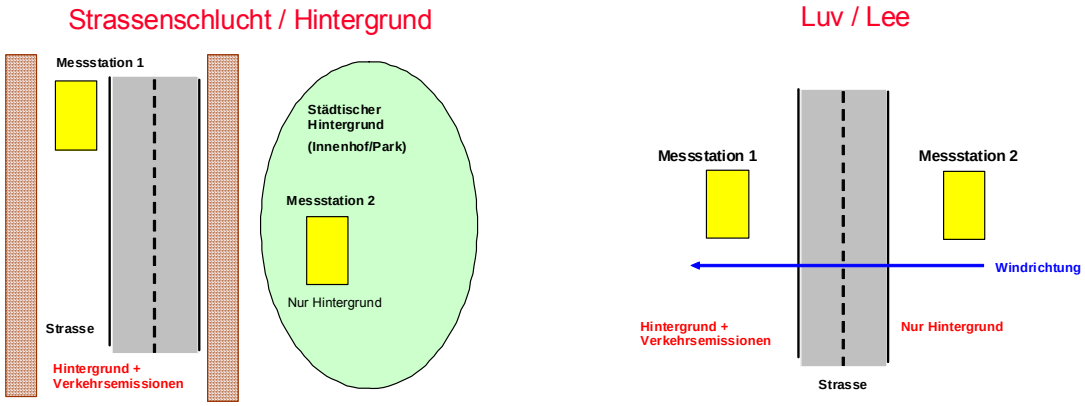

Fig. 1.1: Schematische Darstellung des Strassenrand-Hintergrund-Konzepts (links) und des Lee-Luv-Konzepts (rechts). Die Probenahmehöhe betrug 4.5 m über Boden, basierend auf experimentellen Voraussetzungen (optimierte Ansaugleitungen, freie Anströmbarkeit und Vandalensicherheit).

1.2.3 Messungen in Zürich an der Weststrasse und Kaserne (Februar und März 2007)

Der Messstandort Zürich Weststrasse stellte eine typische städtische Strassenschlucht mit den folgenden Verkehrscharakteristiken dar:

- Innerorts-Hauptverkehrsstrasse mit Lichtsignalanlage und starken Störungen des Verkehrsflusses (Kategorie IO_HVS3 nach *Handbuch Emissionsfaktoren des Strassenverkehrs HBEFA*, http://www.hbefa.net). Kein Durchgangsverkehr zwischen 22:00 und 06:00 Uhr.
- Belag: Asphaltbeton AB12, Einbaujahr 1995/96
- Verkehrszählung: Fahrzeuge <6m: Leichte Motorwagen (davon 9% Lieferwagen); Fahrzeuge >6m: Schwere Motorwagen (inkl. Reisecars); Die Verkehrzählung erfolgte durch die Empa.
- Werktage: 22'000 Fahrzeuge/Tag (Schwerverkehrsanteil 12%)
- Samstage: 21'000 Fahrzeuge/Tag (Schwerverkehrsanteil 5%)
- Sonntage: 19'000 Fahrzeuge/Tag (Schwerverkehrsanteil 4%)

Um die lokalen PM10-Beiträge an der Weststrasse zu quantifizieren, wurden gleichzeitig auch Messungen im ca. 600 m entfernten Zeughaushof der Kaserne Zürich durchgeführt. Die Datenanalyse für beide Standorte zeigte, dass der Standort Kaserne die städtische Hintergrundsbelastung gut widerspiegelte und für den Standort Weststrasse repräsentativ war. Diese Hintergrundbelastung setzte sich aus allen städtischen und regionalen PM10-Quellen zusammen (verkehrsbedingt wie auch nicht verkehrsbedingt, siehe Figur 1.2). Figur 1.3 zeigt beispielhaft den zeitlichen Verlauf der PM10- und Antimonkonzentrationen an den beiden Messorten während einer winterlichen Inversionslage.

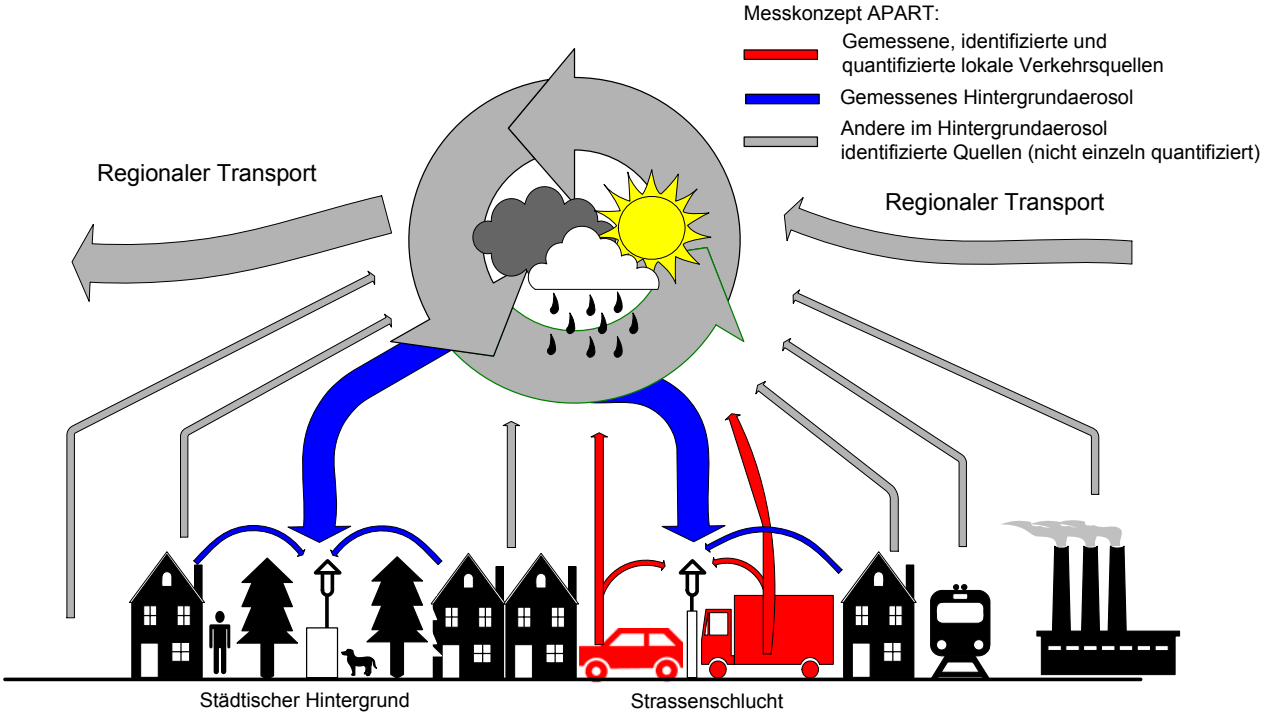

Fig. 1.2: Schematische Darstellung der relevanten Schadstoffflüsse in einer städtischen Umgebung. Um den lokalen Beitrag des Strassenverkehrs zu bestimmen, müssen alle lokalen und regionalen Quellen (auch weiter entfernte Verkehrsemissionen), die meteorologischen Verhältnisse und allfällige chemische Umformungen der Schadstoffe berücksichtigt werden.

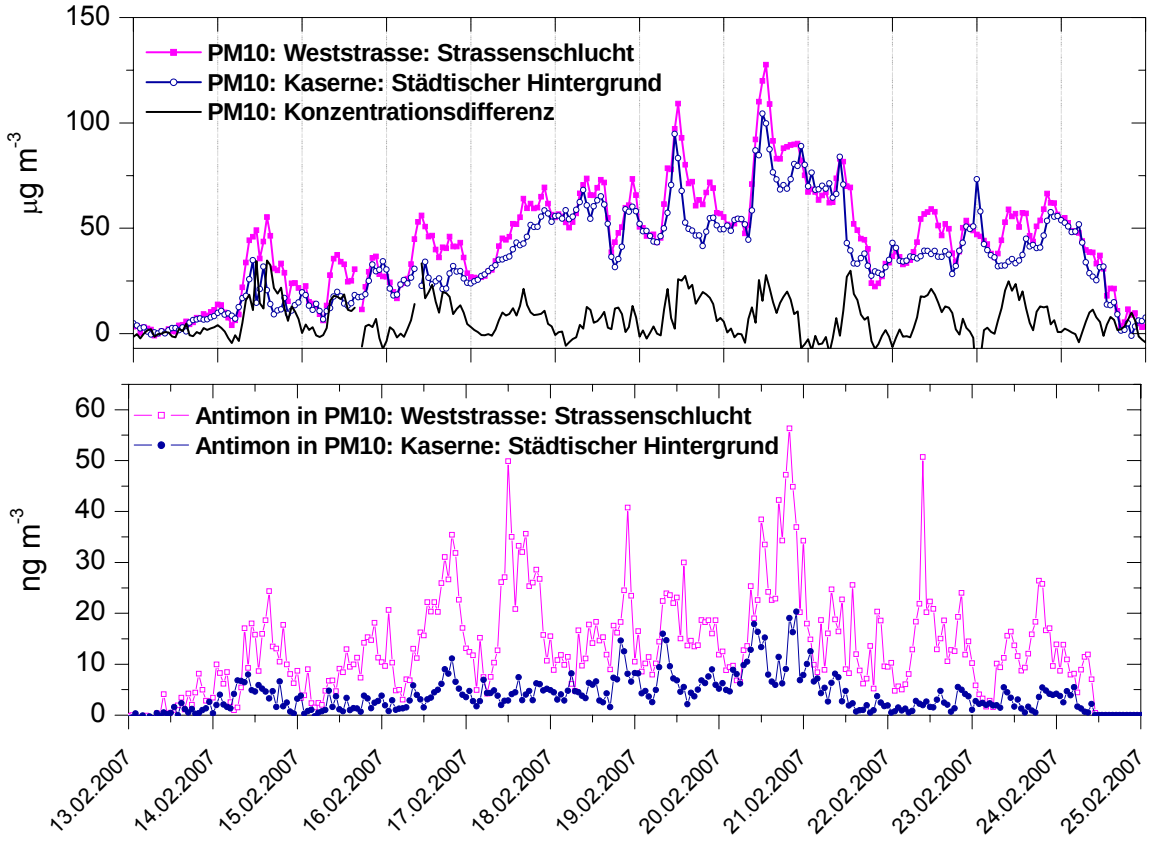

Fig. 1.3: Zeitlicher Verlauf der PM10- und Antimonkonzentrationen (Stundenwerte) in der Strassenschlucht in Zürich-Weststrasse, vor, während und nach einer meteorologischen Inversionslage. Oberes Diagramm: Die schwarze Linie zeigt die Differenz zwischen der Strassenschlucht und der Hintergrundstation und stellt somit den Beitrag des lokalen Verkehrs in der Strassenschlucht zur PM10-Konzentration dar. Die gezeigte Zeitperiode stellt nur einen Ausschnitt aus dem ausgewerteten Datensatz dar.

1.2.4 Messungen in Reiden (LU) (Juli – November 2007)

Der Messstandort in Reiden an der Autobahn A2 repräsentierte folgende Verkehrscharakteristik:

- Autobahn mit flüssigem Verkehr, Tempolimit 120 km h^{-1} (Kategorie AB_120 nach *Handbuch Emissionsfaktoren des Strassenverkehrs HBEFA*, http://www.hbefa.net)
- Belag: Splitt-Mastixbelag (kompakter Belag mit wenig Hohlräumen, vergleichbar mit Asphaltbeton); Richtung Luzern SMA 11 B 80/100+NAF; Richtung Basel SMA 11 B55/70+NAF, Einbaujahr: 1999.
- Verkehrzählung: Unterscheidung: Leichte Motorwagen (davon 9% Lieferwagen) und schwere Motorwagen (inkl. Reisecars). Die Verkehrzählung erfolgte durch ASTRA (Messstelle *lu reiden-s-239*)
- Werktage: 49'000 Fahrzeuge/Tag (Schwerverkehrsanteil 16%)
- Samstage: 45'000 Fahrzeuge/Tag (Schwerverkehrsanteil 7%)
- Sonntage: 41'000 Fahrzeuge/Tag (Schwerverkehrsanteil 2%, inkl. Reisebusse)

Die Messstationen befanden sich zu beiden Seiten der Autobahn (Figur 1.1 links). Während Zeitperioden mit Querwind befand sich somit jeweils eine Station im Luv der Autobahn und war damit nur durch die Hintergrundskonzentrationen belastet. Die andere, im Lee gelegene Station, war hingegen zusätzlich durch

die Emissionen der Autobahn belastet. Figur 1.4 zeigt die gemessenen PM10-Konzentrationen für beide Seiten während einer ausgewählten Messperiode.

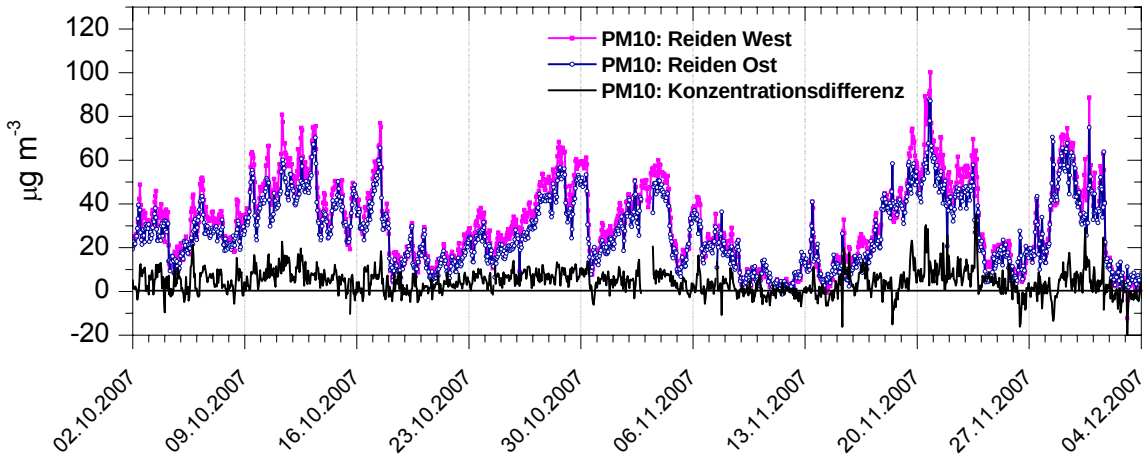

Fig. 1.4: Zeitlicher Verlauf der PM10-Konzentrationen (Stundenwerte) in Reiden. Die schwarze Linie zeigt die Differenz zwischen den beiden Messstationen und repräsentiert somit den Beitrag des lokalen Verkehrs auf der Autobahn zur PM10-Konzentration.

1.2.5 Ergänzende Untersuchungen

Die Feldmessungen an den Strassen lieferten einen umfangreichen und realistischen Datensatz, der für die weiteren statistischen Untersuchungen gut geeignet war. Dennoch konnten nicht alle wichtigen Fragestellungen des Projekts mit Hilfe dieser Feldmessungen beantworten werden. Deshalb wurden als Ergänzung weitere gezielte Untersuchungen durchgeführt.

- **Belagsabrieb oder Aufwirbelung:** Die spezifische Unterscheidung der PM10-Emissionen aus mechanischem Belagsabrieb und Aufwirbelung von Strassenstaub ist ausgesprochen schwierig mittels Datensätzen aus Feldmessungen. Selbst mit detaillierter chemischer Analyse können wichtige Quellen wie Belagsabrieb und Aufwirbelung nicht voneinander getrennt werden, da diese Emissionen sowohl ähnlich zusammengesetzt sind, wie auch zeitlich hoch korrelieren. Eine Möglichkeit, dieses Problem anzugehen bieten sogenannte Verkehrslastsimulatoren, welche von Strassenbauingenieuren zur Prüfung der Verschleissfestigkeit von Belägen eingesetzt werden. In diesem Projekt wurden zwei Typen von Simulatoren mit unterschiedlichen Achslasten eingesetzt, um Abriebsemissionen zu quantifizieren. Die Versuchsanlage wurde so gewählt, dass eine separate Bestimmung der Emissionen durch Belagsabrieb und Aufwirbelung von deponiertem Staub möglich war.

- **Deponierter Strassenstaub:** Die Analyse von auf Strassenoberflächen abgelagertem Staub liefert gute Informationen über die chemische Zusammensetzung des durch den Strassenverkehr aufgewirbelten Feinstaubs. Mit einem speziell konstruierten "PM10-Staubsauger" wurden in Zürich im Februar 2008 Proben von Strassenstaub gesammelt und analysiert.

- **Mobile PM10- und PM1-Messungen:** Um die räumliche Schwankung der Partikelkonzentration in verschiedenen Grössenklassen innerhalb der Stadt Zürich zu untersuchen, wurde im Juni 2007 eine Serie mobiler Messungen mit einem Messfahrzeug durchgeführt.

1.3 Resultate

1.3.1 Verkehrsbedingte PM10-Emissionen in Zürich-Weststrasse

1.3.1.1 Massenrelevante PM10-Verkehrsquellen

Basierend auf den stündlichen Messdaten wurden an der Weststrasse mit dem statistischen PMF-Modell (Positive Matrix Factorization) folgende PM10-Verkehrsquellen als massenrelevant identifiziert:

- **Bremsabrieb:** Dieser war charakterisiert durch ein typisches Muster von Fe, Cu, Zn, Zr, Mo, Sn, Sb und Ba. Diese Elemente werden verbreitet in Bremsbelägen eingesetzt und werden (vermutlich in ihrer oxidierten Form) durch den Abriebsprozess beim Bremsen emittiert.
- **Auspuffemissionen:** Diese bestanden vorwiegend aus organischen und anorganischen Kohlenstoffverbindungen (angegeben als totale verkehrsbedingte Kohlenstoffverbindungen). Den Auspuffemissionen konnten ausserdem keine relevanten Beiträge von Spurenelementen aus Treibstoffadditiven zugeordnet werden. Dies ist ein Hinweis darauf, dass andere Quellen dieser Elemente massenmässig dominieren.
- **Verkehrsbedingte Aufwirbelung von Strassenstaub:** Neben dem typischen Mineralstaub konnten im abgelagerten und aufgewirbelten Strassenstaub charakteristische Beiträge von Bremsstaub und Auspuffpartikeln (Kohlenstoff) klar identifiziert werden.

Mit der statistischen Analyse der Immissionsdaten konnten allfällige Beiträge von Reifenabrieb oder Belagsabrieb mangels spezifischer Leitelemente nicht separat quantifiziert werden. Zu diesen Prozessen lassen sich folgende Aussagen machen:

- **Belagsabrieb und Aufwirbelung:** Zusätzliche gezielte Experimente mit Verkehrslastsimulatoren zeigten, dass Partikelemissionen aus direktem Abrieb von intakten Strassenbelägen von untergeordneter Bedeutung sind. Hingegen können von schadhaften Belägen erhebliche Abriebsemissionen ausgehen.
- **Reifenabrieb:** Über Emissionen von Reifenabrieb gibt es bis heute kaum zuverlässige Untersuchungen. Ältere Untersuchungen, die teilweise von bis zu 10% Reifenabrieb im PM10 berichten, wurden mit aus heutiger Sicht unzulänglichen methodischen Konzepten durchgeführt. Eine neue, noch unveröffentlichte Studie an zwei innerstädtischen Strassen in Wiesbaden (Deutschland) verwendet erstmals eine sehr spezifische Methode (Analyse von Latex-Pyrolyseprodukten) und findet im Mittel einen Anteil des Reifenabriebs im PM10 von 0.5%. In derselben Studie wird auch gezeigt, dass die früher vermuteten bis zu 10% Reifenabrieb durchaus vorhanden sind, jedoch in gröberen Partikelfraktionen (>10µm). Dies wird qualitativ auch durch mikroskopische Aufnahmen bestätigt. Aus unseren Untersuchungen mit den Verkehrslastsimulatoren ergeben sich ebenfalls keine Hinweise auf namhafte Beiträge aus Reifenabrieb. Im Ganzen gesehen kann deshalb eine signifikante Verfälschung der statistischen Quellenzuordnung mit dem PMF-Modell durch Reifenabrieb ausgeschlossen werden.

1.3.1.2 Emissionsfaktoren für verkehrsbedingtes PM10 in Zürich-Weststrasse

Tabelle 1.1 und Figur 1.5 zeigen Emissionsfaktoren für verkehrsbedingtes PM10, mit separaten Werten für leichte und schwere Motorfahrzeuge sowie für die durchschnittliche Flottenzusammensetzung. Die Emissionsfaktoren wurden aus den stündlichen Massenkonzentrationen der einzelnen Verkehrsquellen berechnet. Die für die Berechnung relevante atmosphärische Verdünnung wurde für jede Stunde aus den gemessenen hintergrundkorrigierten NO_x-Konzentrationen sowie aus den bekannten NO_x-Emissionsfaktoren für diese Messstelle berechnet. Die Verkehrszahlen für leichte und schwere Fahrzeuge stammen aus der Verkehrszählung am Messort. Tabelle 1.1 zeigt, dass bei der Aufteilung der Flottenemissionsfaktoren auf leichte und schwere Motorfahrzeuge mit grösseren Unsicherheiten zu rechnen ist.

Die berechneten PM10-Emissionsfaktoren in **Zürich-Weststrasse** zeigen folgende Charakteristiken:

- **Flottenemissionen:** Der durchschnittliche PM10-Emissionsfaktor für die Flottenemission (bezogen auf einen Schwerverkehrsanteil von 10%) wurde von den Auspuffemissionen dominiert (41%), gefolgt von fahrzeugverursachter Aufwirbelung von Strassenstaub (38%) und Bremsabrieb (21%).

- **Emissionsfaktoren für leichte und schwere Motorfahrzeuge:** Auspuffpartikel (63%) und Bremsabrieb (33%) waren die dominanten PM10-Emissionsquellen für **leichte Motorfahrzeuge**. Demgegenüber waren an der Weststrasse die Emissionen durch Aufwirbelung für leichte Motorfahrzeuge nur gering (<5%). Im Vergleich zu den leichten Motorfahrzeugen waren die absoluten PM10-Emissionsfaktoren der **schweren Motorfahrzeuge** etwa 15-mal höher, die Emissionsfaktoren für Bremsabrieb und Auspuffemissionen etwa 10-mal höher. Im Gegensatz zu den leichten Motorfahrzeugen war der Beitrag der schweren Fahrzeuge zur Aufwirbelung bedeutend. Für Zürich-Weststrasse waren 53% der PM10-Emissionen der schweren Motorfahrzeuge der Aufwirbelung zuzuordnen. Der Beitrag der Auspuffemissionen lag bei 31%, von Bremsabrieb bei 16%. In der stark befahrenen Weststrasse scheint der verfügbare Strassenstaub demnach grösstenteils durch die von den schweren Motorfahrzeugen induzierten Turbulenzen in Schwebe gehalten zu werden, so dass die leichten Fahrzeuge nur wenig dazu beitragen. Dies heisst allerdings nicht, dass leichte Motorfahrzeuge kein Potential für Aufwirbelung hätten, was durch die Experimente mit den Verkehrslastsimulatoren deutlich gezeigt werden konnte.

Während eine starke Korrelation des Bremsabriebs und der Auspuffemissionen mit den Verkehrsfrequenzen gefunden wurde, war der Tagesverlauf der fahrzeuginduzierten Aufwirbelung deutlich weniger korreliert und wies zudem eine grössere statistische Streuung auf. Daraus ergibt sich, dass Emissionsfaktoren für Aufwirbelung nicht adäquat in mg/km/Fz ausgedrückt werden können, wie dies für Bremsabrieb und Auspuffemissionen möglich ist. Die Emissionsfaktoren für Aufwirbelung konnten deshalb nicht mit dem multilinearen Regressionsmodell berechnet werden, sondern wurden indirekt abgeschätzt, mit entsprechend höheren absoluten Unsicherheiten. Da Aufwirbelung einen wesentlichen Beitrag zum gesamten verkehrsbedingten PM10 leistete, traf dies auch auf die Berechnung der totalen PM10-Emissionsfaktoren zu.

Tabelle 1.1: PM10-Emissionsfaktoren des Strassenverkehrs für die Verkehrssituation Zürich-Weststrasse (städtische Strassenschlucht). LMW: Leichte Motorfahrzeuge inkl. 9% Lieferwagen, SMW: Schwere Motorfahrzeuge inkl. Reisebusse. Die Bremsabrieb-Berechnung basierte darauf, dass Bremsstaub 1% Antimon und 5% Kupfer enthält. Auspuffemissionen (definiert als totale verkehrsbedingte Kohlenstoffverbindungen) wurden aus 'Black Carbon' - Messungen abgeschätzt, durch Multiplikation mit einem experimentell ermittelten Faktor von 1.45 welcher auf Messungen im Raum Zürich beruht. Die angezeigten Emissionsfaktoren beziehen sich auf 12 Messtage im Februar/März 2007 (ΔNO_x > 20 µg m^{-3}, nur Tage ohne Niederschlag). Die zur Berechnung verwendeten Emissionsfaktoren für NO_x basieren auf dem Handbuch Emissionsfaktoren des Strassenverkehrs (HBEFA, http://www.hbefa.net) und wurden speziell für die Verkehrssituation an der Weststrasse abgeschätzt (Jahr: 2007, EF_{NOx}(LMW) = 286.8 mg km^{-1}, EF_{NOx}(SMW) = 10559 mg km^{-1}, NO_x berechnet als NO_2). Zum Vergleich zeigt die Tabelle auch Emissionsfaktoren für Belagsabrieb und Aufwirbelung aus den Messungen mit Verkehrslastsimulatoren. Die Tabelle zeigt, dass bei der Aufteilung der Flottenemissionsfaktoren auf leichte und schwere Motorfahrzeuge mit grösseren Unsicherheiten zu rechnen ist.

Quelle	**Quantifizierung der Quelle**	**Berechnung Emissionsfaktor**	**Zürich-Weststrasse**		
			Flotte 10% SMW[*1] mg/km/Fz	**LMW [*2] mg/km/Fz**	**SMW[*2] mg/km/Fz**
Verkehrsbedingtes PM10	Gemessen (PM10 – Differenz: Strasse – Hintergrund)	Abgeschätzt aus Massen-bilanzierung	**71**	**24 ± 8**	**498 ± 86**
Bremsabrieb	Statistisches Modell[*3]	Multilineare Regression	**15**	**8 ± 4**	**81 ± 39**
Auspuff (Totale verkehrsbedingte Kohlenstoff-verbindungen)	Statistisches Modell[*3]	Multilineare Regression	**29**	**15 ± 6**	**155 ± 67**
Aufwirbelung von Strassenstaub	Statistisches Modell[*3]	Abgeschätzt aus Massen-bilanzierung	**27**	**1 ± 11**	**262 ± 115**
Strassenbelagsabrieb	Experiment mit Verkehrslastsimulatoren		-	(<3)[*a,d]	(7)[*a] (80[*b])
Aufwirbelung[*d]			-	(5)[*d] (76)[*a]	(110)[*c] (660[*b])

[*1] Mittlerer Schwerverkehrsanteil während der ganzen Messkampagne im Februar/März 2007 (starke Schwankungen im Tagesverlauf)

[*2] Multilineares Modell mit individueller Berücksichtigung der stündlichen Verkehrszusammensetzung

[*3] PMF (Positive Matrix Factorization)

[*a] Neuer Betonasphalt

[*b] Betonasphalt in schlechtem Zustand

[*c] Betonasphalt in gutem Zustand

[*d] Neuer poröser Asphalt

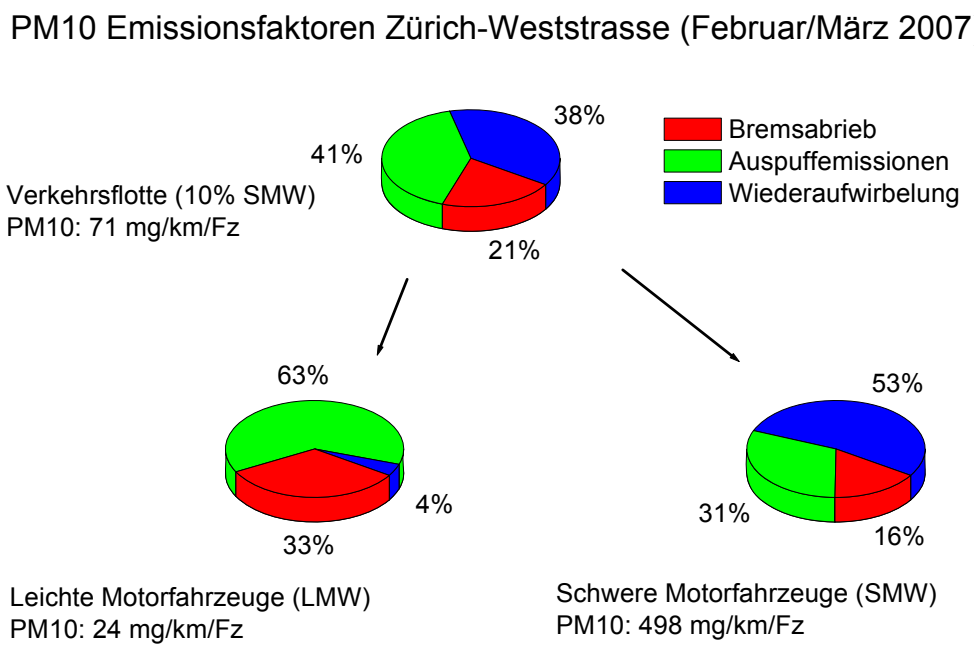

Fig. 1.5: PM10-Emissionsfaktoren Zürich-Weststrasse (prozentuale Anteile der Quellen). Bei der Aufteilung der Flottenemissionsfaktoren auf leichte und schwere Motorfahrzeuge ist mit grösseren Unsicherheiten zu rechnen.

1.3.2 Verkehrsbedingte PM10-Emissionen in Reiden (LU)

1.3.2.1 Massenrelevante PM10-Verkehrsquellen

Basierend auf den stündlichen Messdaten wurden an der Messstelle Reiden mit dem statistischen PMF-Modell (Positive Matrix Factorization) folgende PM10-Quellen als massenrelevant identifiziert:

- **Bremsabrieb:** Dieser war charakterisiert durch ein typisches Muster von Fe, Cu, Zn, Zr, Mo, Sn, Sb und Ba. Das gefundene Muster war demjenigen in Zürich-Weststrasse sehr ähnlich. Diese Elemente werden verbreitet in Bremsbelägen eingesetzt und werden (vermutlich in ihrer oxidierten Form) durch den Abriebsprozess beim Bremsen emittiert.
- **Auspuffemissionen:** Diese bestanden vorwiegend aus organischen und anorganischen Kohlenstoffverbindungen (angegeben als totale verkehrsbedingte Kohlenstoffverbindungen). Wie bereits an der Weststrasse in Zürich konnten den Auspuffemissionen keine relevanten Beiträge von Spurenelementen aus Treibstoffadditiven zugeordnet werden. Dies ist ein Hinweis darauf, dass auch in Reiden andere Quellen dieser Elemente massenmässig dominant sind.

Beiträge von mineralischen Elementen zu den Verkehrsemissionen wurden identifiziert und weisen auf verkehrsverursachte Aufwirbelung von Strassenstaub hin. Eine Hochrechnung der Emissionen der mineralischen Elemente auf die gesamten Aufwirbelungsemissionen war aber nicht möglich, da keine zuverlässige Information über die chemische Zusammensetzung des deponierten Strassenstaubs an dieser Messstelle vorlag.

1.3.2.2 Emissionsfaktoren für verkehrsbedingtes PM10 in Reiden

Tabelle 1.2 und Figur 1.6 zeigen Emissionsfaktoren für verkehrsbedingtes PM10, mit separaten Angaben für leichte und schwere Motorfahrzeuge sowie für die durchschnittliche Flottenzusammensetzung. Die Emissionsfaktoren wurden aus den stündlichen Massenkonzentrationen der einzelnen Verkehrsquellen berechnet. Die für die Berechnung relevante atmosphärische Verdünnung wurde für jede Stunde aus den gemessenen hintergrundkorrigierten NO_x-Konzentrationen sowie aus den bekannten NO_x-Emissionsfaktoren für diese Messstelle berechnet. Die Verkehrszahlen für leichte und schwere Fahrzeuge stammen aus der Verkehrszählung des ASTRA für diesen Strassenabschnitt. Tabelle 1.2 zeigt, dass bei der Aufteilung der Flottenemissionsfaktoren auf leichte und schwere Motorfahrzeuge mit grösseren Unsicherheiten zu rechnen ist.

Die berechneten PM10-Emissionsfaktoren in **Reiden** zeigen folgende Charakteristiken:

- **Flottenemissionen:** Der durchschnittliche PM10 Emissionsfaktor (15% Schwerverkehrsanteil) setzte sich aus 41% Auspuffemissionen und einem mit rund 3% sehr kleinen Bremsabriebanteil zusammen. Die verbleibenden 56% der verkehrsbedingten Emissionen konnten keiner spezifischen Quelle zugeordnet werden. Es handelt sich dabei aber sehr wahrscheinlich hauptsächlich um aufgewirbelten Strassenstaub (und kleinere Beiträge von Reifen- und Strassenabrieb).
- **Emissionsfaktoren für leichte und schwere Motorfahrzeuge:** Der totale PM10-Emissionsfaktor für schwere Motorfahrzeuge war 5.8-mal höher als der entsprechende Wert für leichte Motorfahrzeuge. Da die Massenbeiträge von Bremsabrieb und verkehrsbedingtem Kohlenstoff aus der gleichen, vom PMF-Modell identifizierten Verkehrsquelle interpoliert wurden, sind die Quellenanteile für leichte und schwere Fahrzeuge praktisch identisch. Eine alternative Berechnung der fahrzeugtypspezifischen Quellenanteile direkt aus den gemessenen Konzentrationsdifferenzen einzelner Elemente war statistisch zu unsicher. Anders als in Zürich-Weststrasse wird in Reiden der aufgewirbelte Staub laufend seitlich wegtransportiert (Lee-Luv-Konzept) und wird nicht wie in einer Strassenschlucht durch wenige Fahrzeuge mit hoher Turbulenz (SMW) in Schwebe gehalten. Deshalb entfällt hier auch auf die LMW ein Teil der Aufwirbelung.

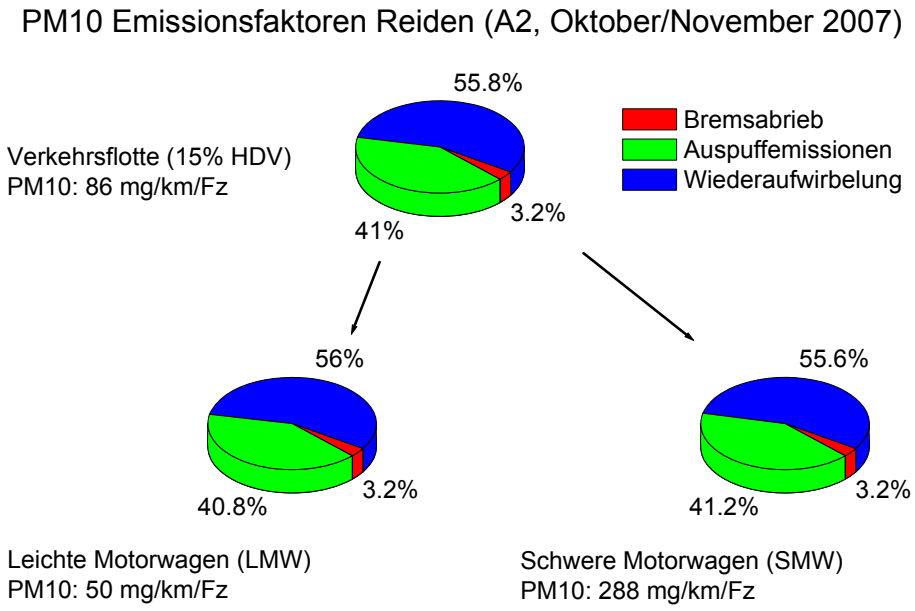

Fig. 1.6: PM10-Emissionsfaktoren für Reiden LU (prozentuale Anteile der Quellen). Bei der Aufteilung der Flottenemissionsfaktoren auf leichte und schwere Motorfahrzeuge ist mit grösseren Unsicherheiten zu rechnen.

Tabelle 1.2: PM10-Emissionsfaktoren des Strassenverkehrs für die Verkehrssituation Reiden LU (Autobahn). LMW: Leichte Motorfahrzeuge inkl. 15% Lieferwagen, SMW: Schwere Motorfahrzeuge inkl. Reisebusse. Die Bremsabrieb-Berechnung basierte darauf, dass Bremsstaub 1% Antimon und 5% Kupfer enthält. Auspuffemissionen (definiert als totale verkehrsbedingte Kohlenstoffverbindungen) wurden aus 'Black Carbon' - Messungen abgeschätzt, durch Multiplikation mit einem experimentell ermittelten Faktor von 1.45 welcher auf Messungen im Raum Zürich beruht (entsprechende Messungen im Raum Reiden fehlen). Die Werte basieren auf 4 Messtagen im Oktober/November 2007 (ΔNO_x > 20 µg m^{-3}, nur Tage ohne Niederschlag). Die zur Berechnung verwendeten Emissionsfaktoren für NO_x basieren auf dem Handbuch Emissionsfaktoren (HBEFA, http://www.hbefa.net) und wurden speziell für die Verkehrssituation an der Autobahn bei Reiden abgeschätzt (Jahr: 2007, EF_{NOx}(LMW) = 448 mg km^{-1}, EF_{NOx}(SMW) = 5421 mg km^{-1}, NO_x berechnet als NO_2). Die Tabelle zeigt, dass bei der Aufteilung der Flottenemissionsfaktoren auf leichte und schwere Motorfahrzeuge mit grösseren Unsicherheiten zu rechnen ist.

Quelle	**Quantifizierung der Quelle**	**Berechnung Emissionsfaktor**	**Reiden (LU) A2**		
			Flotte 15% SMW[*1] mg/km/Fz	**LMW[*2] mg/km/Fz**	**SMW[*2] mg/km/Fz**
Verkehrsbedingtes PM10	Gemessen (PM10 – Differenz: Lee – Luv)	multilineare Regression	**86**	**50.0 ± 13**	**288 ± 72**
Bremsabrieb	statistisches Modell[*3]	multilineare Regression	**3**	**1.6 ± 1.1**	**9 ± 7**
Auspuff (Totale verkehrsbedingte Kohlenstoff-verbindungen)	statistisches Modell[*3]	multilineare Regression	**35**	**20.4 ± 7**	**119 ± 38**
Rest (Aufwirbelung und kleinere Quellen[*4])	abgeschätzt aus Massenbilanz		**48**	**28 ± 14**	**160 ± 82**

[*1] Mittlerer Schwerverkehrsanteil im Oktober/November 2007 (starke Schwankungen im Tagesverlauf)
[*2] Multilineares Modell mit individueller Berücksichtigung der stündlichen Verkehrszusammensetzung
[*3] PMF (positive matrix factorization)
[*4] Reifen- und Strassenabrieb

1.3.3 Vergleich der Emissionsfaktoren mit früheren Untersuchungen

Der Vergleich der verkehrsbezogenen PM10-Emissionsfaktoren für Zürich-Weststrasse und Reiden mit früheren Untersuchungen zeigt Folgendes (Werte siehe Tab. 1.1 und 1.2):

- Der totale PM10-Flottenemissionsfaktor für Reiden (15% schwere Fahrzeuge, flüssiger Verkehr) war 20% höher als für Zürich-Weststrasse (10% schwere Fahrzeuge, stark gestörter Verkehrsfluss). Ursache sind höhere Auspuffemissionen und grössere Beiträge aus der Aufwirbelung von Strassenstaub.
- Im Gegensatz dazu waren die Emissionsfaktoren für Bremsabrieb in Reiden 5-mal tiefer verglichen mit Zürich-Weststrasse. Erwartungsgemäss zeigt sich hier der Einfluss der stark unterschiedlichen Bremsaktivitäten an den beiden Messstellen.

Tabelle 1.3 vergleicht die in dieser Untersuchung erhaltenen Emissionsfaktoren mit entsprechenden Werten aus früheren Untersuchungen an vergleichbaren Standorten.

- Zeitlicher Trend: Bei Zürich-Weststrasse wird ein sinkender Trend der PM10-Emissionsfaktoren der Verkehrsflotte beobachtet. Dagegen sind die PM10-Emissionsfaktoren in Reiden verglichen mit Birrhard (2004, gleiche Verkehrssituation) etwa gleich geblieben.
- Auspuffemissionen: Die abgeschätzten Werte für Auspuffemissionen sind unter Berücksichtigung der Messunsicherheiten konsistent mit den Werten der Emissionsinventare.
- Nicht auspuffbedingte Emissionen und totale verkehrsbedingte PM10-Emissionen: Diese Emissionsfaktoren hängen sehr stark von der fahrzeugverursachten Aufwirbelung zum Zeitpunkt der Untersuchung ab. Unterschiede bei diesen Faktoren reflektieren deshalb eher die lokal herrschenden Bedingungen an den Messorten (Verschmutzung der Strasse, Zustand des Belags) als einen zeitlichen Emissionstrend.

Tabelle 1.3: Emissionsfaktoren für Auspuff- und nicht auspuffbedingte PM10-Emissionen aus Untersuchungen in Zürich-Weststrasse, Zürich-Schimmelstrasse (stark verkehrsbelastete Strasse, 300 m von Zürich-Weststrasse), Reiden (LU, Nationalstrasse A2) und Birrhard (AG, Nationalstrasse A1). Generell ist zu bemerken, dass bei der Aufteilung der Flottenemissionsfaktoren auf leichte und schwere Motorfahrzeuge mit grösseren Unsicherheiten zu rechnen ist.

Parameter	**Untersuchung**	**Ort**	**Bezugsjahr**	**Flotte (mg km^{-1})**	**LMW (mg km^{-1})**	**SMW (mg km^{-1})**
PM10	NFP41[*1]	Zürich-Schimmelstrasse	1998/99	153	59	1420
	BUWAL/ASTRA 2003[*2]	Zürich-Weststrasse	2002/03	104	49	703
	APART	**Zürich-Weststrasse**	**2007**	**71**	**23.7 ± 7.5**	**498 ± 86**
Auspuff-emissionen	NFP41[*1]	Zürich-Schimmelstrasse	1998/99	48	14	507
	BUWAL/ASTRA 2003[*2]	Zürich-Weststrasse	2002/03	29	10	320
	HBEFA [*3]	IO_HVS3[*4]	2002/03	-	11	342
	APART	**Zürich-Weststrasse**	**2007**	**29**	**14.9 ± 6.3**	**155 ± 67**
	HBEFA [*3]	IO_HVS3[*4]	2007	-	12	286
Nicht auspuffbedingte Emissionen (inkl. Aufwirbelung)	NFP41[*1]	Zürich-Schimmelstrasse	1998/99	105	45	913
	BUWAL/ASTRA 2003[*2]	Zürich-Weststrasse	2002/03	75	39	383
	APART	**Zürich-Weststrasse**	**2007**	**42**	**9 ± 11**	**343 ± 122**

Tabelle 1.3 (Fortsetzung).

Parameter	Untersuchung	Ort	Bezugsjahr	Flotte (mg km^{-1})	LMW (mg km^{-1})	SMW (mg km^{-1})
PM10	BUWAL/ASTRA 2003[*2]	Birrhard	2003	83	63	267
	APART	**Reiden**	**2007**	**86**	**50.0 ± 12.6**	**288.0 ± 71.9**
Auspuff-emissionen	BUWAL/ASTRA 2003[*2]	Birrhard	2003	33	16	193
	HBEFA [*3]	AB_120[*5]	2002/03	-	17	176
	APART	**Reiden**	**2007**	**35**	**20.4 ± 6.6**	**119 ± 38**
	HBEFA [*3]	AB_120[*5]	2007	-	16	111
Nicht auspuffbedingte Emissionen (inkl. Aufwirbelung)	BUWAL/ASTRA 2003[*2]	Birrhard	2003	50	47	74
	APART	**Reiden**	**2007**	**51**	**30 ± 14**	**169 ± 82**

[*1] Hüglin, C. (2000). Anteil des Strassenverkehrs an den PM10- und PM2.5-Immissionen; Chemische Zusammensetzung des Feinstaubs und Quellenzuordnung mit einem Rezeptormodell, Nationales Forschungsprogramm NFP41 Verkehr und Umwelt, Bericht C4, Bern.

[*2] Verifikation von PM10-Emissionsfaktoren des Strassenverkehrs, Forschungsauftrag ASTRA/BUWAL 2000/415(52/00), Bern.

[*3] Basierend auf: Handbuch Emissionsfaktoren des Strassenverkehrs (http://www.hbefa.net), Version 2.1 / 2004, INFRAS im Auftrag BUWAL, Bern.

[*4] IO_HVS3: Städtische Hauptverkehrsstrasse mit Lichtsignalanlage, stark gestörter Verkehrsfluss.

[*5] Autobahn mit flüssigem Verkehr bei 120 km h^{-1}.

1.3.4 Emissionsfaktoren für bremsabriebsbezogene Spurenelemente

Der in Zürich-Weststrasse und Reiden identifizierte Bremsabrieb zeigte ein charakteristisches Muster von Fe, Cu, Zn, Mo, Zr, Sn, Sb und Ba, welches gut mit entsprechenden Befunden anderer Studien übereinstimmt, obschon die elementare Zusammensetzung einzelner Bremsbeläge stark variieren kann. Im Gegensatz zu den oben aufgeführten Elementen wurden deutlich tiefere Bleiwerte gefunden als in älteren Studien teilweise angegeben wurde. Dies weist darauf hin, dass dieses unerwünschte Element in Bremsbelägen inzwischen weitgehend durch andere Elemente oder Substanzen ersetzt wurde. Figur 1.7 und Figur 1.8 zeigen Emissionsfaktoren für typische Elemente des Bremsabriebs. Die höchsten Werte wurden für Fe, Cu und Ba gefunden, gefolgt von Zr, Mo, Sn und Antimon mit etwas tieferen Werten. Das Verhältnis der Emissionsfaktoren von schweren zu leichten Motorfahrzeugen betrug für den Partikelgrössenbereich 2.5 – 10 µm im Mittel neun, für den Partikelgrössenbereich 1 - 2.5 µm vier und für den Partikelgrössenbereich 0.1 - 1 µm vierzehn.

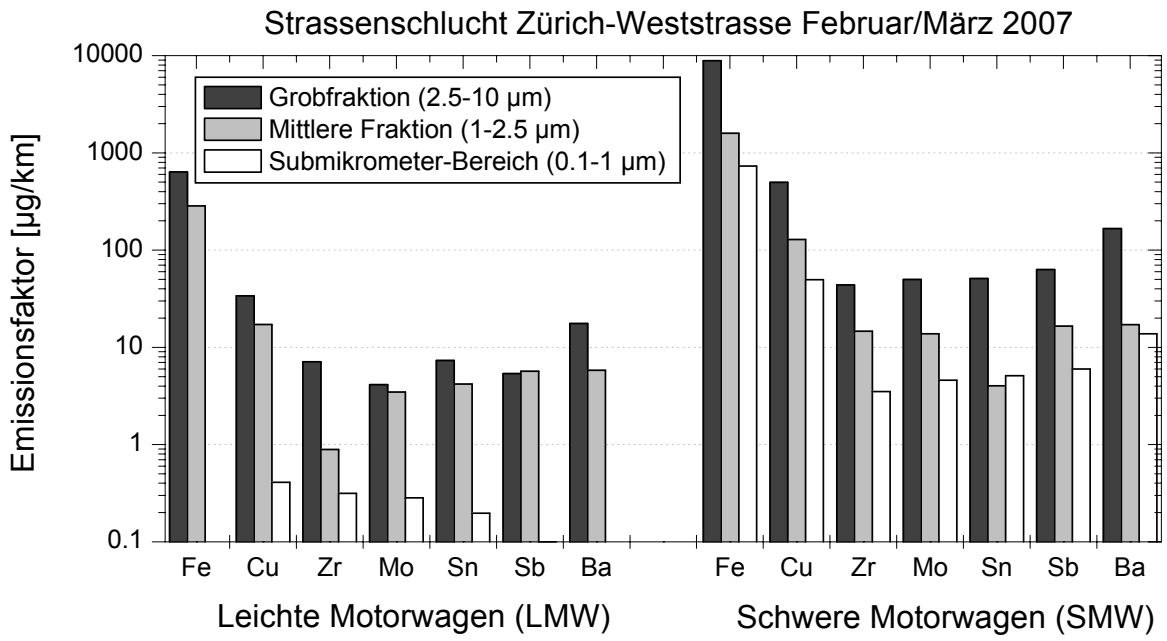

Fig. 1.7: Emissionsfaktoren (EF) für leichte (LMW) und schwere (SMW) Motorfahrzeuge für Zürich-Weststrasse (Strassenschlucht). Der Berechnung lagen 209 Stundenwerte zugrunde (~ 9 Tage, ΔNO_x > 20 µg m^{-3}, nur Zeitabschnitte ohne Niederschlag). Für Zn wurden keine Emissionsfaktoren berechnet, da dieses Element auch durch nicht verkehrsbedingte Quellen stark beeinflusst war.

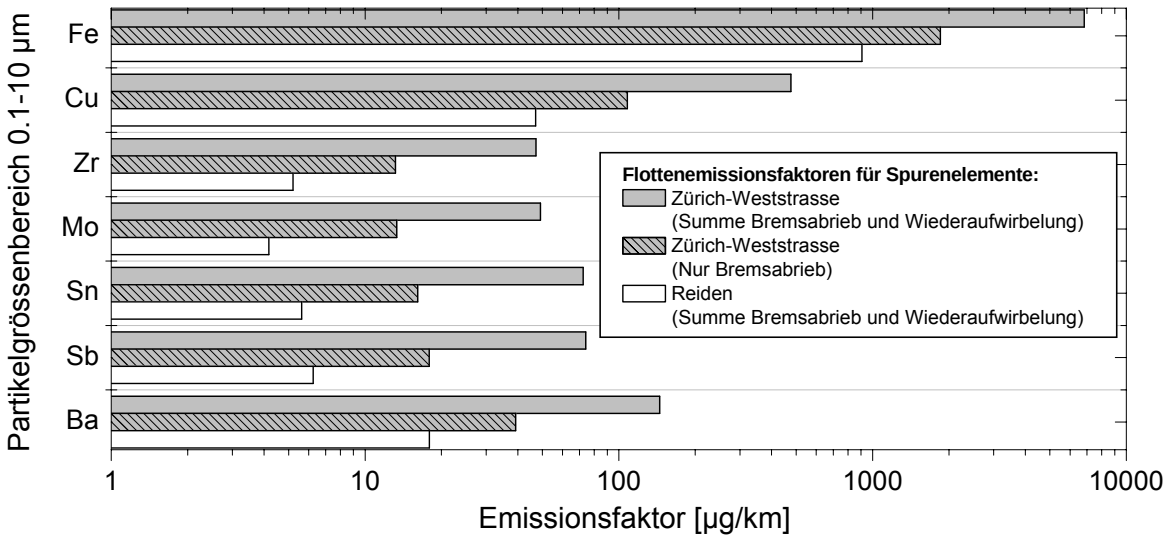

Fig. 1.8: Totale Flottenemissionsfaktoren (Partikelgrössenbereich 0.1 - 10 µm) für Zürich-Weststrasse (10% SMW) und Reiden (15% SMW), für bremsabriebsbezogene Spurenelemente. Den Werten für Zürich-Weststrasse liegen experimentelle Daten von Februar/März 2007 zugrunde (9 Tage, nur Zeitabschnitte ohne Niederschlag), für Reiden von Oktober 2007 (4 Tage, nur Zeitabschnitte ohne Niederschlag).

1.3.5 Partikelgrössenverteilung der Abriebsquellen

Bremsabrieb: Bremsabriebspartikel wurden für leichte Motorfahrzeuge vorwiegend im Partikelgrössenbereich von 1-10 µm gefunden, während der Beitrag im Grössenbereich kleiner als 1 µm sehr tief war. Für schwere Motorfahrzeuge ist die Grössenverteilung noch mehr in Richtung Grobpartikel (2.5-10 µm) verschoben, allerdings ist auch ein leicht höherer Anteil im Submikrometerbereich zu beobachten als bei leichten Motorfahrzeugen. Eine klare Benennung der Ursachen hierfür ist schwierig, dürfte aber mit den sehr unterschiedlichen Konstruktions- und Betriebsmerkmalen von LMW- und SMW-Bremssystemen zusammenhängen.

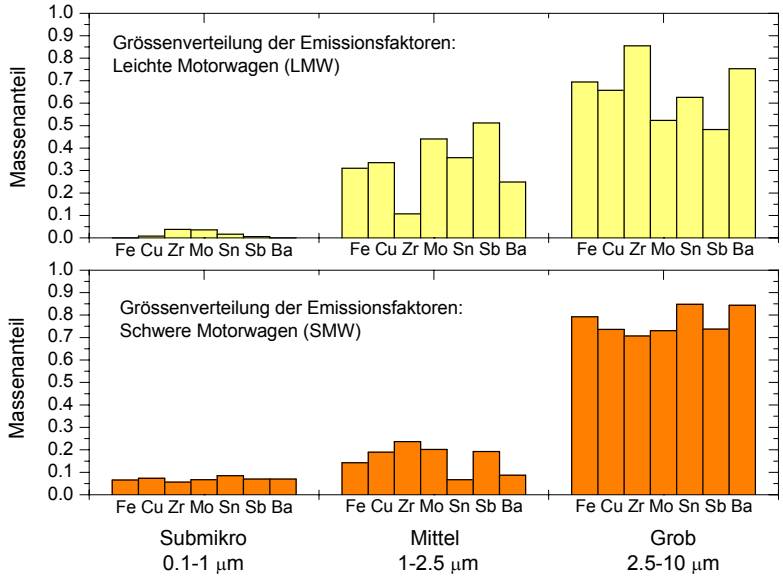

Fig. 1.9 Grössenverteilung von LMW and SMW Emissionsfaktoren für Spurenelemente im Bremsabrieb bei stockendem Verkehr in der Strassenschlucht Zürich-Weststrasse.

Strassenabrieb: Die Experimente mit den Verkehrslastsimulatoren zeigten, dass Partikel aus Strassenabrieb ebenfalls vorwiegend in der Grobfraktion (2.5-10 µm) vorliegen (Figur 1.10). Dies traf auch auf die Grössenverteilung von aufgewirbelten Partikeln zu.

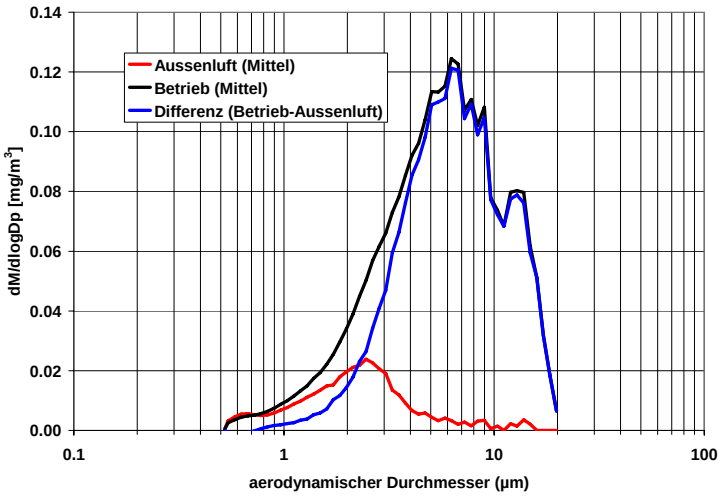

Fig 1.10: Typische Partikelgrössenverteilung im Messbereich 0.5-20 µm aus einem Experiment mit einem Verkehrslastsimulator während einer Versuchsperiode mit dominierendem Strassenabrieb (Aufwirbelung vernachlässigbar). Verglichen mit der Umgebungsluft ist die Grössenverteilung klar Richtung Grobfraktion verschoben.

1.3.6 Räumliche Verteilung und Lebensdauer von städtischem PM10

1.3.6.1 Tagesverlauf der Schadstoffe bei Zürich-Weststrasse

Für eine systematische Beschreibung der zeitlichen Schwankung von lokalen Emissionen in der Strassenschlucht Zürich-Weststrasse werden in Figur 1.11 normierte und hintergrundkorrigierte Tagesverläufe von PM10, NOx, CO_2, Russ (als "black carbon", BC) in PM1, sowie grössenfraktioniertes Antimon und Silizium zusammen mit den Verkehrsfrequenzen dargestellt.

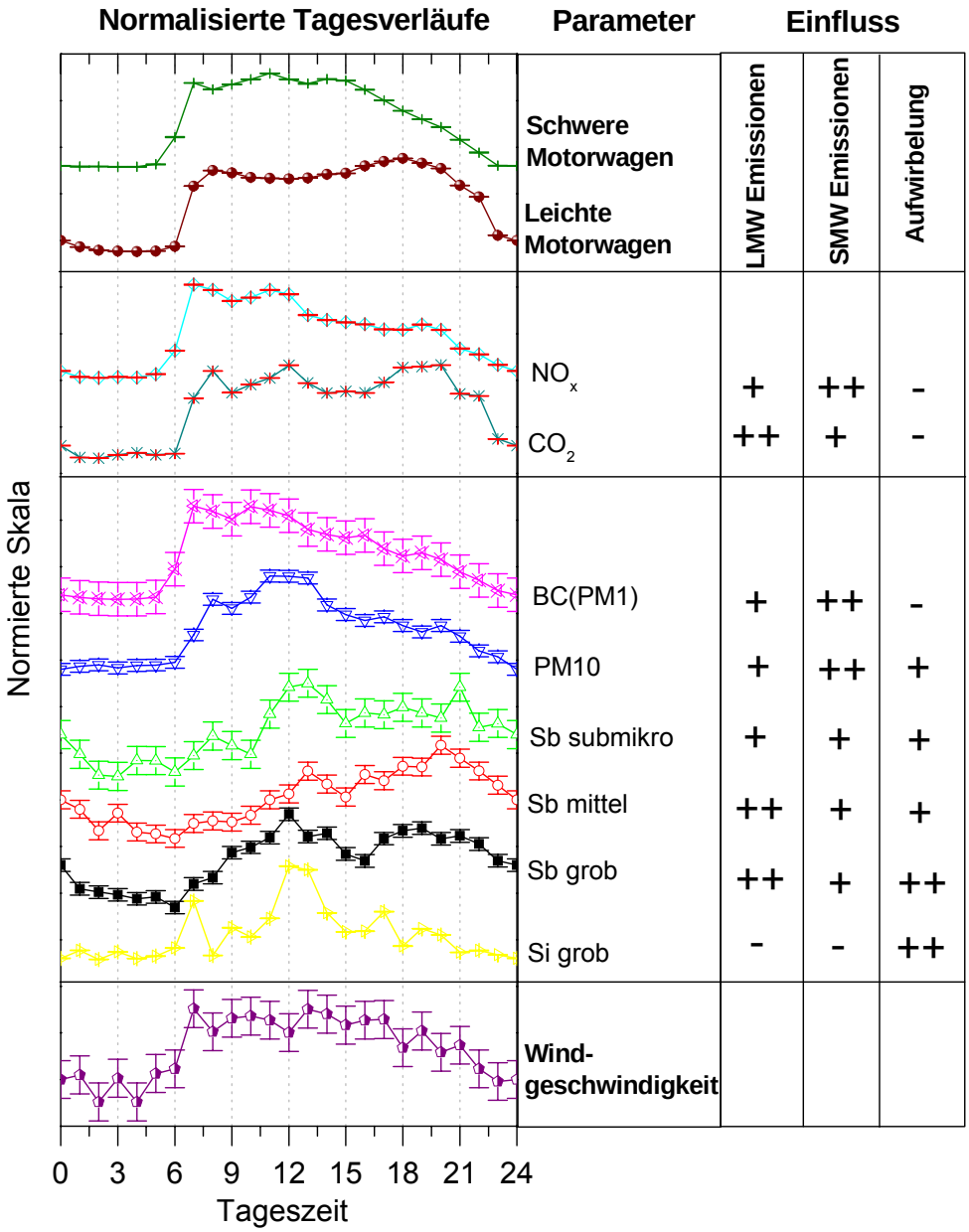

Fig. 1.11: Hintergrundkorrigierte Tagesverläufe (Zürich-Weststrasse, 15 Tage im Februar/März 2007, nur Werktage ohne Niederschlag). Alle Verläufe sind normalisiert auf vergleichbare Amplituden. Fehlerbalken geben die Messunsicherheit an. Die meteorologischen Verhältnisse waren an allen Tagen ähnlich (winterliche Inversionslage).

Die Tagesverläufe von NOx und BC(PM1) waren hoch korreliert mit den Tagesverläufen der schweren Motorfahrzeuge. Dies zeigt, dass diese Emissionen vor allem durch die rund 10% Schwerverkehr dominiert werden. CO_2 hingegen zeigte eine bessere Korrelation des Tagesverlaufs mit den leichten Motorfahrzeugen,

die somit emissionsmässig für CO_2 hauptsächlich verantwortlich sind. Der generelle Konzentrationsabfall zwischen 14 - 16 Uhr, der für die gasförmigen Komponenten beobachtet wurde, hat primär meteorologische Gründe.

Im Gegensatz dazu zeigten PM10 und Antimon keine ganztägige Korrelation mit der Verkehrsfrequenz, sondern ein ausgeprägtes Maximum um die Mittagszeit. Eine mögliche Erklärung für dieses Mittagsmaximum ist der Einfluss der Windgeschwindigkeit und der dadurch induzierten Aufwirbelung von Strassenstaub, aber auch die Anreicherung von frischen Emissionen und von Strassenstaub in der Strassenschlucht im Laufe des Tages. Tatsächlich war Silizium in der Grobfraktion, ein guter Indikator für Aufwirbelung in der Strassenschlucht, mit der Windgeschwindigkeit hoch korreliert. Der markante Anstieg der Windgeschwindigkeiten in der Strassenschlucht mit einsetzendem Verkehr zeigt deutlich, dass hier die Windbewegungen nicht nur meteorologische Gründe haben, sondern wesentlich vom Verkehr mitverursacht sind. Deshalb ist die Aufwirbelung klar dem Verkehr und nicht den natürlichen Windbewegungen zuzuordnen.

Trotz der beschriebenen Bedeutung von nicht strikt verkehrsproportionaler Aufwirbelung und Anreicherung sind auch direkte Einflüsse des Verkehrs auf die Tagesverläufe klar sichtbar. Speziell am Nachmittag und Abend korrelierten die Tagesverläufe von PM10 und Antimon deutlich mit den Verkehrsfrequenzen der leichten Motorfahrzeuge.

1.3.6.2 PM-Massenkonzentrationen aus mobilen Strassenmessungen

Mobile PM-Messungen in Zürich zeigten äusserst komplexe räumliche und zeitliche Schwankungen (Fig. 1.12). Für PM1 war eine Korrelation mit der Verkehrsdichte ersichtlich, welche auf die Emissionen von primären Verbrennungspartikeln hinweist. Auch Partikel >1 µm zeigten noch eine gewisse Korrelation mit der Verkehrsdichte und können daher zumindest teilweise Abriebsprozessen des Verkehrs und der Aufwirbelung von Strassenstaub zugeordnet werden. Allerdings ist das räumliche und zeitliche Muster inhomogener, so dass auch der Einfluss weiterer Partikelquellen in Betracht gezogen werden muss. So ist die hohe Variabilität der Konzentrationen an der Badenerstrasse wahrscheinlich dem Einfluss der Baustelle für das Letzigrundstadion zuzuschreiben, mit dem dadurch induzierten hohen Aufkommen von Baustellenverkehr.

1.3.6.3 Zusammensetzung von deponiertem Strassenstaub

In Zürich besteht Strassenstaub vorwiegend aus Silikat- und Karbonatverbindungen von natürlichen mineralischen Quellen, Baustaub und deponierten Verkehrsemissionen. Figur 1.13 zeigt das chemische Profil (relative Mengen in %) der untersuchten Proben. Dazu wurden alle Strassenstaubproben, welche im Februar 2008 gesammelt wurden, gemittelt. Es zeigte sich, dass 35% des Staubs aus Silikatverbindungen (angegeben als SiO_2) und weitere 35 % aus organischem und elementarem Kohlenstoff (OM und EC) bestanden.

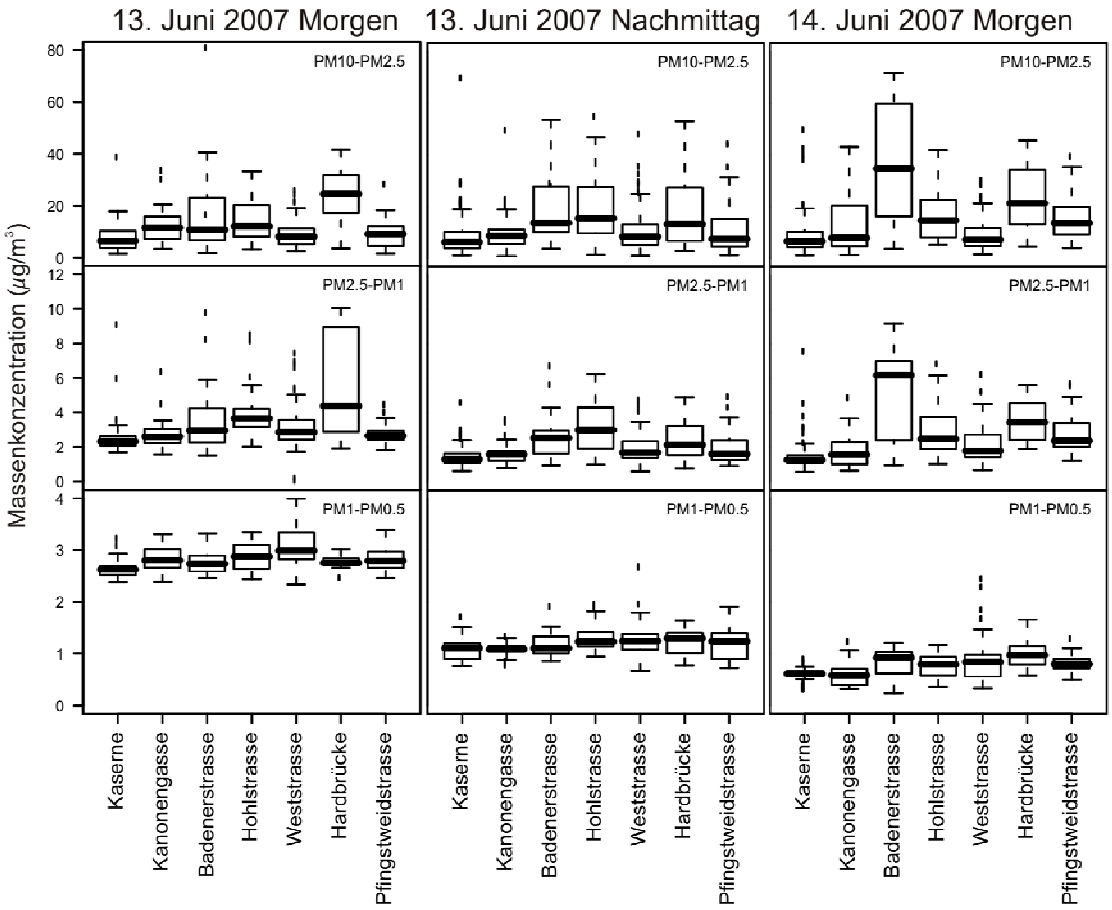

Fig. 1.12: Räumliche Variabilität von PM-Massenkonzentrationen in µg m^{-3} in Zürich, gemessen mit mobilem Messfahrzeug (Massenberechnung basierend auf Einheitsdichte). Die Messorte sind in der Reihenfolge zunehmender durchschnittlicher Verkehrsdichte geordnet (Kaserne: Innenhof ohne Verkehr). Darstellung ohne 6 Extremwerte am 13. Juni 2007.

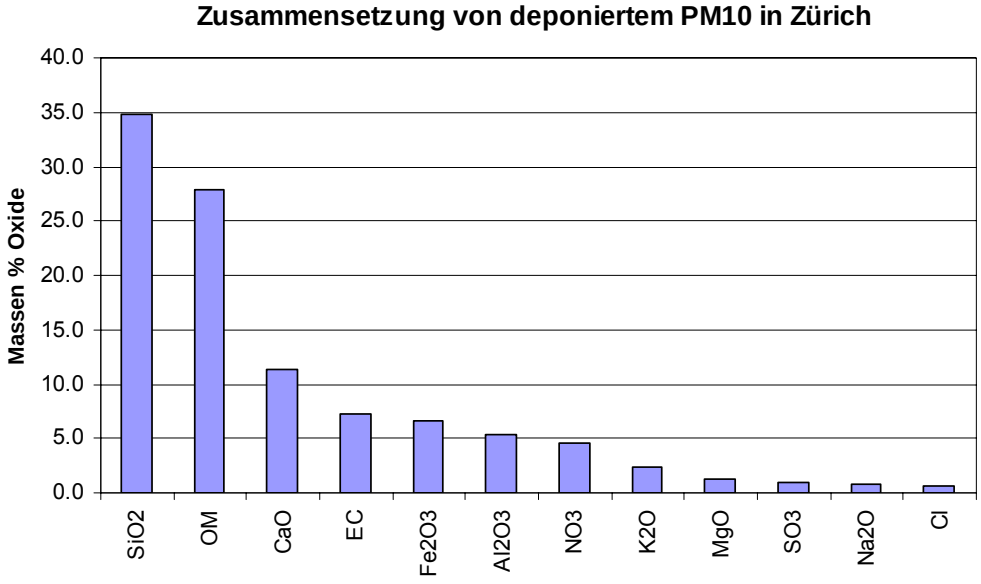

Fig. 1.13: Hauptbestandteile von deponiertem PM10-Staub auf verschiedenen Strassen in Zürich. Die Elemente werden als Oxide angegeben. OM = organisches Material, EC = elementarer Kohlenstoff.

1.4 Schlussfolgerungen und Ausblick

Aus der Gesamtheit der Resultate können folgende Schlussfolgerungen gezogen werden, die auch Anhaltspunkte für künftige Massnahmen zur Emissionsminderung bieten:

- **Massenmässiger PM10-Beitrag nicht-auspuffbedingter Emissionsquellen des Strassenverkehrs:** Während des Untersuchungszeitraums in der Strassenschlucht Zürich-Weststrasse (Februar/März 2007) und entlang der Autobahn A2 in Reiden (Oktober/November 2007) trugen die direkten Abriebsquellen und die fahrzeugverursachte Aufwirbelung von Strassenstaub rund 60% zu den totalen verkehrsbedingten PM10-Emissionen bei.

- **Bremsabrieb:** Bremsabrieb zeigte ein charakteristisches Muster von Fe, Cu, Zn, Mo, Zr, Sn, Sb und Ba, welches gut mit entsprechenden Befunden anderer Studien übereinstimmt. Dagegen kann die elementare Zusammensetzung einzelner Bremsbeläge stark variieren. Im Gegensatz zu den früheren Studien wurden deutlich tiefere Bleianteile gefunden. Dies weist darauf hin, dass dieses unerwünschte Element in Bremsbelägen inzwischen weitgehend durch andere Elemente oder Substanzen ersetzt wurde. Durch den stark gestörten Verkehrsfluss in Zürich-Weststrasse betrugen die Bremsabriebsemissionen rund 20% (15 mg/km/Fz) der totalen verkehrsbedingten PM10-Emissionen. Dagegen war der Beitrag des Bremsabriebs entlang der Autobahn in Reiden mit flüssigem Verkehr deutlich geringer (3%, 3 mg/km/Fz). An beiden Standorten waren die Emissionsfaktoren für Bremsabrieb für schwere Motorfahrzeuge etwa 10 mal höher als für leichte Motorfahrzeuge.

- **Verkehrsinduzierte Aufwirbelung (Resuspension) von Strassenstaub:** Generell ist die Aufwirbelung (Resuspension) von Strassenstaub stark von der zur Verfügung stehenden Staubmasse auf der Strassenoberfläche und damit von der Verschmutzung der Strasse beeinflusst. Im Februar/März 2007 konnten in der Strassenschlucht von Zürich-Weststrasse bis zu 40% der verkehrsbedingten PM10-Emissionen der Aufwirbelung zugeordnet werden. Die Abschätzungen für Aufwirbelung entlang der Autobahn in Reiden im Oktober/November 2007 ergaben einen Anteil von über 50%. In der Strassenschlucht Zürich-Weststrasse wurde der verfügbare Strassenstaub im Wesentlichen durch die Turbulenz schwerer Fahrzeuge aufgewirbelt sodass in dieser Situation der Einfluss der leichten Fahrzeuge klein war. Daraus kann aber nicht generell auf unbedeutende Aufwirbelungsemissionen von leichten Motorfahrzeugen geschlossen werden. In Verkehrssituationen ohne oder mit wenig Schwerverkehr werden auch leichte Fahrzeuge Staub aufwirbeln.

- **Belagsabrieb und Reifenabrieb:** Beiträge zur PM10-Belastung aus Belags- und Reifenabrieb konnten weder in Zürich-Weststrasse noch in Reiden direkt nachgewiesen werden. Spezifische Experimente mit Verkehrslastsimulatoren zeigten, dass direkter Belagsabrieb bei intakten Belägen sehr gering ist im Vergleich zu Aufwirbelung. Schadhafte Beläge hingegen zeigten deutlich erhöhte Abriebsemissionen. Zur Quantifizierung des Abriebs von gängigen Belagstypen unter realen Verkehrsbedingungen sind jedoch weitere Untersuchungen notwendig. Zu Reifenabrieb resultierten aus unserer Studie keine spezifischen Resultate. Andere Studien zeigen aber, dass dieser nur im Grössenbereich über 10 µm massenmässig relevant ist. Für weitere Untersuchungen zu Reifenabrieb könnten gewisse Pyrolyseprodukte des Kautschuks als spezifischer Indikator dienen, wie eine noch unveröffentlichte deutsche Studie zeigt.

- **Emissionsfaktoren:** Die präsentierten Emissionsfaktoren sind grundsätzlich nicht abhängig von der exakten Position der Messstelle entlang der Strasse, da die atmosphärische Verdünnung orts- und

zeitspezifisch berücksichtigt wird. Allerdings können die Emissionen aus Aufwirbelung oft nicht adäquat in mg/km/Fz beschrieben werden, da kein strikt linearer Zusammenhang mit den Verkehrsfrequenzen existiert. Dies liegt an den sehr vielfältigen Ursachen, welche die Aufwirbelung beeinflussen. Dies ist auch der Grund, weshalb spezifische Emissionsfaktoren für Aufwirbelung nur indirekt und mit erhöhter Messunsicherheit abgeschätzt werden konnten. Da Aufwirbelung wesentlich zu den verkehrsbedingten totalen PM10-Emissionen beiträgt, gilt dies auch für PM10. Zukünftige Untersuchungen sollten dieses Problem aufgreifen und geeignete Konzepte zur systematischen Beschreibung der Emissionen aus Aufwirbelung entwickeln.

- **Grössenbereich der Partikel aus nicht auspuffbedingten Verkehrsemissionen:** Im Rahmen dieser Studie wurden Partikel im Grössenbereich von 0.1 bis 10 µm untersucht. Massenrelevante Beiträge aus Abriebs- und Aufwirbelungsemissionen lagen dabei vorwiegend im Grössenbereich oberhalb 1 µm.

- **Auspuffemissionen:** Obwohl grundsätzlich nicht Gegenstand dieser Studie, wurden aus Gründen der PM10-Massenbilanzierung Auspuffemissionen aus "black carbon"-Messungen abgeschätzt. Diese Emissionen beinhalten vorwiegend organische und elementare Kohlenstoffverbindungen und sind dem Grössenbereich unterhalb 1 µm zuzuordnen. Den Auspuffemissionen konnten keine relevanten Beiträge von Spurenelementen aus Treibstoffadditiven (Zn, Ca, S, P) zugeordnet werden. Dies ist ein Hinweis darauf, dass andere Quellen dieser Elemente massenmässig bedeutender sind. Zwar zeigten Zn und P eine relative Anreicherung im Grössenbereich unterhalb 1 µm. Diese konnte aber nicht spezifisch dem Verkehr zugeordnet werden.

- **Vergleich mit früheren Untersuchungen:** Die Quantifizierung der Emissionen für die einzelnen Abriebsprozesse erforderte im Vergleich zur Vorläuferstudie ASTRA2000/415 einen ungleich höheren experimentellen Aufwand. Deshalb beschränkten sich die Messungen auf zwei Messstandorte. Bei Zürich-Weststrasse wurden für die Verkehrsflotte über die letzten 10 Jahre abnehmende Werte der PM10-Emissionsfaktoren beobachtet. Dagegen sind die PM10-Emissionsfaktoren in Reiden verglichen mit einer ähnlichen Verkehrssituation in Birrhard (2004) etwa gleich geblieben. Die Emissionsfaktoren für nicht auspuffbedingte Emissionen und der totalen verkehrsbedingten PM10-Emissionen hängen sehr stark von der fahrzeugverursachten Aufwirbelung von Strassenstaub zum Zeitpunkt der Untersuchung ab. Unterschiede bei diesen Faktoren reflektieren eher die lokal herrschenden Bedingungen an den Messorten (Verschmutzung der Strasse, Zustand des Belags) als einen zeitlichen Emissionstrend.

- **PM10 aus nicht-auspuffbedingten Verkehrsquellen im Vergleich zum städtischen PM10:** Die beiden gewählten Messstandorte dieser Studie waren topographisch sehr unterschiedlich (Strassenschlucht resp. Autobahn in offenem Gelände). Dies hatte einen starken Einfluss auf die Verdünnung des emittierten PM10 und damit auf die lokalen PM10-Konzentrationen. Mobile Messungen in Zürich zeigten, dass die räumliche Schwankung der Partikelkonzentration im Partikelgrössenbereich 0.5 bis 1 µm an den Messtagen durch die lokalen Verkehrsemissionen beeinflusst wurde. Dagegen war der Einfluss des lokalen Verkehrs auf die räumliche Schwankung der Partikelfraktion grösser als 1 µm nicht dominant. Die Schwankungen wurden hier eher durch andere Quellen (z.B. Baustellen) beeinflusst. Während die Grobfraktion des städtischen Hintergrundaerosols vor allem durch mineralische Elemente dominiert wird, enthält die vom Verkehr emittierte Grobfraktion zusätzlich noch signifikante Mengen von Spurenelementen (Fe, Cu, Zn, Mo, Zr, Sn, Sb und Ba), welche vorwiegend vom Bremsabrieb stammen.

1 Summary

1.1 Motivation

Particle emissions of road traffic are generally associated with fresh exhaust emissions. However, the preceding research project ASTRA2000/415 as well as several recent studies identified a clear contribution of non-exhaust emissions to the traffic related PM10 load of the ambient air. These emissions consist of particles produced by abrasion from brakes, road wear, tire wear, as well as vehicle induced resuspension of deposited road dust. For many urban environments, quantitative information about the contributions of the individual abrasion processes is still scarce. For effective PM10 reduction scenarios it is of particular interest to know whether road wear, resuspension or fresh abrasion from vehicles dominates the non-exhaust PM10 emissions.

1.2 Goal, concept and experiments

1.2.1 Main goals

The main scope of the project APART (Abrasion PArticles produced by Road Traffic) was to identify and quantify the non-exhaust fraction of traffic related PM10 for several road-side locations with characteristic traffic regimes.

Specific goals:

- To provide a reliable base for future PM10 reduction scenarios
- Determination of location-specific emission factors (mg/km/vehicle) for *trace elements* emitted by local road traffic.
- Calculation of location-specific emission factors (mg/km/vehicle) for individual *non-exhaust emission sources*.
- Separation of emission factor values for light duty vehicles (LDV) and heavy duty vehicles (HDV).
- Evaluation of the local mass contribution from individual non-exhaust sources (% of traffic related PM10).

Scope exclusion:

- The study focused on traffic related emissions and did not include a quantification of other PM10 sources.
- Exhaust related PM10 was quantified at the investigated locations to establish a mass balance of total traffic related PM10. An in-depth interpretation of the exhaust fraction is however subject of other studies and was not within the scope of the present investigation.

1.2.2 Concept

The selection of the investigated locations was based a) on their traffic and roadside characteristics being typical also for other real-world situations and b) on their experimental and conceptual applicability. To separate traffic related emissions from the total ambient PM10 load, representative background measurements were performed either upwind of the selected measuring location, or at a suitable background site (Figure 1.1). The identification of individual traffic related sources was based on specific elemental fingerprint signatures for the various sources. These fingerprints were obtained by hourly elemental mass concentration measurements in three size classes (2.5-10, 1-2.5 and 0.1-1 micrometers). A rotating drum impactor (RDI) was used as sampling device for this purpose. The collected samples were analyzed by synchrotron radiation X-ray fluorescence spectrometry (SR-XRF). The elemental fingerprint measurements were accompanied by additional aerosol, gas phase and meteorological measurements, and by traffic counting for light and heavy duty vehicles. The mathematical identification of the abrasion sources from the experimental data was performed by positive matrix factorization (PMF), a statistical method widely used for this purpose. The atmospheric dilution of the emissions from their point of emission to the point of sampling (10-20 m) was obtained by background corrected NO_x measurements and known NO_x emissions at the considered site. This dilution, along with the traffic counts, allowed for the calculation of vehicle specific emission factors for the measured tracer species and for the identified abrasion sources with help of a statistical model. To ensure a statistically significant calculation of emission factors, only time periods with distinctively high background corrected NO_x concentrations (ΔNO_x > 20 µg m^{-3}) were considered for analysis. The presented emission factors are independent of the exact measurement position along the road.

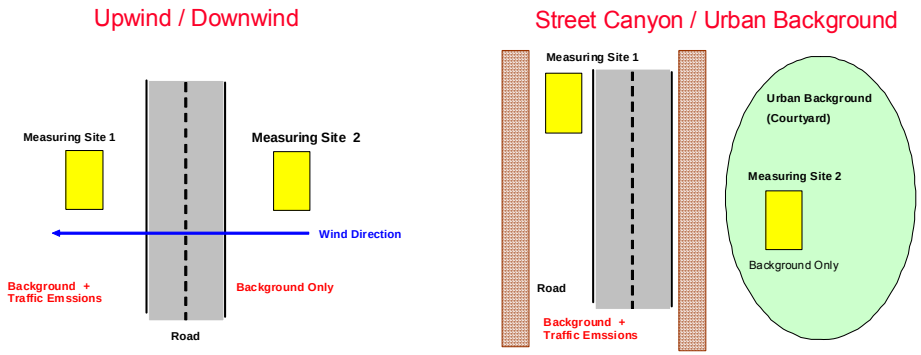

Fig. 1.1: Schematic illustration of the upwind-downwind concept (left) and the traffic vs. background concept (right). The sampling inlets of the measuring sites were located 4.5 m above ground, defined by experimental preconditions.

1.2.3 Measurements in Zürich at Weststrasse and Kaserne (February and March 2007)

The Zürich-Weststrasse site represented an urban street canyon with the following traffic characteristics:

- 'Stop-and-go traffic': Urban main road with traffic lights, strong disturbances (Category 'IO_HVS3' according to *Handbook of Emission Factors,* http://www.hbefa.net). Closed for transit traffic from 22:00 to 06:00.
- Pavement: Asphalt concrete (AB12), year of application: 1995/98
- Vehicle counting: <6m; (Light duty vehicles including 9% delivery vans), >6m (Heavy duty vehicles including motor coaches). Traffic counting was performed by Empa.
- Weekdays: 22000 vehicles per day (heavy duty vehicle fraction 12%)
- Saturdays: 21000 vehicles per day (heavy duty vehicle fraction 5%)
- Sundays: 19000 vehicles per day (heavy duty vehicle fraction 4%)

To quantify the local PM10 contributions at Zürich-Weststrasse, simultaneous measurements of the urban background were performed at Zürich-Kaserne (approximately 600 m distance from Zürich-Weststrasse). During the considered time periods, PM10 at Zürich-Kaserne was shown to also represent the urban background at Zürich-Weststrasse. It consisted of the accumulated contributions of all urban PM10 sources (both traffic and non-traffic related sources), as illustrated in Figure 1.2. Figure 1.3 shows the measured PM10 concentrations at both sites for a selected time period with a prevailing meteorological inversion.

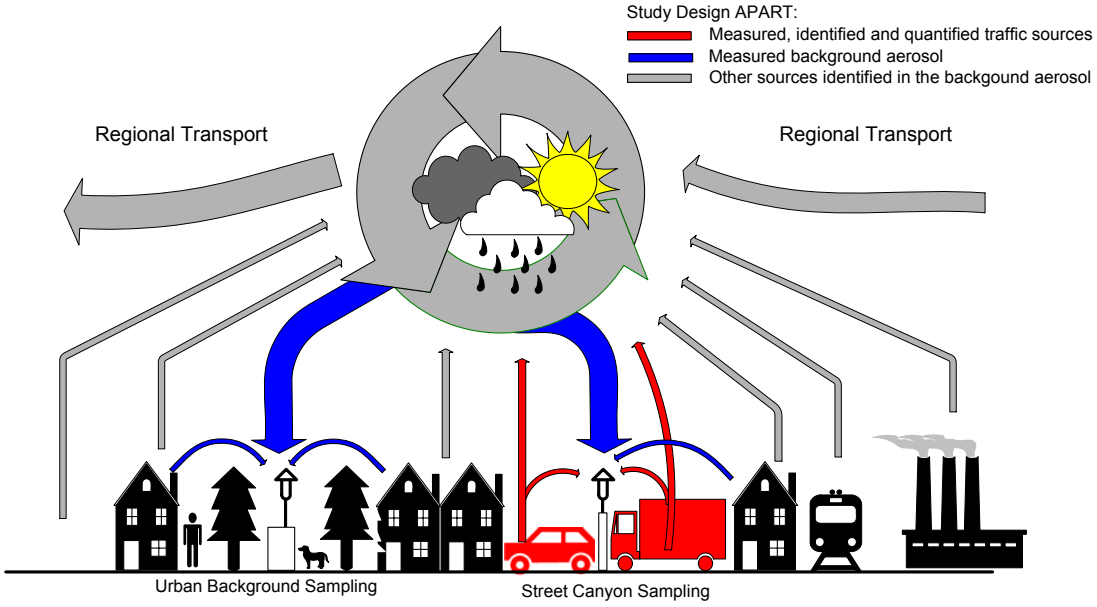

Fig. 1.2: Schematic view of relevant pollutant fluxes in an urban environment. To evaluate the local contribution of road traffic, all local background sources (also traffic emissions from other locations) as well as the meteorological dilution and chemical transformation have to be considered.

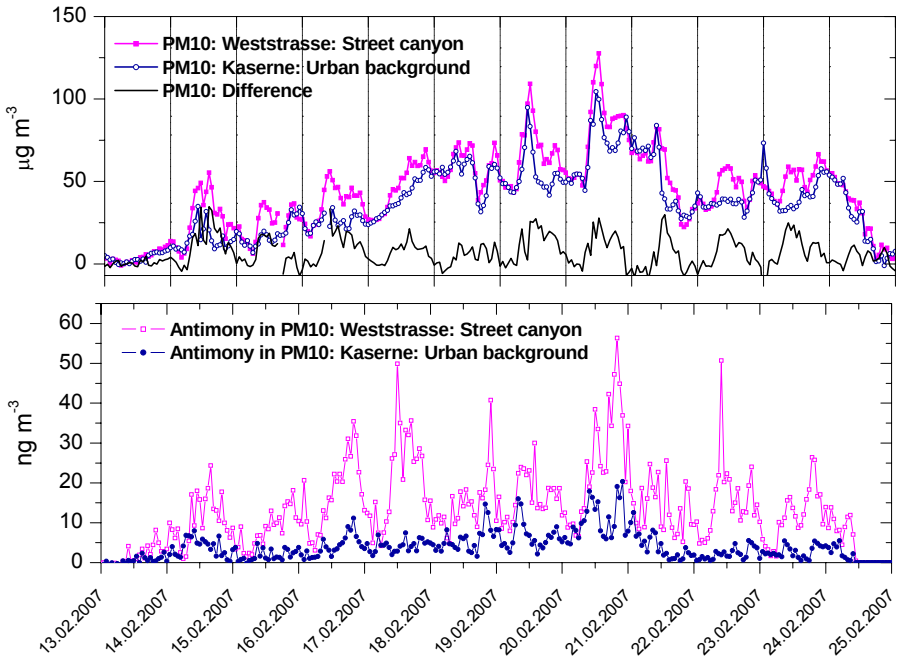

Fig. 1.3: Temporal evolution of PM10 and antimony in a street canyon in Zürich before, during and after a meteorological inversion situation (hourly values). Upper panel: The black line represents the difference between the street canyon and the background and thus represents the local traffic contribution to PM10 in the street canyon.

1.2.4 Measurements in Reiden (July – November 2007)

Measurements were performed in Reiden LU, along the national freeway A2 with the following traffic characteristics:

- Motorway with free-flowing traffic at 120 km h^{-1} (Category 'AB_120' according to *Handbook of Emission Factors,* http://www.hbefa.net)
- Pavement: Splitt-mastix asphalt (compact pavement comparable to asphalt concrete); direction Luzern SMA 11 B 80/100+NAF; direction Basel SMA 11 B55/70+NAF, year of application: 1999.
- Vehicle counting: Light duty vehicles (including 15% delivery vans) versus heavy duty vehicles (including motor coaches). Traffic counting was performed by ASTRA (lu_reiden-s-239)
- Weekdays: 49000 vehicles per day (heavy duty vehicle fraction 16%)
- Saturdays: 45000 vehicles per day (heavy duty vehicle fraction 7%)
- Sundays: 41000 vehicles per day (heavy duty vehicle fraction 2%, including coaches)

Measuring stations were placed at both sides of the freeway. For time periods with perpendicular wind, the upwind station measured the local background PM10 load, while the downwind station detected the background plus the local traffic PM10 emissions (Figure 1.1). Figure 1.4 shows the measured PM10 concentrations at both sites for a selected time period.

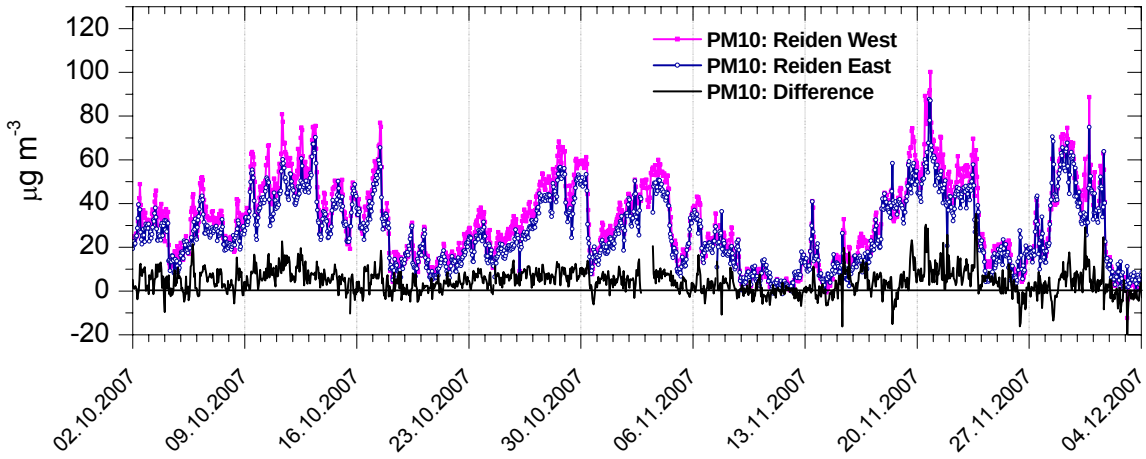

Fig. 1.4: Temporal evolution of PM10 in Reiden (hourly values). The solid black line represents the difference between the PM10 concentrations measured at both sides of the freeway, which was strongly dependent on the wind direction.

1.2.5 Complementing experiments

The road-side measurements provided a robust real-world data base, allowing for extensive data treatment and evaluations of PM10 related sources. To complete the overall results of the study, additional experiments were performed:

- **Resuspended road dust versus road wear:** A separation between road wear and resuspension of deposited dust can not easily be obtained from field measurements. Even with detailed chemical speciation these two sources can hardly be distinguished due to their similar elemental composition and highly correlated variation in time. A so-called "mobile load simulator" offered a possibility to tackle this issue. These devices are designed and used by road engineers to test the properties and durability of road pavements in the field. In this study emission rates for road wear were derived from measurements with two different types of mobile load simulators on different types of road pavement

(asphalt concrete, porous asphalt). The experimental set-up allowed for a separate characterization of the emissions caused by fresh in-situ abrasion and by resuspension of previously deposited dust.

- **Deposited road dust:** Deposited PM10 collected from the surface of a road provides important information on the chemical composition of vehicle induced PM10 resuspension. A specialized instrument for the collection of road dust was used in a sampling campaign in Zurich in February 2008.

- **Mobile PM10 and PM1 measurements:** To investigate the spatial variation of individual particle size ranges within the city of Zürich, a series of mobile measurements was performed in Zürich in June 2007 using a mobile measurement platform.

1.3 Results

1.3.1 Traffic related PM10 emissions in Zürich-Weststrasse

1.3.1.1 Mass relevant PM10 traffic sources

For Zürich-Weststrasse, the following mass relevant traffic related PM10 sources were identified from the hourly measurements by the applied statistical method (positive matrix factorization):

- **Brake wear.** Brake wear was characterized by a specific pattern of Fe, Cu, Zn, Zr, Mo, Sn, Sb and Ba. These elements are widely used constituents of brake linings and are likely to be oxidized during the brake abrasion process.

- **Exhaust emissions:** Exhaust emissions predominantly consisted of organic and inorganic carbon species, expressed as total traffic related carbon. Trace elements originating from fuel additives were not specifically identified from the road side measurements, indicating that these contributions are low on a mass base and other emission sources of these elements are more relevant.

- **Vehicle induced resuspension of road dust:** Besides the large abundance of mineral elements in deposited and resuspended road dust, characteristic contributions of brake wear and exhaust particles (carbon) were clearly identified.

Road wear and tire wear were not identified as separate sources from the measurements at Zürich-Weststrasse, due to the absence of unique tracer species. With the applied approach of analysis, any unidentified contributions from road wear and tire wear were added to the other sources. However, the presented source apportionment is only minimally biased by undetermined contributions from these sources:

- **Road wear versus road dust resuspension:** The controlled experiments with a mobile load simulator showed that direct abrasion wear from the road surface is of minor importance for pavements in good condition. However, damaged pavement surfaces can cause quite significant PM10 emissions.

- **Tire wear:** Reliable information for PM10 emissions from tire wear can hardly be found in literature. Some older works report contributions up to 10% to urban PM10 concentrations. However, none of the applied methods was specific enough to be convincing. A new, still unpublished study at two urban traffic sites in Wiesbaden (Germany) for the first time uses a method that seems to be really specific (analysis of pyrolysis products of tire rubber) and find a mean contribution of tire wear of

0.5% to PM10. The same work shows that the earlier assumed contribution of up to 10% tire wear assumed earlier really exists, but in particle fractions >10 µm and not in PM10. This was also qualitatively confirmed by microscopic evidence. In agreement with these findings, PM10 tire wear emissions for the simulator experiments performed during APART were found to be negligible.

1.3.1.2 Emission factors for traffic related PM10 at Zürich-Weststrasse

Table 1.1 and Figure 1.5 show emission factors for the traffic related PM10 sources, with separate values for light and heavy duty vehicles, and for the average vehicle fleet. Emission factors were calculated from the hourly mass concentrations of the individual traffic sources. For the calculations, the atmospheric dilution of the emissions was taken into account, which was obtained from background corrected NO_x measurements and known NO_x emissions at the considered site. The applied calculation models also considered individual vehicle counts for light and heavy duty vehicles, which allowed for the calculation of separate emission factors for light and heavy duty vehicles. Table 1.1 shows that considerable uncertainties were introduced by splitting the fleet emission factors into vehicle type specific emission factors.

The calculated PM10 emission factors for **Zürich-Weststrasse** show the following characteristics:

- **Vehicle Fleet :** The average PM10 emission factor, related to a HDV fraction of 10%, was mainly caused by exhaust emissions (41%) and vehicle induced resuspension of road dust (38%), followed by brake wear (21%).
- **Light and heavy duty vehicles:** Exhaust (63%) and brake wear (33%) were the dominant PM10 emissions for **light duty vehicles**. In contrast, emissions from resuspension of road dust were estimated to be totally less than 5 % for light duty vehicles. Compared to light duty vehicles, the absolute emission factors for **heavy duty vehicles** were 15 times higher for total PM10 and 10 times higher for brake wear and the exhaust emissions. For heavy duty vehicles, the road dust resuspension capability of an individual heavy duty vehicle was estimated to be substantial. 53% of the PM10 emissions of an individual heavy duty vehicle were attributed to road dust resuspension. Exhaust emissions (31%) and brake wear (16%) are additional important contributions. In the heavily trafficked street canyon at Zürich-Weststrasse, the emissions from resuspension are likely to be limited by the amount of resuspendable dust. The available dust on the surface was resuspended and kept in suspended state mainly by the turbulence induced by the heavy duty vehicles, leaving only small amounts of dust to be resuspended by the light duty vehicles. From this finding at Weststrasse, however, it can not be concluded, that resuspension is generally not induced by LDV. In the case of little or no heavy duty vehicle traffic, the resuspension would also be induced by the light duty vehicle fleet.

While a strong correlation of brake wear and exhaust emissions with the hourly traffic frequencies was found, the diurnal pattern of vehicle induced resuspension was less correlated and characterized by a larger statistical variation. Therefore emission factors expressed as mg/km/vehicle are not appropriate for road dust resuspension. As a consequence, vehicle specific emission factors could not be calculated using the multilinear regression model, but could only be indirectly estimated with accordingly high absolute uncertainties. Since resuspension was found to be a relevant contributor to total traffic related PM10, the same applies to PM10.

Table 1.1: Emission factors for the individual sources contributing to traffic related PM10, valid for Zürich-Weststrasse (urban street canyon). LDV: Light duty vehicles (including 9% delivery vans), HDV: Heavy duty vehicles (including motor coaches). Brake wear was quantified assuming a brake dust antimony content of 1% and a copper content of 5%. Total traffic related carbon was estimated from black carbon measurements, using an experimentally determined ratio of 1.45 for traffic related carbon to emitted black carbon. Values are based on 12 days of measurements in February an March 2007, ΔNO_x > 20 µg m^{-3}, dry time periods only) and are based on NO_x emission factors estimated for Zürich-Weststrasse (Year: 2007, EF_{NOx}(LDV) = 286.8 mg km^{-1}, EF_{NOx}(HDV) = 10559 mg km^{-1}, NO_x calculated as NO_2, *Handbook of Emission Factors,* http://www.hbefa.net) For comparison, emission factors for road wear and resuspension from mobile load simulator experiments are shown. The Table shows that considerable uncertainties were introduced by splitting the fleet emission factors into vehicle type specific emission factors.

Source	**Source quantification**	**Emission factor calculation**	**Zürich-Weststrasse**		
			Fleet 10% HDV[*1] mg/km/veh	**LDV [*2] mg/km/veh**	**HDV[*2] mg/km/veh**
Traffic related PM10	Measured (PM10-Difference: Street canyon - background	Estimated from mass balance	**71**	**24 ± 8**	**498 ± 86**
Brake wear	Statistical modelling[*3]	Multilinear regression	**15**	**8 ± 4**	**81 ± 39**
Exhaust (Total traffic related carbon species)	Statistical modelling[*3]	Multilinear regression	**29**	**15 ± 6**	**155 ± 67**
Road dust resuspension	Statistical modelling[*3]	Estimated from mass balance	**27**	**1 ± 11**	**262 ± 115**
Road Wear	Mobile load simulator experiments		-	(<3)[*a,d]	(7)[*a] (80[*b])
Resuspension[*d]			-	(5)[*d] (76)[*a]	(110)[*c] (660[*b])

[*1] Average heavy duty vehicle fraction during the entire field campaign in February and March 2007 (varies strongly within a day)

[*2] Multilinear model with individual consideration of hourly traffic composition

[*3] PMF (positive matrix factorization)

[*a] new asphalt concrete

[*b] asphalt concrete in poor condition

[*c] asphalt concrete in good condition

[*d] new porous asphalt

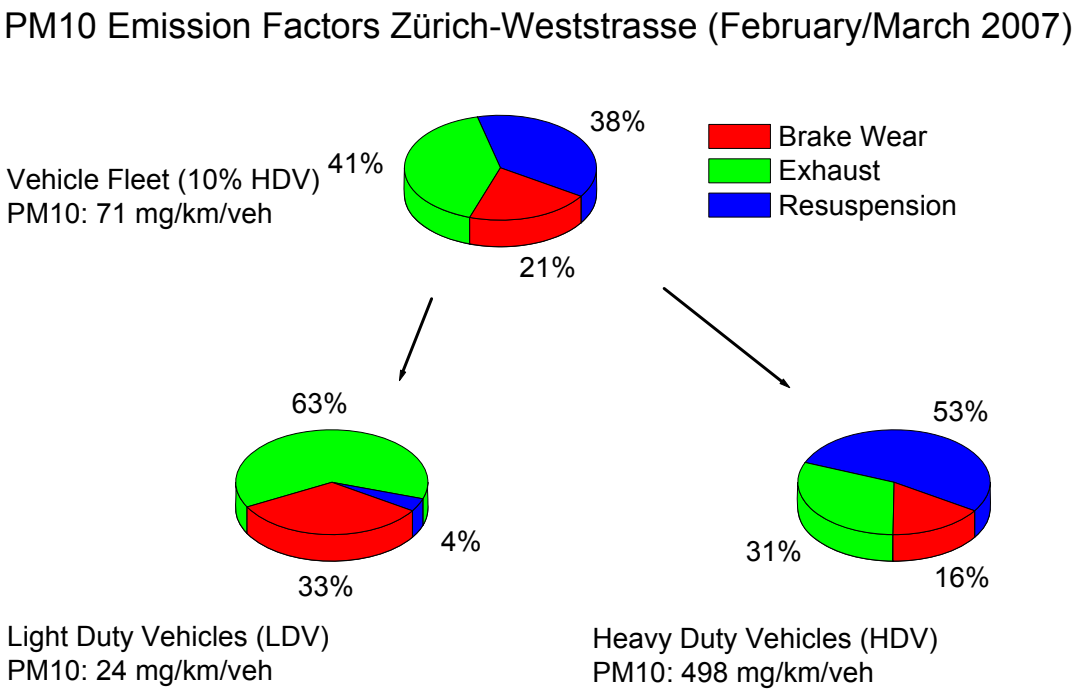

Fig. 1.5: Traffic PM10 emission factors determined for Zürich-Weststrasse and their composition. Considerable uncertainties were introduced by splitting the fleet emission factors into vehicle type specific emission factors.

1.3.2 Traffic related PM10 emissions in Reiden LU

1.3.2.1 Mass relevant PM10 traffic sources

For Reiden, the following mass relevant traffic related PM10 sources were identified from the hourly measurements by the applied statistical method (positive matrix factorization):

- **Brake wear:** Brake wear was characterized by a specific pattern of Fe, Cu, Zn, Zr, Mo, Sn, Sb and Ba. The pattern was very similar to the one found at Zürich-Weststrasse. These elements are widely used constituents of brake linings and are likely to be oxidized during the brake abrasion process.
- **Exhaust emissions:** The exhaust emissions were predominantly formed by organic and inorganic carbon species, expressed as total traffic related carbon. Like at Zürich-Weststrasse, trace elements originating from fuel additives were not specifically identified from the road side measurements, indicating that the contributions are low and other emission sources of these elements were more relevant on a mass base.

Contributions of mineral dust elements to traffic emissions were identified, pointing to vehicle induced road dust resuspension. A specific quantification for resuspension based on these contributions was however not possible, because no reliable composition profile was available for road dust deposited on the freeway.

1.3.2.2 Emission factors for traffic related PM10 at Reiden

Table 1.2 and Figure 1.6 show emission factors for the traffic related PM10 sources, with separate values for light and heavy duty vehicles, and for the average vehicle fleet. Emission factors were calculated from the hourly mass concentrations of the individual traffic sources. For the calculations, the atmospheric dilution of the emissions was taken into account, which was obtained from background corrected NO_x measurements and known NO_x emissions at the considered site. The applied calculation models also considered individual vehicle counts for light and heavy duty vehicles, which allowed for the calculation of separate emission factors for light and heavy duty vehicles. Table 1.2 shows that considerable uncertainties were introduced by splitting the fleet emission factors into vehicle type specific emission factors.

The calculated PM10 emission factors for **Reiden** show the following characteristics:

- **Vehicle fleet:** The average PM10 emission factor for Reiden (15% HDV fraction during the entire campaign) was caused by exhaust emissions (41%) and very low contributions from brake wear emissions (3.2%). The remaining 56% of the traffic emissions were not directly identified, but probably represented contributions from road dust resuspension (and minor contributions from tire wear and road wear).

- **LDV and HDV emission factors:** The PM10 emission factor for HDV was 5.8 times higher than for LDV. Because the mass contributions of both brake wear and traffic related carbon were extrapolated from the same traffic source identified by PMF, the resulting LDV and HDV emission factors showed virtually identical source contributions. An alternative calculation of LDV and HDV emission factors for brake wear and exhaust directly from measured concentration differences of specific marker species (Sb, BC) did not lead to statistically significant results. In contrast to Zürich-Weststrasse, the resuspended dust was removed laterally due to the perpendicular winds (upwind/downwind concept), rather than being kept in suspended state by the turbulence induced by heavy duty vehicles. Therefore a part of the resuspended road dust was also attributed to light duty vehicles.

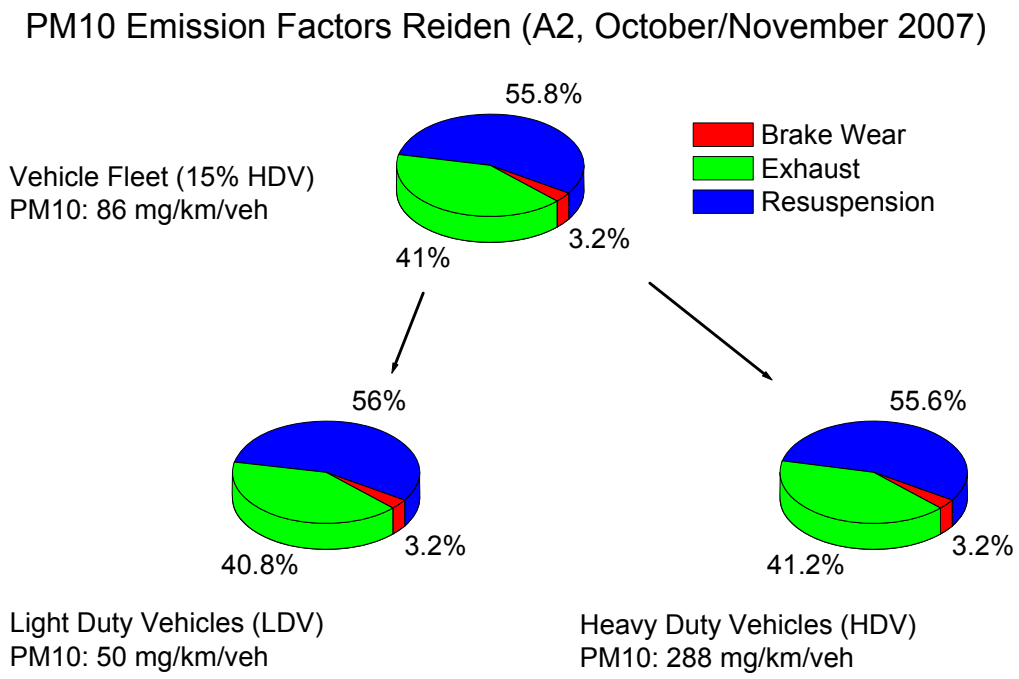

Fig. 1.6: Traffic PM10 emission factors determined for Reiden (A2) and their composition. Considerable uncertainties were introduced by splitting the fleet emission factors into vehicle type specific emission factors.

Table 1.2: Emission factors for the individual sources contributing to traffic related PM10, valid for Reiden LU (Autobahn). LDV: Light duty vehicles (including 15% delivery vans), HDV: Heavy duty vehicles (including motor coaches). Brake wear was quantified assuming a brake dust antimony content of 1% and a copper content of 5%. Total traffic related carbon was estimated from black carbon using the same empirical conversion factor of 1.45 as for Zürich-Weststrasse, due to the lack of a specific factor for Reiden. Values are based on 4 days of measurements in October and November 2007, dry time periods only) and are based on NO_x emission factors estimated for Reiden LU (Year: 2007, EF_{NOx}(LDV) = 448 mg km^{-1}, EF_{NOx}(HDV) = 5421 mg km^{-1}, NO_x calculated as NO_2, *Handbook of Emission Factors,* http://www.hbefa.net). The table shows that considerable uncertainties were introduced by splitting the fleet emission factors into vehicle type specific emission factors.

Source	Source quantification	Emission factor calculation	Reiden (LU) A2		
			Fleet 15% HDV[*1] mg/km/veh	**LDV[*2] mg/km/veh**	**HDV[*2] mg/km/veh**
Traffic related PM10	Measured (PM10-Difference: Downwind - Upwind	Multilinear regression	**86**	**50.0 ± 13**	**288 ± 72**
Brake Wear	Statistical modelling[*3]	Multilinear regression	**3**	**1.6 ± 1.1**	**9 ± 7**
Exhaust (Total traffic related carbon species)	Statistical modelling[*3]	Multilinear regression	**35**	**20.4 ± 7**	**119 ± 38**
Rest (Resuspension and minor sources[*4])	Estimated from mass balance		**48**	**28 ± 14**	**160 ± 82**

[*1] Average heavy duty vehicle fraction in October and November 2007 (varies strongly within a day)
[*2] Multilinear model with individual consideration of hourly traffic composition
[*3] PMF (positive matrix factorization)
[*4] Tire wear and road wear

1.3.3 Emission factor comparison with earlier research

The comparison of the traffic related PM10 emission factors for Zürich-Weststrasse and Reiden (A2) showed the following (values see Tables 1.1 and 1.2):

- The total PM10 fleet emission factor for Reiden (15% HDV, free-flowing traffic) was 20% higher than for Zürich-Weststrasse (10% HDV, heavily disturbed traffic), due to higher exhaust emissions and larger contributions from vehicle induced road dust resuspension.
- In contrast, the fleet emission factor for brake wear was found to be 5 times lower in Reiden compared to Weststrasse, due to the absence of relevant braking activity in the mainly free-flowing freeway traffic.

Table 1.3 compares the determined emission factors to values from earlier studies and emission inventory values for comparable locations in Switzerland:

- Temporal tendency: At Zürich-Weststrasse, a decrease in the PM10 fleet emission factors over time is observed. In contrast, the fleet emission value determined for Reiden is about equal to a value obtained for Birrhard in 2004, a site with a similar traffic regime.

- Exhaust emissions: The estimated values for exhaust emissions are in line with inventory values, considering the uncertainty of determination.
- Non-exhaust emissions and total traffic related PM10: These emission factors strongly depend on the influence of vehicle induced road dust resuspension during the time periods considered in the respective investigations. Therefore, differences rather reflect local conditions at the measurement sites (dirt load on the road surface, condition of pavement) than a reliable emission trend.

Table 1.3: Emission factors for exhaust and non-exhaust PM10 emissions determined at Zürich-Weststrasse, Zürich-Schimmelstrasse (heavily trafficked road intersection, 300 m from Zürich-Weststrasse), Reiden (LU, national freeway A2) and Birrhard (AG, national freeway A1). Generally, considerable uncertainties were introduced by splitting the fleet emission factors into vehicle type specific emission factors.

Parameter	Study	Location	Year	Fleet (mg km^{-1})	LDV (mg km^{-1})	HDV (mg km^{-1})
PM10	NFP41[*1]	Zürich-Schimmelstrasse	1998/99	153	59	1420
	BUWAL/ASTRA 2004[*2]	Zürich-Weststrasse	2002/03	104	49	703
	APART	**Zürich-Weststrasse**	**2007**	**71**	**23.7 ± 7.5**	**498 ± 86**
Exhaust emissions	NFP41[*1]	Zürich-Schimmelstrasse	1998/99	48	14	507
	BUWAL/ASTRA 2003[*2]	Zürich-Weststrasse	2002/03	29	10	320
	HBEFA [*3]	IO_HVS3[*4]	2002/03	-	11	342
	APART	**Zürich-Weststrasse**	**2007**	**29**	**14.9 ± 6.3**	**155 ± 67**
	HBEFA [*3]	IO_HVS3[*4]	2007	-	12	286
Non-exhaust emissions (including resuspension)	NFP41[*1]	Zürich-Schimmelstrasse	1998/99	105	45	913
	BUWAL/ASTRA 2004[*2]	Zürich-Weststrasse	2002/03	75	39	383
	APART	**Zürich-Weststrasse**	**2007**	**42**	**9 ± 11**	**343 ± 122**

Parameter	Study	Location	Year	Fleet (mg km^{-1})	LDV (mg km^{-1})	HDV (mg km^{-1})
PM10	BUWAL/ASTRA 2003[*2]	Birrhard	2003	83	63	267
	APART	**Reiden**	**2007**	**86**	**50.0 ± 12.6**	**288.0 ± 72**
Exhaust emissions	BUWAL/ASTRA 2003[*2]	Birrhard	2003	33	16	193
	HBEFA [*3]	AB_120[*5]	2002/03	-	17	176
	APART	**Reiden**	**2007**	**35**	**20.4 ± 6.6**	**119 ± 38**
	HBEFA [*3]	AB_120[*5]	2007	-	16	111
Non-exhaust emissions (including resuspension)	BUWAL/ASTRA 2003[*2]	Birrhard	2003	50	47	74
	APART	**Reiden**	**2007**	**51**	**30 ± 14**	**169 ± 82**

[*1] Hüglin, C. (2000). Anteil des Strassenverkehrs an den PM10- und PM2.5-Immissionen; Chemische Zusammensetzung des Feinstaubs und Quellenzuordnung mit einem Rezeptormodell, Nationales Forschungsprogramm NFP41 Verkehr und Umwelt, Bericht C4, Bern.

[*2] Verifikation von PM10-Emissionsfaktoren des Strassenverkehrs, Forschungsauftrag ASTRA/BUWAL 2000/415(52/00), Bern.

[*3] Based on: Handbuch Emissionsfaktoren des Strassenverkehrs, Version 2.1 / 2004, INFRAS im Auftrag BUWAL, Bern, http://www.hbefa.net.

[*4] IO_HVS3: Urban main road with traffic lights, strong disturbances.

[*5] Motorway with free-flowing traffic at 120 km h^{-1}.

1.3.4 Emission factors for brake wear related trace elements

Both at Zürich-Weststrasse and Reiden, brake wear was characterized by a characteristic pattern of Fe, Cu, Zn, Mo, Zr, Sn, Sb and Ba. This pattern is similar to real-world fleet brake wear compositions reported in other studies. In contrast, the respective pattern for individual brake linings is extremely inhomogeneous. Compared to older studies, the measured emission factors for brake wear related lead (Pb) were considerably lower, indicating that lead has in the mean time largely been replaced by other elements or substances in brake linings. Emission factors are shown in Figure 1.7 and Figure 1.8. Highest emission factors were found for Fe, Cu and Ba, followed by similar values for Zr, Mo, Sn and Sb. The average ratios between the emission factors for heavy and light duty vehicles were 9, 4 and 14 for the coarse, intermediate and submicron mode, respectively.

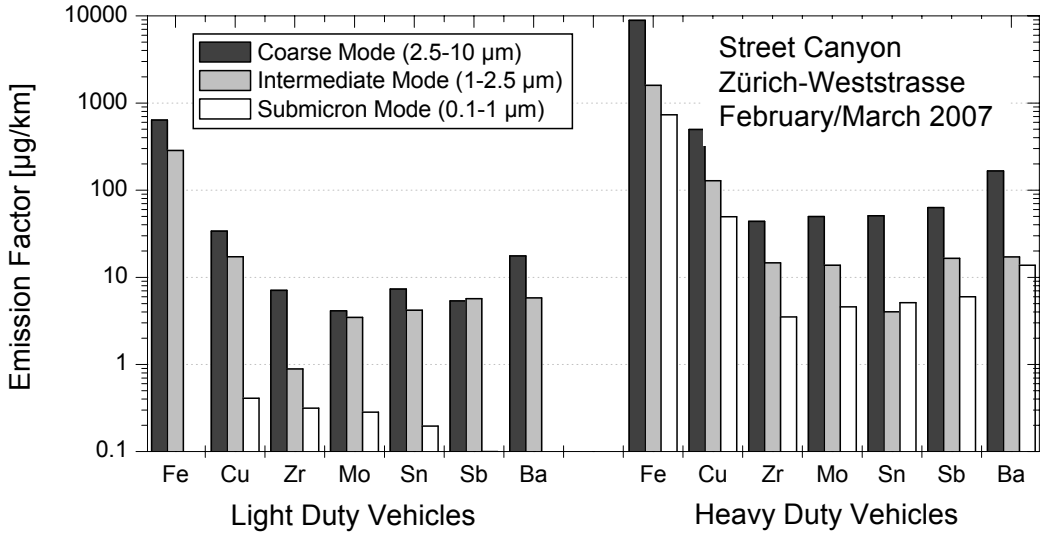

Fig. 1.7: Light duty vehicle (LDV) and heavy duty vehicle (HDV) emission factors (EF) for Zürich-Weststrasse (street canyon). The calculation was performed using 209 hourly values (~ 9 days, ΔNO_x > 20 µg m^{-3}, dry time periods only). For Zn no emission factors were calculated because the significant presence of other sources for this element did not allow for the determination of the contribution of local road traffic within the street canyon.

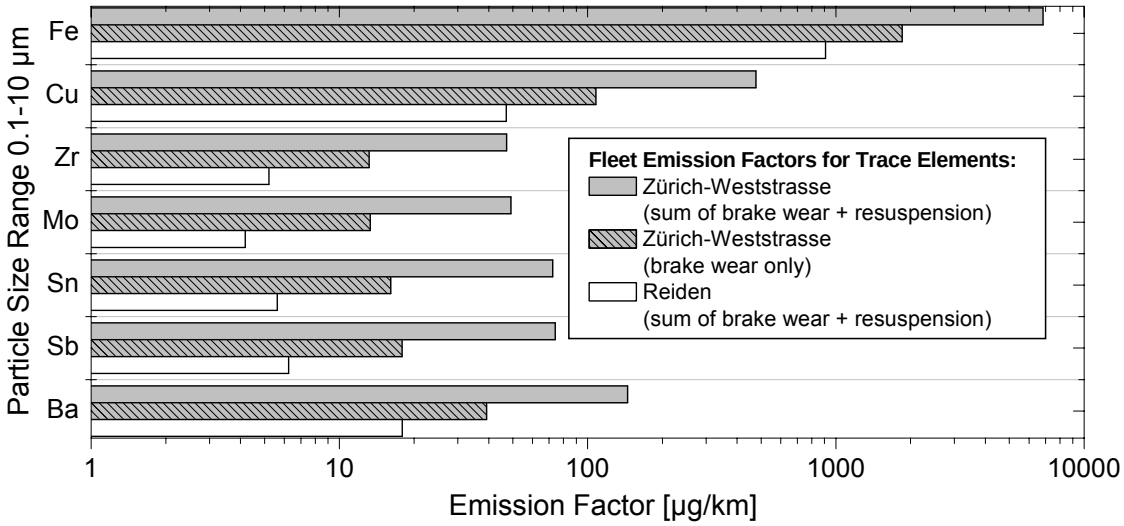

Fig. 1.8: Sum fleet emission factors (particle size range 0.1 - 10 µm) for Zürich-Weststrasse (10% HDV) and Reiden (15% HDV), for trace elements associated to brake wear. The values for Zürich-Weststrasse were calculated from experimental data from February and March 2007 (9 days, dry time periods only), while the values for Reiden refer to October 2007 (4 days, dry time periods only).

1.3.5 Particle size of non-exhaust emissions

Brake wear: Brake wear particles from light duty vehicles were distributed in the entire size range larger than 1 µm, while the contribution from the submicron mode was very low (Figure 1.9). In contrast, more than 75% of the brake wear particles from heavy duty vehicles were found in the coarse mode (2.5-10 µm). A comprehensive explanation of these different size distributions remains difficult, but is likely due to the strongly different design and operation conditions of LDV and HDV brake systems.

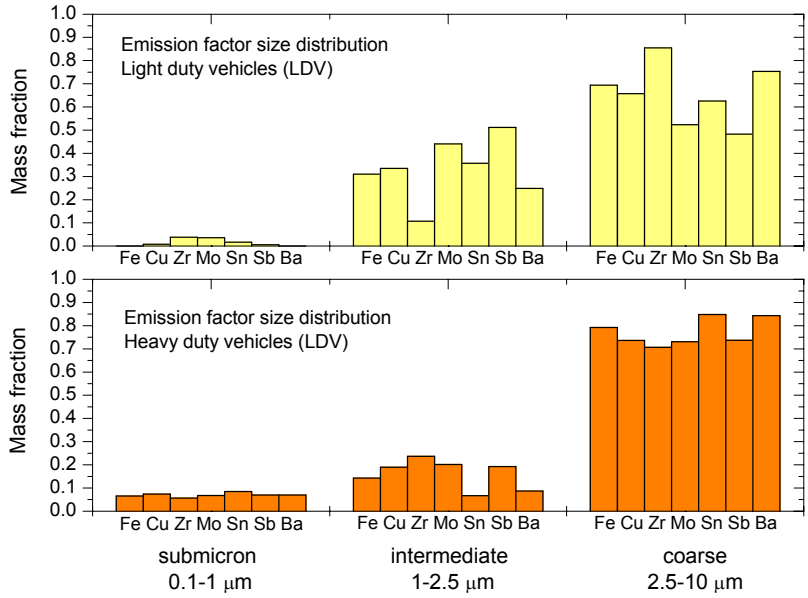

Fig. 1.9: Fractional size contribution for LDV and HDV emission factors determined for brake wear related trace elements and stop-and-go traffic in Zürich-Weststrasse (street canyon).

Road wear: The controlled mobile load simulator experiments showed that road wear was predominantly found in the coarse mode (Figure 1.10). The same also applied to resuspended particles.

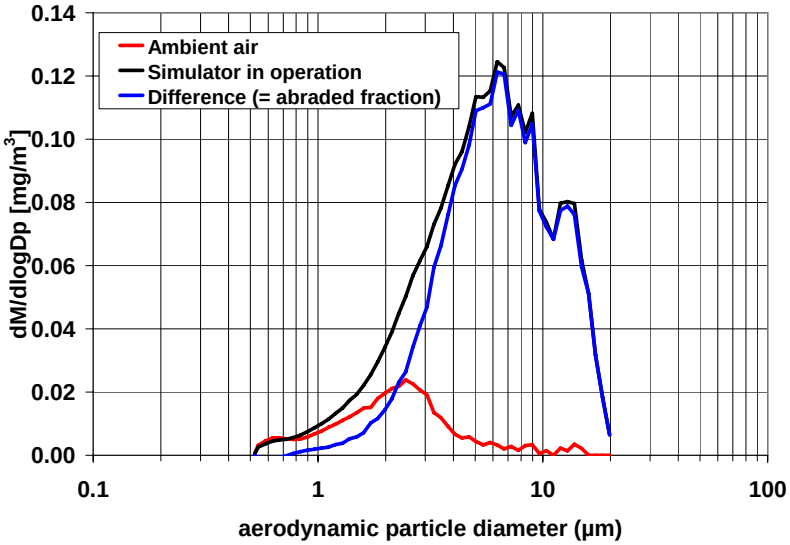

Fig 1.10: Typical particle size distribution obtained from an experiment with the mobile load simulator (measured size range 0.5-20 µm), during a measurement period with dominating abrasion (negligible resuspension). The size distribution of the abrasion particles is clearly shifted towards the coarse side compared to the ambient size distribution.

1.3.6 Spatial distribution and lifetime of urban PM10

1.3.6.1 Diurnal variation of pollutants in Zürich-Weststrasse

For a comprehensive description of the temporal variability of local emissions within the street canyon at Zürich-Weststrasse, normalized and background corrected diurnal variations of NO_x, CO_2, black carbon (BC) in PM1, PM10, size-segregated antimony and coarse mode silicon are shown in Figure 1.11, along with the vehicle frequencies for light and heavy duty vehicles.

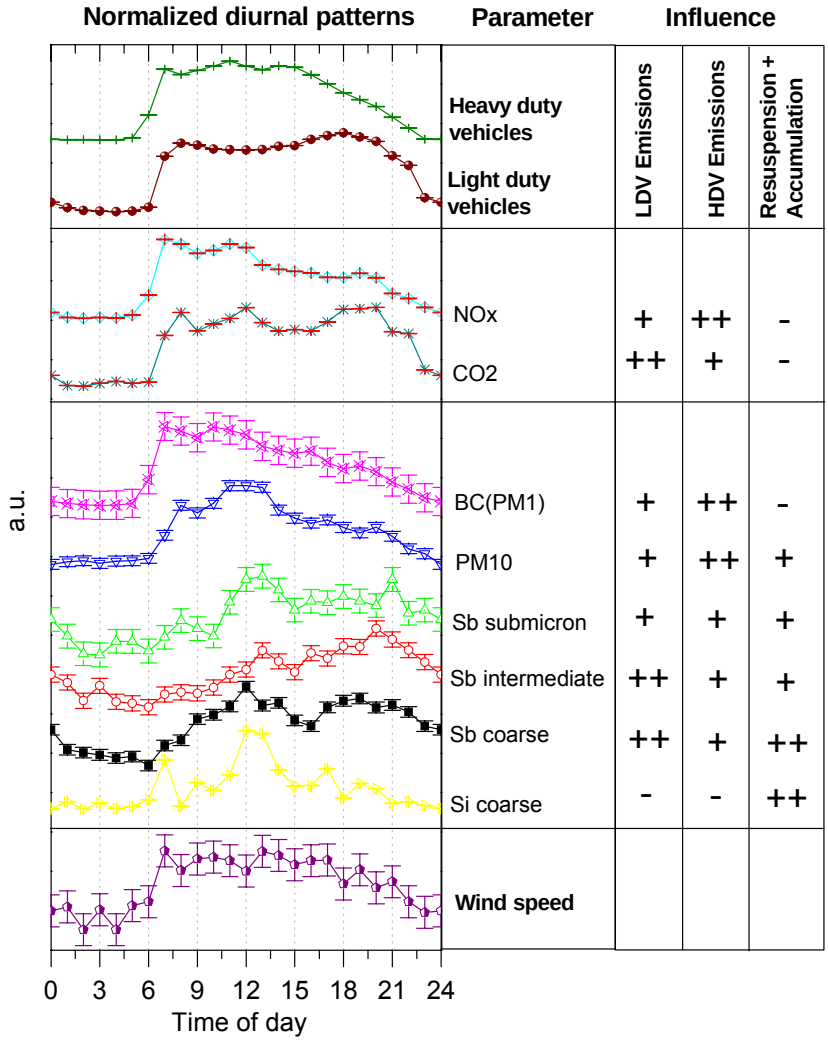

Fig. 1.11: Background corrected diurnal variations (Zürich-Weststrasse, 15 days in February and March 2007, weekdays and dry periods only). Diurnal variations were normalized to have comparable amplitudes. Error bars indicate the measurement precision. The meteorological conditions were comparable for the considered days (wintertime inversion layer).

The diurnal patterns for NOx and BC(PM1) were highly correlated to the diurnal pattern for heavy duty vehicles, indicating that their emissions by the traffic fleet (approx. 10% heavy duty vehicles) were mainly dominated by high emissions from heavy duty vehicles. On the other side, CO_2 showed a better correlation to the diurnal pattern of light duty vehicles, which accordingly implies a high net emission contribution from light duty vehicles. The slight concentration decrease from 14:00 until 16:00, observed for all gaseous and aerosol species, was partly attributed to meteorology.

In contrast, the diurnal patterns of PM10 and antimony showed no all-day correlation to traffic frequencies, but additionally exhibited a distinct midday maximum. A likely explanation for this midday maximum is an increased influence of wind speed induced resuspension of road dust, as well as the enrichment of fresh emissions and resuspended dust throughout the day within the street canyon. Coarse mode silicon, used as proxy for road dust resuspension in this context, was correlated to the wind speed within the street canyon and did not show any correlation to traffic numbers except for the initial traffic increase at 07:00. As seen from this distinct peak in wind speed with beginning morning traffic, the wind speed within the street canyon was not triggered by meteorology, but by the traffic fleet. Thus, resuspension has clearly to be assigned to traffic and not to natural wind movements.

Despite this distinct effect from road dust resuspension and emission enrichment within the street canyon, there were still clear indications for an influence of direct traffic emissions. In the afternoon and evening, the diurnal variations for PM10 and antimony showed a distinct correlation to light duty vehicle frequencies.

1.3.6.2 On-road PM10 mass concentrations

Mobile PM measurements in Zürich showed a complex variation with space and time (see Figure 1.12). For PM1 a correlation with traffic density could be discerned which hinted towards emissions of primary particles produced in combustion processes. Particles larger than 1 µm still showed a relationship with traffic density and hence can be attributed to abrasion processes and road dust resuspension. However, the pattern is spatially and temporally more inhomogeneous, such that other sources have to be taken into account. For example, the large variability of the concentrations at Badenerstrasse is probably due to the influence of the nearby construction site of the Letzigrund sport stadium with its HDV traffic.

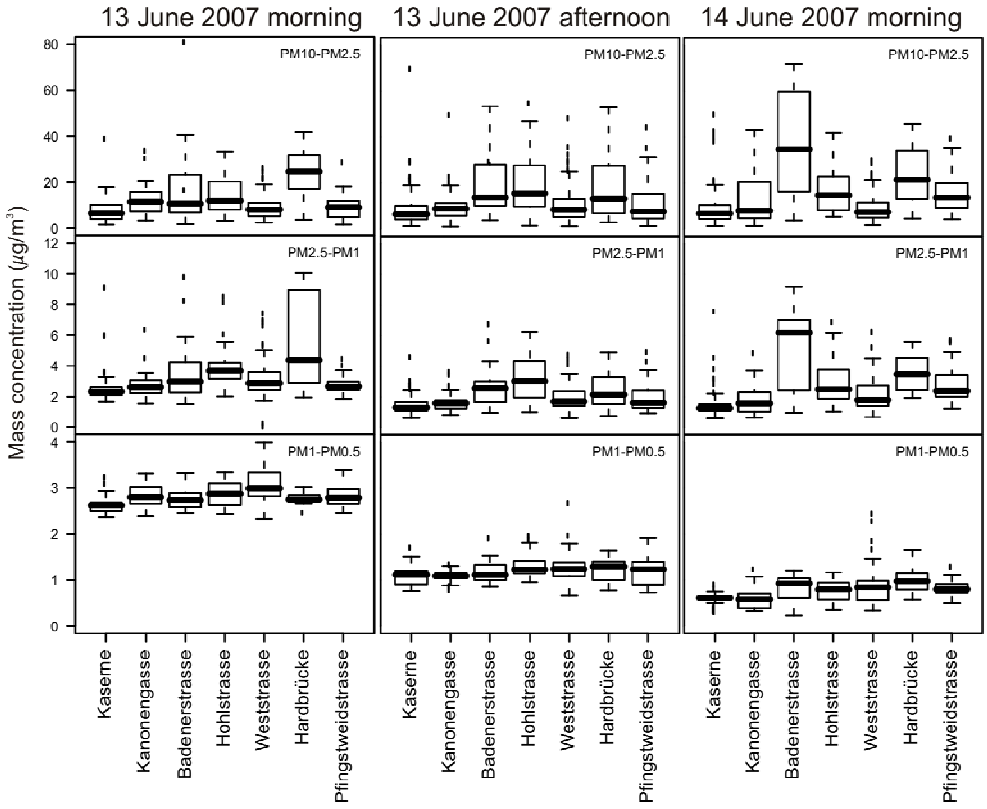

Fig. 1.12: Spatial variation of PM mass concentrations in µg m^{-3} in Zürich, determined by on-road experiments (assuming unit density for the collected particles). The sites are ordered according to increasing traffic density (averaged over 24 h), with Kaserne being the background site without traffic. For a better graphical representation 6 extreme outliers have been cropped on 13 June.

1.3.6.3 Composition of the PM10 fraction of deposited road dust

Zürich road dust consists mainly of silicate and carbonate compounds originating from mineral sources, building material and deposited traffic emissions. Fig. 1.13 shows the chemical profile or relative amount of the chemical constituents in a sample. The values of all road dust samples collected during the campaign in February 2008 were averaged to obtain a reference. Hence, on average 35% of a dust sample were silicate compounds (calculated as SiO_2), and further 35% of mass were organic matter (OM) and elemental carbon (EC).

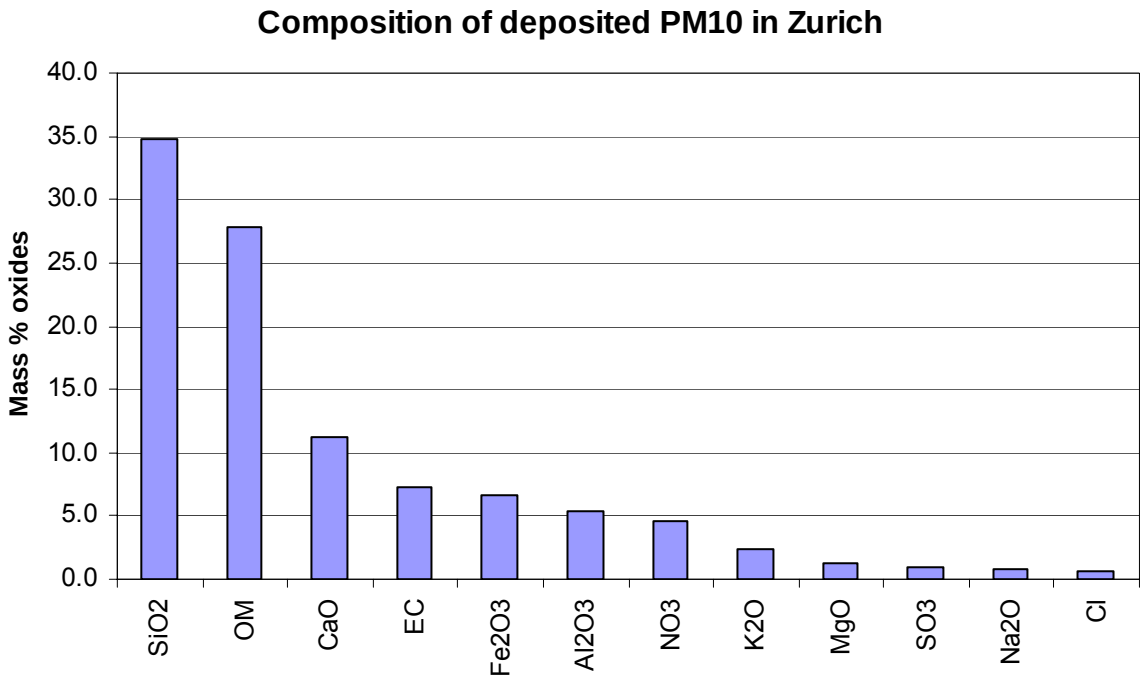

Fig. 1.13: Major element abundances of deposited PM10 collected from different roads in Zürich. Elements are shown in oxide form. OM = Organic matter, EC = elemental carbon.

1.4 Overall Conclusions and Outlook

The following statements are made based on the performed investigations and provide indications for future pollution abatement strategies:

- **Mass contribution of non-exhaust sources:** During the time periods considered for the measurements in the street canyon at Zürich-Weststrasse (February and March 2007) and along the national freeway A2 in Reiden LU (October and November 2007), the sum of direct abrasion sources and vehicle induced road dust resuspension made up 60% of the total traffic related PM10 emissions.

- **Brake wear:** Brake wear was characterized by a characteristic pattern of Fe, Cu, Zn, Mo, Zr, Sn, Sb and Ba, which is similar to real-world fleet emissions for brake wear reported in other studies. In contrast, the pattern of these elements in individual brake linings is extremely inhomogeneous. Compared to older studies, the measured emission factors for brake wear related lead (Pb) were considerably lower, indicating that lead has in the mean time largely been replaced in brake linings. At Zürich-Weststrasse, the heavily disturbed traffic flow resulted in brake wear emissions that made up 20% (15 mg/km/vehicle) of the total PM10 emissions from traffic. In contrast, brake wear emissions contributed less along the freeway in Reiden (3%, 3 mg/km/vehicle), due to the free-flowing traffic regime. For both locations the brake wear emissions from heavy duty vehicles were approximately 10 times higher than from light duty vehicles.

- **Traffic induced resuspension of road dust:** Generally, road dust resuspension is strongly influenced by available road dust and thus by the pollution of the road surface. In the street canyon at Zürich-Weststrasse, up to 40% of the traffic related PM10 emissions were assigned to resuspended road dust during the period of measurements in February and March 2007. Along the freeway in Reiden, the contribution of resuspended road dust to traffic related PM10 emissions was estimated to be higher than 50% in October and November 2007. In the heavily trafficked street canyon at Zürich-Weststrasse, the available dust on the surface was resuspended and kept in suspended state mainly by the turbulence induced by the heavy duty vehicles, leaving only small amounts of dust to be resuspended by the light duty vehicles.

- **Road wear and tire wear:** PM10 contributions from road wear and tire wear were not directly identified from the measurements at Zürich-Weststrasse and Reiden. Controlled experiments with a mobile load simulator showed that for intact pavements road wear is negligible compared to resuspension of deposited road dust, which shows a similar composition. Damaged pavements however led to significantly higher road wear emissions. Quantitative information for road wear under real-world traffic conditions has to be gained by further investigations. While not specifically investigated in this study, tire wear has been found by other investigations to be only relevant in the size range above 10 µm. Recent work indicates that certain pyrolytic products of rubber might be suitable tracers for tire wear.

- **Emission factors:** The presented emission factors are independent of the exact measurement position along the road, because the emissions were corrected for their atmospheric dilution. However, for road dust resuspension at Zürich-Weststrasse emissions were only insufficiently described in terms of mg/km/vehicle, because there was no strictly linear relation with hourly traffic counts due to the complex mechanisms of these emissions. As a consequence, vehicle specific emission factors could only be indirectly estimated with high absolute uncertainties. Since

resuspension of road dust was found to be a relevant contributor to total traffic related PM10, the same applied to PM10. Future work will have to address this problem and define refined models for emission inventories.

- **Particle size of non-exhaust emissions:** The investigated particle size ranged from 0.1 to 10 µm. Mass relevant contributions from abrasion related particles and resuspended road dust to traffic related PM10 were mainly found for particles larger than 1 µm.

- **Exhaust:** Although not in the scope of APART, exhaust emissions were estimated from black carbon measurements to complete the mass balance for traffic related PM10. These emissions were assigned to the particle size range below 1 µm. Trace elements originating from fuel additives (Zn, Ca, S, P) were not specifically identified from the road side measurements, indicating that other emission sources of these elements are more relevant on a mass base. Zn and P show a relative enrichment in the submicron particle fraction which was however not attributed to traffic.

- **Comparison of results to earlier investigations:** At Zürich-Weststrasse, a net decrease in the PM10 fleet emission factors over the last 10 years was observed. In contrast, the fleet emission value determined for Reiden is about equal to a value for a comparable freeway location near Birrhard in 2004. Generally, the emission factors for non-exhaust emissions and total traffic related PM10 strongly depend on the influence of vehicle induced road dust resuspension during the time periods considered in the respective investigations. Therefore, differences rather reflect local conditions at the measurement sites (dirt load on the road surface, condition of pavement) than a reliable emission trend.

- **Comparison of PM10 from non-exhaust sources to general urban PM10:** The locations selected for this study exhibited a different local topography (street canyon at Zürich-Weststrasse versus the open-field situation in Reiden), which strongly influenced the dilution of emitted PM10 and consequently the total local PM10 concentration. Mobile measurements in Zürich showed that the spatial mass concentration variation in the particle size range 0.5 - 1 µm was influenced by local traffic emissions on the days selected for measurements. In contrast, the traffic related emissions in the PM10-PM1 fraction were not dominant compared to emissions from other urban emission sources in this size range (e.g. construction sites). While the coarse mode contribution of the urban background aerosol is dominated by mineral dust elements, the coarse mode of the traffic related emissions contributes trace elements (Fe, Cu, Zn, Mo, Zr, Sn, Sb and Ba) produced by brake wear.

1 Résumé

1.1 Situation initiale

Souvent les émissions de poussière fine du trafic routier ne sont attribuées qu'aux seules émissions dans les gaz d'échappement (suie) et longtemps les particules produites par les processus d'abrasion mécanique ont été négligées. Le projet de recherche ASTRA2000/415 et quelques études plus récentes montrent toutefois que les particules d'abrasion contribuent pour une part importante aux émissions de PM10. Ces particules proviennent de l'abrasion des revêtements routiers, des freins et des pneus ainsi que de la resuspension de la poussière déposée sur les routes. On ne connaît cependant encore que mal la part de chacun de ces processus dans les émissions de PM10. Des données quantitatives sont toutefois indispensables pour la prise de mesures de réduction efficaces des PM10. Il était dès lors intéressant de savoir si les particules d'abrasion proviennent principalement des revêtements routiers ou des véhicules et de connaître pour combien la resuspension contribue à ces émissions.

1.2 Buts du projet, concept de recherche et expériences

1.3 Buts du projet

Le projet APART (particules abrasives du trafic routier) avait pour but principal l'identification et la quantification pour des situations de trafic typiques des émissions de PM10 du trafic routier ne provenant pas des gaz d'échappement.

Buts spécifiques:

- Etablissement d'une base factuelle en vue de la prise de mesures de réduction futures
- Détermination de facteurs d'émission (mg/km/V) pour les éléments traces typiques des émissions du trafic routier.
- Calcul des facteurs d'émission (mg/km/V) pour les sources d'émission de PM10 du trafic routier non attribuables au gaz d'échappement.
- Etude de diverses situations de trafic.
- Distribution des facteurs d'émissions entre véhicules légèrs et poids lourds
- Evaluation spécifique pour chaque site de la contribution des différentes sources de PM10 du trafic routier.

N'étaient pas l'objet du projet:

- L'étude quantitative des sources de PM10 non attribuées au trafic routier.
- Bien que les PM10 provenant des gaz d'échappement aient aussi été mesurées afin d'établir un bilan massique global, cette étude n'avait pas pour objet l'interprétation détaillée des ces émissions.

1.3.1 Concept de recherche

Les sites étudiés dans ce projet ont été choisis avant tout en fonction de leur régime de trafic et de leur environnement local, typiques de nombreuses situations de trafic suisses. A côté de cela, ces sites devaient présenter une infrastructure adéquate pour les mesures et satisfaire toutes les exigences méthodologiques du concept de mesure. Pour différencier la contribution locale du trafic aux PM10 du niveau de fond des PM10, le plus souvent dominant sur les sites de mesure, on a recouru soit à des mesures « sous le vent et au vent», soit à des mesures simultanées directement au bord de la route et sur une station de fond située à proximité (figure 1.1). L'identification des différentes sources de poussière imputables au trafic reposait sur la mesure des signatures élémentaires (fingerprints) spécifiques des sources. Pour cela, on a procédé à la récolte horaire de la poussière fine en 3 classes de taille (2.5-10, 1-2.5 et 0.1-1 µm) à l'aide d'un «Rotating Drum Impactor» (RDI). Les éléments traces contenus dans ces échantillons ont ensuite été analysés par spectrométrie de fluorescence X induite par rayonnement synchrotron (SR-XRF). Ces mesures ont été complétées par d'autres mesures d'une large gamme des propriétés des gaz et des aérosols, de paramètres météorologiques ainsi que par des comptages du trafic des différentes catégories de véhicules. L'identification proprement dite des différentes sources d'émission à partir des données de mesure a été réalisée à l'aide d'une factorisation en matrices positive (FMP), une méthode fréquemment utilisée à cette fin. La dilution atmosphérique locale entre le point d'émission et l'endroit de mesure (distants de 10 à 20 m) a été calculée à partir de mesures de concentration de NO_x et des facteurs d'émission de NO_x connus des différentes situations de trafic. En tenant compte de cette dilution, et avec les fréquences et la composition du trafic mesurées, des modèles statistiques permettent de calculer les facteurs d'émission par véhicule pour les différentes sources d'émission. La dilution atmosphérique étant un paramètre important dans les calculs, seules les périodes temporelles où la contribution locale aux NO_x est élevée sont utilisables pour l'évaluation. (ΔNO_x > 20 µg m^{-3}). Les facteurs d'émission présentés sont en principe indépendants de la position exacte de la station de mesure le long de la route car leur détermination tient compte, tant de manière spatiale que temporelle, de la dilution atmosphérique.

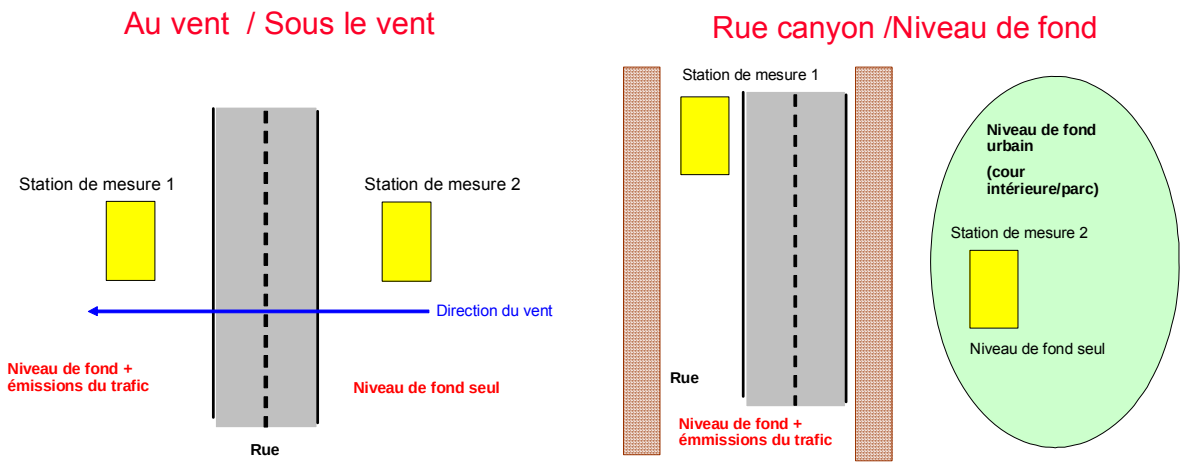

Fig. 1.1: Représentation schématique du concept «au vent-sous le vent» (à gauche) et du concept «bordure de route-fond» (à droite). Hauteur de prélèvement: 4.5 m au-dessus du sol, déterminée pour obtenir de bonnes conditions expérimentales (conduites d'aspiration optimisées, écoulement libre de l'air à proximité, sécurité contre le vandalisme).

1.3.2 Mesures sur les sites Weststrasse et Kaserne à Zurich (février et mars 2007)

Le site de mesure Weststrasse à Zurich, représentatif d'une rue canyon urbaine typique, présente les caractéristiques de trafic suivantes:

- Route principale urbaine avec feux de signalisation et écoulement du trafic fortement perturbé (catégorie IO_HVS3 du manuel des coefficients d'émission[1]). Pas de trafic de transit entre 22.00 et 06.00 heures.
- Revêtement: béton bitumineux AB12, année de pose 1995/96
- Comptage du trafic: véhicules <6m: véhicules légers (dont 9% de véhicules utilitaires légers); véhicules >6m: poids lourds (autocars compris). Le comptage du trafic a été effectué par l'Empa.
- Jours ouvrables: 22'000 véhicules/jour (part du trafic poids lourds 12%)
- Samedis: 21'000 véhicules/jour (part du trafic poids lourds 5%)
- Dimanches: 19'000 véhicules/jour (part du trafic poids lourds 4%)

Pour la quantification de la contribution locale aux émissions de PM10 à la Weststrasse, on a aussi procédé simultanément à des mesures dans la cours de la caserne de Zurich éloignée d'environ 600 m. Ce site est représentatif de la pollution de fond urbaine résultant de toutes les sources de PM10 urbaines et régionales (dues ou non au trafic, voir figure 1.2). La figure 1.3 donne un exemple de courbe temporelle des concentrations de PM10 sur les deux sites de mesure lors d'une situation d'inversion hivernale.

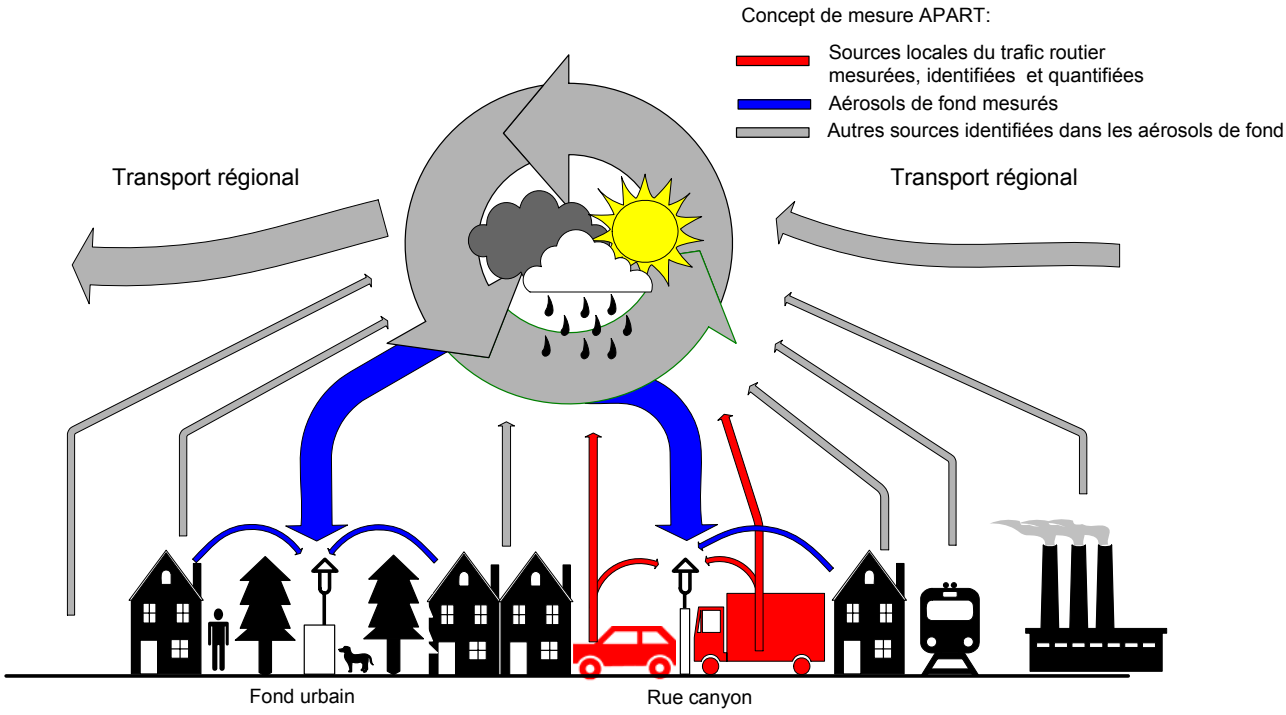

Fig. 1.2: Représentation schématique des principaux flux de polluants dans un milieu urbain. La détermination de la contribution locale du trafic routier demande la prise en compte de toutes les sources locales et régionales (y compris des émissions plus lointaines du trafic), des conditions météorologiques et des transformations chimiques éventuelles des polluants.

[1] Manuel informatisé des coefficients d'émission du trafic routier (MICET, http://www.hbefa.net)

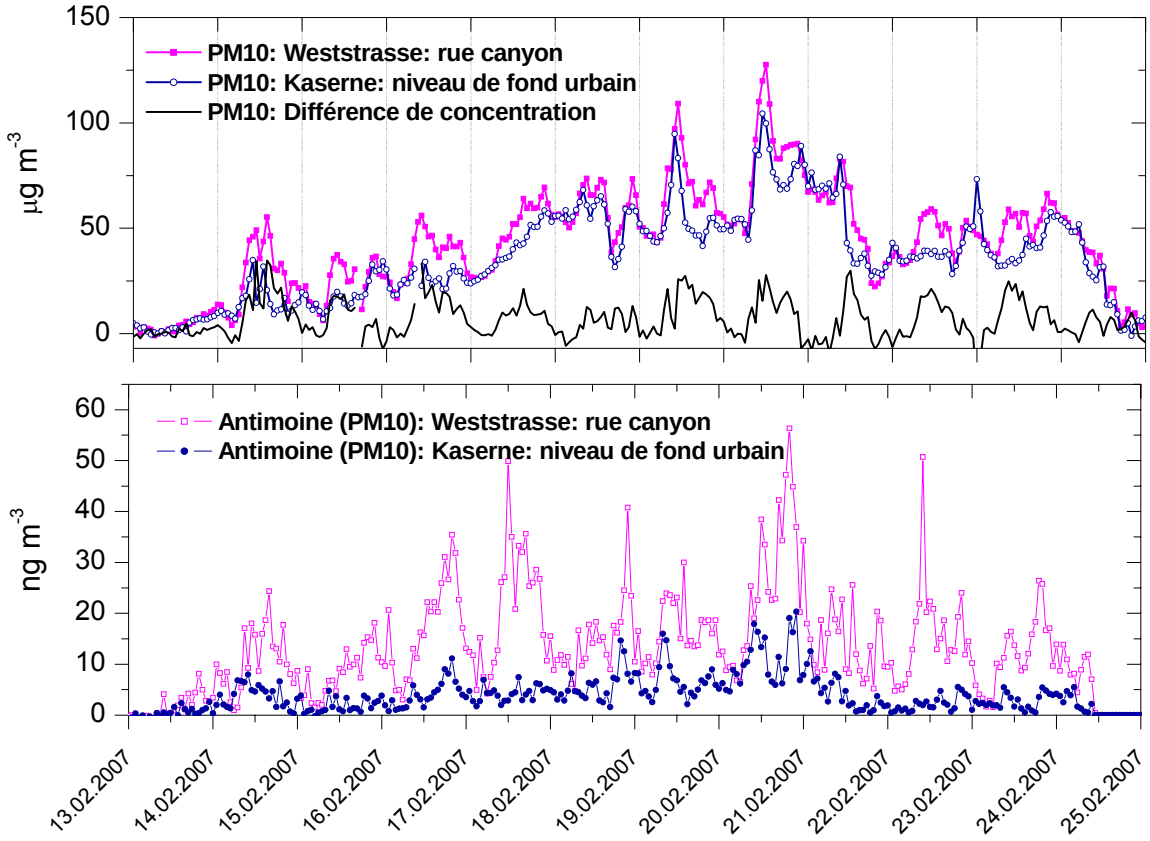

Fig. 1.3: Courbe temporelle des concentrations de PM10 (valeurs horaires) dans la rue canyon de la Weststrasse à Zurich avant, pendant et après une situation météorologique d'inversion. 22.09.09. Diagramme du haut: La ligne noire indique la différence entre la rue canyon et la station de fond et représente ainsi la contribution du trafic local dans la rue canyon à la concentration de PM10. La période représentée sur les graphiques ne correspond qu'à ne partie des données évaluées.

1.3.3 Mesures à Reiden (LU) (juillet – novembre 2007)

Le site de mesure de Reiden sur l'autoroute A2 est représentatif des caractéristiques de trafic suivantes:

- Autoroute avec trafic fluide, limitation de vitesse à 120 km h^{-1} (catégorie du manuel des coefficients d'émission AB_120[2])
- Revêtement: splittmastixasphalt (revêtement compact à faible teneur en vides, comparable au béton bitumineux); direction Lucerne SMA 11 B 80/100+NAF; direction Bâle SMA 11 B55/70+NAF, année de pose: 1999.
- Comptage du trafic: différenciation: véhicules légers (dont 9% de véhicules utilitaires légers) et poids lourds lourdes (autocars compris). Le comptage du trafic a été effectué par l'OFROU (site de mesure lu reiden-s-239)
- Jours ouvrables: 49'000 véhicules/jour (part du trafic poids lourds 16%)
- Samedis: 45'000 véhicules/jour (part du trafic poids lourds 7%)
- Dimanches: 41'000 véhicules/jour (part du trafic poids lourds 2%, autocars compris)

[2] Manuel informatisé des coefficients d'émission du trafic routier (MICET, http://www.hbefa.net)

Les stations de mesure étaient situées de part et d'autre de l'autoroute (figure 1.1, à gauche). Lors des périodes de vent transversal, une des stations se trouvait au vent par rapport à l'autoroute et n'était ainsi exposée qu'aux concentrations de fond. L'autre station, située dans le vent, subissait en plus les émissions de l'autoroute. La figure 1.4 donne les concentrations de PM10 pour les deux côtés de l'autoroute durant une période de mesure.

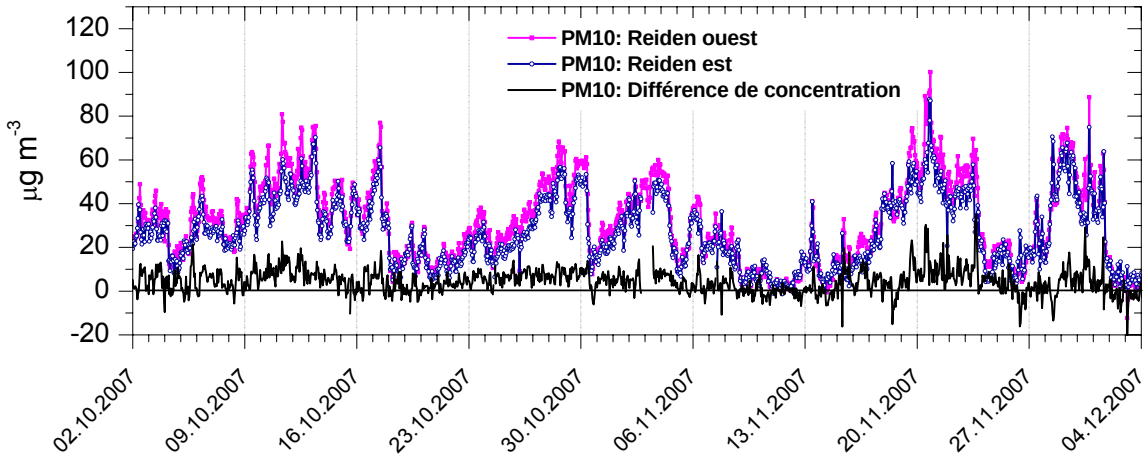

Fig. 1.4: Courbe temporelle des concentrations de PM10 (valeurs horaires) à Reiden. La ligne noire indique la différence entre les deux stations de mesure et représente ainsi la contribution du trafic local sur l'autoroute à la concentration de PM10.

1.3.4 Etudes complémentaires

Les mesures sur place sur les routes ont fourni un vaste fichier de données réalistes bien adapté pour les études statistiques prévues. Toutefois ces mesures sur place ne permettaient pas de répondre à toutes les questions posées dans ce projet et c'est pourquoi on a encore procédé à d'autres études ciblées pour y répondre.

Abrasion du revêtement ou resuspension: La différenciation spécifique des émissions de PM10 dues à de l'abrasion mécanique du revêtement de celles provenant de la resuspension des particules est particulièrement difficile. Même des analyses chimiques détaillées ne permettent pas de distinguer ces sources de particules importantes que sont l'abrasion du revêtement et la resuspension des particules déposées car ces émissions présentent à la fois une composition semblable et une corrélation temporelle élevée. Une possibilité de résoudre ce problème consiste à faire appel à des simulateurs de charge du trafic que les ingénieurs routiers utilisent pour tester la résistance à l'abrasion des revêtements. Dans ce projet, on a utilisé deux types de simulateurs avec différentes charges par essieu pour quantifier les émissions par abrasion. L'installation d'essai a été conçue de manière à permettre la détermination séparée des émissions par abrasion du revêtement de celles dues à la resuspension de la poussière déposée.

- **Poussière déposée sur les routes:** L'analyse de la poussière déposée fournit de bonnes informations sur la composition chimique de la poussière fine remise en suspension par le trafic routier. A l'aide d'un «aspirateur de PM10» spécialement construit à cet effet, on a procédé à Zurich au mois de février 2008 au prélèvement de poussière routière à des fins d'analyse.

- **Mesures mobiles des PM10 et des PM1:** Afin d'étudier la variation spatiale des concentrations des particules de différentes classes granulométriques dans la ville de Zurich, on a effectué au mois de juin 2007 une série de mesures mobiles avec un véhicule de mesure.

1.4 Résultats

1.4.1 Emissions de PM10 du trafic routier à la Weststrasse à Zurich

1.4.1.1 Sources d'importance massique de PM10 du trafic routier

Les données de mesure horaires enregistrées ont permis d'identifier à l'aide du modèle statistique FMP (factorisation en matrices positives) les sources d'importance massique de PM10 attribuables au trafic routier suivantes:

- **Abrasion des freins:** Cette source se caractérise par une signature élémentaire typique de Fe, Cu, Zn, Zr, Mo, Sn, Sb et Ba. Ces éléments sont largement utilisés dans les revêtements de freins et sont émis (probablement sous forme d'oxydes) lors des processus d'abrasion au cours lors du freinage.

- **Gaz d'échappement:** Ces émissions de poussière fine étaient formées principalement de composés inorganiques et organiques du carbone (indiqué sous forme de carbone total provenant du trafic routier) Il n'a pas été possible d'identifier d'éléments traces provenant spécifiquement des additifs des carburants, ce qui constitue un indice que leurs quantités sont faibles ou que d'autres sources de ces éléments sont dominantes.

- **Resuspension de poussière routière par le trafic:** A côté de la poussière minérale typique, on a identifié clairement dans la poussière routière déposée et remise en suspension les contributions caractéristiques de la poussière d'abrasion des freins et des particules émises dans les gaz d'échappement (carbone).

Du fait de l'absence d'éléments indicateurs spécifiques, la méthode d'analyse choisie n'a pas permis de quantifier séparément les contributions éventuelles de l'abrasion des pneus et du revêtement routier:

- **Abrasion du revêtement et resuspension:** Des essais effectués avec des simulateurs de trafic ont montré que les émissions de particules provenant directement de l'abrasion de revêtements routiers intacts n'ont qu'une importance secondaire. Par contre, les revêtements endommagés peuvent provoquer des émissions importantes par abrasion.

- **Abrasion des pneus:** Il n'existe actuellement encore guère d'études fiables sur les émissions dues à l'abrasion des pneus. Des études anciennes, dont certaines attribuent une part atteignant jusqu'à 10% de l'abrasion des pneus aux émissions de PM10, reposent sur des concepts méthodologiques considérés aujourd'hui comme inadéquats. Une étude récente, encore non publiée, portant sur deux routes urbaines à Wiesbaden en Allemagne, qui utilise pour la première fois une méthode très spécifique (analyse des produits de pyrolyse du latex), montre qu'en moyenne la part de l'abrasion des pneus dans les PM10 est de 0.5%. Cette même étude révèle que le pourcentage de 10% supposé par le passé existe bel et bien mais toutefois sous forme de particules plus grossières (>10µm). Ces résultats ont aussi été confirmés par des examens microscopiques. Nos essais avec les simulateurs de trafic ne fournissent pas non plus d'indices d'une contribution importante de l'abrasion des pneus aux PM10. D'une manière générale, peut conclure le modèle FMP ne conduit pas à une erreur significative dans l'attribution statistique aux différentes sources de particules.

1.4.1.2 Facteurs d'émission de PM10 du trafic routier à Zurich-Weststrasse

Le tableau 1.1 et la figure 1.5 donnent les facteurs d'émission de PM10 provenant du trafic routier, avec des valeurs séparées pour les véhicules légers et les poids lourds ainsi que pour une composition moyenne de la flotte de véhicules. Ces facteurs d'émission ont été calculés à partir des concentrations massiques horaires des différentes sources du trafic avec un modèle statistique multilinéaire. La dilution atmosphérique, elle aussi importante pour le calcul, a été déterminée pour chaque heure à partir des concentrations mesurées de NO_x et des facteurs d'émission du NO_x connus pour ce site de mesure. Les nombres de véhicules légers et de poids lourds proviennent de comptages effectués sur le site de mesure.

Les facteurs d'émission de PM10 calculés pour **Zurich-Weststrasse** présentent les caractéristiques suivantes:

- **Emissions de la flotte de véhicules:** Le facteur d'émission moyen de PM10 pour la flotte de véhicules (avec un pourcentage de poids lourds de 10%) était dominé par les émissions des gaz d'échappement (41%), suivies par la resuspension de la poussière routière et de l'abrasion des freins (21%).

- **Facteurs d'émission pour les véhicules légers et les poids lourds:** Les particules des gaz d'échappement (63%) et l'abrasion des freins (33%) étaient les sources d'émission dominantes des **véhicules légers**. En comparaison, les émissions dues à la resuspension par les véhicules légers n'étaient que faible à la Weststrasse (<5%).Par contre les facteurs d'émission absolus des **poids lourds** étaient environ 15 fois plus élevés, alors que leurs facteurs d'émission pour l'abrasion des freins et les émissions à travers les gaz d'échappement étaient elles environ 10 fois plus élevées. Au contraire de ce qui était le cas pour les véhicules légers, la contribution des émissions à travers les gaz d'échappement atteignait 31% et celle de l'abrasion des freins, 16%. A la Weststrasse, soumise à un fort trafic, il semble donc que la poussière routière présente est en majeure partie maintenue en suspension par les turbulences induites par les poids lourds, de sorte qu'il n'en reste que peu pour les véhicules légers. Ceci ne signifie toutefois pas que les véhicules légers ne possèdent pas de potentiel pour la resuspension, comme l'ont démontré clairement les essais effectués avec les simulateurs de trafic.

Alors que l'on a pu mettre en évidence une corrélation élevée de l'abrasion des freins et des émissions des gaz d'échappement avec les fréquences du trafic, la corrélation entre la courbe journalière de la resuspension induite par les véhicules et les fréquences de trafic était nettement plus faible et présentait de plus une plus grande dispersion statistique. Il s'ensuit que les facteurs d'émission pour la resuspension ne peuvent pas être exprimés sous la forme adéquate de mg/km/V, comme cela peut se faire pour l'abrasion des freins et les émissions des gaz d'échappement. Les facteurs d'émission de la resuspension n'ont ainsi pas pu être calculés avec le modèle de régression multilinéaire mais ont été estimés de manière indirecte et sont donc entachés d'une incertitude absolue élevée. Comme la resuspension contribuait ici pour une bonne part aux PM10 attribuables au trafic routier, ceci a aussi influencé, quoique dans une mesure moindre, le calcul des facteurs d'émission totaux des PM10.

Tableau 1.1: Facteurs d'émission de PM10 du trafic routier pour la situation de trafic Zurich-Weststrasse (rue canyon) : VL: véhicules légers, y compris 9% de véhicules utilitaires légers, PL: poids lourds, y compris autocars. Le calcul de l'abrasion des freins repose sur une teneur de 1% en antimoine et de 5% en cuivre de la poussière d'abrasion des freins. Les émissions à travers les gaz d'échappement (définies sous forme de carbone total provenant du trafic) ont été estimées à partir de mesures du «Black-Carbon», par multiplication avec un facteur de 1.45 reposant sur des mesures effectuées en ville de Zurich. Les facteurs d'émission mentionnés se rapportent à 12 jours de mesure en février/mars 2007 (ΔNO_x > 20 µg m^{-3}, uniquement jours sans précipitations). Les facteurs d'émission de NO_x utilisés dans les calculs ont été estimés pour la situation de trafic spécifique à la Weststrasse à partir du manuel des coefficients d'émission[3] (Année: 2007 EF_{NOx} (VL = 286.8 mg km^{-1}, EF_{NOx}(PL) = 10559 mg km^{-1}, NO_x calculé comme NO_2). A titre de comparaison, le tableau indique aussi les facteurs d'émission pour l'abrasion du revêtement et la resuspension établis à partir de mesures réalisées avec des simulateurs de trafic.

Source	**Quantification de la source**	**Calcul du facteur d'émission**	**Zurich-Weststrasse**		
			Flotte 10% PL[*1] mg/km/V	**VL [*2] mg/km/V**	**PL[*2] mg/km/V**
PM10 dues au trafic routier	Mesure (Différence PM10 route-fond)	Estimation à partir du bilan massique	**71**	**24 ± 8**	**498 ± 86**
Abrasion des freins	Modèle statistique[*3]	Régression multilinéaire	**15**	**8 ± 4**	**81 ± 39**
Gaz d'échappement (composés carbonés totaux dus au trafic routier)	Modèle statistique[*3]	Régression multilinéaire	**29**	**15 ± 6**	**155 ± 67**
Resuspension de la poussière routière	Modèle statistique[*3]	Estimation à partir du bilan massique	**27**	**1 ± 11**	**262 ± 115**
Abrasion du revêtement routier	Essais avec simulateurs de trafic		-	(<3)[*a,d]	(7)[*a] (80[*b])
Resuspension[*d]	Essais avec simulateurs de trafic		-	(5)[*d] (76)[*a]	(110)[*c] (660[*b])

[*1] Pourcentage moyen de poids lourds en février/mars 2007 (fortes variations journalières)
[*2] Modèle multilinéaire avec prise en compte individuelle de la composition horaire du trafic
[*3] FMP (factorisation en matrices positives)
[*a] Revêtement de béton bitumineux neuf
[*b] Revêtement de béton bitumineux en mauvais état
[*c] Revêtement de béton bitumineux en bon état
[*d] Revêtement bitumineux poreux neuf

[3] Manuel informatisé des coefficients d'émission du trafic routier (MICET, http://www.hbefa.net))

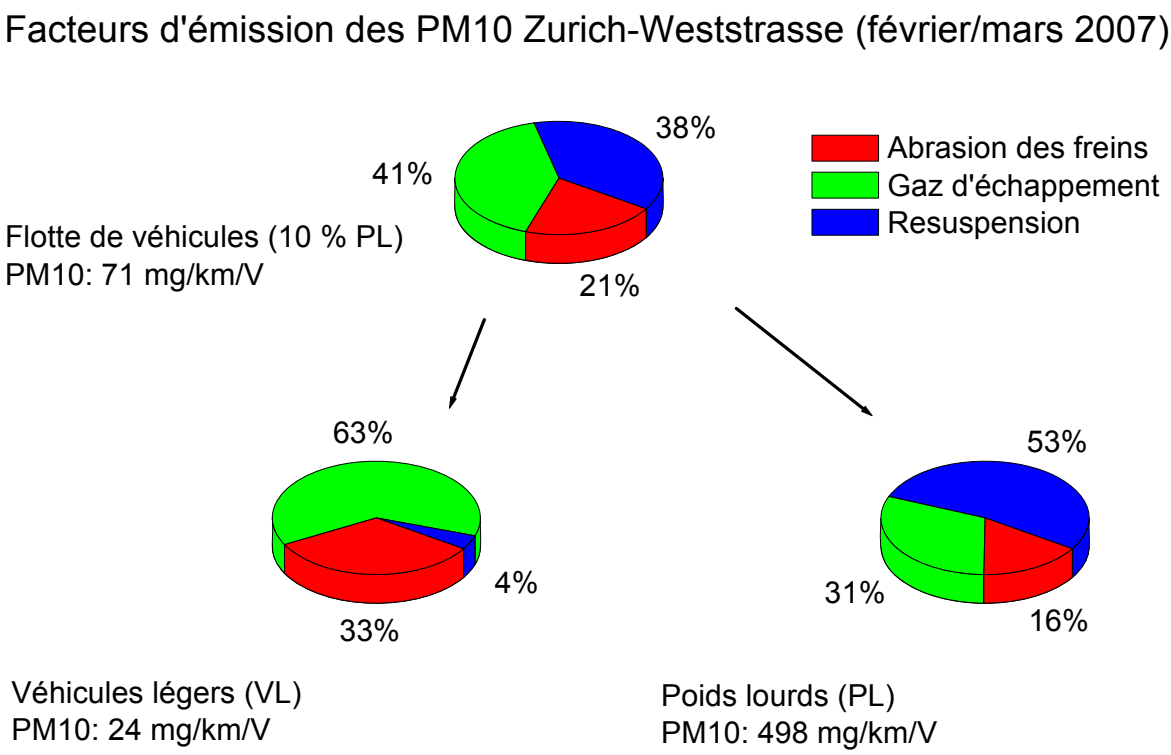

Fig. 1.5: Facteurs d'émissions de PM10 à Zurich-Weststrasse (en pourcentages).

1.4.2 Facteurs d'émission de PM10 du trafic routier à Reiden (LU)

1.4.2.1 Sources d'importance massique de PM10 du trafic routier

Les données de mesure horaires enregistrées ont permis d'identifier à l'aide du modèle statistique FMP (factorisation en matrices positives) les sources d'importance massique de PM10 attribuables au trafic routier suivantes:

- **Abrasion des freins:** Cette source se caractérise par une signature élémentaire typique de Fe, Cu, Zn, Zr, Mo, Sn, Sb et Ba. La signature élémentaire déterminée ici est très semblable à celle trouvée à Zurich-Weststrasse. Ces éléments sont largement utilisés dans les revêtements de freins et sont émis (probablement sous forme d'oxydes) lors des processus d'abrasion au cours du freinage.
- **Gaz d'échappement:** Ces émissions de PM10 étaient principalement formées de composés inorganiques et organiques du carbone (indiqué sous forme de carbone total provenant du trafic routier). Tout comme à la Weststrasse à Zurich, il n'a pas été possible d'identifier d'éléments traces provenant spécifiquement des additifs des carburants, ce qui constitue un indice que leurs quantités sont faibles ou que d'autres sources de ces éléments sont dominantes.

On a identifié une contribution d'éléments minéraux aux émissions du trafic qui signent l'existence d'une resuspension de poussière routière. Il n'a pas été possible de quantifier cette resuspension du fait du manque de données fiables sur la composition chimique de la poussière routière sur ce site de mesure.

1.4.2.2 Facteurs d'émission de PM10 du trafic routier à Reiden

Le tableau 1.2 et la figure 1.6 donnent les facteurs d'émission de PM10 provenant du trafic routier, avec des valeurs séparées pour les véhicules légers et les poids lourds ainsi que pour une composition moyenne de la flotte de véhicules. Ces facteurs d'émission ont été calculés à partir des concentrations massiques horaires des différentes sources du trafic avec un modèle statistique multilinéaire. La dilution atmosphérique, elle aussi importante pour le calcul, a été déterminée pour chaque heure à partir des concentrations mesurées de NO_x et des facteurs d'émission du NO_x connus pour ce site de mesure. Les nombres de véhicules pour les véhicules légers et les poids lourds proviennent de comptages effectués par l'OFROU sur ce tronçon de route.

Les facteurs d'émission de PM10 calculés pour **Reiden** présentent les caractéristiques suivantes:

- **Emissions de la flotte de véhicules:** Le facteur d'émission moyen de PM10 pour la flotte de véhicules (avec un pourcentage de poids lourds de 15%) était formé pour 41% des émissions à travers les gaz d'échappement et d'un très faible pourcentage, soit 3% de l'abrasion des feins. Les 56% restants des émissions dues au trafic routier n'ont pas pu être attribués à une source spécifique. Il doit très probablement s'agir là essentiellement de poussière routière remise en suspension et d'une contribution plus faible de l'abrasion des pneus et du revêtement.

- **Facteurs d'émission pour les véhicules légers et les poids lourds:** Le facteur d'émission total des poids lourds était 5.8 fois plus élevé que celui des véhicules légers. Comme les contributions massiques de l'abrasion des pneus et du carbone attribuable au trafic ont été interpolées à partir de la même source de trafic identifiée à l'aide du modèle FMP, les parts de ces sources sont pratiquement identiques pour les véhicules légers et les poids lourds. Un calcul direct des parts respectives des deux catégories de véhicules à partir des différences de concentrations mesurées était statistiquement eu sûr. Contrairement à Zurich-Weststrasse, à Reiden la poussière remise en suspension est continuellement évacuée latéralement (mesure au vent-sous le vent) et n'est pas maintenue en suspension par un petit nombre de véhicules (PL) provoquant de fortes turbulences. C'est pourquoi ici une part de la resuspension est aussi à mettre au compte des véhicules légers.

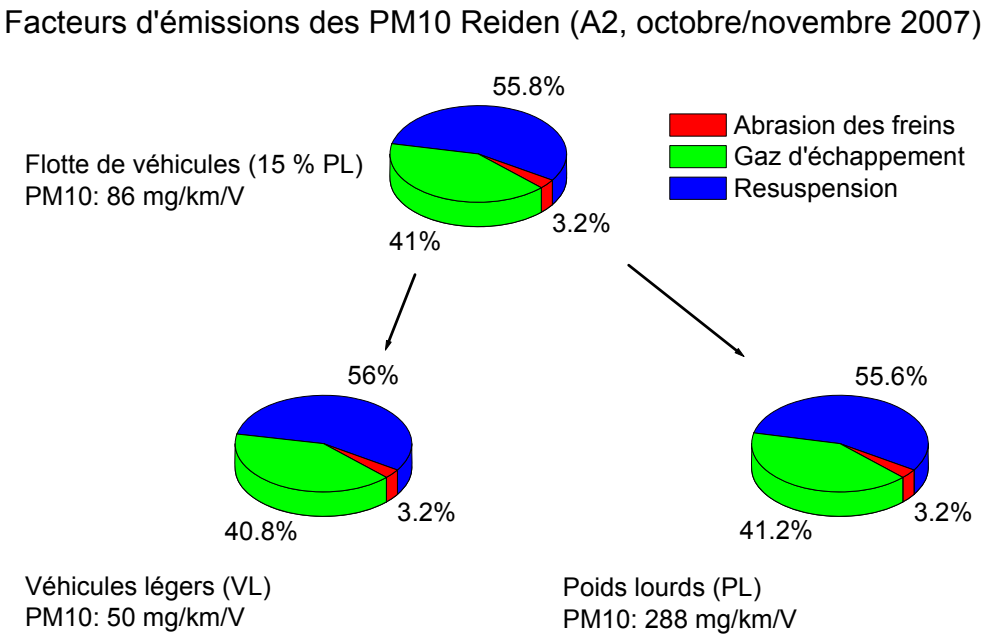

Fig. 1.6: Facteurs d'émissions de PM10 à Reiden LU (en pourcentages).

Tableau 1.2: Facteurs d'émission de PM10 du trafic routier pour la situation de trafic Reiden LU (autoroute): VL: véhicules légers, y compris 15% de véhicules utilitaires légers), PL: poids lourds, y compris autocars. Le calcul de l'abrasion des freins repose sur une teneur de 1% en antimoine et de 5% en cuivre de la poussière d'abrasion des freins. Les émissions à travers les gaz d'échappement (définies sous forme de carbone total provenant du trafic) ont été estimées à partir de mesures du «Black-Carbon», par multiplication avec un facteur de 1.45 reposant sur des mesures effectuées en ville de Zurich (absence de mesures correspondantes dans la région de Reiden) . Les facteurs d'émission mentionnés se rapportent à 4 jours de mesure en octobre/novembre 2007 (ΔNO_x > 20 µg m^{-3}, uniquement jours sans précipitations). Les facteurs d'émission de NO_x utilisés dans les calculs ont été estimés pour la situation de trafic spécifique sur l'autoroute à Reiden à partir du manuel des coefficients d'émission[4] (Année: 2007 EF_{NOx} (VL = 448 mg km^{-1}, EF_{NOx}(PL) = 5421 mg km^{-1}, NO_x calculé comme NO_2).

Source	Quantification de la source	Calcul du facteur d'émission	Reiden (LU) A2		
			Flotte 15% PL[*1] mg/km/V	**VL[*2] mg/km/V**	**PL[*2] mg/km/V**
PM10 dues au trafic routier	Mesure (Différence PM10 route-fond)	Régression multilinéaire	**86**	**50.0 ± 13**	**288 ± 72**
Abrasion des pneus	Modèle statistique[*3]	Régression multilinéaire	**3**	**1.6 ± 1.1**	**9 ± 7**
Gaz d'échappement (composés carbonés totaux dus au trafic routier)	Modèle statistique[*3]	Régression multilinéaire	**35**	**20.4 ± 7**	**119 ± 38**
Reste (resuspension et sources moins importantes[*4])	Estimation à partir du bilan massique		**48**	**28 ± 14**	**160 ± 82**

[*1] Pourcentage moyen de poids lourds en octobre/novembre 2007 (fortes variations journalières)
[*2] Modèle multilinéaire avec prise en compte individuelle de la composition horaire du trafic
[*3] FMP (factorisation en matrices positives)
[*4] Abrasion des pneus et du revêtement

1.4.3 Comparaison des facteurs d'émission avec ceux d'études antérieures

La comparaison des facteurs d'émission de PM10 du trafic routier à Zurich-Weststrasse et à Reiden avec ceux d'études antérieures montre ce qui suit (valeurs, cf. tableaux 1.1 et1.2):

- Le facteur d'émission total de PM10 à Reiden (15% de poids lourds, trafic fluide) était supérieur de 20% à celui de Zurich-Weststrasse (10% de poids lourds, trafic fortement perturbé). Cette différence est due à des émissions plus élevées dans les gaz d'échappement et à une contribution plus importante de la resuspension de la poussière routière.

[4] Manuel informatisé des coefficients d'émission du trafic routier (MICET, http://www.hbefa.net))

- Par contre à Reiden, les facteurs d'émission pour l'abrasion des freins étaient cinq fois plus bas qu'à Zurich-Weststrasse. Comme attendu, ceci est dû à l'influence des activités de freinages fort différentes entre les deux sites de mesure.

Le tableau 1.3 compare les facteurs d'émission obtenus dans la présente étude avec ceux d'études antérieures sur des sites comparables.

- Tendance temporelle: A Zurich-Weststrasse on observe une tendance à la baisse des facteurs d'émission de la flotte de véhicules. Par contre à Reiden, ces facteurs d'émission sont demeurés à peu près identiques en comparaison de ceux obtenus à Birrhard (2004, situation de trafic comparable).

- Emissions des gaz d'échappement: En tenant compte des incertitudes de mesure, les valeurs estimées des émissions des gaz d'échappement sont consistantes avec celles des inventaires des émissions.

- Emissions non attribuables aux gaz d'échappement et émissions totales de PM10 du trafic routier: Ces facteurs d'émission dépendent très fortement de la resuspension de poussière provoquée par les véhicules au moment des mesures. Les différences de ces facteurs reflètent ainsi davantage les conditions locales sur le site de mesure (degré de salissure de la route, état du revêtement) qu'une tendance temporelle des émissions.

Tableau 1.3: Facteurs d'émission de PM10 attribuables et non attribuables aux gaz d'échappement à Zurich-Weststrasse, Zurich-Schimmelstrasse (route à fort trafic, située à 300 m de Zurich-Weststrasse), Reiden (LU, route nationale A2) et Birrhard (AG, route nationale A1).

Paramètre	**Etude**	**Lieu**	**Année**	**Flotte (mg km^{-1})**	**VL (mg km^{-1})**	**PL (mg km^{-1})**
PM10	NFP41[*1]	Zurich-Schimmelstrasse	1998/99	153	59	1420
	OFEV/OFROU 2004[*2]	Zurich-Weststrasse	2002/03	104	49	703
	APART	**Zurich-Weststrasse**	**2007**	**71**	**23.7 ± 7.5**	**498 ± 86**
Emissions des gaz d'échappement	NFP41[*1]	Zurich-Schimmelstrasse	1998/99	48	14	507
	OFEV/OFROU 2003[*2]	Zurich-Weststrasse	2002/03	29	10	320
	MICET [*3]	IO_HVS3[*4]	2002/03	-	11	342
	APART	**Zurich-Weststrasse**	**2007**	**29**	**14.9 ± 6.3**	**155 ± 67**
	MICET [*3]	IO_HVS3[*4]	2007	-	12	286
Emissions non attribuables aux gaz d'échappement (y compris resuspension)	NFP41[*1]	Zurich-Schimmelstrasse	1998/99	105	45	913
	OFEV/OFROU 2004[*2]	Zurich-Weststrasse	2002/03	75	39	383
	APART	**Zurich-Weststrasse**	**2007**	**42**	**9 ± 11**	**343 ± 122**

Tableau 1.3 (suite)

Paramètre	Etude	Lieu	Année	Flotte (mg km^{-1})	VL (mg km^{-1})	PL (mg km^{-1})
PM10	OFEV/OFROU 2003[*2]	Birrhard	2003	83	63	267
	APART	**Reiden**	**2007**	**86**	**50.0 ± 12.6**	**288.0 ± 71.9**
Emissions des gaz d'échappement	OFEV/OFROU 2003[*2]	Birrhard	2003	33	16	193
	MICET [*3]	AB_120[*5]	2002/03	-	17	176
	APART	**Reiden**	**2007**	**35**	**20.4 ± 6.6**	**119 ± 38**
	MICET [*3]	AB_120[*5]	2007	-	16	111
Emissions non attribuables aux gaz d'échappement (y compris resuspension	OFEV/OFROU 2003[*2]	Birrhard	2003	50	47	74
	APART	**Reiden**	**2007**	**51**	**30 ± 14**	**169 ± 82**

[*1] Hüglin, C. (2000). Contribution du trafic routier aux émissions de PM10 et de PM2.5; composition chimique de la poussière fine et attribution aux sources avec un modèle de récepteur (Anteil des Strassenverkehrs an den PM10- und PM2.5-Immissionen; Chemische Zusammensetzung des Feinstaubs und Quellenzuordnung mit einem Rezeptormodell), programme national de recherche PNR41, Transport et environnement, rapport C4, Berne.

[*2] Vérification des facteurs d'émissions de PM10 de la circulation routière (Verifikation von PM10-Emissionsfaktoren des Strassenverkehrs), mandat de recherche AFROU/OFEV 2000/415(52/00), Berne.

[*3] Sur la base de: Manuel informatique des coefficients d'émission du trafic routier, Version 2.1 / 2004, INFRAS sur mandat de l'OFROU, Berne.

[*4] IO_HVS3: Route principale urbaine avec feux de signalisation et écoulement du trafic fortement perturbé.

[*5] Autoroute avec trafic fluide à 120 km h^{-1}.

1.4.4 Facteurs d'émission des éléments traces associés à l'abrasion des feins

Les particules identifiées à Zurich-Weststrasse et à Reiden comme provenant de l'abrasion des freins présentaient une signature élémentaire typique de Fe, Cu, Zn, Zr, Mo, Sn, Sb et Ba qui concorde bien avec celle déterminée dans d'autres études, cela bien que la composition élémentaire des différents types de revêtements de freins puisse varier fortement. Par contre, on a trouvé des concentrations de plomb nettement plus basses que celles mentionnées en partie dans des études plus anciennes, signe que cet élément indésirable a depuis lors été largement remplacé par d'autres dans les revêtements de freins. Les figures 1.7 et 1.8 donnent les facteurs d'émission d'éléments typiques des particules d'abrasion des revêtements de freins. Ce sont les éléments Fe, Cu et Ba qui présentent les valeurs les plus élevées, suivis de Zr, Mo, Sn et Sb avec des valeurs légèrement plus basses. Le rapport entre les facteurs d'émission des poids lourds et ceux des véhicules légers était en moyenne de 9 pour les particules de 2.5 – 10 µm, de quatre pour celles de 1 - 2.5 µm et de quatorze pour celles de 0.1 - 1 µm.

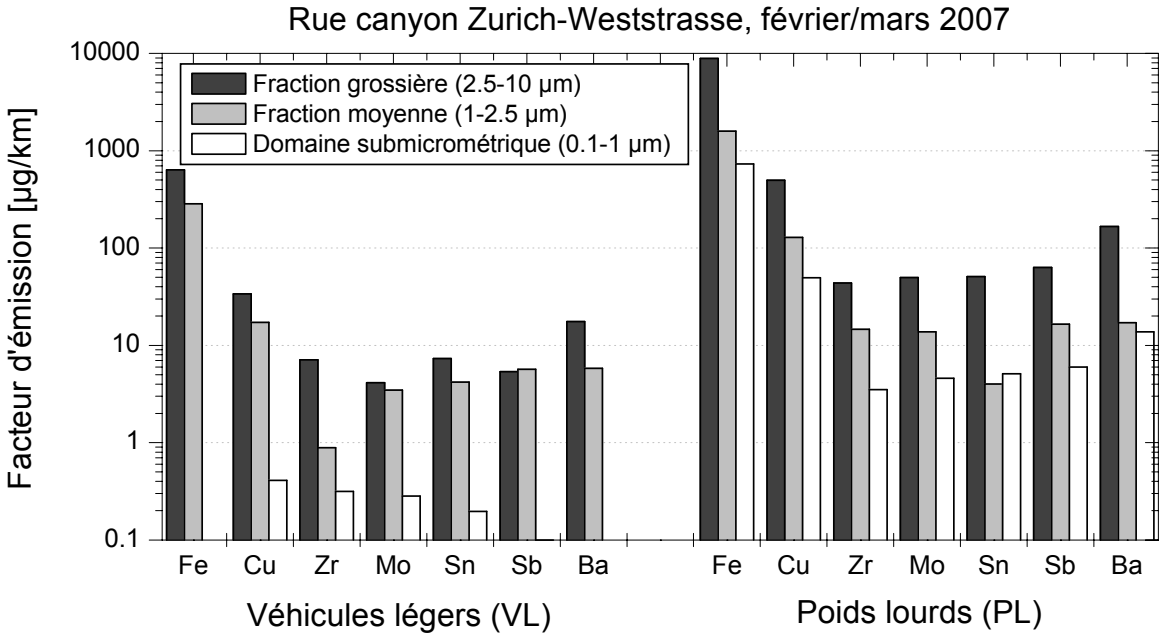

Fig. 1.7: Facteurs d'émission (FE) pour les véhicules légers (VL) et les poids lourds (PL) à Zurich-Weststrasse (rue canyon). Le calcul repose sur 209 valeurs horaires (~ 9 jours, ΔNO_x > 20 µg m^{-3}, uniquement jours sans précipitations). On n'a pas calculé de facteurs d'émission pour Zn car cet élément était aussi fortement influencé par d'autres sources étrangères au trafic.

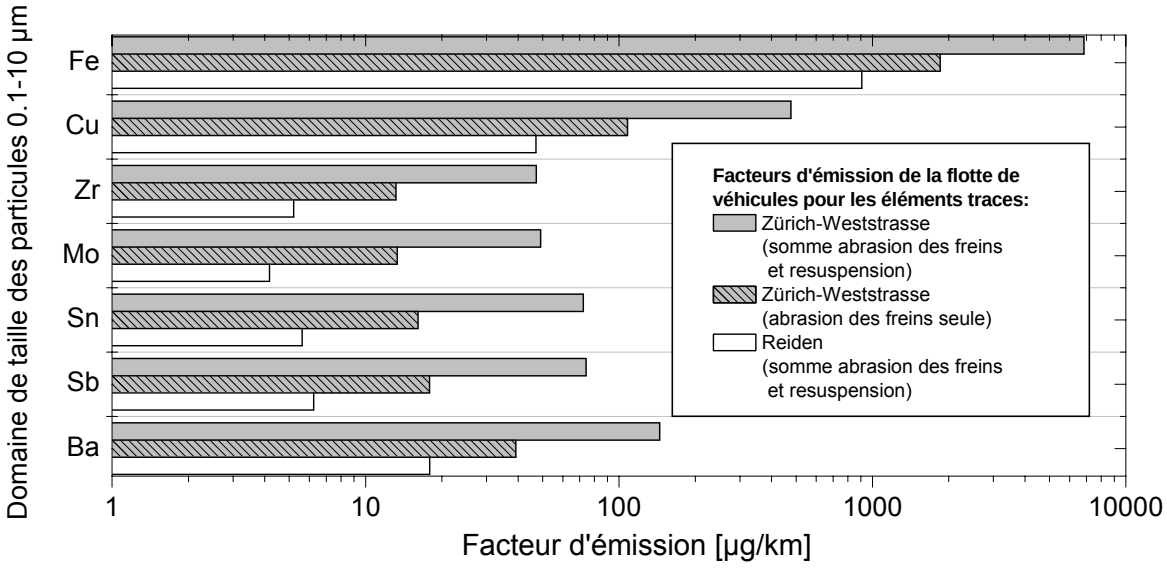

Fig. 1.8: Facteurs d'émission totaux de la flotte de véhicules (domaine de taille des particules 0.1 - 10 µm) à Zurich-Weststrasse (10% PL) et Reiden (15% PL) pour les éléments provenant de l'abrasion des freins. Les valeurs pour Zurich-Weststrasse reposent sur les données de mesure de février/mars 2007 (9 jours, uniquement périodes sans précipitations) et pour Reiden, sur celles d'octobre 2007 (4 jours, uniquement périodes sans précipitations).

1.4.5 Distribution granulométrique des particules d'abrasion

Abrasion des freins: Pour les véhicules légers, les particules d'abrasion des freins se situaient principalement dans le domaine de taille de 1 – 10 µm, alors que la fraction inférieure à 1 µm était très faible. Pour les poids lourds la distribution granulométrique était encore plus nettement décalée vers les particules grossières (2.5-10 µm). Les causes de cette disparité sont difficiles à élucider, mais elles pourraient être en relation avec les différences de construction et de fonctionnement entre les systèmes de freinage des véhicules légers et ceux des poids lourds.

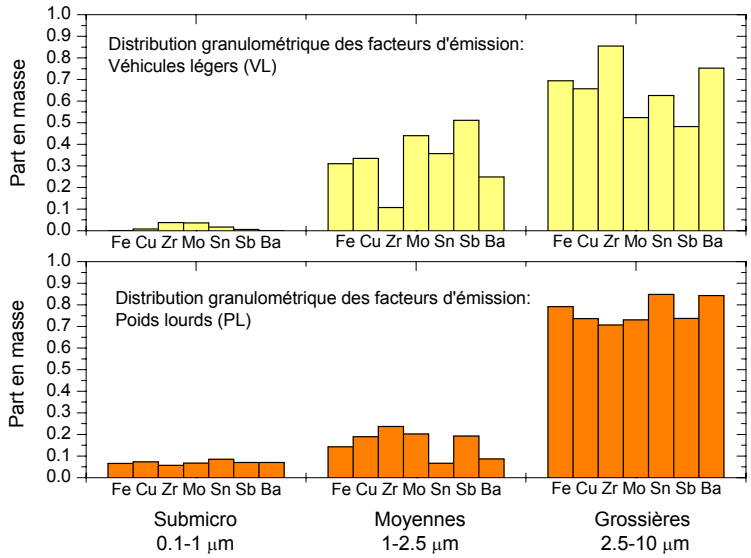

Fig. 1.9 Distribution des facteurs d'émission des éléments traces des particules d'abrasion pour les véhicules légers et les poids lourds lors d'un trafic perturbé dans la rue canyon de Zurich-Weststrasse.

Abrasion du revêtement routier et resuspension: Les essais réalisés avec des simulateurs de trafic ont montré que les particules provenant de l'abrasion du revêtement routier et de la resuspension se trouvaient elles aussi principalement dans la fraction grossière (2.5-10 µm), (figure 10).

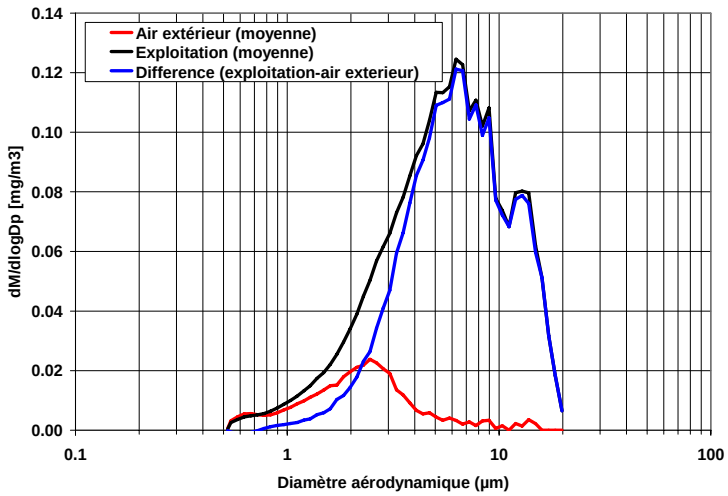

Fig. 1.10: Distribution granulométrique typique lors d'un essai avec un simulateur de trafic pour une période avec dominance de l'abrasion du revêtement routier (resuspension négligeable). On constate un net décalage de la courbe granulométrique vers la fraction grossière par rapport à celle des particules de l'air ambiant.

1.4.6 Distribution spatiale et durée de vie des PM10 urbaines

1.4.6.1 Courbes journalières des émissions de polluants à Zurich-Weststrasse

Afin d'obtenir une représentation systématique des variations temporelles des émissions locales dans la rue canyon de Zurich-Weststrasse, on a représenté sur la figure 1.11, en échelle normalisée, les courbes journalières des fréquences du trafic et celles des émissions locales corrigées en fonction des émissions de fond de PM10, NOx, CO_2, suie dans PM1 (exprimée sous forme de «Black Carbon, BC) ainsi que celles de l'antimoine et du silicium dans les différentes fractions granulométriques.

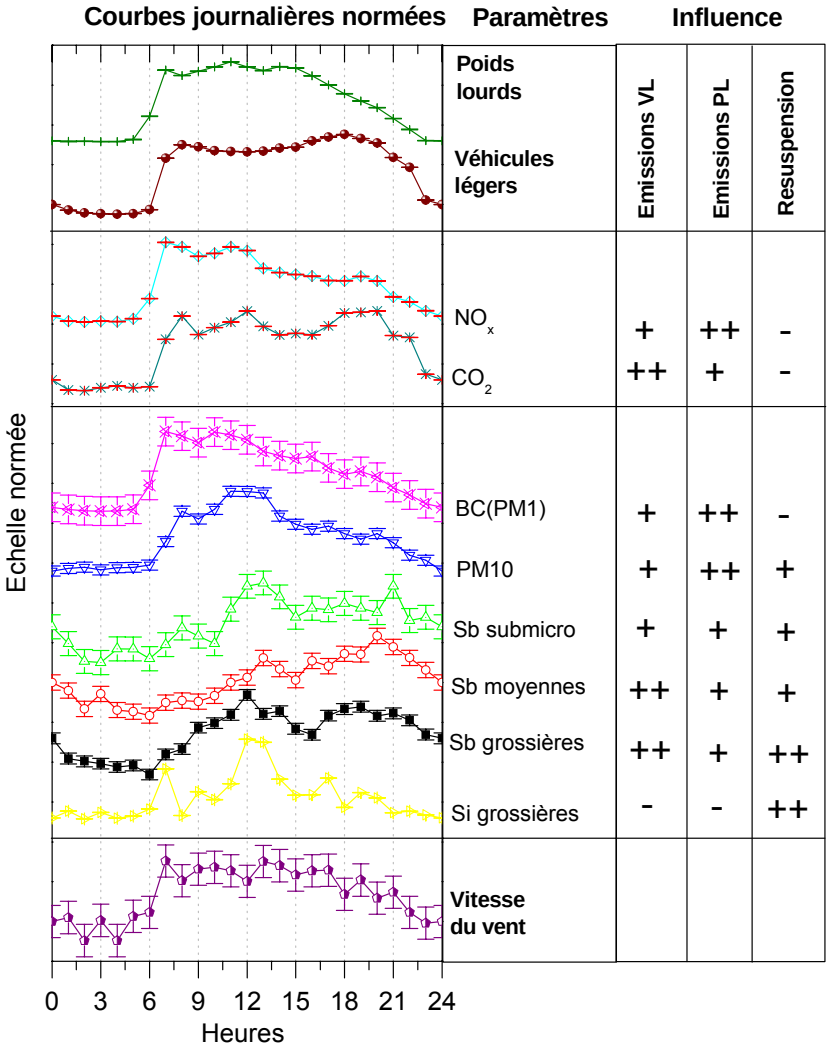

Fig. 1.11: Courbes journalières corrigées en fonction des émissions de fond (Zurich-Westatrasse, 15 jours en février/mars 2007, uniquement jours de semaine sans précipitations). Toutes les courbes sont normalisées à des amplitudes comparables. Les barres d'erreur indiquent l'incertitude de mesure. Les conditions météorologiques étaient semblables pour tous les jour considérés (situation d'inversion hivernale).

Les courbes journalières de NOx et BC(PM1) sont étroitement corrélées à celle des fréquences du trafic des poids lourds. Ceci montre que le trafic des poids lourds exerce une influence dominante sur ces émissions. La courbe du CO_2 est par contre mieux corrélée à celle des fréquences du trafic des véhicules légers, qui sont ainsi les principaux responsables des émissions de ce polluant. La diminution générale des concentrations entre 14 et 16 heures constatée pour les composants gazeux est à mettre essentiellement au compte des conditions météorologiques.

Les courbes de PM10 et de l'antimoine ne sont par contre pas corrélées avec celles des fréquences du trafic mais présentent un maximum marqué vers midi. Une explication possible à ce maximum à la mi-journée est l'influence de la vitesse du vent et la resuspension de poussière routière qui en découle, mais aussi un enrichissement provenant des émissions fraîches dans la rue canyon dans le cours de la journée. Le silicium dans la fraction grossière, qui est un bon indicateur de la resuspension, est effectivement étroitement corrélé avec la vitesse du vent. L'augmentation marquée des vitesses du vent avec l'accroissement du trafic montre clairement qu'ici les mouvements de l'air n'ont pas qu'une origine météorologique mais sont aussi pour une grande part provoqués par le trafic et qu'ainsi la resuspension est clairement à attribuer au trafic et non pas aux mouvements naturels de l'air.

Malgré l'importance décrite ci-dessus d'une resuspension non strictement proportionnelle au trafic et d'un enrichissement, l'influence directe du trafic sur les courbes journalières est nettement visible. Plus spécialement l'après-midi et le soir, les courbes journalières de PM10 et de l'antimoine sont nettement corrélées à celles des fréquences du trafic des véhicules légers.

1.4.6.2 Concentrations massiques des PM obtenues lors de mesures mobiles sur les routes

Les mesures mobiles des PM réalisées à Zurich ont montré l'existence de variations spatiales et temporelles extrêmement complexes (figure 1.12). Pour les PM1, on décèle une corrélation visible avec les fréquences du trafic qui est le signe d'une émission de particules primaires issues de la combustion. Les particules >1 µm présentent elles aussi encore une certaine corrélation avec les densités du trafic et peuvent ainsi être attribuées, du moins en partie, aux processus d'abrasion du trafic routier et à la resuspension de poussière routière. Toutefois leurs signatures spatiales et temporelles sont inhomogènes de sorte qu'il faut aussi considérer l'influence d'autres particules. C'est ainsi que la variabilité élevée des concentrations à la Badenerstrasse est à attribuer à l'influence du chantier du stade du Letzigrund avec le trafic de chantier élevé qu'il implique.

1.4.6.3 Composition de la poussière routière déposée

A Zurich, la poussière routière se compose principalement de silicates et de carbonates provenant de sources minérales naturelles ainsi que de poussière provenant de chantiers et du trafic routier. La figure 1.13 montre le profil chimique (quantités relatives en %) des échantillons analysés. A côté de cela, on a formé un échantillon moyen à partir de tous les échantillons de poussière routière récoltés au mois de février 2008 dont l'analyse montre que la poussière sont formés pour 35% de silicates (exprimés sous forme de SiO_2) et pour 35% aussi, de carbone organique et de carbone élémentaire (OM et CE).

.

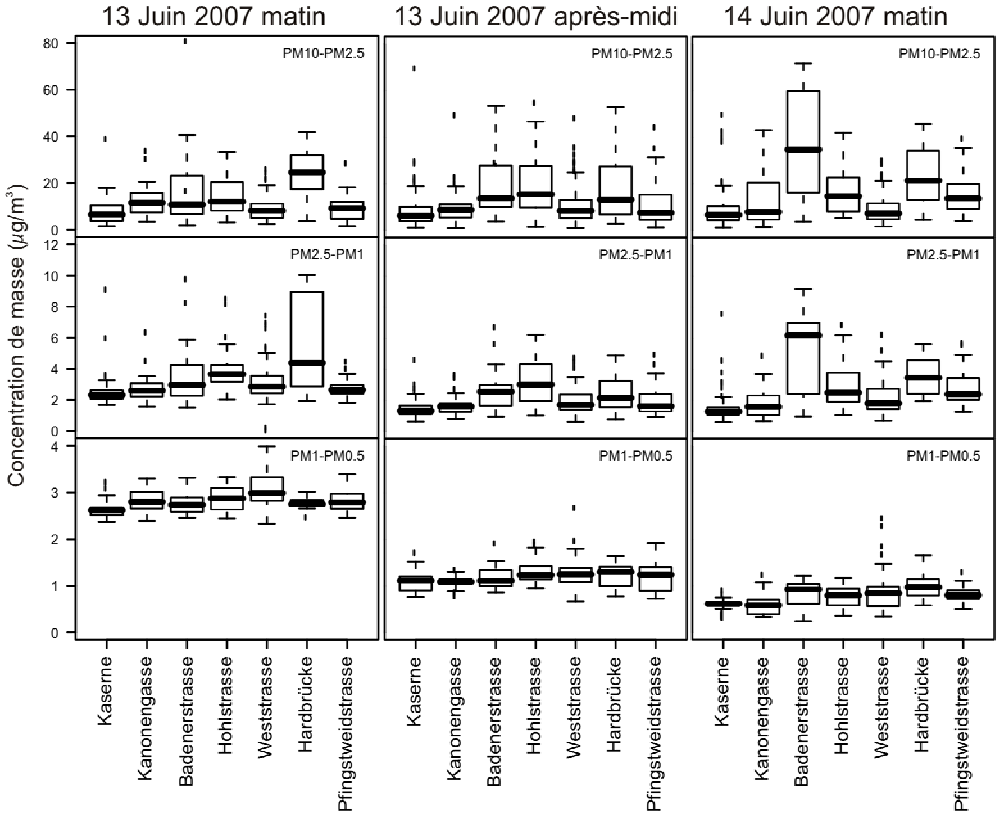

Fig. 1.12: Variabilité spatiale des concentrations de PM10 en µm m^{-3} à Zurich, mesurées avec un véhicule de mesure mobile. Les lieux de mesure sont classés dans l'ordre croissant de la densité de trafic moyenne (Kaserne: cour intérieure sans trafic). La représentation ne tient pas compte de 6 valeurs extrêmes enregistrées le 13 juin 2007.

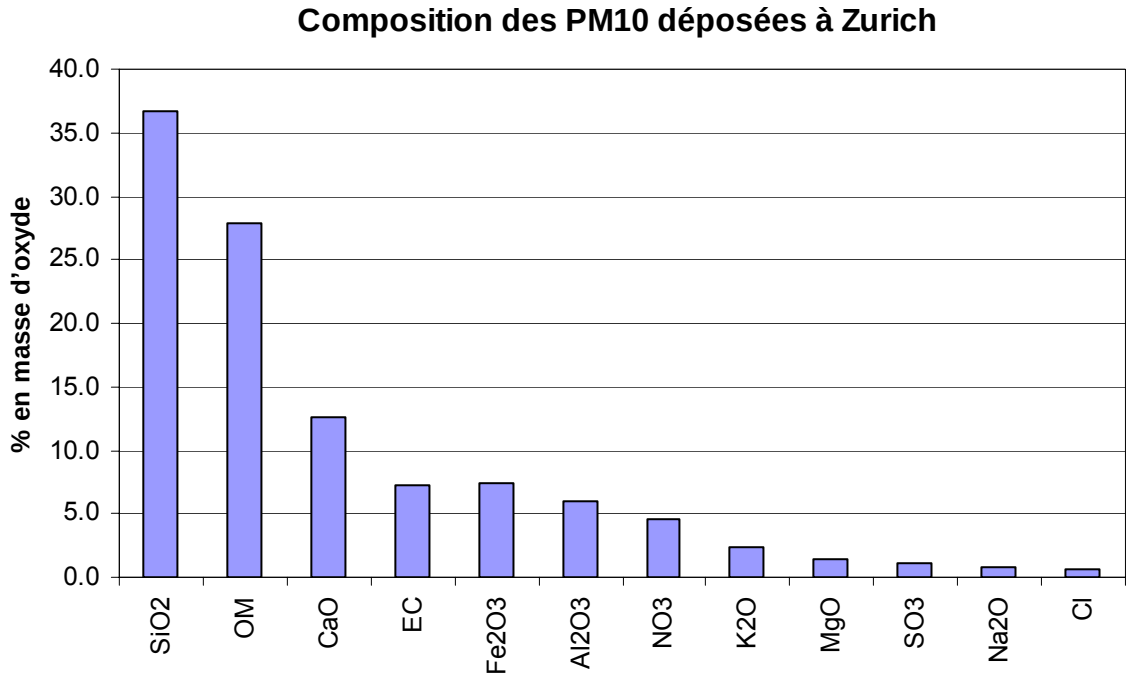

Fig. 1.13: Composants principaux des PM10 déposées dans différentes rues de Zurich. Les éléments sont indiqués sous forme d'oxydes. OM = matériel organique, EC = carbone élémentaire.

1.5 Conclusions et perspectives

Les conclusions que l'on peut tirer de l'ensemble des résultats, qui peuvent aussi servir de points de référence pour la prise de mesures de réduction des émissions de poussière fine provoquées par le trafic routier, sont les suivantes:

- **Contribution massique des sources du trafic routier aux PM10:** Durant les périodes sur lesquelles s'est déroulée cette étude à Zurich-Weststrasse (février/mars 2007) et le long de l'autoroute A2 à Reiden (octobre/novembre 2007), les sources directes de particules d'abrasion et la resuspension des poussière routière contribuaient pour environ 60% aux émissions totales de PM10 attribuables au trafic routier.
- **Abrasion des freins:** Les particules d'abrasion des freins présentent une signature élémentaire caractéristique de Fe, Cu, Zn, Mo, Zr, Sn, Sb et Ba qui concorde bien avec celle déterminée dans d'autres études. Par contre la composition élémentaire des revêtements de freins peut varier fortement. Au contraire de ce qui avait été constaté dans des études antérieures, les teneurs en plomb relevées ici sont nettement inférieures, signe que cet élément indésirable a depuis lors été en majeure partie remplacé par d'autres dans les revêtements de freins. Du fait du trafic très perturbé régnant à Zurich-Weststrasse, les émissions dues à l'abrasion des freins représentaient environ 20% (15 mg/km/V) des émissions totales de PM10. Par contre, la contribution de l'abrasion des freins le long de l'autoroute à Reiden, où le trafic était fluide, était nettement moins élevée (3%, 3 mg/km/V). Sur ces deux sites, les émissions dues à l'abrasion des freins des poids lourds étaient environ 10 fois plus élevées que celles des véhicules légers.
- **Resuspension de poussière fine induite par le trafic routier:** D'une manière générale la resuspension de la poussière routière dépend fortement de la masse de poussière présente sur la surface de la route et elle est donc influencée par le degré de salissure de cette dernière. En février/mars 2007 dans la rue canyon de Zurich-Weststrasse jusqu'à 40% des émissions de PM10 du trafic routier étaient attribuables à la resuspension. Les estimations de la resuspension le long de l'autoroute à Reiden aboutissent à une part de plus de 50%. Dans la rue canyon de Zurich-Weststrasse, ce sont essentiellement les turbulences provoquées par les poids lourds qui remettent en suspension la poussière disponible de sorte que, dans cette situation, l'influence des véhicules légers est faible. Ceci ne permet toutefois pas de déduire que les émissions dues à la resuspension de poussière par les véhicules légers sont d'une manière générale insignifiantes. Dans les situations de trafic sans ou avec ou avec un faible nombre de poids lourds, les véhicules légers provoqueront eux aussi une resuspension de la poussière routière.
- **Abrasion du revêtement routier et des pneus**: Pas plus à Zurich-Weststrasse qu'à Reiden il n'a été possible de déterminer directement les contributions de l'abrasion du revêtement routier et des pneus à la charge de PM10. Des essais spécifiques réalisés avec des simulateurs de trafic ont montré que sur les revêtements routiers intacts l'abrasion de ces derniers est très faible par rapport à la resuspension. Par contre, les revêtements routiers endommagés présentaient des émissions par abrasion nettement plus élevées. Des études supplémentaires seraient nécessaires pour quantifier l'abrasion des types de revêtements courants dans des conditions de trafic réelles. Notre étude ne fournit pas de résultats spécifiques sur les émissions de particules dues à l'abrasion des pneus. D'autres études montrent cependant que seule la fraction granulométrique supérieure à 10 µm a une importance massique. Certains produits de la pyrolyse du caoutchouc pourraient servir d'indicateurs pour des études complémentaires sur l'abrasion des pneus ainsi que le montre une étude allemande non encore publiée.

- **Facteurs d'émission:** Les facteurs d'émission présentés sont en principe indépendants de la position exacte de la station de mesure le long de la route car leur détermination tient compte, tant de manière spatiale que temporelle, de la dilution atmosphérique. Toutefois les émissions provenant de la resuspension n'ont souvent pas pu être exprimées de manière adéquate en mg/km/V car il n'existe pas de relation strictement linéaire entre ces émissions et les fréquences de trafic. Ceci est dû à la grande variété des facteurs qui exercent une influence sur la resuspension. C'est là aussi la raison pour laquelle les facteurs d'émission spécifiques de la resuspension n'ont pu être qu'estimé indirectement avec l'incertitude plus élevée qui en découle. La resuspension contribuant pour une grande part aux émissions de PM10 du trafic routier, ceci s'applique aussi aux PM10. Des études futures devraient s'attaquer à ce problème pour développer des concepts appropriés pour la description systématique des émissions provenant de la resuspension.
- **Domaine de taille des particules du trafic routier ne provenant pas des gaz d'échappement:** Cette étude était consacrée aux particules du domaine de taille de 0.1 à 10 µm. Les contributions massiques importantes des émissions par abrasion et resuspension se situaient en majeure partie dans le domaine de taille supérieur à 1 µm.
- **Emissions des gaz d'échappement:** Bien qu'elles ne fussent en principe pas l'objet de cette étude, les émissions de particules des gaz d'échappement ont été estimées à partir de mesures du «Black Carbon» pour l'établissement du bilan massique des PM10. Les particules de ces émissions se situent dans le domaine de tailles inférieures à 1 µm. Dans cette campagne de mesure, il n'a pas été possible d'identifier de manière spécifique les éléments traces provenant des additifs des carburants (Zn, Ca, S, P), ce qui indique que d'autres sources de ces éléments sont massiquement plus importantes. On a certes décelé un enrichissement relatif en Zn et P dans les particules du domaine de tailles inférieures à 1 µm, mais cet enrichissement n'a pas pu être attribué de manière spécifique au trafic routier.
- **Comparaison avec des études antérieures**: La quantification des émissions des différents processus d'abrasion a exigé une somme de travail expérimental bien supéreure à celle de l'étude antérieure ASTRA2000/415. A Zurich-Weststrasse on a observé une tendance à la baisse des facteurs d'émissions de PM10 de la flotte de véhicules au cours de ces dix dernières années. Par contre, à Reiden, les facteurs d'émission de PM10 sont restés à peu près inchangés par rapport à une situation de trafic semblable à Birrhard (2004). Les facteurs d'émission pour les émissions ne provenant pas des gaz d'échappement et les émissions totales de PM10 du trafic routier dépendent fortement de la resuspension de la poussière routière provoquée par les véhicules lors des mesures. Les différences de ces facteur reflètent ainsi davantage les conditions locales régnant sur les sites de mesure (salissure de la route, état du revêtement) qu'une tendance temporelle des émissions.
- **Comparaison entre PM10 des sources du trafic routier autres que celles des gaz d'échappement et PM10 urbaines**: Les deux sites de mesure choisis pour cette étude différaient fortement par leur situation topographique (rue canyon et autoroute en terrain découvert), ce qui exerçait une forte influence sur la dilution des PM10 émises et ainsi aussi sur leurs concentrations locales. Les mesures mobiles réalisées à Zurich ont montré que, pour un jour donné, les variations spatiales des concentrations de PM1 étaient déterminées par les émissions locales du trafic. Par contre, le trafic local n'exerçait pas d'action dominante sur les variations spatiales de la fraction des particules de taille supérieure à 1 µm. Ces variations étaient davantage influencées par d'autres sources telles que les chantiers. Alors que la fraction grossière de l'aérosol de fond urbain est dominée avant tout par les éléments minéraux, la fraction grossière émise par le trafic routier renferme encore en plus des quantités significatives d'éléments traces (Fe, Cu, Zn, Mo, Zr, Sn, Sb et Ba) qui proviennent principalement de l'abrasion des freins.

2 Conceptual Outline and Methodological Overview

2.1 State of Research

Particle emissions of road traffic are generally associated with fresh exhaust emissions only. However, recent studies identified a clear contribution of non-exhaust emissions to the traffic related PM10 load of the ambient air. These emissions consist of particles produced by abrasion from brakes, road wear, tire wear, as well as vehicle induced resuspension of deposited road dust. For many urban environments, quantitative information about the contributions of the individual abrasion processes is still scarce.

A main difficulty is the reliable identification of the individual non-exhaust sources based on source-specific tracers (see recent review by Thorpe and Harrison, 2008). In an increasing number of studies, airborne antimony and other trace elements in urban areas are being correlated with road traffic and more specifically with emissions emerging from brake wear (Furusjo et al. 2007; Furuta et al. 2005; Garg et al. 2000; Gomez et al. 2005; Grieshop et al. 2005; Hjortenkrans et al. 2007; Johansson 2008; Lough et al. 2005; Sternbeck et al. 2002; von Uexkull et al. 2005; Weckwerth 2001). Besides steel as brake pad support material, the agents present in brake linings usually consist of Cu, Mo, Sn, Sb and Ba. Additionally, Zn has been reported to be further constituents of brake wear, although it is a less specific markers for brake wear than the other elements (Johansson 2008). Lead (Pb) has largely been replaced in modern brake lining. In laboratory experiments, abraded brake wear particles showed a size distribution with >90% within PM10 (Furuta et al. 2005; von Uexkull et al. 2005). In contrast to brake wear, the experimental identification of tire wear emissions is more difficult. Zinc or black carbon have been used as tracers for tire wear (Adachi and Tainosho 2004; Camatini et al. 2001; Councell et al. 2004), these species are however ubiquitous in urban ambient air due to their emission by various other sources.

Due to their similar chemical composition, emissions from road wear and resuspended road dust are not easy to separate from field data and thus have been examined with controlled laboratory-type experiments. In Scandinavian countries, the use of studded tires has been shown to cause relevant road wear emissions. Quantified PM10 emissions by road wear and/or resuspension of road dust are reported for a number of locations (Hussein et al. 2008; Ketzel et al. 2007; Ropertz and Suritsch 2006) or controlled laboratory experiments (Gustafsson et al. 2009; Kupiainen et al. 2003; Kupiainen et al. 2005).

For effective PM10 reduction scenarios it is of particular interest to know whether road wear, resuspension or fresh abrasion from vehicles is dominating the non-exhaust PM10 contribution. A comprehensive review on existing emission inventory models for non-exhaust emissions was given by Lohmeyer and Düring (2001). The number of studies reporting a comprehensive real-world source apportionment for traffic related non-exhaust PM10 emissions is still low (Abu-Allaban et al. 2003; Furusjo et al. 2007; Quass et al. 2008). Possible adverse health effects of emissions by traffic related non-exhaust emissions have recently been addressed (Gustafsson et al. 2008; Lindbom et al. 2006; von Uexkull et al. 2005).

2.2 Project goals

The main scope of the project APART (Abrasion Particles produced by Road Traffic) was to identify and quantify the non-exhaust fraction of traffic related PM10 for several road-side locations with characteristic traffic regimes.

Specific goals:

- To provide a reliable base for future PM10 reduction scenarios
- Determination of location-specific emission factors (mg/km/vehicle) for *trace elements* emitted by local road traffic.
- Calculation of location-specific emission factors (mg/km/vehicle) for individual *non-exhaust emission sources*.
- Separation of emission factor values for light duty vehicles (LDV) and heavy duty vehicles (HDV).
- Evaluation of the local mass contribution from individual non-exhaust sources (% of traffic related PM10).

Scope exclusion:

- The study focused on traffic related emissions and did not include a quantification of other PM10 sources.
- Exhaust related PM10 was quantified at the investigated locations to establish a mass balance of total traffic related PM10. An in-depth interpretation of the exhaust fraction is subject of other studies and was not within the scope of the present investigation.

2.3 Experiments

2.3.1 Roadside measurements

To separate traffic related emissions from the total ambient PM10 load, representative background measurements were performed either upwind of the selected measuring location, or at a suitable background site (Figure 2.1). The selection of the investigated locations was based a) on their traffic and roadside characteristics being typical also for other real-world situations and b) on their experimental and conceptual applicability. ► ***Report Section 4.1***

The following roadside measurements were performed:

- Zürich-Weststrasse: Urban street canyon with 'Stop-and-go traffic' (Urban main road with traffic lights, strong disturbances). Simultaneous urban background measurements were performed at an urban courtyard park (Zürich-Kaserne).
- Reiden LU: Upwind/downwind measurements along a national freeway (A2) with mainly free-flowing traffic at 120 km h^{-1}.

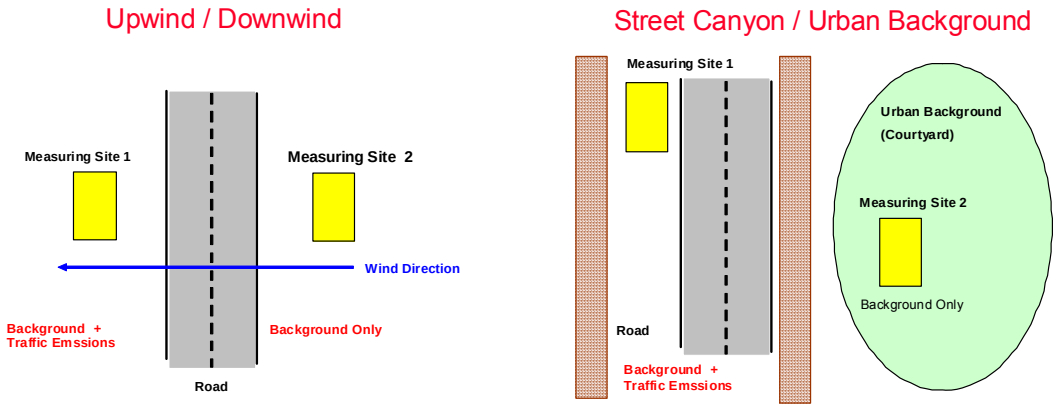

Fig. 2.1: Schematic illustration of the traffic vs. background concept.

2.3.2 Time and size resolved trace element measurements

To allow an identification of individual traffic related sources, specific elemental fingerprint signatures for the various sources were used. These were obtained by hourly elemental mass concentration measurements in three size classes (2.5-10, 1-2.5 and 0.1-1 micrometers) with a rotating drum impactor (RDI) as sampling device and subsequent analysis with synchrotron radiation X-ray fluorescence spectrometry (SR-XRF). The elemental fingerprint measurements were embedded into a large set of aerosol, gas phase, meteorological and traffic count measurements. ► ***Report Sections 3.1 and 3.2***

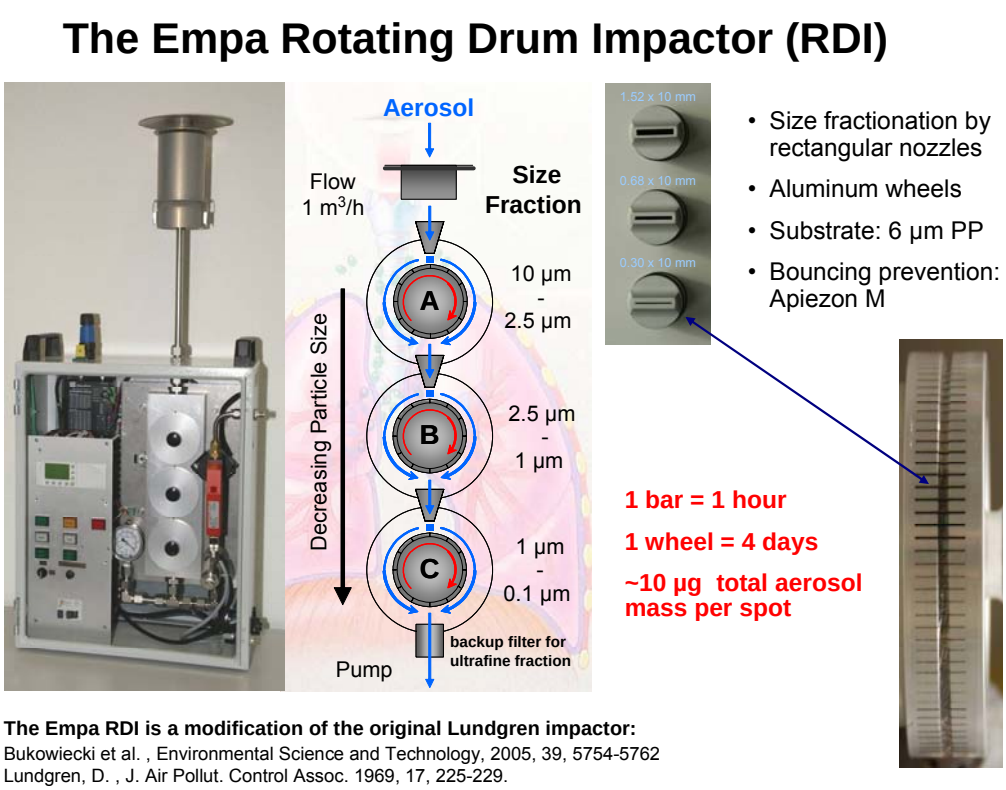

The Empa RDI is a modification of the original Lundgren impactor:
Bukowiecki et al. , Environmental Science and Technology, 2005, 39, 5754-5762
Lundgren, D. , J. Air Pollut. Control Assoc. 1969, 17, 225-229.

Fig. 2.2: The Empa Rotating Drum Impactor (RDI).

2.3.3 Additional experiments

- **Road wear simulator experiments:** Specific quantification of PM10 emissions due to abrasion and resuspension from road pavement can not easily be obtained from field measurements at traffic sites because a large variety of potential sources could affect local PM concentrations. It is quite difficult to quantitatively attribute the measured PM to the individual sources. For emissions with specific elemental composition (e.g. brake wear) it is possible to do so. But even with detailed chemical speciation locally produced abrasion particles from the road surface and resuspension of previously deposited dust of mainly mineral origin from other sources can hardly be distinguished due to their similar elemental composition and highly correlated variation in time. However, so-called "mobile load simulators" offer a possibility to tackle this issue. These devices are designed and used by road engineers to test the properties and durability of road pavements in the field. In this study emission rates were derived from measurements with two different types of mobile load simulators on different types of road pavement (asphalt concrete, porous asphalt). The experimental set-up allowed for a separate characterisation of the emissions caused by fresh in-situ abrasion and by resuspension of previously deposited dust. ► ***Report Sections 3.3 (Method) and 5.2 (Results)***

- **Road dust sampling and analysis:** Dust collected from the surface of a road gives important clues about the general chemical composition and to some degree the size distribution of particles resuspended by traffic. As a specialized instrument for the collection of road dust has been developed at the Institute of Earth Sciences 'Jaume Almera' in Barcelona, Spain, and was used in a sampling campaign in Zurich in February 2008. ► ***Report Sections 3.4 (Method), 4.2 (Field campaigns) and 5.3 (Results)***

- **Mobile measurements: Mobile PM10 and PM1 measurements:** To investigate the intra-urban spatial variation of individual particle size ranges, a series of mobile measurements was performed in Zürich in June 2007 using a mobile measurement platform. ► ***Report Sections 3.5 (Method), 4.3 (Field campaigns) and 5.5 (Results)***

2.4 Source identification

For the identification and quantification of the different pollutant sources contributing to the measured PM10 mass concentrations at the individual locations, positive matrix factorization (PMF) was applied. This statistical procedure represents a state-of-the-art method widely used in atmospheric chemistry and physics. The input to the model is a set of time series for individual PM10 constituents, along with a uncertainty value for every individual data point. While tracer species (in our case trace elements) help for the source identification, the mass dominant PM10 constituents (usually secondary aerosols etc.) contribute to a complete mass balance. The source separation capacity of the PMF method relies on the different temporal evolution of the tracer species, which allows for the distinction of an individual source. The main model assumption of PMF is that the chemical composition of the identified sources remains constant throughout time. The input species are considered to be independent, and the number of relevant sources (factors) is not determined by the model, but has to be estimated by the user. The output of the model is a set of factor profiles (source composition) and factor contribution (source time series) for every individual source, which is illustrated in Figure 2.3. In cases where the sum of measured input species add up to the full PM10 mass concentration at the considered location, the PMF source contributions allow for a full PM10 mass balance.

In urban air, the temporal dynamics and the emission characteristics of most pollution sources occur within a few hours. For the trace element measurements performed within APART, the time resolution of one hour as well as the size-segregation represent a strong benefit for the source identification by PMF. The measured species covered only a fraction of total PM10. The sources identified by the PMF analysis had to be empirically extrapolated to their full mass contributions.► ***Report Section 5.6***

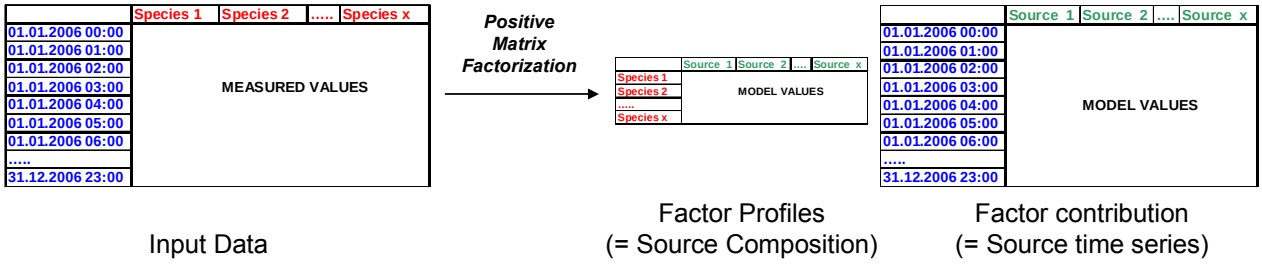

Fig. 2.3: Schematic illustration of PMF.

2.5 Calculation of source emission factors

Emission factors (EF) are used by researchers and regulating agencies as a tool to quantify the emission of a specified pollutant by an individual vehicle or a vehicle fleet mixture. In most studies, emission factors are expressed in mass per vehicle km or mass per amount of fuel. While emission factor determinations for an individual vehicle in the laboratory are straightforward, the atmospheric dilution of the emitted species is a main parameter that has to be taken into account for the calculation of real-world emission factors.

To separate traffic related emissions from the total ambient PM10 load, representative background measurements were performed either upwind of the selected measuring location (Field campaign Reiden LU), or at a suitable background site (Field campaign Zürich Weststrasse / Zürich Kaserne). The atmospheric dilution of the emissions from their point of emission to the point of sampling (10-20 m) was obtained by background corrected NO_x measurements and known NO_x emissions at the considered site (available from emission inventories). This, together with information on traffic frequencies, allowed for the calculation of emission factors (expressed as mg/km/vehicle) for the measured tracer species and for the abrasion sources (see Figure 2.4). Calculations were performed with help of a multilinear regression model, which also allowed for the determination of individual emission factors for light and heavy duty vehicles (based on individual traffic counts for these categories). Time periods with distinctively high background corrected mass concentrations were required for statistically significant emission factor calculations. ► ***Report Sections 5.1 and 5.6***

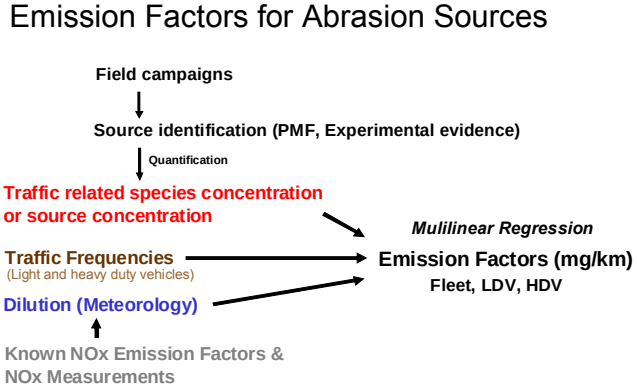

Fig. 2.4: Schematic illustration of emission factor calculation.

3 Instrumentation and Techniques

3.1 Field Campaign Containers

Two air quality monitoring containers were placed at different near-road locations on occasion of APART. The two monitoring containers were equipped with the instruments listed in Table 3.1a. The sampling inlets for the instruments were positioned on the container roofs at a height of 4.5 m above road level. Table 3.1b shows the calibration procedures and measurement uncertainties for the instruments used for the determination of emission factors. Propagated instrumental uncertainties will be discussed in the Result Section.

Table 3.1a: Measured parameters.

Measured Parameter	**Purpose**	**Instrument**	**Time Resolution**	**Container 1**	**Container 2**
PM2.5-PM10, PM1-PM2.5 PM0.1 -1	Size-resolved sampling of trace elements	Rotating Drum Impactor (RDI), manufactured at Empa	1 h		
PM10	Mass balancing of identified particle sources	TEOM (Tempered Oscillating Microbalance, R&P Inc. USA)	10 min		
Black Carbon in PM1	Information on the PM1 carbon fraction	Aethalometer (7-Wavelength, Magee Sci. Inc., USA), plus 1 µm cyclone	5 min		
CO2 concentration	Calculation of atmospheric dilution	LICOR 840 (LICOR Inc., USA)	1 min		
NO,NO_2 and NO_x concentration		HORIBA NO_x-Monitor	1 min		
Wind direction Wind speed	Identification of upwind/downwind situations	Metek Meteo (Metek Inc.)	1 min		
Relative humidity, temperature	Meteorological information	Common standard products	1 min		
Daily PM10 filter samples	Quality assurance: PM10 measurements and trace element analysis using an external method	HIVOL (High Volume) – Sampler (Digitel AG, CH)	1 day		
Particle size distributions	Complementary investigation of PM10 (Sections 5.4/5.5)	APS (Atmospheric Particle Sizer, TSI Inc., USA)	1 min		

Table 3.1b: Calibration and adjustment procedures for the instruments used for the later determination of source emission factors. Before and after the field campaigns, instrument cross-comparisons were performed at the NABEL site in Dübendorf. Standard instrument and inlet air flow checks were performed in regular intervals during the campaigns. MC1, MC2: Measurement containers 1 and 2. Propagated instrumental uncertainties are discussed in the Result Section.

Parameter	**Instrument**	**Calibration and adjustments**	**Uncertainty of measurement**
Trace element mass concentrations	Rotating Drum Impactor (RDI), SR-XRF analysis	See Section 3.2	Precision: ±5% Accuracy: ± 20%
PM10	TEOM/FDMS (Tempered Oscillating Microbalance, R&P Inc. USA)	PM10(MC2) was adjusted to PM10(MC1) based on instrument cross-comparisons: Weststrasse/Kaserne: PM10(MC2)= 1.011*PM10(MC1)+0.574 r^2 = 0.899 Reiden: PM10(MC2)= 1.104*PM10(MC1)+1.652 r^2 = 0.929	Precision: ±2.5 µg/m³ (1-hour ave.) Accuracy : ±0.75%
Black Carbon in PM1	Aethalometer (7-Wavelength, Magee Sci Inc., USA), plus 1 µm cyclone	BC(MC2) was adjusted to BC(MC1) based on instrument cross-comparisons: Weststrasse/Kaserne: BC(MC2)= 1.011*BC(MC1)+0.574 r^2 = 0.0.956 Reiden: BC(MC2)= 1.104*BC(MC1)+1.652 r^2 = 0.0.955	Precision: 0.1 µg/m3 @ 1-min resolution @ 3 LPM
CO2 concentration	LICOR 840 (LICOR Inc., USA)	Direct calibration using span gases with different concentrations.	Accuracy: ± 1.5%
NO,NO_2 and NO_x concentration	HORIBA NO_x-Monitor	Direct calibration using span gases with different concentrations.	Repeatability: ±2.0% of full scale

Fig. 3.1: Inside the measurement container.

Fig. 3.2: Measurement container at Zürich-Weststrasse.

3.2 Synchrotron radiation based trace element analysis

For hourly resolved and size-segregated ambient aerosol sampling, a rotating drum impactor (RDI) has been deployed at Empa and PSI in recent years. The RDI collected ambient aerosol in 3 size ranges (2.5-10 µm, 1-2.5 µm and 0.1-1 µm, see Bukowiecki et al. 2008). The sampling time resolution, achieved by stepwise rotation of the impactor substrate wheels, was set to 1 hour for the measurements in Zürich-Weststrasse and Zürich-Kaserne, and to 2 hours for Reiden, respectively (see Section 4). After collection, the aerosol loaded RDI samples were scanned through a synchrotron radiation generated X-ray beam and analyzed using energy-dispersive X-ray fluorescence spectrometry (SR-XRF) in an automated routine and without further sample treatment. This combined sampling and analysis technique allowed for the detection of the ng amounts of trace elements contained in the individual aerosol deposition bars (Bukowiecki et al. 2008). The method does not include any chemical preparation of the aerosol samples prior to the trace element analysis, which makes it very efficient for the analysis of a large number of samples within a short time. To cope with the large number of samples collected with an RDI, the low sample mass and the need for an efficient analysis, the use of synchrotron X-rays represents a *conditio sine qua non* for the XRF analysis of the RDI samples.

The RDI sampler type was originally designed several decades ago by (Lundgren 1967) and consists of rectangular jet nozzles for particle size separation. The RDI (Figure 3.3) used by Empa represents a redesign of the original impactor, designed for the collection of ambient aerosol in 3 size ranges (2.5-10 µm, 1-2.5 µm and 0.1-1 µm) on aluminum substrate holder wheels. A polypropylene (PP) film with 6 µm thickness was used as collection substrate. This substrate produced minimal scattering during the subsequent spectrometric analysis and does not contain relevant contaminations of trace elements. The aerosol samples show a bar-code like deposition pattern (see Figure 3.3), determined by the nozzle dimensions of the impactor stages. For a typical ambient aerosol mass concentration of 20 µg m^{-3} (annual

average value in Switzerland) the total mass deposited on an individual hourly RDI deposition bar is less than 10 µg on each stage. A minimal detection limit in the region of 1-10 ppm was achieved for most trace elements in the size-segregated hourly samples containing approx. 10 µg total aerosol mass. This corresponds to ambient air mass concentrations in the range of pg m-3 to ng m-3 (see Tables S1 and S2). Trace elements with Kα fluorescence line energies in the higher energy range (5-35 keV, corresponding to Ca-Sb in the Periodic Table) were detected at the beamline L of HASYLAB (Hamburger Synchrotronstrahlungslabor at Deutsches Elektronen-Synchrotron, Germany). For the detection of trace elements with Kα fluorescence line energies in the lower energy range (1-8 keV, corresponding to Si-Fe), the samples were additionally analyzed at the Advanced Light Source (ALS, beamline 10.3.1) at Berkeley National Laboratory, USA. Absolute calibration of the measured XRF spectral data and the conversion to hourly elemental mass concentrations was performed by external calibration (ICP-OES) of homogenous standard samples prepared with an ink jet printer. The average accuracy (uncertainty of the absolute values) of the measurements was ±20%. This introduced a systematic uncertainty to the measured mass concentrations, which was identical for all measured samples. On the other hand, the average precision (hour-to-hour variation) of the elemental mass concentrations was only ±5%, reached by the high sensitivity of the Synchrotron-XRF analysis and a sufficient sample homogeneity, and by the analysis of the samples directly on the substrate (Bukowiecki et al. 2008; Bukowiecki et al. 2009). The high precision of the time series was essential for the purpose of this study, where mass concentration differences play an important role.

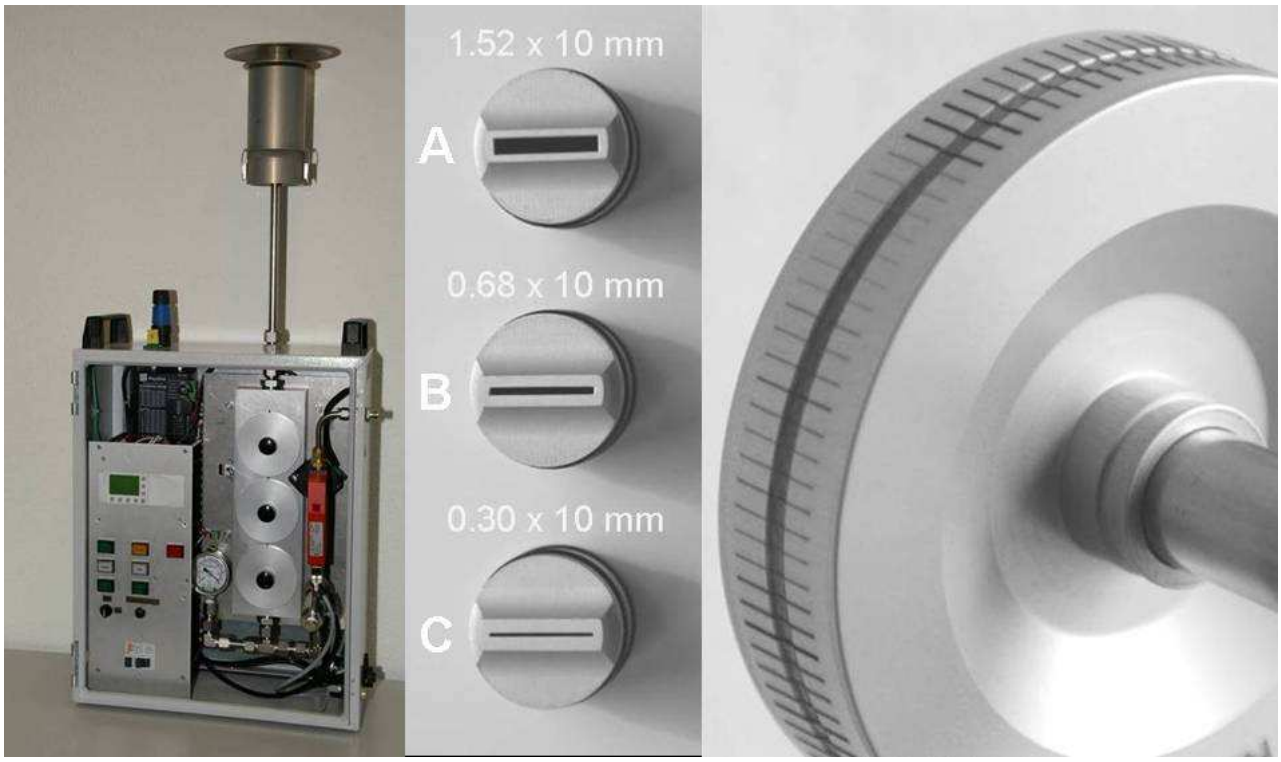

Fig. 3.3: Rotatings drum impactor (RDI) with PM10 inlet (left picture), Size-segregating nozzles of the RDI (middle), RDI sampling wheel with a sample of urban submicrometer particles (right picture). Each dark bar represents one hour of collected ambient aerosol with a total aerosol mass of approx. 10 µg.

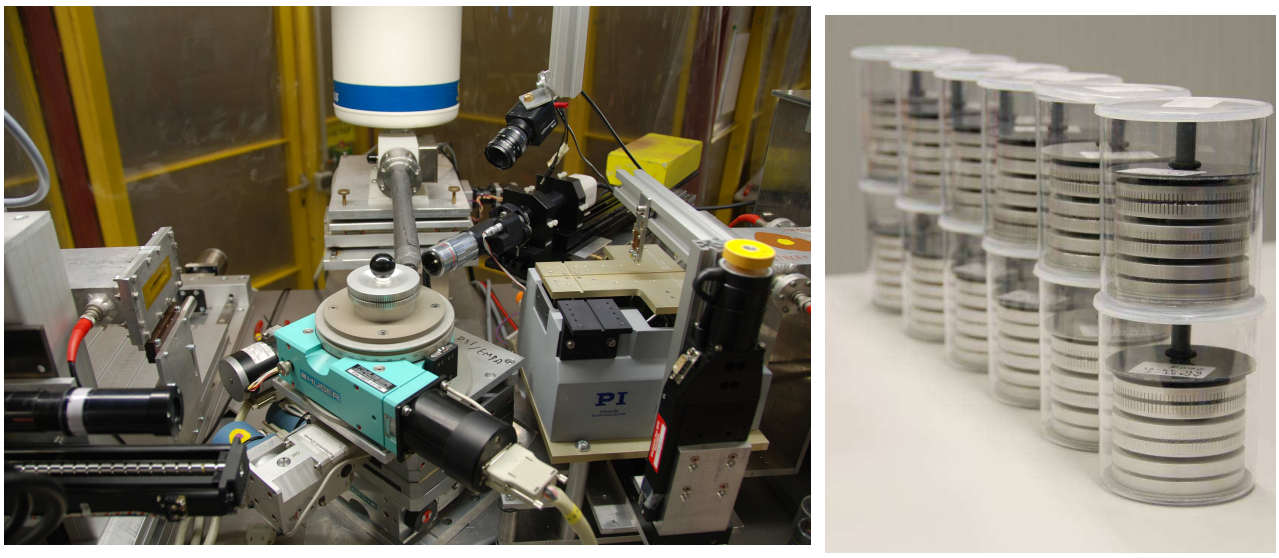

Fig. 3.4: Left: Experimental setup for trace element analysis at HASYLAB (Hamburg), right: Collected RDI samples.

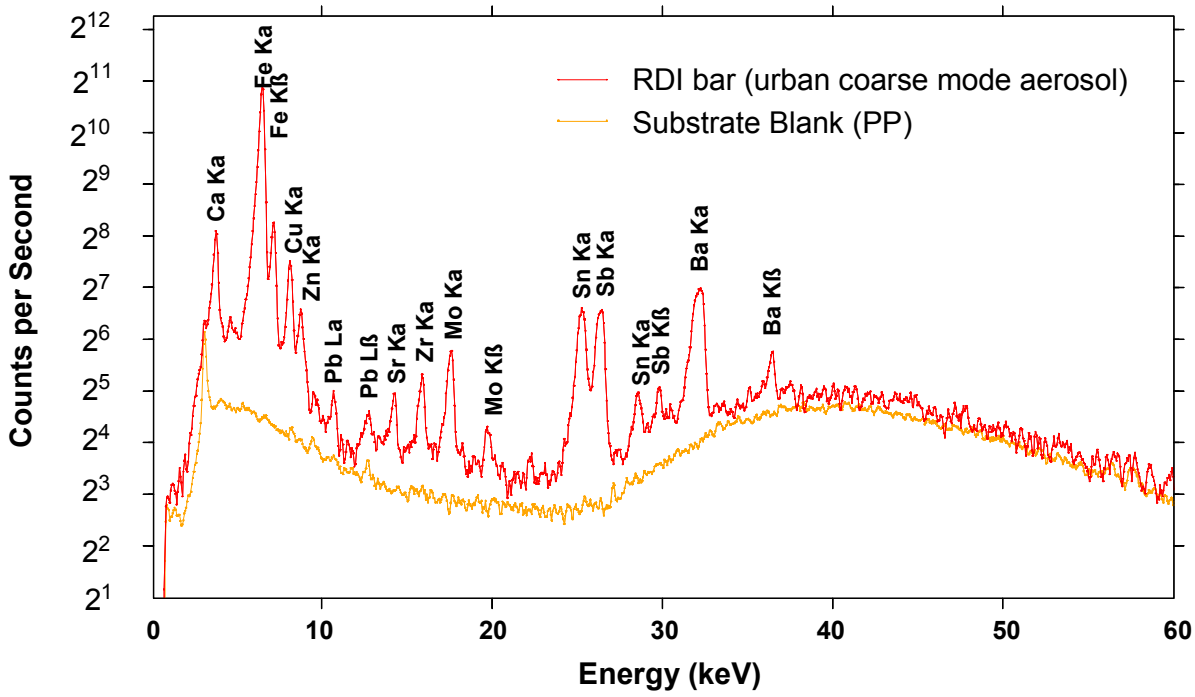

Fig. 3.5: Example SR-XRF spectrum for an RDI sample collected at Zürich-Weststrasse.

3.3 Mobile Load Simulators

Two different types of mobile load simulators were employed. The operation principle of both simulators is the same. Wheels are pulled in a closed loop over a defined distance of road surface at a defined speed and with a defined axle weight (Figure 3.6). The MMLS (Model Mobile Load Simulator, Figure 3.7) is a relatively small device simulating approximately one third of the load of a normal passenger car (LDV) at a low speed of 9 km/h. The big device MLS (Mobile Load Simulator, Figure 3.8) simulates the abrasion processes of a full size heavy duty vehicle (HDV) at a speed of 25 km/h. Table 3.2 gives an overview of the characteristics of the two mobile load simulators.

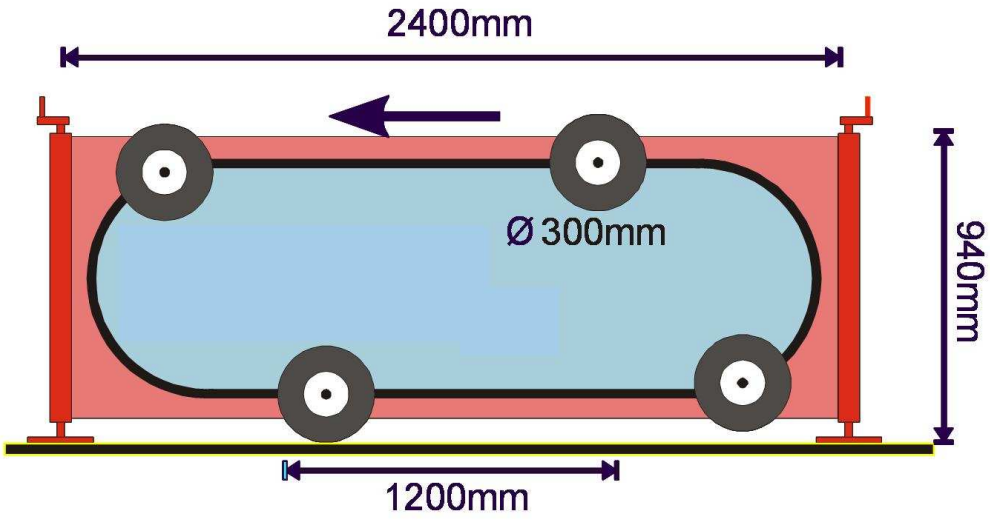

Fig. 3.6: Operation principle of a mobile load simulator, exemplified with a schematic view of the MMLS.

Fig. 3.7: Model Mobile Load Simulator (MMLS, simulating approx. 1/3 of the axle load of LDV): View with opened top (top) and in operation on AC pavement (bottom).

Fig. 3.8: View of the large Mobile Load Simulator (MLS, simulating the full axle load of HDV) in service position. During operation the whole device is lowered to the level of the road surface.

Table 3.2: Characteristics of the two mobile load simulators.

	MMLS	**MLS**
Speed	9 km/h	25 km/h
Driving distance on pavement /wheel passage	1.2 m	4 m
Number of wheel passages/minute	125 (single wheels)	100 (double wheels)
Axle weight	2.1 kN (212 kg)	65 kN (6570 kg)
Comments	simulating approx. 1/3 of the load of a LDV wheel	simulating the full load of a HDV double wheel

For the abrasion particle study the devices were placed on the road pavement to be investigated and then started. The motion of the wheels created an air flow under the device in the direction of the moving wheels. In order to avoid this air stream to escape at the sides the free volume under the devices was canalized by attaching plastic screens along the sides. The measurement set-up is schematically illustrated in Figure 3.9. It involved size fractionated particle measurements in the range of 0.5 – 20 µm with an aerodynamic particle size monitor (TSI APS Model 3321) and the dilution of a tracer gas (sulphurhexafluoride SF_6). This latter measurement was used to characterize the air dilution in the induced air stream under the mobile load simulator and allows the calculation of the volume rate of this air stream and thus the establishment of absolute emission factors from measured particle concentrations. Table 3.3 gives the experimental conditions and the results of the tracer experiments for both types of mobile load simulators.

From the measured tracer gas flows and concentrations the induced volume flow is calculated as follows:

$$dil = \frac{c_{tr} \cdot 10^6}{c_{meas}}$$

$$\dot{V} = \frac{f_{tr} \cdot dil}{10^6} = \frac{f_{tr} \cdot c_{tr}}{c_{meas}}$$

where:

dil Dilution rate

$\dot{V}$ Air flow through simulator (m^3/min)

f_{tr} Flow of tracer gas injection (ml/min)

c_{tr} Concentration of injected tracer gas (ppm)

c_{meas} Measured tracer gas concentration at sampling point (ppt)

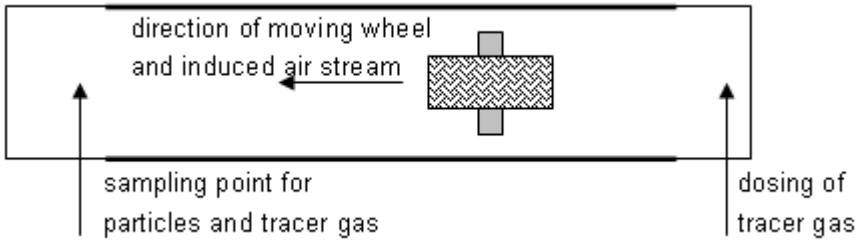

Fig 3.9: Schematic view of the measurement set-up at the mobile load simulators

Table 3.3: Experimental conditions and results of the tracer gas measurements

	MMLS	**MLS**
Dosing of tracer gas injection(SF_6)	52 ml/min	150 ml/min
Concentration of injected tracer gas (SF_6)	53 ppm	150 ppm
Measured concentration at sampling point (SF_6)	625 ppt	200 ppt
Dilution rate	84'800	750'000
Volume rate of air flow through simulator	4.41 m^3/min	112.5 m^3/min

Two different types of pavements of high practical importance were investigated. Asphalt concrete (AC) is a relatively compact pavement with low porosity and represents one of the most used types on Swiss roads. Porous asphalt (PA) is now often used because of its acoustic advantages (low noise emissions) and its favourable properties under wet conditions. As the name suggests it has a surface of high porosity. Fig 5 shows the preparation of the test area for MMLS measurements with these two pavements.

Fig. 3.10: Preparation of the two pavements investigated with MMLS (AC bottom right, PA centre, work in progress).

From the particle concentrations measured at the sampling point, the covered wheel distance and the volume rates of air flow through the simulators emission factors can be derived. Mass concentrations were calculated from the number size distributions by assuming a particle density of 1 g/cm^3. The plausibility of this assumption was checked by comparing the calculated mass concentrations of the APS during measurement of ambient air with the simultaneous PM10 readings at the nearby NABEL site Dübendorf (distance approx. 100 m). The APS concentrations were always in the range of 50-75% of the PM10 readings. This is quite plausible in view of the fact that PM1 is typically approx. 50% of PM10 and the evaluated APS range was 0.5 to 10 µm.

$$EF = \frac{(c_{op} - c_{amb}) \cdot \dot{V}}{d}$$

where:

EF Emission factor for 1 wheel (mg/km)

c_{op} Particle concentration during operation (mg/m^3)

c_{amb} Particle concentration of ambient air (mg/m^3)

$\dot{V}$ Air flow through simulator (m^3/min)

d Driving distance of the simulator wheels on the pavement (km/min)

3.4 Road Dust Sampling (Deposited Dust)

Dust collected from the surface of a road gives important clues about the general chemical composition and to some degree the size distribution of particles resuspended by traffic. A specialized instrument for the collection of road dust has been developed at the Institute of Environmental Assessment and Water Research (IDAEA) in Barcelona, Spain, and was used in a sampling campaign in Zurich in February 2008.

The dust sampler (Figure 3.11) consisted of a PVC deposition/resuspension chamber with a subsequent trap (a Negretti stainless steel elutriation filter designed to allow passage to only PM10 material of average density) and a filter on which the passing dust was deposited. A pump sucked 25 l/min of air through the chamber and the filter. Either quartz fiber or Teflon membrane filters were used to collect the samples.

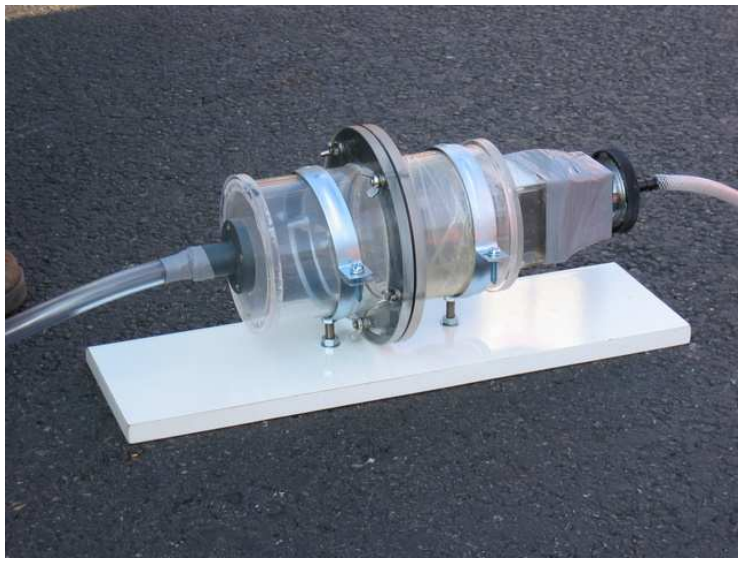

Fig. 3.11: The dust sampler. Air enters the chamber through the tube on the left. Large particles are deposited in the plexiglas tube. The particle trap is located at the right-hand side in the square block. The filter is mounted in the round, black filter holder at the right. The tube at the right connects to the pump.

Sampling was performed by means of a new methodology devised by IDAEA (Amato et al. 2009) which allows collecting the road dust particle fraction with aerodynamic diameter lower than 10 µm directly from the road pavement onto the filters. For each location four different filters were collected by sampling in four different square meters, to collect enough PM10 mass for further chemical analyses and to get information about the variability of the four samples. Sampling time was 30 min for each square meter.

The collection of deposited PM_{10} onto the filters was done as follows (Figure 3.12):

- On a quartz fiber filter (47mm) for the determination of the total concentration of major and trace elements (by ICP-AES and ICP-MS, (Querol et al. 2001), and for Elemental Carbon (EC), Organic Carbon (OC) and Carbonate Carbon (CC) determination using a thermal-optical transmission technique (Sunset Laboratory OCEC Analyzer, performed at Institute of Earth Sciences “Jaume Almera” (IJA), Barcelona).

- On a Teflon-membrane filter (47mm) for the determination of sulfate, nitrate, ammonium, chloride (by ion-chromatography), soluble metals (by ICP-AES and ICP-MS), pH and conductivity (performed at IJA).

- On a Teflon-membrane filter (47mm) for determining the silica concentration by XRF analysis (performed at PSI and Empa). Quartz fiber filters are not suitable for this purpose.

- On a quartz fiber filter (47mm) to be kept for further analyses.

A further square meter was selected to sample the total deposited matter:

- On a Teflon-membrane filter (47mm) for the determination of the mass (Figure 3.13).

Furthermore, road dust was swept with a brush into a plastic bag for a bulk analysis of the coarse material. After a day of sampling, the dust sampler was cleaned with ethanol. The Negretti filter unit was cleaned in an ultrasonic bath.

Fig. 3.12: PM10 sampling at Pfingstweidstrasse in Zürich.

Fig. 3.13: Coarse dust sampling in the Milchbuck tunnel.

Particles with aerodynamic diameter >10 µm were deposited in the PVC chamber. Electrostatic adhesion might have caused some losses of particles <10 µm, which was not possible to quantify. Nevertheless this loss is likely to be negligible compared to losses of traditional sampling procedures (i.e. sweeping). Results

showed that the PM10 fraction was on average only 0.6% and 0.1% (in volume) of the samples (Amato et al. 2009). 47-mm diameter Munktell quartz fiber filters were used to determine the concentration of major and trace elements, OC and EC, and 47-mm diameter Schleicher & Schuell Teflon membrane filters (1 μm pore) to determine the concentration of water-soluble ions. Before sampling, the quartz fiber filters were dried at 205°C for 5 h and conditioned for 48 h at 20°C and 50% relative humidity. Weights of blank filters were measured three times every 24 h by a Sartorius LA 130 S-F micro-balance (1 μg sensitivity).

After sampling, filters were brought back to the laboratory for mass determination and analytical treatments. One quartz fiber filter per site was cut into two sections. Half of the filter was acid digested (5 ml HF, 2.5 ml HNO_3, 2.5 ml $HClO_4$) for the determination of major and trace elements and analyzed by inductively coupled plasma mass and atomic emission spectrometry (ICP-MS and ICP-AES, Querol et al. 2001). Blank measurements were performed in the laboratory, by connecting the sampling device to an empty drum for 2 h. Blank concentrations were subtracted from the sampled filter concentrations, being on average 3.6% (for the major chemical analyses done with elements) and 5.4% (for trace elements) of uncorrected concentrations in sampled filters. A section of 1.5 cm^2 from the other half of the filter was used for the determination of OC and EC by a thermal-optical transmission technique (Birch and Cary 1996) using a Sunset Laboratory OCEC Analyzer with the default temperature program. Total carbon (TC) was determined as the sum of OC + EC. Teflon membrane filters were leached in 20 ml of bi-distilled water for the extraction of water-soluble anions and subsequent analysis by ion chromatography (IC) for sulfate, nitrate and chloride and by an ion specific electrode for ammonium.

SiO_2 concentrations were determined from the Teflon filters of each sampling site with XRF measurements at Empa. The Si counts were compared to those of other elements by calculating the ratios Si/element. Mg proved to be best related to Si (i.e. the mean ratio for all sites showed the least standard deviation), and therefore Mg was used to transform the counts of Si to masses. The resulting numbers were multiplied with a factor of 44/28 (molar mass ratio of SiO_2/Si) to obtain the SiO_2 deposition.

The variability of the masses was determined as the standard deviation of all (≤4) filters analyzed at the respective site. At two sites (Milchbuck Tunnel and Weststrasse) not the full set of filters could be analyzed due to technical problems, and the uncertainties (error bars) of these measurements were larger than at the other sites (see also Fig. 5.3.2).

3.5 Mobile Measurements (Airborne Particles)

3.5.1 Mosquita I

PSI's mobile laboratory Mosquita I was built into an IVECO Turbo Daily van (Bukowiecki et al. 2002) and consisted of a set of instruments for gas phase and aerosol measurements besides supporting instrumentation for geographical position, meteorological parameters, and video surveillance during driving. A schematic of the equipment is given in Figure 3.14, and the instruments are described in Table 3.4.

The inlet system on the roof of Mosquita I at a height of 2.8 m above the road surface had a diameter of 5 cm. Air was sucked through the tube with a flow rate of ~4000 l min^{-1}. An 8-mm (internal diameter) stainless steel tube with several bends led the air from the main inlet tube to the APS with a flow rate of 5 l min^{-1}. Total path length between the main inlet and the APS was about 2 m. Two smaller inlet lines made of 8-mm stainless steel tubes led the sampled air to the other instruments. The inlet for the different instrumentation had a particle diameter cutoff of 1 μm. No cutoff size was specified for the APS, however, as this instrument was used to sample the full range of particle sizes (0.5 - 20 μm). Due to significant sampling losses occurring

for large particles, only the size distribution below 10 µm was considered for analysis. Test runs on 11 and 12 June 2007 showed that the optimum on-road sampling rate for the APS was 5 s. This allowed for collecting sufficient aerosols with acceptable spatial resolution.

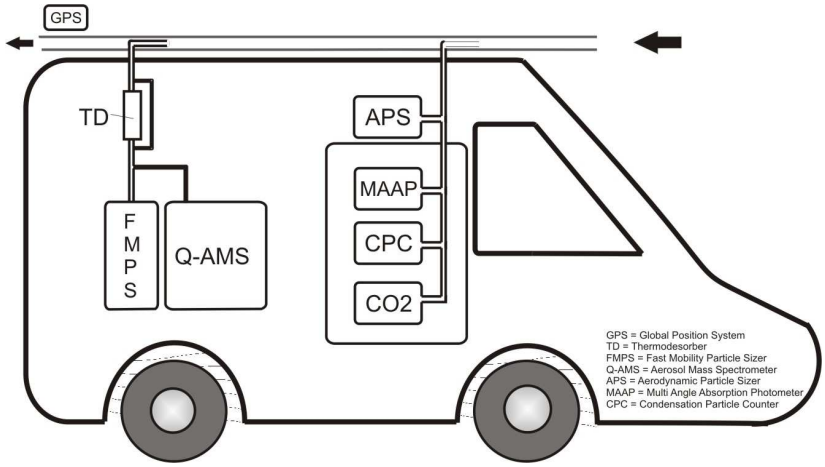

Fig. 3.14: Schematic of Mosquita I instrumentation for the Zurich-Hardplatz campaign in June 2007. Instrument characteristics are given in Table 3.4.

3.5.2 Mosquita II

In 2008 a new IVECO Daily 2006 Euro4 van was equipped with the same concept of instrumentation, hence its name Mosquita II. An improvement compared to Mosquita I was the van's particle filter which reduced self-contamination of the sampled air during stand-by operation or at traffic lights. The new van was not equipped with an APS, however, and thus did not collect larger particles originating from mechanical wear or resuspended road dust.

Table 3.4: Instrumentation of the mobile platforms Mosquita I and II.

Parameter	**Instrument / Name / Type and Manufacturer / Particle Size Range**	**Unit**	**Maximum sampling frequency**
Particle surface area concentration	DC / Diffusion Charging Particle Sensor / LQ1-DC Matter Engineering	µm²/ cm³	1 s
Particle number concentration	CPC / Condensation Nuclei Counter / 3010s TSI / ≥10 nm	#/cm³	1 s (500 s*)
CO_2, H_2O	CO2/H2O Gas Analyzer / LI-7000 LI-COR	ppm	1 s
Particle size spectra	FMPS / Fast Mobility Particle Sizer Spectrometer / 309100 TSI / 20 nm .. 800 nm	#/cm³, nm²/cm³, nm³/cm³, µg/m³	1 s
Chemical composition of particles	Q-AMS / Quadrupole Aerosol Mass Spectrometer / Aerodyne / 60 nm .. 1 µm	µg/m³	6 s
Soot concentration	MAAP / Multi Angle Absorption Photometer / 5012 Thermo	ng/m³	1 s
Particle size spectra *	APS / Aerodynmic Particle Sizer Spectrometer / 3321 TSI / 500 nm .. 20 µm	#/cm³, µm²/cm³, µm³/cm³, µg/m³	5 s
Thermodesorber **	TD / Thermodesorber / Burtscher	-	-
Meteorological parameters, geographical coordinates	Temperature, solar irradiation, relative humidity, pressure sensor, GPS	°C, W/m², %, bar, °, m	1 s, 2 s (GPS)

* Mosquita I only

** The thermodesorber removes volatile material from aerosol particles. It is not a sampler.

3.6 Particle Size Distributions

3.6.1 APS – Aerodynamic Particle Sizer Spectrometer

Because particles generated mechanically by break abrasion, tire wear and resuspension are typically quite large, size spectra are best measured with an instrument that covers a broad range of particle sizes. The Aerodynamic Particle Sizer Spectrometer by TSI Inc. covers a range from 0.5 to 20 μm and is thus well-suited for this purpose. The measuring principle is based on the time delay in an accelerated air flow, where the particles are detected by light scattering with a double crest optical system that illuminates the particle. The time of flight of the particle from one crest to the other is measured and can directly be converted into the aerodynamic particle diameter. Sampling during a selected time interval yields size spectra with the number of particles counted in a specified size range (Figure 3.15). Under the assumption of a constant density of 1 kg m^{-3}, the number density can be converted into mass, and mass spectra can be calculated from the raw data (Figure 3.15). This type of data can also be extracted from the raw data with the Aerosol Instrument Manager software by TSI Inc.

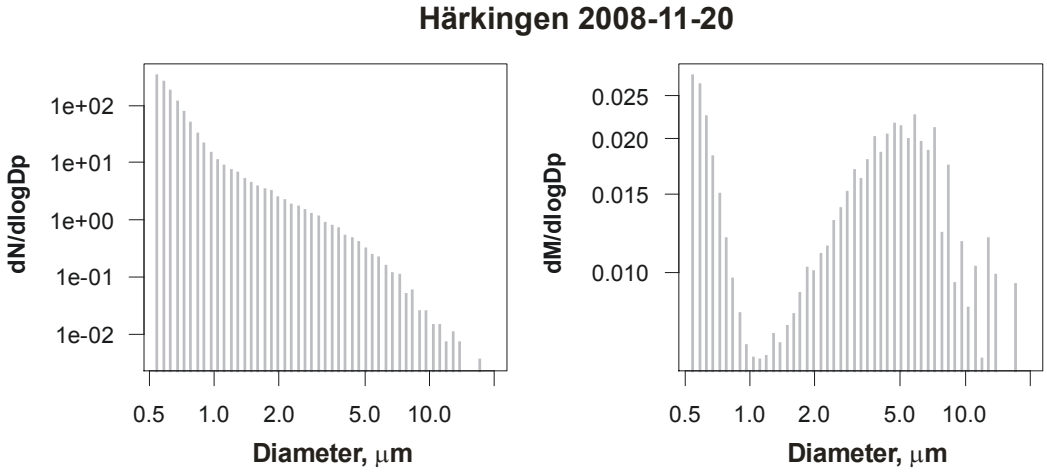

Fig. 3.15: Example size spectrum measured with the PSI Aerodynamic Particle Sizer spectrometer (APS). Left: Particle number concentration dN/dlogDp in counts. Right: Mass concentration dM/dlogDp in mg m^{-3}.

For particle sizes larger than 8 μm the scatter increases, because the number of collected particles becomes more arbitrary. The bimodal mass distribution indicates that most of the particle mass is concentrated in submicron particles (due to their large numbers) and in particles between 2.5 and 10 μm diameter. The scatter in the larger particle diameters is more evident in this representation of the data.

The particle size range of the APS (0.5 – 20 μm) prevents the particles smaller than 0.5 μm from being sampled. These are mostly fresh emissions from combustion processes of vehicle engines or heating devices, and they contribute considerably to total particle mass. This cut-off has to be taken into account when interpreting the APS measurements, as the total mass sampled with the APS will be systematically lower by PM0.5 than the standard PM measurements. This will be indicated in the notation of PMx-PM0.5, where x is 10, 2.5 or 1.

4 Field Campaigns

4.1 Roadside Measurements

4.1.1 Zürich Weststrasse/Kaserne (Street Canyon vs. Urban Background)

The Zürich-Weststrasse urban monitoring station was located in the city center of Zürich (Switzerland), in a narrow street canyon (20 m) with 10-20 m high buildings and two traffic lanes with one-way traffic. The site was chosen because of its high transit traffic frequency (22 000 vehicles per day, >1000 vehicles h^{-1} during rush hour). While there was only negligible heavy duty vehicle traffic during weekends, the light duty vehicle frequencies were similar to weekdays. The permitted traffic speed was 50 km h^{-1}, which was only reached during evening and nighttime, because the high vehicle frequency in combination with the traffic lights did not allow a speed higher than 30 km h^{-1} during daytime. Queues regularly developed at red lights, which resolved temporarily during the following green phase. At night from 22:00 to 6:00 the road was closed for transit, with only residents having driving permission. Consequently, traffic density was very low (<100 vehicles h^{-1}) during the night. The prevailing wind direction within the street canyon was along the street axis (NW to SE), influenced both by traffic induced turbulence and frequent regional winds from NW. Measurements were performed from January to March 2007.

Simultaneously to the measurements at Zürich-Weststrasse, measurements were performed at Zürich-Kaserne, a site located in a courtyard in the downtown area of Zürich in 600 m distance from Zürich-Weststrasse. The site represents an urban background site and has been extensively characterized by a number of previous air quality studies (Gehrig et al. 2004; Hueglin et al. 2005; Szidat et al. 2004). Additionally, it has served as a long-term air pollution monitoring site of the Swiss monitoring network NABEL for 20 years (BUWAL 2003).

Table 4.1: Campaign key parameters.

Duration/ Season	22.1.2007 – 26.3.2007
Total number of days	64
Number of days with trace element data	24
Coordinates (Swiss Grid)	Weststrasse 74, LK 681.81/ 247.27
Pavement	Asphalt concrete (AB12), year of application: 1995/98, in good condition
Traffic regime	50 km h^{-1},'Stop-and-go traffic': Urban main road with traffic lights, strong disturbances (Category 'IO_HVS3' according *Handbook of Emission Factors (INFRAS 2004)*).

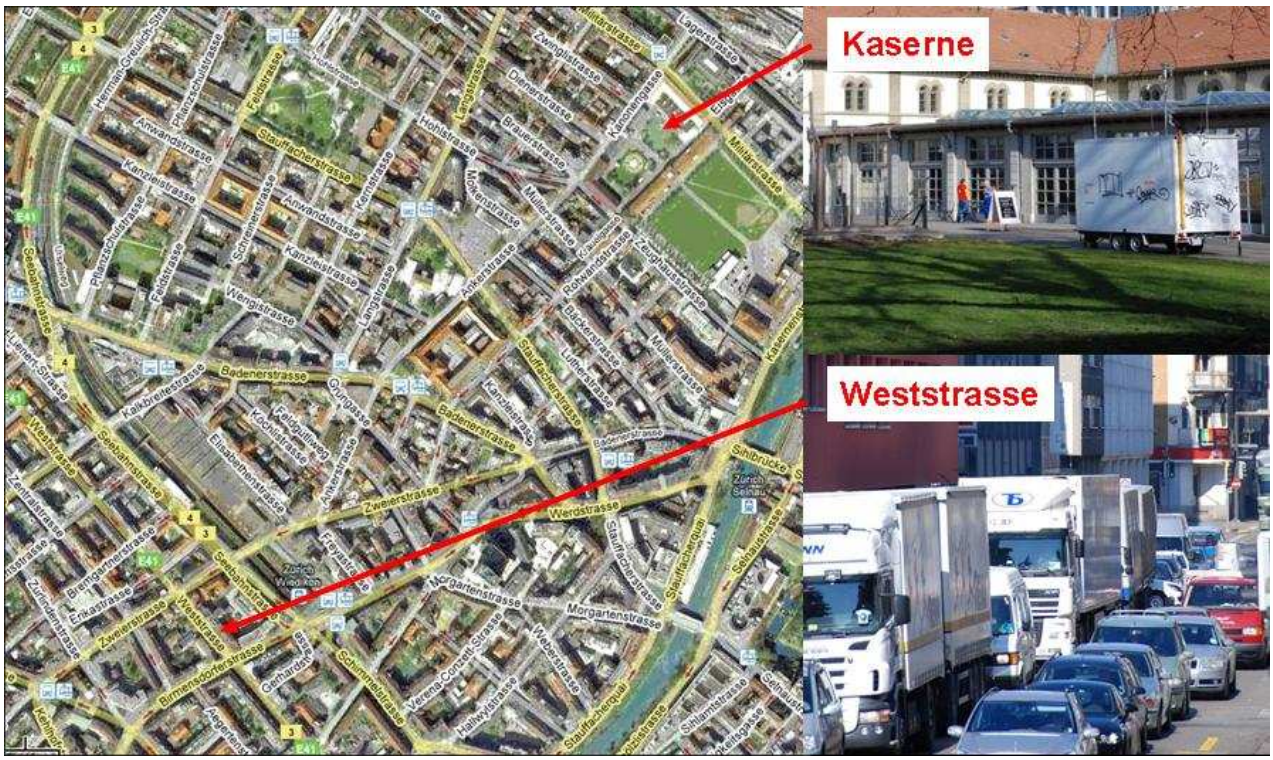

Fig. 4.1: Aerial and street view of the Zürich measuring sites (http://maps.google.ch).

Table 4.2: Input emission factors, based on the *Handbook of Emission Factors (INFRAS 2004).*

Weststrasse 2007						
Case 2: Emission factors "warm + 30%-cold start" Weststrasse (Year 2007, IO_HVS3, Longitudinal gradient =0%; LDV = 31.1km/h, HDV = 28.7km/h, Coaches = 18.7 km/h)						
IO_HVS3, 'iO-Hauptverkehrsstrasse, starke Störungen, 30% Kaltstart' (Urban main road with traffic lights, strong disturbances)						
Vehicle Category	CH-VehKm (urban main road)	EF Exhaust [g/km]			Abrasion, Resuspension [g/km]	Total [g/km]
	[Mio. VehKm]	NOx[1]	CO	Particles		PM10
LDV Gasoline	13'708	0.2010	2.9064	0.0020	0.0540	0.0560
LDV Diesel	3'618	0.4491	0.3473	0.0310	0.0540	0.0814
Delivery Vans Gasoline	471	0.8748	6.9644	0.0020	0.0540	0.0560
Delivery Vans Diesel	912	0.8128	0.4521	0.0682	0.0540	0.1209
MR Motorcycles	505	0.0870	6.5372	0.0310	0.0270	0.0580
Mopeds	337	0.0870	6.5372	0.0310	0.0135	0.0445
LDV Total	**19'550**	**0.2868**	**2.5723**	**0.0117**	**0.0526**	**0.0636**
HDV	396	10.5220	2.7236	0.2855	0.5400	0.8255
Coaches	19	11.3410	2.4576	0.2966	0.5400	0.8366
Public transit bus	0	12.9512	3.3151	0.3209	0.5400	0.8609
HDV Total	**551**	**10.5588**	**2.7116**	**0.2860**	**0.5400**	**0.8260**

[1] calculated as NO_2

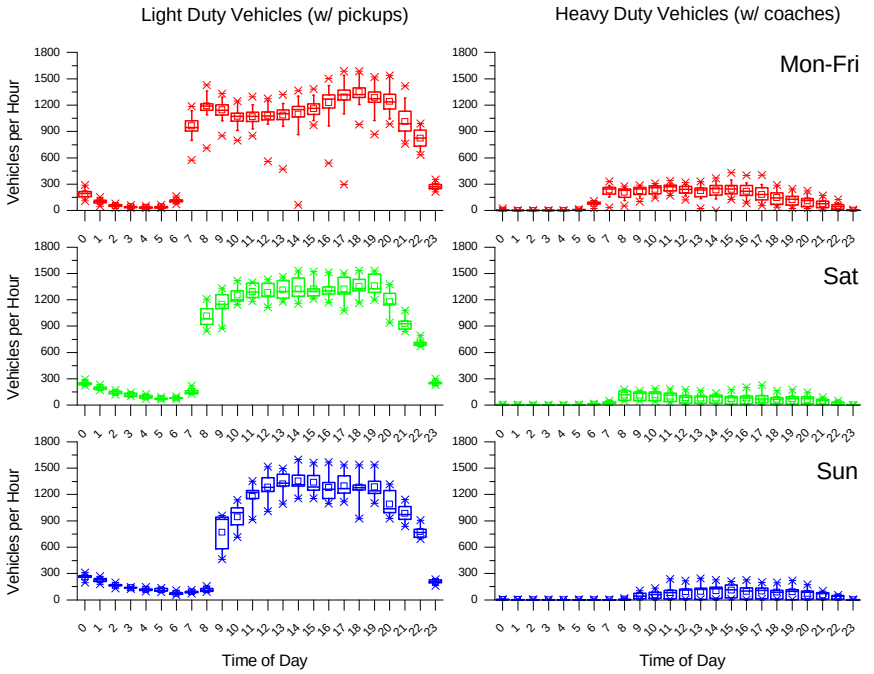

Fig. 4.2: Traffic frequencies Zürich-Weststrasse (unidirectional, two lanes).

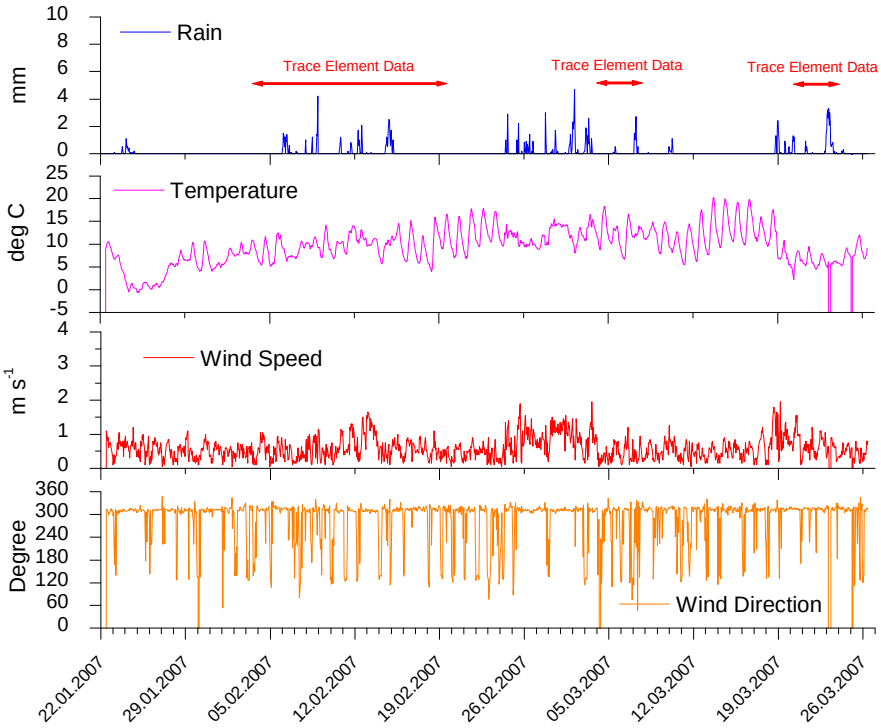

Fig. 4.3: Meteorological conditions during the Zürich-Weststrasse/Kaserne campaign. The allocated time for SR-XRF analysis at the Synchrotron facilities was limited, thus not all of the collected RDI samples could be analyzed. Time periods with priority for SR-XRF analysis were selected based on distinct concentration differences for PM10 and NO_x, and on the completeness of the measured data for the parameters required for emission factor calculations.

4.1.2 Reiden (Upwind/Downwind)

To compare the urban street canyon measurements to measurements next to a freeway, an additional campaign was performed from September to December 2007 next to a Swiss main interurban motorway with four lanes in total, surrounded by agricultural areas. The next village (Reiden) was in 1 km distance, and there were several industrial areas within a radius of 20-30 km. Traffic was mainly free flowing with a 120 km h^{-1} speed limit, with 50 000 vehicles per day.

Table 4.3: Campaign key parameters

Duration/ Season	27.8.2007 – 6.12.2007
Total number of days	100
Number of days with trace element data	50 (2 h Time resolution)
Coordinates (Swiss Grid)	LK 639.560/232.110
Pavement	Splitt-mastix asphalt (compact pavement comparable to asphalt concrete); direction Luzern SMA 11 B 80/100+NAF; direction Basel SMA 11 B55/70+NAF, year of application: 1999, in good condition.
Traffic regime	Motorway with free-flowing traffic at 120 km h^{-1} (Category 'AB_120' according *Handbook of Emission Factors (INFRAS 2004)*)

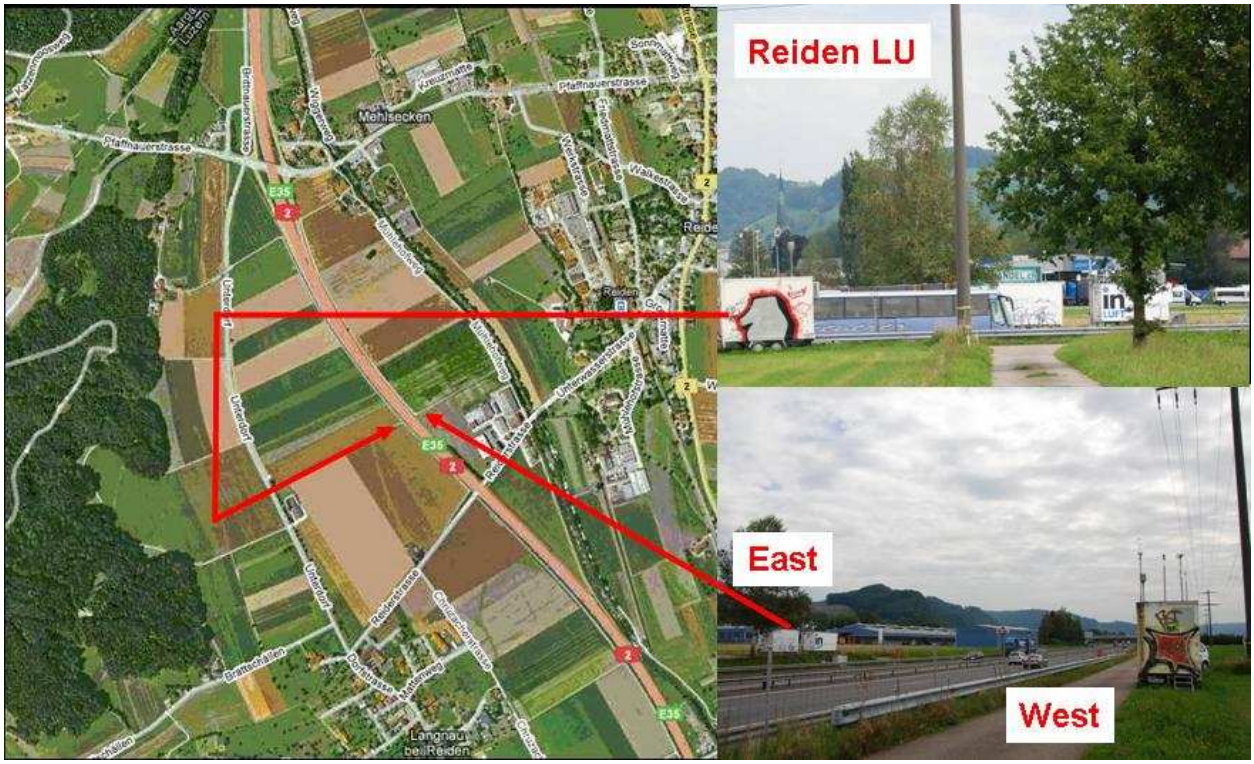

Fig. 4.4: Aerial and street view of the Reiden measuring sites (http://maps.google.ch).

Table 4.4: Input emission factors, based on the *Handbook of Emission Factors (INFRAS 2004).*

Reiden 2007						
Case 1: Emission factors "warm" Reiden (Year 2007, AB_120, Longitudinal gradient =0%; LDV = 116 km/h, HDV = 86 km/h)						
AB_120: Autobahn, Speed limit 120 km/h, LMW= 116 km/h, SMW: 86 km/h (Motorway with free-flowing traffic at 120 km h^{-1})						
Vehicle Category	CH-VehKm (urban main road)	EF Exhaust [g/km]			Abrasion, Resuspension [g/km]	Total [g/km]
	[Mio. VehKm]	NOx[2]	CO	Particles		PM10
LDV Gasoline	15'443	0.3077	0.9835	0.0020	0.0470	0.0490
LDV Diesel	4'076	0.5102	0.0781	0.0355	0.0470	0.0825
Delivery Vans Gasoline	571	1.4410	9.6966	0.0020	0.0470	0.0490
Delivery Vans Diesel	1'106	1.5997	0.1448	0.1416	0.0470	0.1886
MR Motorcycles	534	0.5853	10.4677	0.0310	0.0235	0.0545
Mopeds	0	0.5853	10.4677	0.0310	0.0118	0.0428
LDV Total	**21'730**	**0.4481**	**1.2330**	**0.0161**	0.0464	**0.0625**
HDV	1'144	5.3722	0.9492	0.1105	0.0740	0.1845
Coaches	47	6.6101	0.8283	0.1387	0.0740	0.2127
Public transit bus	0	0.0000	0.0000	0.0000	0.0000	0.0000
HDV Total	**1'191**	**5.4207**	**0.9444**	**0.1116**	0.0740	**0.1856**

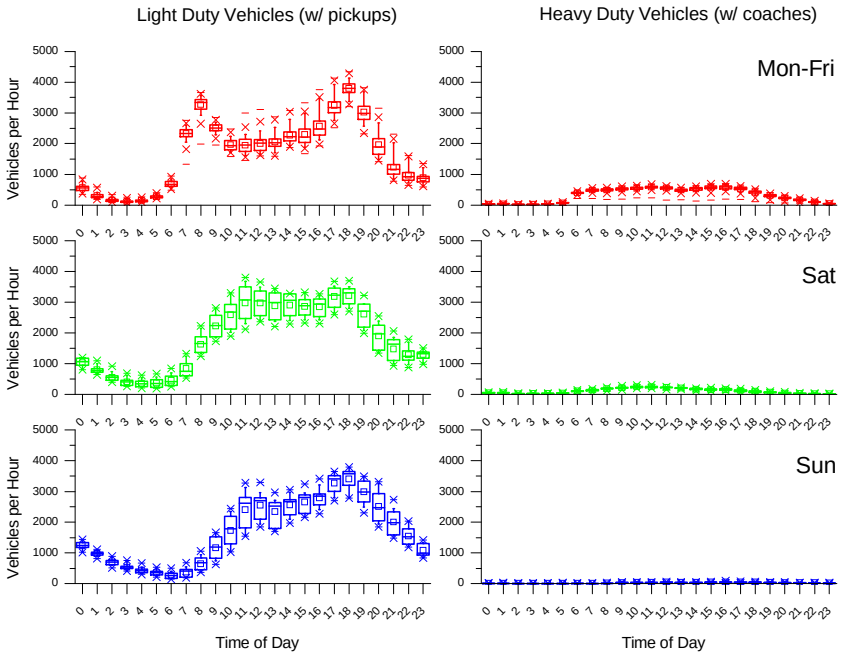

Fig. 4.5: Total traffic frequencies Reiden LU (A2, two directions with 2 lanes each).

[2] calculated as NO_2

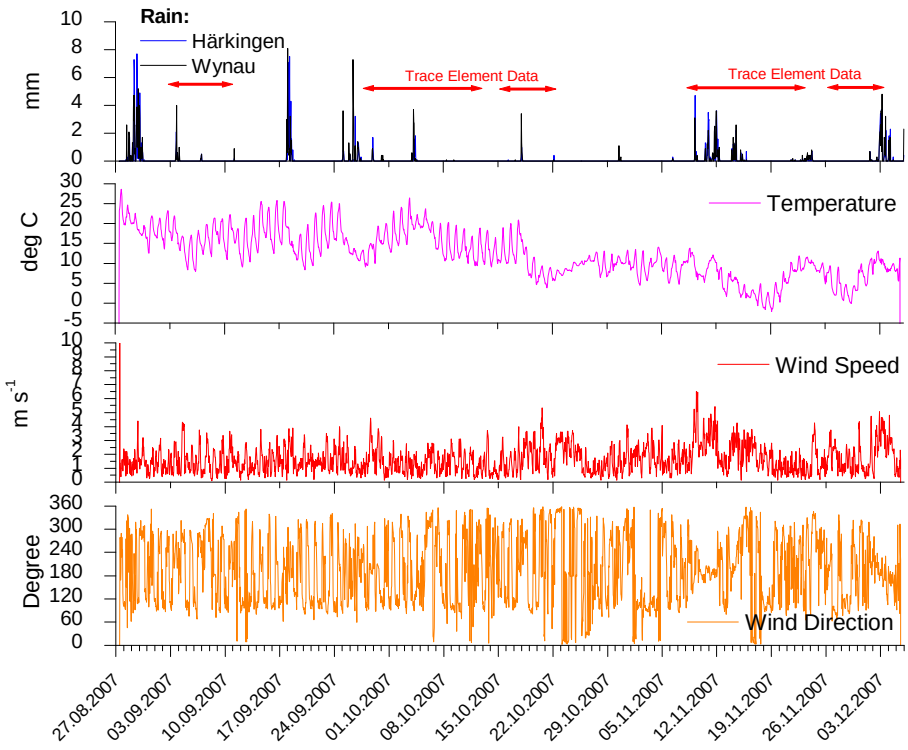

Fig. 4.6: Meteorological conditions during the Reiden campaign. The allocated time for SR-XRF analysis at the Synchrotron facilities was limited, thus not all of the collected RDI samples could be analyzed. Time periods with priority for SR-XRF analysis were selected based on distinct concentration differences for PM10 and NO_x, and on the completeness of the measured data for the parameters required for emission factor calculations. Rain data was not available for Reiden and was taken from nearby NABEL stations (Härkingen, Wynau).

4.2 Road Dust Sampling (Deposited Dust)

4.2.1 Goal

The road dust sampling campaign was intended for collecting road dust to study its composition and mass, and to learn about the characteristics of dust resuspended by traffic (and other activities). 8 sites were selected on roads with different traffic densities and characteristics within the city of Zurich, where the sampling could be done directly on the road surface without constricting the traffic too much.

4.2.2 Organizational Issues

The coordination of the sampling campaign was quite labor intensive. However, the support from the different authorities (City Police, Civil Engineering Department of the City and the Canton of Zurich) was quick and un-bureaucratic and facilitated the organization significantly. Advice for safety measures was obtained from the police (Figure 4.7).

For the sampling itself the traffic had to be by-passed around the sampling allotment. Measures to protect the personnel during the sampling consisted of an appropriate signalization and obstacles. A small truck with a flashing arrow was provided by the Civil Engineering Department of the City and accompanied the

sampling team to all sites in the city. A similar truck was provided by the Canton for the sampling in the Milchbuck tunnel. During the whole campaign the sampling team was in contact with the authorities by mobile phone. The necessary blocking of the lanes was scheduled to times when traffic density was reduced, e.g. in the early afternoon or at night. Rush hours were omitted.

Fig. 4.7: Typical installation of a sampling site (here: Duttweilerstrasse) with trucks and signalization.

Weather information was obtained freely from the internet and partly from MeteoSwiss. After a long standby time due to unfavorable weather conditions, a dry period began in February 2008, and a campaign alert was issued by eMail to all involved persons. Considering all technical, logistic and meteorological boundary conditions, the campaign start was issued for the 18th, and the campaign could take place from 18 – 20 February 2008.

4.2.3 Sampling Sites

The sampling campaign was carried out in as short a period as possible to avoid accumulation of road dust with time during the sampling period. This allowed for a comparison of the amount of mass and element concentrations of the selected sampling sites. Eight locations were selected with the aims of characterizing the urban area of Zurich and to better understand the factors controlling the mass and chemistry of the PM_{10} fraction of road dust in such an environment:

- Urban background sites were selected in order to detect background levels of traffic tracers (brake pads and tire wear, gasoline and diesel exhausts) and of construction work tracers (use of concrete and aggregates) and to obtain a road dust chemical profile next to the air quality monitoring station site (*Kaserne*).

- Sampling sites located in less busy (residential areas) and very busy roads of the city were chosen in order to evaluate the impact of traffic to the levels of pollutants, which are available for resuspension.

- A tunnel site (*Milchbucktunnel*) was selected to investigate a specific situation with high traffic volume, low brake frequency and minimal addition of dust from external sources.

The selected sites are listed in Table 4.5 and indicated in the map (Figure 4.8). All sites but one are in the flat area of the city. Milchbuck Tunnel is slightly inclined, and the sampling took place in the rightmost uphill lane.

Table 4.5: Listing of sites where road dust was collected in Zürich. Notice that some sites do not coincide with the road sections measured with the mobile laboratory.

No.	Name	Traffic characteristics (No. of vehicles in 24 h)	Road characteristics	Sampling date and time (CET)
1	Weststrasse	Heavy traffic during the day, only residential traffic during the night. (857)	Street canyon. Old surface with many repair patches, Asphalt concrete (AB12), year of application: 1995/98.	2008-02-19, 2100 – 2300 h
2	Schimmelstrasse	Heavy traffic. (1084)	Street canyon close to intersections. Old surface (2002), Stone Mastic Asphalt or Stone Asphalt.	2008-02-18, 2000 – 2200 h
3	Hardplatz	Heavy traffic (1273)	Open intersection. Bus stop. New surface (ca. 2006), Stone Mastic Asphalt.	2008-02-19, 1300 – 1500 h
4	Eichbühlstrasse	Residential traffic (not available)	Street canyon with trees. Old surface. Small construction site nearby.	2008-02-19, 1000 – 1200 h
5	Pfingstweidstrasse	Heavy traffic (1685)	Large buildings on one side, green open area with scattered small buildings on the other side. Old surface, many repair patches. Asphalt type: Asphalt concrete (AB 16), partly OB, HMT 25 or AB 11.	2008-02-18, 1600 – 1800 h
6	Duttweilerstrasse	Medium traffic (535)	Street canyon close to intersection. New surface (Nov. 2007), Stone Mastic Asphalt (11 PmB).	2008-02-18, 1300 – 1500 h
7	Milchbuck Tunnel	Heavy traffic (1237)	Tunnel.	2008-02-20, 1330 – 1530 h
8	Kaserne	No traffic. Urban background site. Sampling reduced due to beginning rain. (0)	Green courtyard surrounded by buildings. Old surface with cracks.	2008-02-20, 1600 – 1800 h

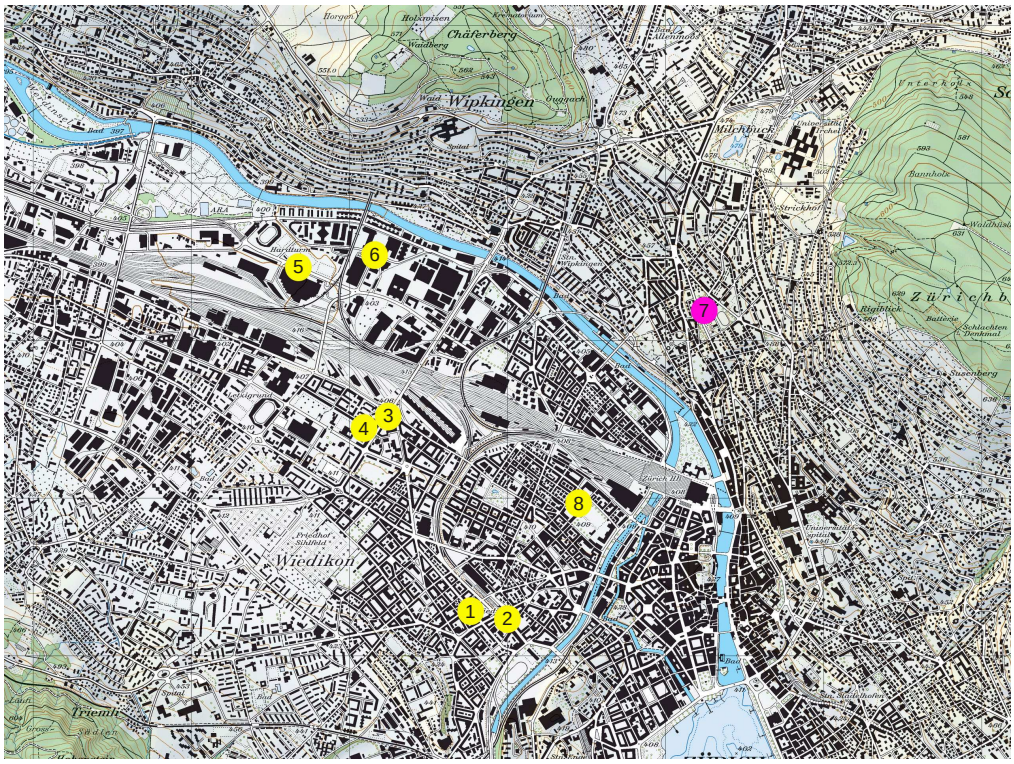

Fig. 4.8: Map of Zurich showing the sampling sites for dust collection. 1 – Weststrasse; 2 – Schimmelstrasse; 3 – Hardplatz; 4 – Eichbühlstrasse; 5 – Pfingstweidstrasse; 6 – Duttweilerstrasse; 7 – Milchbuck Tunnel; 8 Kaserne. © 2009 swisstopo (JD082777).

4.2.4 Weather Conditions

The key weather feature for a successful sampling campaign was a dry period of at least three consecutive days such that the road surfaces could completely dry out. This was typically not the case in late November, December and January. Only in February 2008 a longer dry spell began on the 6th, lasting until the 20th (Figure 4.9).

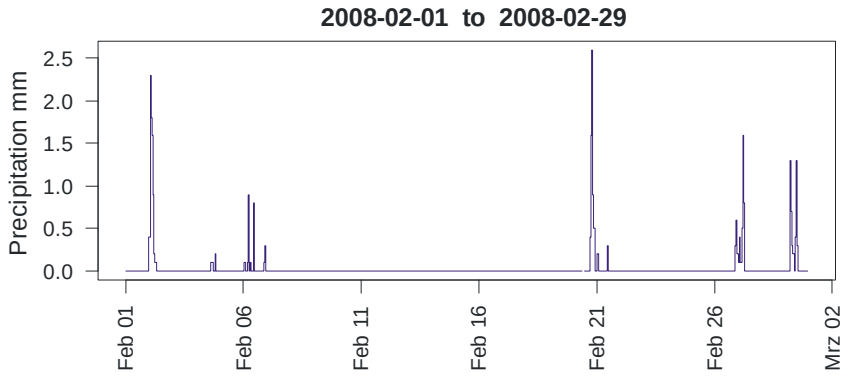

Fig. 4.9: 1-hour sums of precipitation in mm at the NABEL station Zürich-Kaserne for February 2008. Source: NABEL (BAFU and Empa).

During the sampling campaign the weather was dry and sunny until the afternoon of the third day, when an occluded front passed nearby and brought some rain after a dry period of 14 days. Daily maximum temperatures were between 8 and 10 ℃, which was ra ther mild for the season. Minimum temperatures were around or below 0 ℃ early in the morning, but not during the sampling times. During the whole period the ambient PM10 concentration was above the 1-day threshold of 50 µg m^{-3}. Winds were quite weak with wind speeds around 1 m s^{-1} until the afternoon of the 20th (see Figure 4.10).

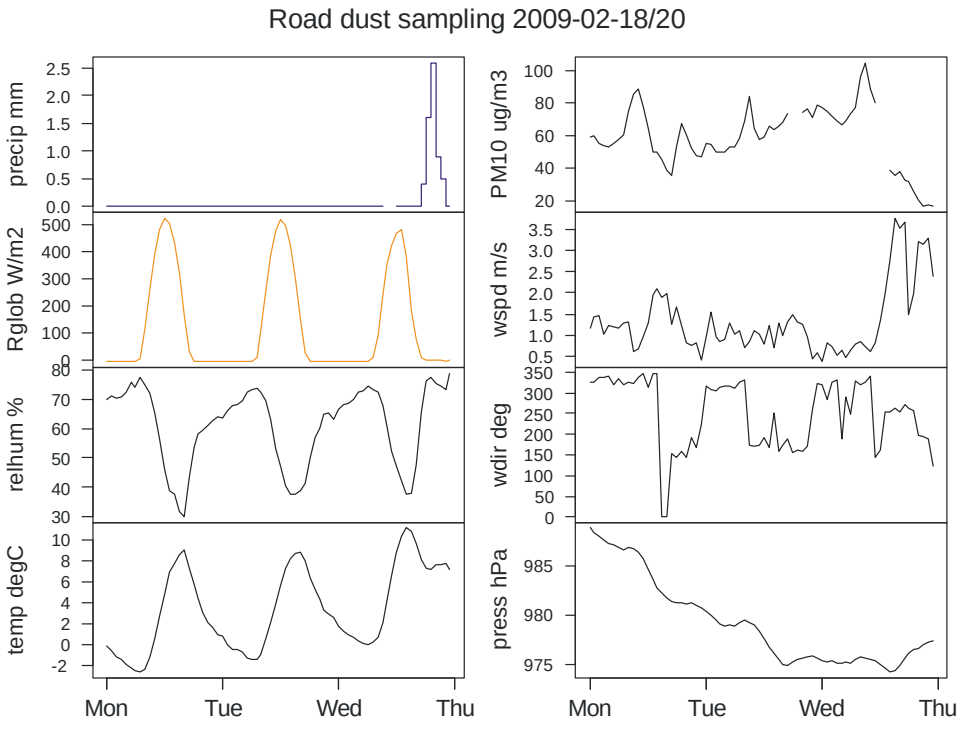

Fig. 4.10: Overview of the meteorological parameters and the PM10 concentration at the NABEL station Zürich-Kaserne. Precip: precipitation; Rglob: global radiation; relhum: relative humidity; temp: temperature; PM10: PM10 concentration; wspd: wind speed; wdir: wind direction; press: pressure. Source: NABEL (BAFU and Empa).

Depending on the orientation of the streets and the time of the day, some sampling was done in the shadow of the adjacent buildings (Pfingstweidstrasse, Eichbühlstrasse), while other sites were sampled in full sunshine (Duttweilerstrasse, Hardplatz). Schimmelstrasse and Weststrasse were sampled at night, the Milchbuck Tunnel in the early afternoon. The Gubrist Tunnel was planned for the last evening, but when the rain started in the afternoon, the traffic lanes were soon wetted throughout the tunnel, and sampling had to be cancelled.

4.3 Field Campaigns: Mobile Laboratory (Airborne Particles)

4.3.1 June 2007

A first series of measurements with the mobile laboratory Mosquita I of PSI was performed in Zurich in June 2007 (Table 4.6). The goal of the campaigns was to investigate the spatial distribution of aerosol at road level within the city.

This was the first deployment of PSI's newly acquired APS (Aerodynamic Particle Sizer), and the defective optical component was not yet recognized. Thus the APS data can only be discussed qualitatively for each test run. The AMS, on the other hand, operated well despite its also being deployed in the mobile laboratory for the first time. Another issue of the APS measurements was the optimization of the sampling frequency, which was finally set to 5 s. A sampling frequency of 60 s was too long and did not provide sufficient data points for each road section. 1-s sampling led to data acquisition problems on the notebook computer and regularly produced gaps in the time series. We therefore concentrate on the successful Mosquita test runs of 13 and 14 June 2007 for further analysis and discussion.

Table 4.6: Campaign overview of the June 2007 Mosquita I test runs.

Campaign	**20070608**	**20070611**	**20070612**	**20070613 morning**	**20070613 afternoon**	**20070614 morning**
Date	2007-06-08	2007-06-11	2007-06-12	2007-06-13	2007-06-13	2007-06-14
Start time, CEST	09:43:22	14:47:00	14:14:10	09:30:30	13:35:44	09:13:27
End time, CEST	12:02:22	17:54:46	17:13:10	11:51:01	17:21:30	12:44:47
APS sampling time, s	60	60	1	5	5	5
Number of APS samples	140	187	6553	1407	2260	2115

Mosquita I followed a prescribed route within the city (Figure 4.11) along roads with different traffic characteristics (heavy, moderate, residential traffic).

Weather conditions were very favorable for the measurements: A subtropical air mass led to cloudy, but dry summer weather with a weak pressure gradient and temperatures increasing from 23 to 30 ℃. Average humidity was 63%. Precipitation occurred on 11 June around noon and in the night from 14-15 June, when a front moved across Switzerland. Ozone concentrations reached values between 60 and 70 ppb, while peak PM10 concentrations were between 20 and 30 μg m^{-3} (Figure 4.12).

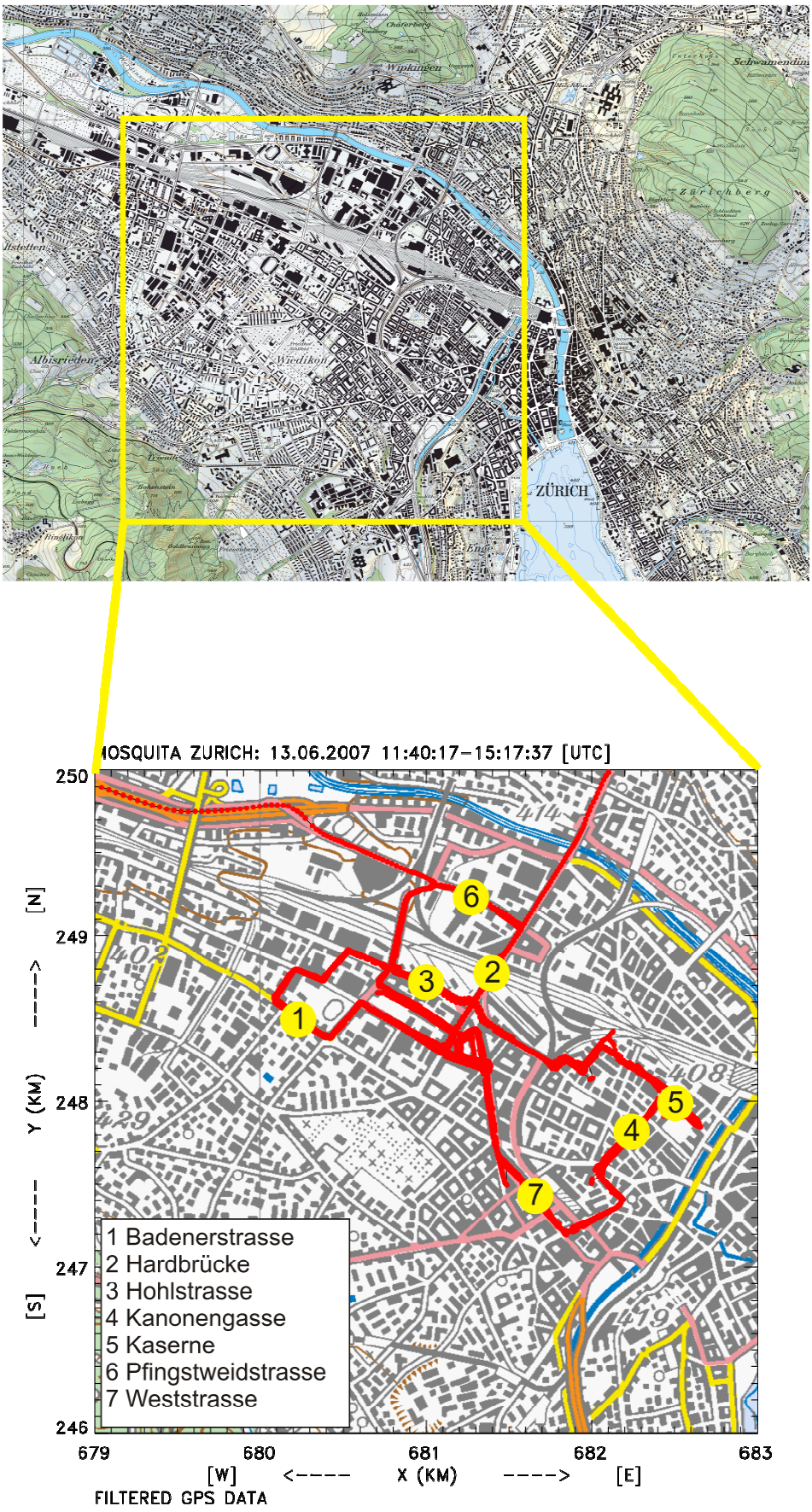

Fig. 4.11: Route of 2007-06-13 afternoon Mosquita test run in Zurich. © 2009 swisstopo (JD082777).

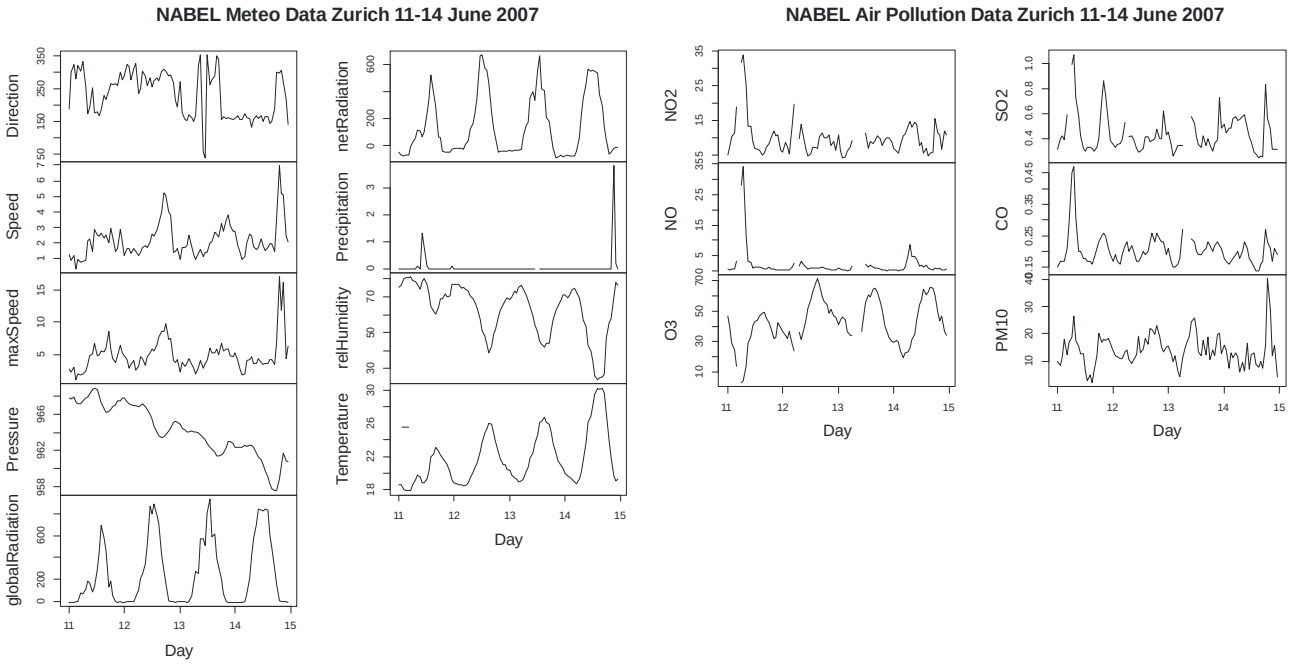

Fig. 4.12: 1-hourly meteo (left) and air quality (right) data from the NABEL station at Kaserne during the June 2007 field campaign. Source: NABEL (BAFU and Empa).

4.3.2 November 2007, February and November 2008

Additional test runs with Mosquita II were performed in November 2007, and in February and November 2008, the last one coinciding with the road dust sampling campaign (Figure 4.13). During these test runs, exclusively PM1 was sampled and chemically analyzed with the aerosol mass spectrometer (AMS). The results of these test runs were published elsewhere (Mohr et al. 2009). With respect to the APART objectives, the chemical composition of PM1 gives some clues on the composition of deposited and resuspended material as collected during the road dust sampling campaign. Therefore only data most relevant for APART are considered for this report and the focus will be put on the test run of 19 February 2008. On 19 February 2008 weather conditions were characterized by a weak bise situation (Wanner and Furger 1990) with a mean temperature of -2 ℃ in Zu rich, northeasterly winds and an inversion at a height of 1400-1600 m asl.

Fig. 4.13: Mosquita II test run on 19 February 2008. Road dust sampling is ongoing in the foreground at Eichbühlstrasse.

5 Results

5.1 Brake wear: Size distribution and emission factors

5.1.1 Average mass concentrations and temporal variability of antimony and other pollutants

In an increasing number of studies, airborne antimony in urban areas is being correlated with road traffic and more specifically with emissions emerging from brake wear (Furusjo et al. 2007; Furuta et al. 2005; Gomez et al. 2005; Grieshop et al. 2005; Hjortenkrans et al. 2007; Johansson 2008; von Uexkull et al. 2005; Weckwerth 2001). Besides steel as brake pad support material, the agents present in brake linings usually consist of Cu, Mo, Sn, Sb and Ba. Additionally, Zn has been reported to be a further constituent of brake wear, although it is a less specific marker for brake wear than the other elements (Johansson 2008). Lead (Pb) has largely been replaced in modern brake lining.

Antimony is present in brake pads as Sb_2S_3 and is oxidized to Sb_2O_3 at temperatures above 380 ^oC during the braking process. Sb_2O_3 is a compound that is categorized as a possibly carcinogenic substance and has been shown not to be soluble in water but partially soluble in physiological fluids (von Uexkull et al. 2005), therefore special attention is drawn to its atmospheric concentration levels. In laboratory experiments, abraded particles showed a size distribution with >90% within PM10 (Furuta et al. 2005; Thorpe and Harrison 2008; von Uexkull et al. 2005).

The trace element mass concentrations measured in Zürich and Reiden are listed in Tables 5.1.1 and 5.1.2. The antimony mass concentrations ranged from 1.6 ng m^{-3} (Reiden, sum of all size ranges) to 11.9 ng m^{-3} (Zürich-Weststrasse street canyon) and compare well with values reported in literature. In Tokyo, Sb mass concentrations in the size range 2-11 µm were 10±2 ng m^{-3} for wintertime and 5±2 ng m^{-3} for summertime (Furuta et al. 2005). In Buenos Aires, Sb mass concentrations ranged from 0.1 up to 20 ng m^{-3} (Gomez et al. 2005), and a concentration range from 1 up to 50 ng m^{-3} was reported for Valencia (Moreno et al. 2007).

Figure 5.1.1 shows a 12-day time series for PM10 and antimony at the street canyon site (Weststrasse) and the urban background site (Kaserne) in February 2007. The shown time period illustrates the build-up of a high pollution episode in Zürich after a rainfall period. This is a rather typical example for a wintertime inversion condition in Zürich. According to equation (1), the difference between the two measuring sites represents the mass concentration related to local traffic at the street canyon site (see equation 1). For PM10 this difference is rather small compared to the high background concentration, which consists of bulk contributions from all intra-urban and imported emission sources. Due to the inversion, the urban background was increasing rapidly over time. In contrast, the urban antimony background was quasi negligible, except in time periods with exceptionally high PM10 concentration levels (> 50 µg m^{-3}). This indicates a small net contribution of antimony to the intra-urban background aerosol. The antimony street canyon mass concentrations were dominated by the coarse mode, peaking during the day due to the local emissions and dropping down to near-zero values during the night. In contrast to ∆PM10, the amplitude of the ∆Sb peaks varied considerably from day to day (bottom plot). This indicates that antimony mass concentrations were strongly influenced not only by fresh vehicle emissions, but also by vehicle induced resuspension of road dust and accumulation of emissions within the street canyon.

Table 5.1.1: Elemental mass concentrations measured in Zürich-Weststrasse (urban street canyon) and Zürich-Kaserne (urban background). Only data with ΔNOx > 20 µg m^{-3} (street canyon minus urban background) were considered (dry time periods only). The values represent averages of 285 hourly values for Zürich (~ 12 days). Values in brackets indicate concentrations below the MDL[*b].

	Coarse mode (2.5-10 µm)			Intermediate mode (1-2.5 µm)			Submicron mode (0.1-1 µm)		
	MDL[*b]	Zürich-Weststrasse (street canyon)	Zürich-Kaserne (urban background)	MDL[*b]	Zürich-Weststrasse (street canyon)	Zürich-Kaserne (urban background)	MDL[*b]	Zürich Weststrasse (street canyon)	Zürich - Kaserne (urban background)
	ng m^{-3}	ng m^{-3}	ng m^{-3}	ng m^{-3}	ng m^{-3}	ng m^{-3}	ng m^{-3}	ng m^{-3}	ng m^{-3}
Si	11.2	299	210	5.01	60.5	82.3	2.21	17.6	18.5
P	7.73	27.3	12.6	3.46	7.94	7.66	1.52	15.8	19.2
S	5.48	201	156	2.45	101	119	1.08	274	359
Cl	3.88	473	331	1.74	97.8	91.3	0.77	10.4	12.5
K	1.88	87.6	77.2	0.84	29.4	44.1	0.37	62.4	70.9
Ca	1.27	658	517	0.57	134	192	0.25	27.9	23.2
Ti	0.47	8.01	6.33	0.21	2.45	3.06	0.09	7.95	0.64
Cr	0.18	7.72	3.25	0.08	2.24	1.71	0.04	0.72	0.47
Mn	0.15	18.6	10.7	0.07	5.88	5.43	0.03	2.23	1.82
Fe	11.11	1020	406	4.97	411	200	2.19	69.8	35.1
Cu	5.6	63.3	20.9	2.50	27.8	11.0	1.11	4.52	2.35
Zn	4.72	21.5	9.56	2.11	13.6	9.43	0.93	6.02	7.29
Sr	1.76	(1.58)	(1.18)	0.79	(0.67)	(0.41)	0.35	(<0.1)	(<0.1)
Zr	1.43	5.80	1.73	0.64	2.72	0.90	0.28	(0.31)	(0.10)
Mo	1.18	6.41	1.98	0.53	2.94	1.06	0.23	0.41	(0.17)
Sn	0.55	8.03	1.52	0.25	3.30	0.81	0.11	0.61	0.32
Sb	0.51	8.60	1.88	0.23	3.75	1.03	0.10	0.58	0.24
Ba	1.09	18.6	5.74	0.49	8.40	3.33	0.22	1.27	0.54
Pb	3.36	(2.81)	(1.36)	1.50	(1.46)	(1.06)	0.66	1.18	1.19

[*b] MDL (Minimal detection limit): Experimental detection limit as described in (19). The elements Si to Mn were determined at ALS (Berkeley National Laboratory), Fe to Pb at HASYLAB (Deutsches Elektronen-Synchrotron), see Section 3.

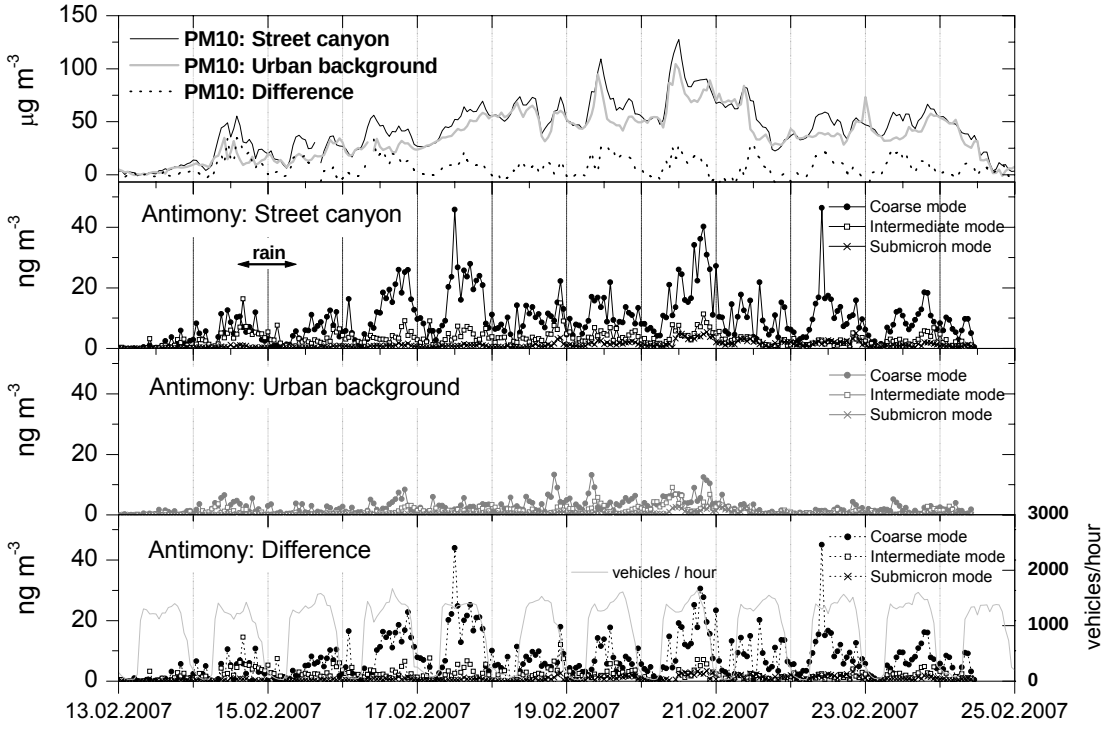

Fig. 5.1.1: Twelve-day time series showing hourly mass concentrations of PM10 (top panel) and size-segregated antimony (Sb, lower three panels) for an urban street canyon (Weststrasse) and an urban background site (Kaserne) in Zürich (Switzerland). Additionally, the difference between the street canyon and urban background mass concentration is shown (dotted lines). While there was only negligible heavy duty vehicle traffic during weekends (17.02 and 18.02), the light duty vehicle frequencies were similar to weekdays.

Table 5.1.2: Elemental mass concentrations measured in Reiden (rural freeway, both sides of freeway). The values represent averages of 97 hourly values (~ 4 days). Only data with ΔNO_x > 20 µg m^{-3} (downwind-upwind concentration) were considered (dry time periods only). Due to prevailing east wind conditions in Reiden during high-traffic periods (average wind speed 2.0 m s^{-1}), the west side station was predominantly downwind of the freeway with the above exclusion criteria. Values in brackets indicate concentrations below the MDL[*b].

	Coarse mode (2.5-10 µm)			Intermediate mode (1-2.5 µm)			Submicron mode (0.1-1 µm)		
	MDL[*b]	Reiden: Downwind	Reiden: Upwind	MDL[*b]	Reiden: Downwind	Reiden: Upwind	MDL[*b]	Reiden: Downwind	Reiden: Upwind
	ng m^{-3}	ng m^{-3}	ng m^{-3}	ng m^{-3}	ng m^{-3}	ng m^{-3}	ng m^{-3}	ng m^{-3}	ng m^{-3}
Si	5.60	254	251	2.51	123	131	1.10	45.4	41.4
P	3.87	22.1	19.1	1.73	12.8	10.9	0.76	31.8	40.0
S	2.74	145	145	1.23	196	163	0.54	660	839
Cl	1.94	358	226	0.87	24.0	23.1	0.38	3.15	2.75
K	0.94	108	106	0.42	53.5	56.9	0.19	56.3	70.9
Ca	0.64	424	402	0.28	123	145	0.13	19.3	15.5
Ti	0.23	7.90	6.48	0.10	3.60	3.81	0.05	0.94	0.81
Cr	0.09	2.02	1.59	0.04	1.23	0.96	0.02	0.44	0.35
Mn	0.08	6.75	6.09	0.03	3.51	3.27	0.02	1.55	1.46
Fe	5.56	165	122	2.48	94.3	67.2	1.10	21.7	23.5
Cu	2.80	10.4	8.37	1.25	6.00	4.21	0.55	1.58	2.59
Zn	2.36	7.31	7.72	1.06	6.65	5.58	0.47	3.55	9.98
Sr	0.88	(0.41)	(0.27)	0.39	(0.09)	(0.09)	0.17	(<0.01)	(<0.01)
Zr	0.71	1.77	1.91	0.32	0.98	0.77	0.14	0.27	0.23
Mo	0.59	0.84	(0.53)	0.26	0.49	0.35	0.12	0.13	0.21
Sn	0.27	1.28	1.04	0.12	0.78	0.50	0.05	0.33	0.53
Sb	0.26	0.92	0.58	0.11	0.59	0.35	0.05	0.16	0.27
Ba	0.55	2.95	2.13	0.24	1.82	1.17	0.11	0.37	0.50
Pb	1.68	(1.49)	(1.61)	0.75	1.06	1.12	0.33	1.17	1.77

[*b] MDL (Minimal detection limit): Experimental detection limit as described in (19). The elements Si to Mn were determined at ALS (Berkeley National Laboratory), Fe to Pb at HASYLAB (Deutsches Elektronen-Synchrotron), see Section 3.

5.1.2 Local trace element emissions at Zürich-Weststrasse

For antimony and the other brake wear related elements (Fe, Cu, Zr, Mo, Sn and Ba), the concentration differences between the roadside location and the defined background site were significantly larger than the urban background concentration (see Figure 5.1.1 for Sb) and were almost strictly positive in all size ranges (see Figures 5.1.3 and 5.1.4 for Zürich-Weststrasse and Reiden). This indicates that there were no relevant local emissions of these elements at the background site and that the spatial background homogeneity was constant and sufficiently high. These were boundary conditions for a reliable determination of the contribution of local emissions within the street canyon (see Section 5.1.3). Zn and Pb showed entirely positive differences for the coarse mode, but not for the other size ranges. All other elements showed both positive and negative differences and thus could not be exclusively related to fresh traffic emissions (for example Ca, due to local constructions at the background site).

For a systematic investigation of the temporal variability of local emissions within the street canyon, normalized and background corrected diurnal variations of NO_x, CO_2, black carbon (BC) in PM1, PM10, size-segregated antimony and coarse mode silicon are shown in Figure 5.1.2, along with the vehicle frequencies. The diurnal patterns for NO_x and BC(PM1) were highly correlated to the diurnal pattern for heavy duty vehicles, indicating that their emissions by the traffic fleet (approx. 10% heavy duty vehicles) were mostly dominated by high emissions from heavy duty vehicles. On the other side, CO_2 showed a better correlation to the diurnal pattern of light duty vehicles, which accordingly implies a high net emission contribution from light duty vehicles. The concentration decrease around 15:00, observed for all gaseous and aerosol species, was partly attributed to meteorology (see explanation in Figure 5.1.5 and 5.1.6).

For PM10 and antimony, only a partial influence of direct traffic emissions on the diurnal variations was observed. The morning increase of heavy duty vehicles is reflected in the diurnal patterns of PM10 and less pronounced also in submicron antimony. Moreover, an afternoon/evening maximum evolving in the diurnal patterns for intermediate and coarse mode antimony is correlated with the evening peak for light duty vehicles. Apart from that, the diurnal patterns of PM10 and antimony showed no exclusive correlation to traffic frequencies, but additionally exhibited a distinct midday maximum. A likely explanation for this midday maximum is an increased influence of wind speed induced resuspension of road dust, as well as the accumulation of fresh emissions and resuspended dust throughout the day within the street canyon. Street canyon specific coarse mode silicon, used as proxy for road dust resuspension (with reasonable background correction for the time period considered in Figure 5.1.2), was highly correlated to the wind speed within the street canyon and did not correlate with traffic numbers except for the initial traffic increase at 07:00. As seen from this distinct peak in wind speed with beginning morning traffic, the wind speed within the street canyon was not only triggered by meteorology, but indirectly also by the traffic fleet.

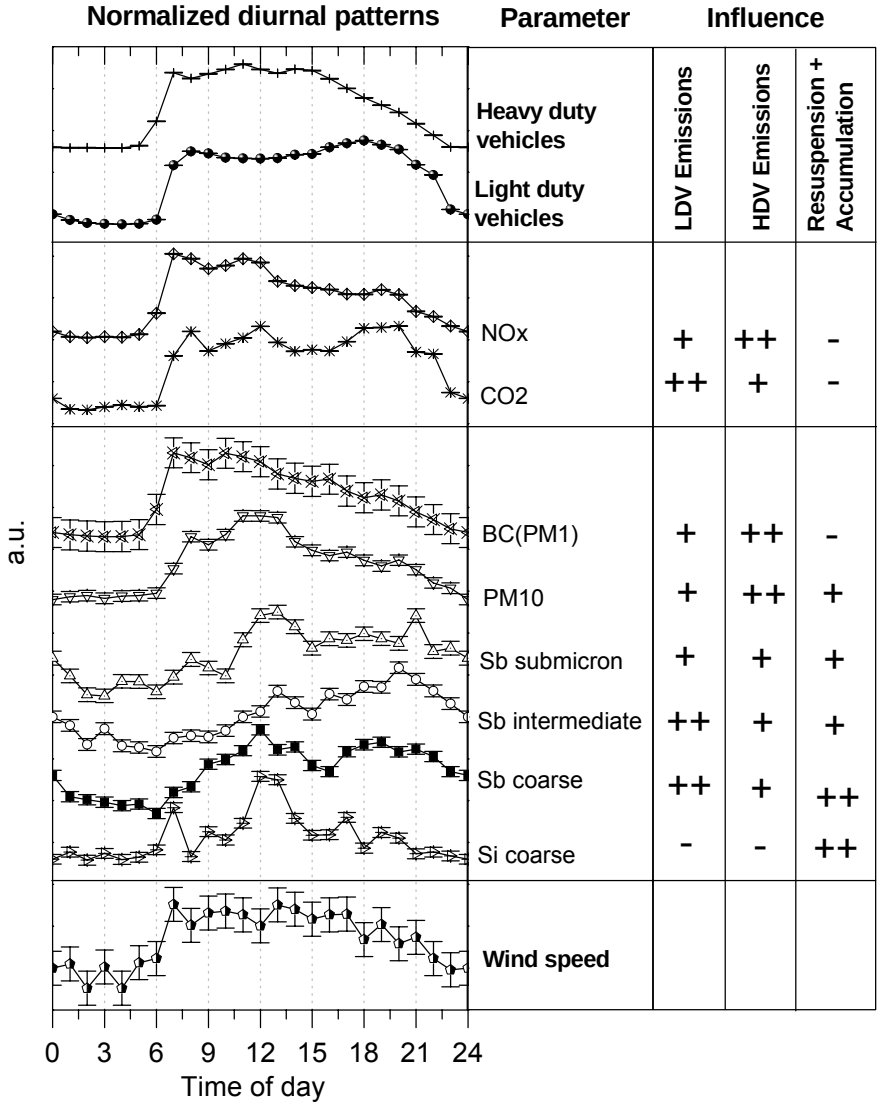

Fig. 5.1.2: Background corrected diurnal variations (Zürich-Weststrasse, 15 days in February and March 2007, weekdays and dry periods only, not identical to the time window shown in Figure 5.1.1). Diurnal variations were normalized to have comparable amplitudes. Error bars indicate the measurement precision. The meteorological conditions were comparable for the considered days (wintertime inversion layer). The categorization of the emissions in the right part is based on the discussion in the text.

Figures 5.1.3 and 5.1.4 shows boxplots for the trace elements measured in this study. For Fe, Cu, Zr, Mo, Sn, Sb and Ba the concentration difference is significantly positive for all size ranges, which confirms that these elements are most likely emitted by brake wear in the street canyon and along the freeway, and that they thus are exclusive tracers for their emission source. Cr, Mn, Zn and Pb show entirely positive differences in the coarse mode, but not for the other size ranges. All other elements show both positive and negative differences and thus cannot be exclusively related to fresh traffic emissions.

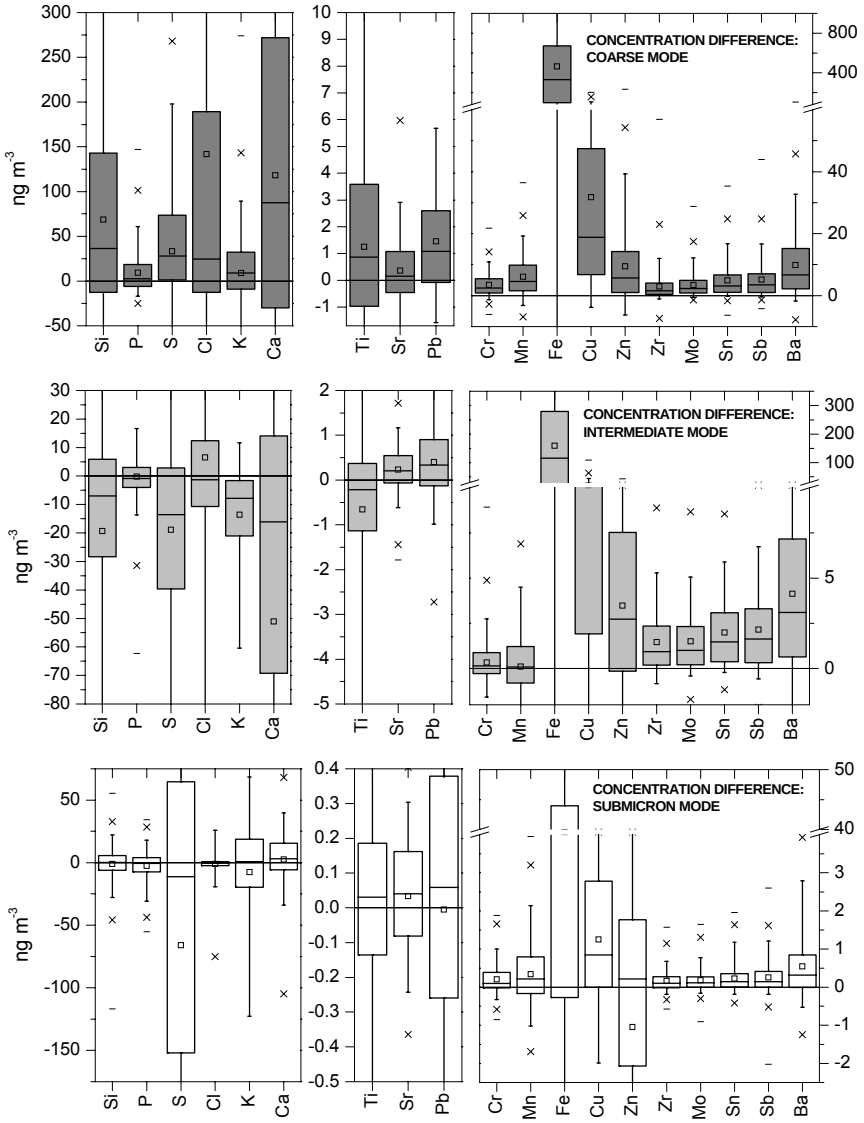

Fig. 5.1.3: Box plots for the background corrected street canyon mass concentrations of the measured trace elements (concentration difference between street canyon and background site) in Zürich-Weststrasse. Only time periods used for emission factor calculations were considered (15 days, dry periods only, weekdays and weekends, ΔNO_x > 20 µg m^{-3}). Boxes represent the 0.25-0.75 percentile range including median (line) and average (squares). The shown standard deviation is dominated by sample statistics rather than methodological uncertainties.

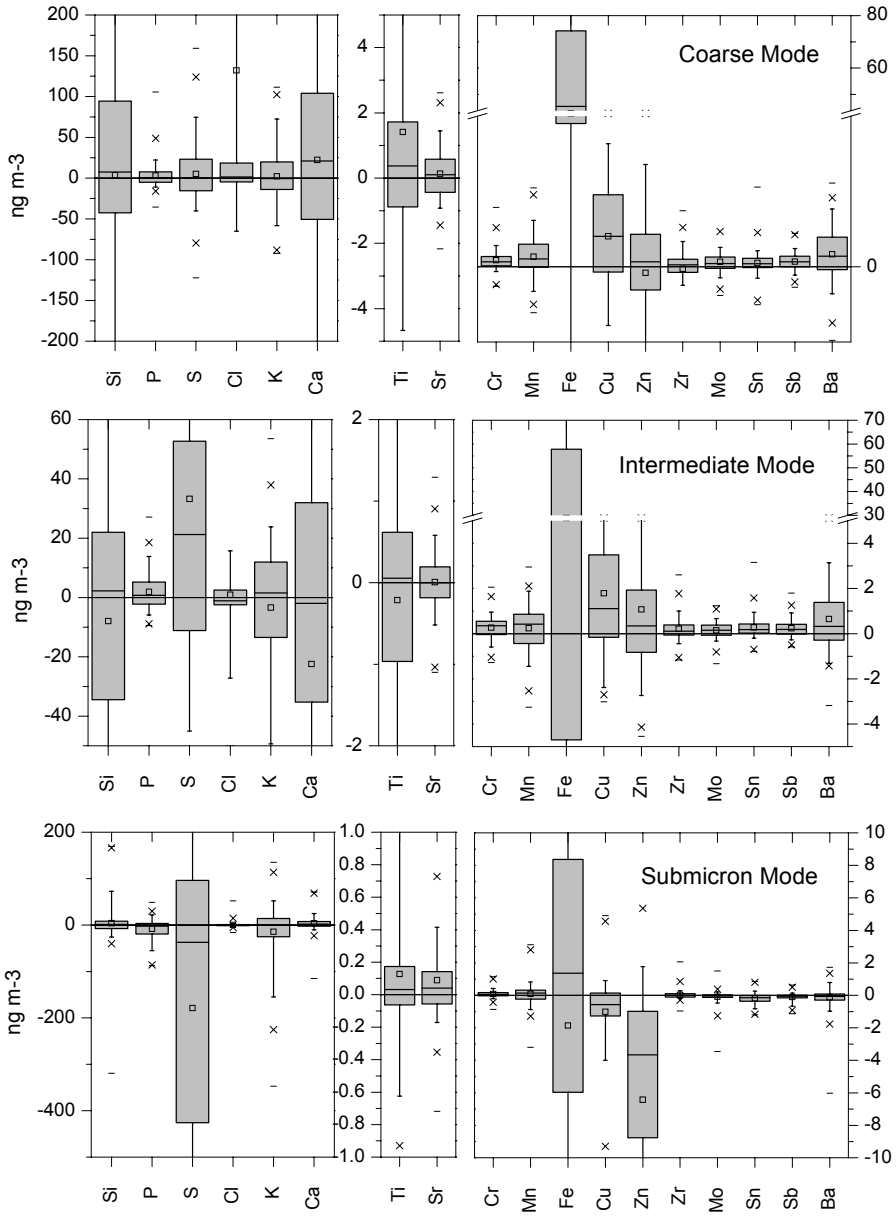

Fig. 5.1.4: Box plots for the background corrected mass concentrations of the measured trace elements in Reiden (upwind/downwind concentration difference). A: Coarse mode. Only time periods used for emission factor calculations were considered (4 days, dry periods only, weekdays and weekends, ΔNO_x > 20 µg m^{-3}). Boxes represent the 0.25-0.75 percentile range including median (line) and average (squares). The shown standard deviation is dominated by sample statistics rather than methodological uncertainties.

The relation of the diurnal PM10 and antimony mass concentration variation to the traffic frequency in the street canyon is shown in Figure 5.1.5 (15 days, dry weekdays only). While PM10 was enriched by a maximal factor of 1.5 within the street canyon during the day, coarse mode antimony was enriched by a factor of 3 to 6. The afternoon concentration decrease was attributed to meteorology, as explained in Figure 5.1.6. The urban courtyard site (Kaserne) was not directly influenced by any fresh contributions of traffic from Zürich-Weststrasse (distance 600 m) or other nearby roads, but was only exposed to urban background aerosol and local non-traffic related sources. The urban background aerosol contained mixed and diluted bulk contributions from all urban emission sources and thus also included diffuse contributions from dispersed urban traffic emissions. As a result, PM10 and antimony mass concentrations show a concentration increase at Kaserne in the morning, which is however slightly delayed compared to the average urban morning rush hour.

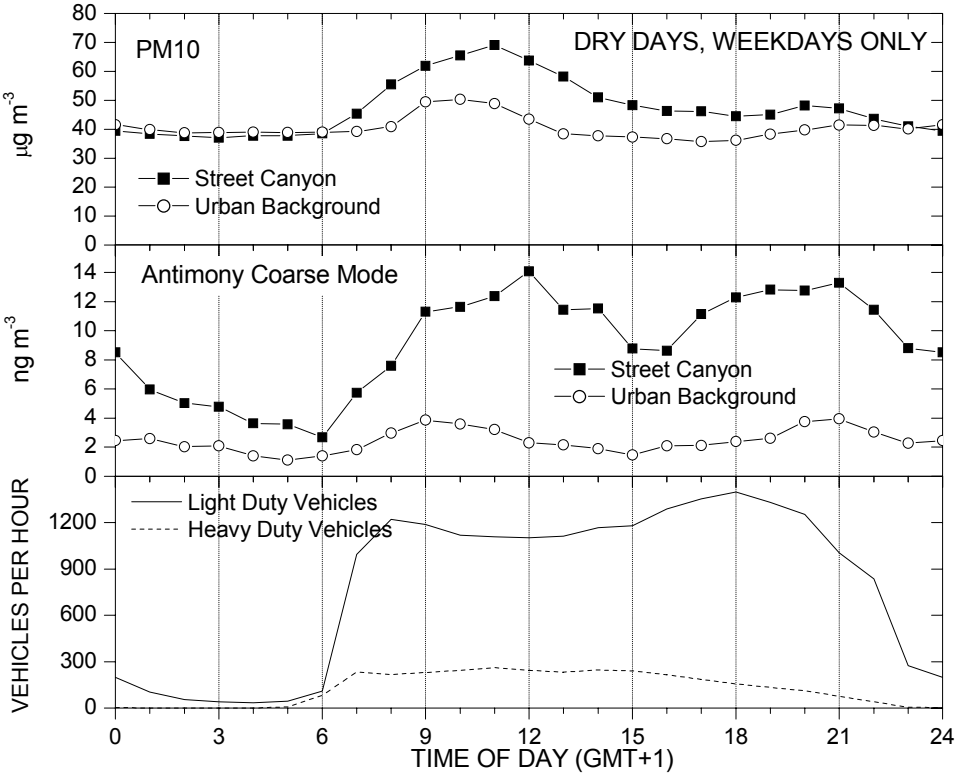

Fig. 5.1.5: Average diurnal variation for PM10 and coarse mode antimony (Zürich-Weststrasse, 15 days in February and March 2007, weekdays and dry periods only). The meteorological conditions were comparable for the considered days (wintertime inversion layer). The traffic frequency at the street canyon site (Zürich-Weststrasse) was 22 000 vehicles per day.

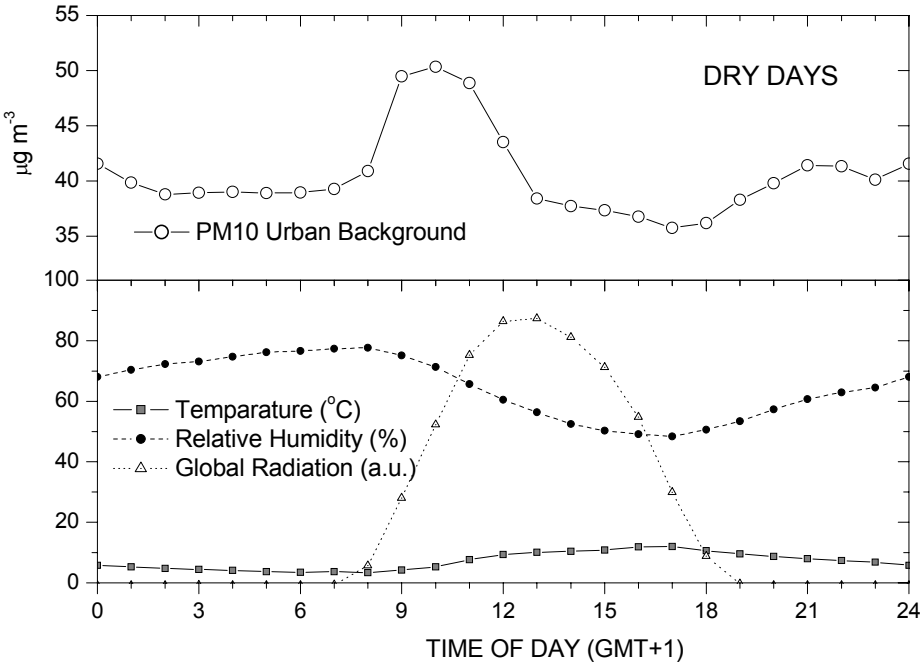

Fig. 5.1.6: The relation of the urban background PM10 mass concentration variation to meteorological parameters (15 days, dry weekdays only). The morning increase in both parameters reflects the advection of nearby emissions (traffic rush hour, industrial activities) to the urban background site. The rather drastic concentration drop in the afternoon was explained by the development of the boundary layer, which was triggered by the sunlight (global radiation) and higher temperatures. In the evening a new stable surface layer developed, again resulting in an enrichment of PM10.

The different temporal behavior of fresh vehicle emissions and road dust resuspension was also reflected in a time series correlation analysis for the background corrected elemental mass concentrations (Figure 5.1.7). A strong correlation within the considered group of brake wear associated elements was observed for all particle size ranges, which indicates that abrasion from brake pads was the dominating origin for these elements within the street canyon. The correlation between the brake wear associated elements and mineral elements related to road dust resuspension was weaker, because the brake wear associated elements were present both in fresh emissions as well as in resuspended dust with a different temporal evolution. Zn and Pb (not longer used in modern brake pads), which have been related to brake wear by several previous studies, are not correlated to the other brake wear tracer species, indicating a significant contribution of other sources for these elements. A thorough source apportionment by means of positive matrix factorization (PMF) is subject to further work and will be published elsewhere. A further group of correlated elements is formed by Si, K, Ca, Ti, Cr, and Mn and indicate mineral sources, road dust, corrosion (coarse mode), or combustion (submicron mode). Chlorine shows no relevant correlation to other elements and was assigned to time periods with road salting activities.

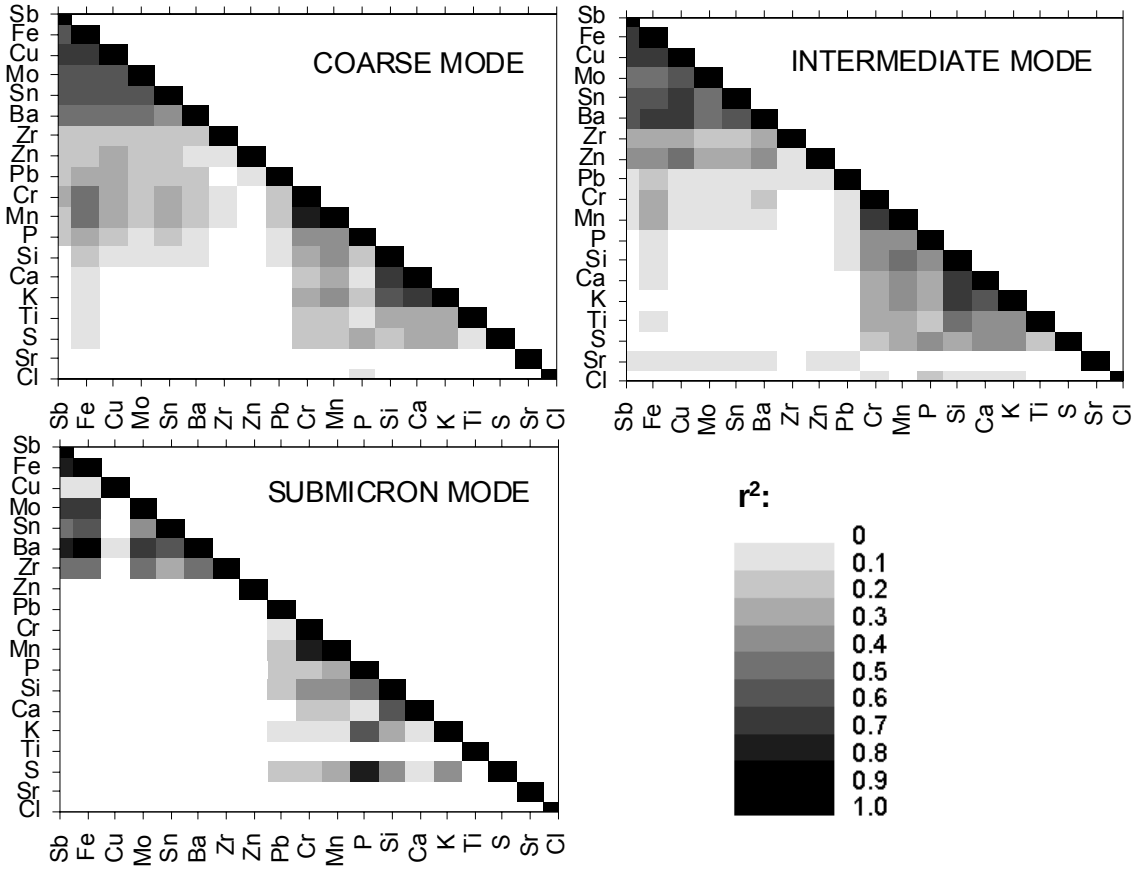

Fig. 5.1.7: Correlation matrices for the background corrected street canyon mass concentrations. The selected time period included 5x4 days in February and March 2007 and included all meteorological conditions. The squared Pearson correlation coefficients are displayed. Elements are sorted by their anticipated emission sources for better optical clarity.

5.1.3 Calculation of emission factors for brake wear associated trace elements

In the urban street canyon of Zürich-Weststrasse, the aerosol load was dominated a) by the local contribution of the road traffic, b) the urban background aerosol and c) other local sources. In contrast, the urban courtyard site (Kaserne) was not directly influenced by any fresh contributions of traffic from Zürich-Weststrasse (distance 600 m) or other nearby roads, but was only exposed to urban background aerosol and local non-traffic related sources. The urban background aerosol contained mixed and diluted bulk contributions from all intra-urban and imported emission sources and thus also included diffuse contributions from dispersed traffic emissions.

The mass concentration for pollutant *x* entirely related to the traffic emissions at the street canyon sampling site ($\Delta c_{x,local\ traffic}$) was assumed to be the difference between the mass concentration measured in the street canyon $c_{x,street\ canyon}$ and the mass concentration simultaneously measured at the urban background site $c_{x,urban\ background}$:

$$c_{x,local\ traffic} = c_{x,street\ canyon} - c_{x,urban\ background} \quad (1)$$

This hypothesis is only true if $c_{x,urban\ background}$ is adequately homogeneous within the spatial area comprising the street canyon and the background site, and if the background site is not significantly influenced by local emissions of the considered pollutant

These two bias scenarios were difficult to separate based on experimental data. For affected species, the sum effect of these scenarios will however result in reduced or negative concentration differences in equation (1).

For the freeway site (Reiden), $c_{x,\ freeway\ traffic}$ was accordingly defined as:

$$c_{x,\ freeway\ traffic} = c_{x,downwind} - c_{x,upwind} \quad (2)$$

In this case the subtraction of the local background is less prone to bias compared to the street canyon case.

The atmospheric dilution d of the vehicle related emissions from the point of emission to the sampler inlets was calculated using background corrected NO_x concentrations (ΔNO_x) and known NO_x emission factors valid for the considered location

$$d = \frac{EF_{NO_x,LDV} \cdot n_{LDV} + EF_{NO_x,HDV} \cdot n_{HDV}}{\Delta NO_x} \quad (3)$$

where n_{LDV}, $EF_{NO_x,LDV}$ and n_{HDV}, $EF_{NO_x,HDV}$ are the vehicle frequencies (vehicles h^{-1}) and NO_x fleet emission factors (mg km^{-1}) for light and heavy duty vehicles, respectively. Both for Zürich-Weststrasse and Reiden, reliable NO_x emission factors from emission inventories were available (Handbook of Emission Factors, see (INFRAS 2004)). The use of equation (3) implied that the dilution of the vehicle related emissions from the point of emission to the sampler inlets (on average 10 and 20 m for Zürich-Weststrasse and Reiden, respectively) was comparable for NO_x and the considered pollutants. To ensure robust dilution values, only hourly values with ΔNO_x > 20 µg m^{-3} (Zürich-Weststrasse – Reiden) were considered for subsequent emission factor calculations.

Emission factors for light duty vehicles (EF_{LDV}) and heavy duty vehicles (EF_{HDV}) were estimated for the individual species using multilinear fitting of the following equations:

Model A: $$c_{x,local\ traffic} = EF_{x,LDV} \cdot \left(\frac{n_{LDV}}{d} \right) + EF_{x,HDV} \cdot \left(\frac{n_{HDV}}{d} \right) + C \quad (4)$$

where $c_{x,local\ traffic}$ is the measured mass concentration difference (µg m^{-3}) of the considered species *x* (see equations 1 and 2) and C the fitting constant. Model A was only applicable for locations where $c_{x,local\ traffic}$ showed no autocorrelation. Time series of $c_{x,local\ traffic}$ exhibited relevant autocorrelation for antimony and other pollutants in the Zürich-Weststrasse street canyon, due to road dust resuspension and emission accumulation effects. To account for this, Model A was extended by a term representing the mass concentration measured one hour earlier (autocorrelation term):

Model B:

$$c_{x,local\ traffic,t=0} = EF_{x,LDV} \cdot \left(\frac{n_{LDV}}{d} \right) + EF_{x,HDV} \cdot \left(\frac{n_{HDV}}{d} \right) + f \cdot c_{x,local\ traffic,t-1} + C \quad (5)$$

where $c_{x,local\ traffic,t=0}$ is the measured mass concentration at a considered hour, $c_{x,local\ traffic,t-1}$ the mass concentration measured one hour earlier and f the respective fractional coefficient (obtained by the multilinear fit). The lag of one hour corresponded to the maximal time resolution of the trace element measurements.

In addition to the estimation of specific LDV and HDV emission factors, an average fleet emission factor ($EF_{x,Fleet}$) was calculated using (eq. 6):

$$EF_{x,Fleet} = \frac{c_{x,local\ trafic} \cdot d}{n_{tot}} \quad (6)$$

The fleet emission factor is valid for the average traffic composition during the considered time period and includes contributions from local emissions not directly correlated to vehicle frequencies such as road dust resuspension.

5.1.4 Assessment of the Emission Factor Calculation Models

The wind speed and traffic induced road dust resuspension as well as the accumulation of direct traffic emissions resulted in an autocorrelational behavior of the time series for the brake wear related elements. The autocorrelation functions (ACF) and partial autocorrelation functions (PACF) for NO_x, CO_2, BC(PM1) and PM10 showed no significant autocorrelation (correlation coefficient < 0.15), whereas coarse mode antimony showed a clear autocorrelation for lag 1 (1 hour, correlation coefficient 0.4) both in the ACF and PACF (for details see Figure 5.1.8). A systematic examination of the application of model A (eq. 4) and model B (eq. 5) for the emission factor calculation is presented in Table 5.1.3 Based on model test runs with the above parameters it was concluded that model B (eq. 5), by taking into account the autocorrelational behavior of the background corrected mass concentrations, provided more robust estimates for emission factors of brake wear related elements than model A (eq. 4). Since the contribution of resuspension and the accumulation of vehicle emissions are considered as separate sum parameter in this model (autocorrelation coefficient),

these emission factors represent fresh brake wear emissions for the stop-and-go situation within the street canyon.

To check the performance of the two models A and B, the NO_x emission factors, used as model input to calculate the dilution, were re-estimated by multilinear regression of (eq. 4) and (eq. 5), respectively. For all emission factor calculations presented in this paper, only hourly data for dry periods with $\Delta NO_x > 20$ µg m^{-3} were considered. For the upwind-downwind approach used for the Reiden freeway site only data with wind speeds higher than 0.5 m s^{-1} were used, while for the street canyon vs. urban background also lower wind speeds were considered.

Table 5.1.3 shows that the fits for CO_2, black carbon in PM1 (BC_{PM1}), for PM10 and for coarse mode antimony show that the autoregressive term becomes more relevant for more coarse-mode based parameters. For BC_{PM1}, the unexplained fraction is <10% using either of the models. The emission factors obtained by the two models are only slightly different and the quality of the fits is comparable (similar r^2 values, small and randomly distributed residuals). For PM10 the autoregressive term improved the fit quality from $r^2 = 0.42$ to $r^2 = 0.68$ and resulted in a negative fitting constant, reflecting the slightly negative mass concentration difference between Weststrasse and Kaserne (see Figure 5.1.5) during nighttime. In contrast to NO_x, BC_{PM1} and PM10, the model without the autoregressive term resulted in a very poor fit for coarse mode antimony. Introducing the postulated autoregressive term strongly improved the model solution. The unexplained fraction dropped from >40% to <20%, accompanied by an increase in r^2 from 0.10 to 0.45.

NO_x:

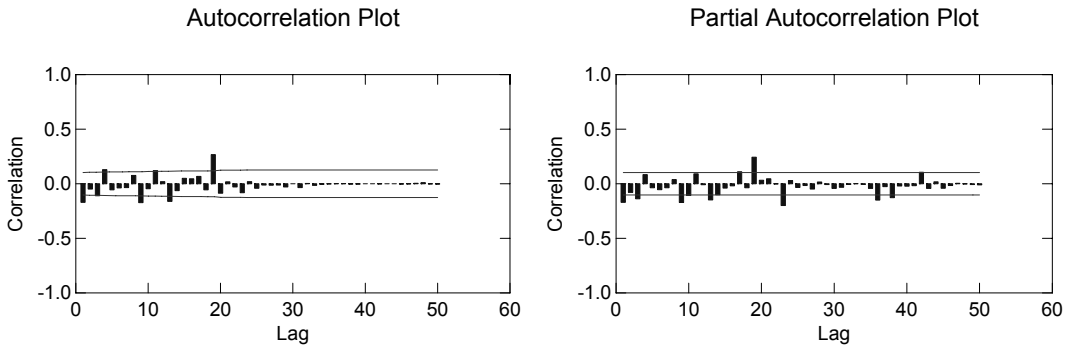

BC(PM1):

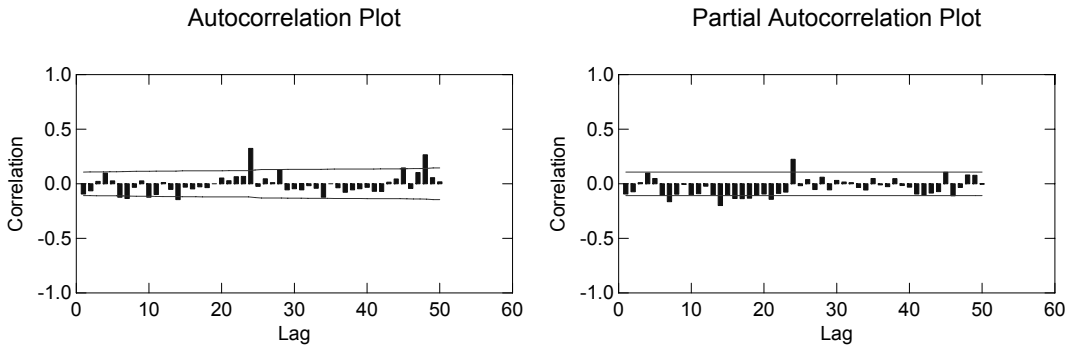

Fig. 5.1.8: Autocorrelation function (ACF) and partial autocorrelation function (PACF) plots for the time series used for emission factor calculations, obtained using the SYSTAT 10.0 software. The lag is expressed in hours. The time series were differenced once.

PM10:

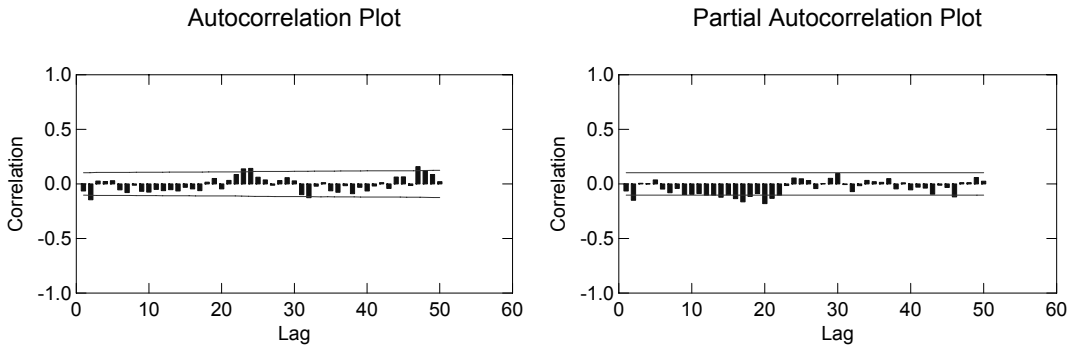

Sb coarse mode:

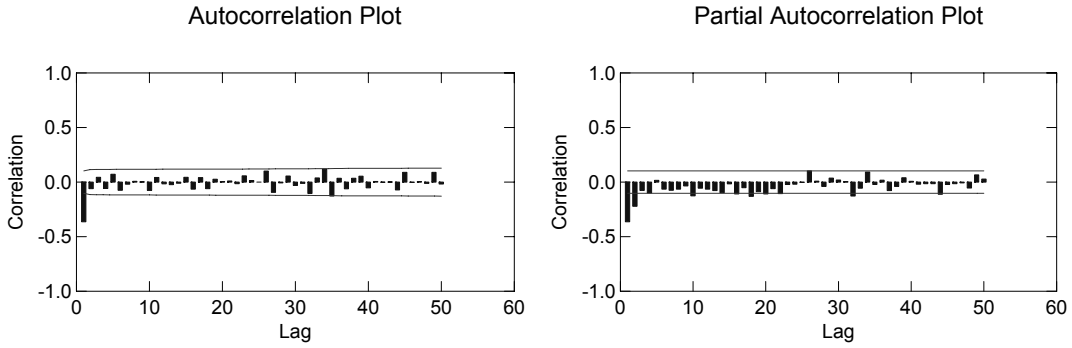

Fig. 5.1.8: continued

5.1.5 Emission factors for brake wear associated trace elements

The model results listed in Table 5.1.3 for Zürich-Weststrasse (street canyon) show that for Fe, Cu, Mo, Sn, Sb and Ba, the average contribution resulting from autocorrelation was 52% (coarse mode 49%, intermediate mode 47% and submicron mode 59%). The autocorrelation is likely related to the dynamic process of road dust resuspension followed by airborne accumulation within the street canyon. The high contributions that were obtained underline the major influence of this process within the considered street canyon. The fitting constant, accounting for additional contributions which are neither correlated with traffic nor follow the autocorrelation, explained further 25% (coarse mode), 29% (intermediate mode) and 8% (submicron mode), respectively. These non-zero fitting constants indicate that there may be additional minor local sources and/or that the selected model approach is not able to fully describe the road dust resuspension process.

Accordingly, the contribution of direct traffic emissions to the total site specific (background corrected) trace element mass concentrations was estimated by the model to be 27% (coarse mode), 24% (intermediate mode) and 33 % (submicron mode). These contributions were split into emission factors for light and heavy duty vehicles by the model. The propagated total uncertainty of the absolute emission factor values was rather high in many cases, influenced by large uncertainty ranges for the model fits and the experimental accuracy. Due to the high precision of the measurements (±5%), the multilinear regression model was at all able to resolve separate emission factors for LDV and HDV with sufficient significance of the model results. The propagated total uncertainty of the absolute emission factor values was rather high in many cases (75-100% for LDV and 46-84% for HDV), influenced by large uncertainty ranges for the model fits and the accuracy of the trace element measurements (±20%). Despite these high uncertainties, the absolute values were plausible and provided sufficient quality for further interpretation within the scope of this work. The

resulting emission factors are shown in Figure 5.1.9. Highest emission factors were found for Fe, Cu and Ba, followed by similar values for Zr, Mo, Sn and Sb and very low values for Pb. The average ratio between the emission factors for heavy and light duty vehicles was 9, 4 and 14 for the coarse, intermediate and submicron mode, respectively.

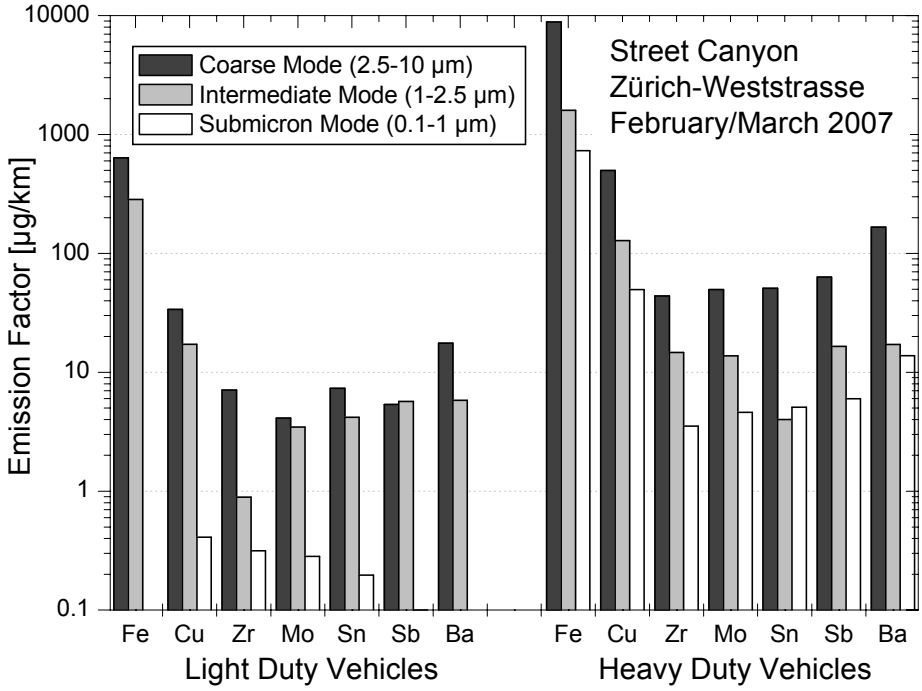

Fig. 5.1.9: Light duty vehicle (LDV) and heavy duty vehicle (HDV) emission factors (EF) for Zürich-Weststrasse (street canyon). The emission factors were calculated using equation (5), corresponding to model B. The input emission factors for NO_x were EF(LDV) = 286.8 mg km^{-1}, EF(HDV) = 10559 mg km^{-1} (INFRAS 2004). The calculation was performed using 209 hourly values (~ 9 days, ΔNO_x > 20 µg m^{-3}, dry time periods only). The average wind speed was 0.55 m s^{-1}. For Zn no emission factors were calculated because the significant presence of other sources for these elements did not allow for the determination of the contribution of local road traffic within the street canyon.

Figure 5.1.10 shows the average fractional size distribution of the LDV and HDV emission factors. The similar distribution for most of the considered elements suggests that these elements origin from the same source, i.e. from individual brake wear particles. Brake wear particles from light duty vehicles were distributed in the entire size range larger than 1 µm, while the contribution from the submicron mode was very low. In contrast, more than 75% of the brake wear emissions from heavy duty vehicles were found in the coarse mode (2.5-10 µm). An explanation of these different size distributions remains difficult, but is likely due to the different design and operating conditions of LDV and HDV brake systems. The found LDV size fractionation agrees with controlled abrasion experiments described in literature (Thorpe and Harrison 2008; von Uexkull et al. 2005), where the size distribution maximum of the brake dust was found to be in the range 1-5 µm. Other laboratory studies (Furuta et al. 2005) found 70% of brake pad dust in the 0.5 – 2 µm size range and only 30 % in the 2-11 µm size range.

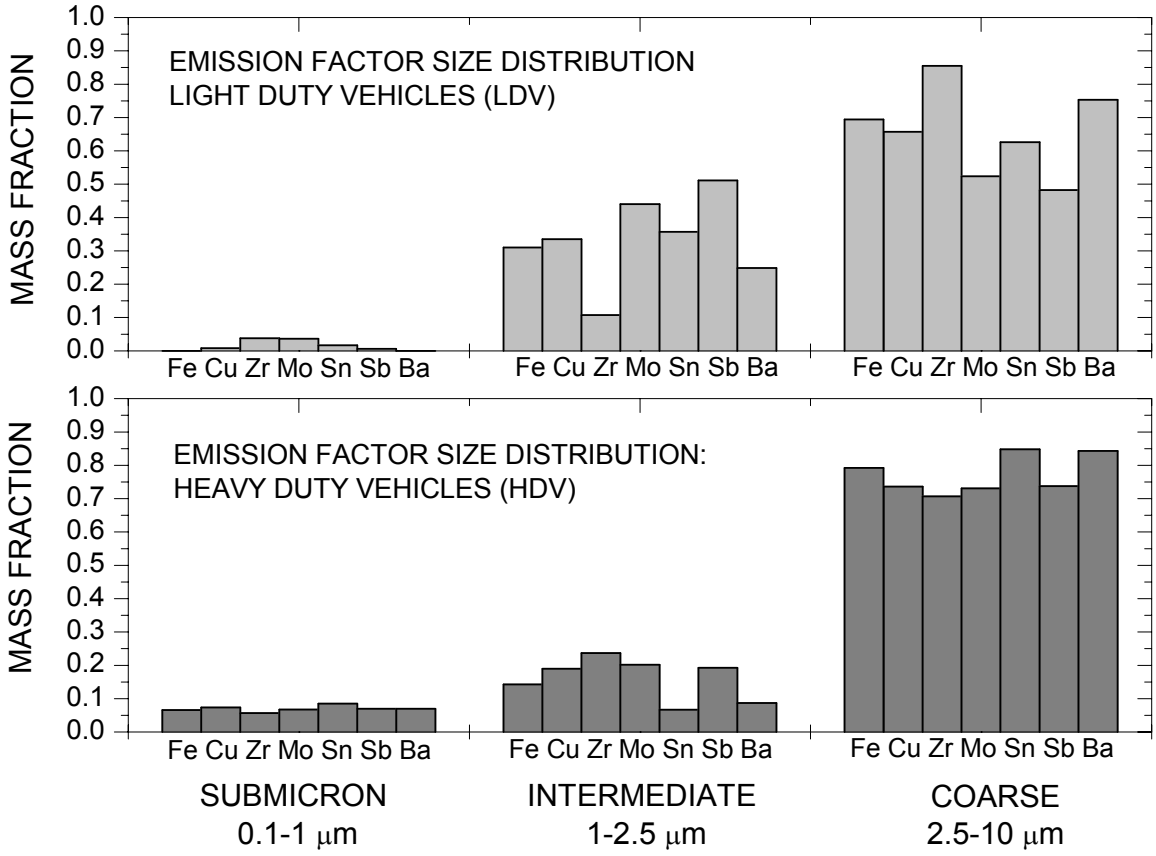

Fig. 5.1.10: Fractional size distribution for LDV and HDV emission factors determined for brake wear related trace elements and stop-and-go traffic in Zürich-Weststrasse (street canyon). The indicated size contributions were calculated from mean emission factor values determined by the multilinear model.

For the freeway site outside of Zürich (Reiden), the downwind-upwind mass concentration difference for the brake wear related elements was measurable but very low (see Figure 5.1.4), since no significant amount of fresh brake wear was expected to be produced by the free-flowing freeway traffic. The only non-zero contributions of the brake wear related elements along the freeway were expected due to resuspension of road dust or due to a steady spin-off of previously deposited brake wear particles from the wheel rims. Compared to Zürich-Weststrasse, the background subtraction was less bias prone due to the simultaneous upwind/downwind measurements. Since the concentration differences were small and even the mass concentrations themselves were close to or below the experimental detection limit (MDL) for some elements, a separate determination of LDV and HDV emission factors was not feasible. Average fleet emission factors for Reiden are listed in Table 5.1.5.

Figure 5.1.11 shows fleet emission factors for Zürich-Weststrasse (10% heavy duty vehicles) and Reiden (15% heavy duty vehicles). For Zürich-Weststrasse, fleet emission factors were calculated a) using equation (6) and b) using the determined LDV and HDV emission factors. The calculation of fleet emission factors according to equation (6) also includes road dust resuspension or other source contributions. As a consequence, the fleet emission factors for Zürich-Weststrasse and Reiden calculated with equation (6) cannot be interpreted as specific values for brake wear emissions, but rather have to be considered as very rough estimates of net emission factors for brake wear and resuspension. The fleet emission factor containing both brake wear and resuspension was up to 11 times higher for Zürich-Weststrasse compared to Reiden. This factor decreases to 2.7 if the isolated brake wear fleet emissions from Zürich-Weststrasse are compared to the total fleet emissions in Reiden.

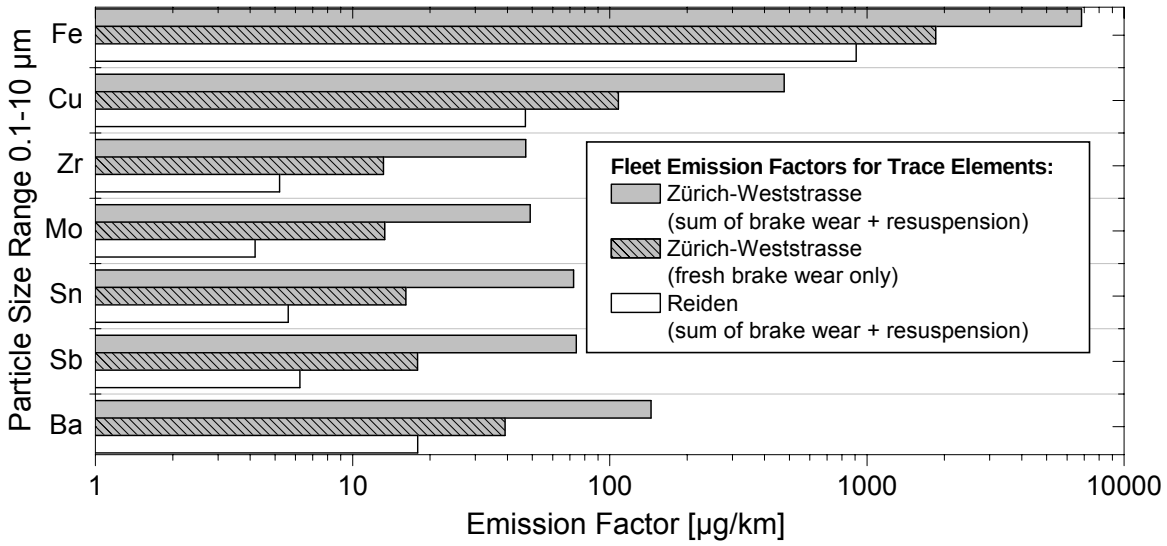

Fig. 5.1.11: Sum fleet emission factors (particle size range 0.1 - 10 µm) for Zürich-Weststrasse (10% HDV) and Reiden (15% HDV), for trace elements associated to brake wear. The values for Zürich-Weststrasse were calculated from experimental data from February and March 2007 (9 days, dry time periods only), while the values for Reiden refer to October 2007 (4 days, dry time periods only).

The antimony average fleet emission factors for Zürich-Weststrasse (88 µg km^{-1} including resuspension, 19 µg km^{-1} without resuspension) and Reiden (8.1 µg km^{-1}) fit well in the range of values reported in literature. A recent study Johansson (2008) found a value of 144 µg km^{-1} for a street canyon in Stockholm, and for two roadway tunnels in Sweden values of 32 µg km^{-1} (Tingstad tunnel) and 51 µg km^{-1} (Lundby tunnel) were reported (Sternbeck et al. 2002). Moreover, the relative elemental patterns for the brake wear related elements were not only similar for both sites considered in this study, but compare also well with other real-world data (see detailed comparison in Figure 5.1.12). Despite large compositional differences for individual brake pads there is a high degree of agreement within the real-world results and emission inventory values.

The reported set of elemental emission factors for LDVs and HDVs, split in three health-relevant particle size classes, contributes towards a better understanding of brake wear emissions. Beside brake wear directly emitted by vehicles, resuspension of road dust has been found highly relevant in the street canyon in Zürich-Weststrasse. While the process of resuspension itself is partly caused by the traffic induced turbulence, the amount of resuspendable dust is limited by the local deposition of dust from different sources to the road surface (atmospheric deposition of urban aerosol, dust introduced by dirty wheels or losses from truck loadings, debris from plants). For traffic situations with low traffic and plenty of resuspendable dust on the road surface a direct correlation between resuspension and vehicle counts is likely. However, in streets with high traffic frequencies like Zürich-Weststrasse the emissions from resuspension are limited by the amount of resuspendable dust. The model used in this work represents an attempt to distinguish the contribution of resuspension from the contribution of direct traffic emissions, but more advanced models and concepts for emission factor calculations will have to be developed in future work.

Table 5.1.3: Emission factors (EF) for light duty vehicles (LDV) and heavy duty vehicles (HDV), calculated for gas phase and aerosol parameters using two different multilinear calculation models (models A (eq. 4) and model B (eq. 5)). The input emission factors for NO_x were specifically estimated for Zürich-Weststrasse (Year: 2007, EF(LDV) = 286.4 mg km^{-1}, EF(HDV) = 10559 mg km^{-1}, NO_x calculated as NO_2, based on emission inventories (INFRAS, 2004). The average wind speed was 0.55 m s^{-1}, ΔNO_x > 20 µg m^{-3}. *The emission factor values presented in this Table are based on a data subset which was specifically selected to test the individual statistical calculation models. It is not representative for the entire campaign and must therefore not be compared to the final PM10 and exhaust emission factors presented in Section 1 and to the refined emission factors for Sb in Tables 5.1.4 and 5.1.5.*

Parameter	Location	Model	Unit	EF LDV	Model error	EF HDV	Model error	Auto-correlation fraction	Model error	Constant	Model error	Average difference	Fraction explained by constant (%)	R^2	Direct traffic Influence	Autocorrelation (resuspension+ enrichment)	Background subtraction	Fit Quality	EF Solutions
CO_2	Weststrasse	B	g/km	183	28	1771	160	0.25	0.04	3.1	3.2	58.5	5	0.62	high	low	appropriate	good	robust
		A	g/km	232	29	1998	165			9.9	3.2	58.5	17	0.57	high		appropriate	good	robust
	Reiden	B	g/km	166	17	511	66	0.11	0.06	25.0	2.9	46.5	54	0.78	distinct	negligible	high unexplained contributions	good	robust
		A	g/km	166	17	531	66			30.1	1.2	46.5	65	0.77	distinct		high unexplained contributions	good	robust
BC(PM1)	Weststrasse	B	mg/km	2.45	1.08	230.8	8.7	0.09	0.03	0.17	0.14	3.36	5	0.90	dominant	negligible	appropriate	very good	very robust
		A	mg/km	2.53	1.10	247.6	6.5			0.28	0.14	3.36	8	0.89	dominant		appropriate	very good	very robust
	Reiden	B	mg/km	9.80	2.38	94.1	9.8	0.07	0.06	0.01	0.19	1.85	0	0.67	dominant	negligible	appropriate	very good	very robust
		A	mg/km	9.78	2.39	97.9	9.2			0.10	0.17	1.85	6	0.67	dominant		appropriate	very good	very robust
PM10	Weststrasse	B	mg/km	9.1	6.7	385	42	0.56	0.04	-1.35	0.76	9.13	-15	0.68	medium	considerable	background partly higher	good	robust
		A	mg/km	9.7	8.9	629	51			0.91	0.99	9.13	10	0.42	medium		background partly higher	fair	weak
	Reiden	B	mg/km	2.1	15.8	206	61	0.40	0.09	1.99	1.13	7.17	28	0.34	medium	considerable	some unexplained contributions	poor-fair	weak
		A	mg/km	14.4	17.0	259	65			3.37	1.18	7.17	47	0.20	medium		some unexplained contributions	poor	weak

Sb coarse	Weststrasse	B	µg/km	9.8	6.3	74.0	34.6	0.61	0.05	0.94	0.68	7.07	13	0.45	medium	high	appropriate	fair	robust
		A	µg/km	35.2	7.6	35.3	43.8			2.76	0.84	7.07	39	0.10	medium		appropriate	weak	weak
	Reiden	B	µg/km	3.2	1.9	17.1	7.4	0.11	0.11	-0.13	0.14	0.31	-43	0.17	medium	low	background partly higher	weak	weak
		A	µg/km	3.3	1.9	19.1	7.1			-0.13	0.14	0.31	-41	0.16	medium		background partly higher	weak	weak
Sb intermediate	Weststrasse	B	µg/km	6.6	2.6	8.7	14.6	0.55	0.05	0.52	0.29	2.96	18	0.38	medium	high	appropriate	fair	robust
		A	µg/km	15.0	3.0	-18.6	17.3			1.48	0.33	2.96	50	0.09	medium		appropriate	weak	weak
	Reiden	B	µg/km	2.0	1.4	2.5	5.4	0.49	0.09	-0.04	0.10	0.24	-15	0.29	medium	high	background partly higher	weak	very weak
		A	µg/km	3.1	1.6	4.8	6.2			-0.02	0.12	0.24	-9	0.06	medium		background partly higher	weak	very weak
Sb submicron	Weststrasse	B	µg/km	0.0	0.4	7.1	2.5	0.68	0.04	0.06	0.05	0.38	14	0.51	medium	high	appropriate	fair	robust
		A	µg/km	0.7	0.6	9.5	3.5			0.20	0.07	0.38	52	0.05	medium		appropriate	weak	weak
	Reiden	B	µg/km									-0.10			below MDL				
		A	µg/km									-0.10			below MDL				
Si coarse	Weststrasse	B	µg/km	-54	271	4540	1566	0.60	0.05	-10.0	30.4	90.1	-11	0.39	negligible	high	background partly higher	fair	meaningless
		A	µg/km	-228	339	6651	1954			39.9	37.9	90.1	44	0.04	negligible		background partly higher	weak	meaningless
	Reiden	B	µg/km	-334	421	2734	1695	0.50	0.10	26.3	30.8	60.4	44	0.29	negligible	high	high unexplained contributions	weak	meaningless
		A	µg/km	-64	480	3449	1944			30.4	35.4	60.4	50	0.04	negligible		high unexplained contributions	weak	meaningless

Table 5.1.4: Elemental emission factors (EF) for light duty vehicles (LDV), heavy duty vehicles (HDV) and average fleet for Zürich-Weststrasse (street canyon). The emission factors for LDV and HDV were calculated using model B (eq. 5), while the average fleet emission factors were obtained by eq. (6). The input emission factors for NO_x were EF(LDV) = 286.8 mg km^{-1}, EF(HDV) = 10559 mg km^{-1}, NO_x calculated as NO_2, based on emission inventories (INFRAS, 2004). The calculation was performed using 209 hourly values (~ 12 days, ΔNO_x > 20 µg m^{-3}, dry time periods only). The average wind speed was 0.55 m s^{-1}. Values in brackets indicate concentrations below the MDL[*1]. For Zn and Pb only coarse mode emission factors could be determined due to background correction constraints (see text).

		Average Difference (Δc)	MDL[*1]	Emission Factor LDV (EF_{LDV})		Emission Factor HDV (EF_{HDV})		Auto-regressive term *f*		Unexplained	R^2	Emission Factor Average Fleet (EF_{tot})[*a]	Emission Factor Average Fleet (EF_{tot})[*b]
		ng m^{-3}	ng m^{-3}	µg km^{-1}		µg km^{-1}		--		%		µg km^{-1}	µg km^{-1}
Coarse mode (2.5-10 µm)	Fe	614	11	635.9	±583.7	8854.8	±3288.0	0.62	±0.05	10	0.44	4893.4	1383.8
	Cu	42.4	5.6	33.7	±49.9	496.8	±277.7	0.48	±0.06	29	0.26	330.7	75.9
	Zr	4.09	1.43	7.1	±6.1	43.8	±34.7	0.36	±0.07	33	0.16	32.3	10.4
	M	4.43	1.18	4.1	±4.4	49.7	±24.7	0.66	±0.06	11	0.43	34.1	8.3
	Sn	6.53	0.549	7.3	±7.6	50.9	±43.1	0.51	±0.06	28	0.28	50.5	11.3
	Sb	6.74	0.512	5.4	±6.5	63.1	±35.9	0.65	±0.05	15	0.45	51.0	10.6
	Ba	12.9	1.1	17.6	±14.1	166.2	±79.5	0.51	±0.06	19	0.30	100.3	31.1
Intermediate mode (1-2.5 µm)	Fe	211	5.0	284.3	±271.6	1596.0	±1541.8	0.63	±0.05	14	0.43	1685.3	403.7
	Cu	16.7	2.5	17.2	±18.8	128.2	±106.4	0.59	±0.06	21	0.36	130.6	27.3
	Zr	1.83	0.639	0.9	±2.7	14.7	±15.1	0.33	±0.07	52	0.12	13.3	2.1
	M	1.89	0.526	3.5	±2.0	13.7	±11.1	0.50	±0.06	17	0.30	13.3	4.4
	Sn	2.49	0.245	4.2	±2.5	4.0	±14.3	0.57	±0.06	23	0.36	19.7	4.2
	Sb	2.72	0.229	5.7	±2.8	16.5	±15.7	0.53	±0.06	15	0.36	20.6	6.7
	Ba	5.08	0.489	5.8	±6.4	17.1	±36.0	0.47	±0.06	36	0.25	39.5	6.8
Submicron mode (0.1-1 µm)	Fe	34.6	2.2	-3.8	±58.4	731.3	±331.3	0.66	±0.05	8	0.47	247.6	63.1
	Cu	2.17	1.11	0.4	±3.7	49.6	±21.0	0.64	±0.05	6	0.42	15.3	4.9
	Zr	(0.208)	0.282	(0.3)	±0.4	(3.5)	±2.3	0.46	±0.06	17	0.23	(1.6)	(0.6)
	M	0.243	0.232	0.3	±0.4	4.6	±2.1	0.56	±0.06	5	0.37	1.7	0.7
	Sn	0.290	0.108	0.2	±0.5	5.1	±2.6	0.60	±0.05	13	0.40	2.3	0.6
	Sb	0.348	0.101	0.1	±0.5	6.0	±2.6	0.62	±0.05	14	0.45	2.5	0.6
	Ba	0.732	0.216	0.0	±1.1	13.8	±6.4	0.67	±0.05	8	0.46	5.2	1.2
Coarse mode	Zn	12.0	4.7	-0.6	±19.9	268.5	±112.3	0.28	0.06	45	0.13	94.3	23.9
	Pb	(1.88)	3.36	(5.7)	±2.9	(0.1)	±0.1	0.30	0.07	33	0.12	(14.6)	(5.2)

[*a] Brake wear and resuspension, related to an average HDV fraction of 0.1.
[*b] Brake wear only, related to an average HDV fraction of 0.1.
[*1] MDL (Minimal detection limit): Experimental detection limit (see also Table 5.1.1)

Table 5.1.5: Average fleet emission factors (EF) for Reiden (rural site next to freeway), obtained using eq. (5). The input emission factors for NO_x were EF(LDV) = 448 mg km^{-1}, EF(HDV) = 5421 mg km^{-1}, NO_x calculated as NO_2, based on emission inventories (INFRAS, 2004). The calculation was performed using 97 hourly values (~ 4 days, ΔNO_x > 20 µg m^{-3}, dry time periods only). The average wind speed was 2.0 m s^{-1}. Calculations were only possible for the coarse and intermediate mode, due to negative concentration differences across the freeway as a bias from nearby fine particle sources. Values in brackets indicate concentrations below the MDL[*1].

		Average Difference (Δc)	MDL[*1]	Emission Factor Average Fleet (EF_{tot})[*a]
		ng m^{-3}	ng m^{-3}	µg km^{-1}
Coarse mode (2.5-10 µm)	Fe	43.4	5.60	557.4
	Cu	(2.02)	2.80	26.6
	Zr	n.a.[*c]	0.714	2.6
	Mo	(0.318)	0.588	2.6
	Sn	(0.248)	0.274	2.7
	Sb	0.343	0.256	3.7
	Ba	0.822	0.547	11.9
	Zn	n.a.	2.361	350.8
	Pb	(0.001)	1.68	20.5
Intermediate mode (1-2.5 µm)	Fe	27.0	2.50	2.6
	Cu	1.79	1.25	1.6
	Zr	0.215	0.319	3.0
	Mo	(0.144)	0.263	2.5
	Sn	0.276	0.123	6.0
	Sb	0.242	0.114	28.6
	Ba	0.650	0.245	<0.1
	Zn	1.076	1.056	0.1
	Pb	(0.116)	0.75	<0.1

[*a] related to an average HDV fraction of 0.15.
[*1] MDL (Minimal detection limit): Experimental detection limit (see also Table 5.1.1)
[*c] n.a.: negative concentration difference

Figure 5.1.12 compares elemental patterns for brake wear related elements, including results from this and other studies. For this specific comparison, the individual elemental patterns are normalized to Cu=1, because Cu is a brake pad component which is not expected to have encountered a significant change in application within the last years. In contrast, the growing concern about limited antimony resources has led to extended efforts by material engineers to reduce the use of antimony in brake pads. Despite the different nature of the experiments reported in literature (real-world studies versus laboratory studies), the Sb/Cu ratio does not vary more than an order of magnitude. In contrast, there are large differences within the other elements. The variation is particularly large for single brake pad investigations, reflecting that manifold brake pad formulations have been used by different manufacturers over the years. Despite this heterogeneity there is a high degree of agreement within the real-world results and the emission inventories, indicating a rather uniform geographical distribution of the different brake pad types.

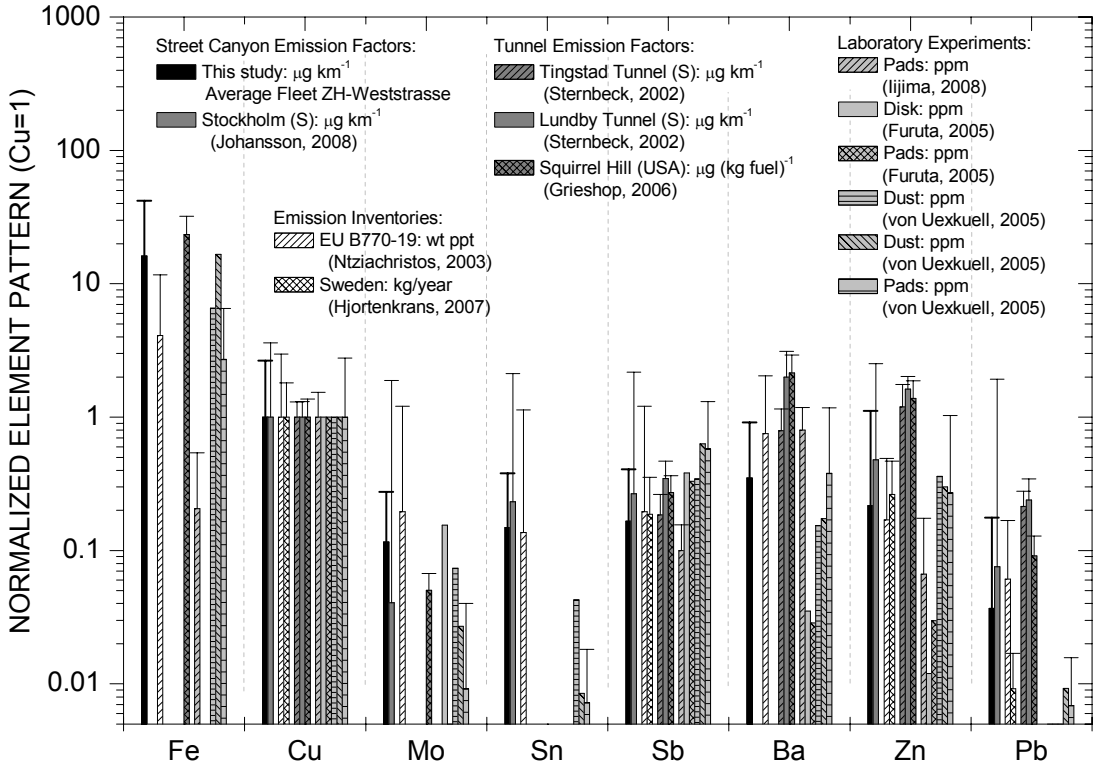

Fig. 5.1.12: Literature comparison for the elemental patterns of brake wear related trace elements. Reported emission factors and mass fractions were normalized to Cu=1.

5.2 Road Wear and Resuspension

Figure 5.2.1 shows a typical particle size distribution obtained during the abrasion experiments with the mobile load simulators. The particle concentrations of the air at the sampling point during operation of the simulator are clearly different from the concentrations in the ambient air. The difference of these two distributions represents the size distribution of the produced abrasion particles. As expected it is clearly shifted towards the coarse side compared to the size distribution in the ambient air.

In Figures 5.2.2 – 5.2.5 the trends of the PM10 concentrations before, during and after the mobile load simulator experiments are illustrated. The measurement cycle of the APS monitor was selected to be 6 min for MMLS experiments and 5 min for MLS experiments in order to ensure stable particle counts for all size classes. Thus every data point in the bar plots represents a measuring time of 5 or 6 minutes. As described in the instrumental section every minute the investigated pavement is overrun by 125 single wheels (MMLS measurements) or 100 double wheels (MLS measurements). This is important to get an impression of how much time or how many wheel passages are needed to remove the resuspendable dust from the road surface after the start of the simulator. In all Figures red bars indicate measurements of ambient air, i.e. the simulators were not operating. The black bars indicate measurements during operation of the simulators.

Figure 5.2.2 shows the measured PM10 concentrations during a measurement with the MLS on an AC pavement in relatively poor condition with an already slightly damaged surface. While measurements of ambient air showed low particle concentrations, very high concentrations can be observed during the first minutes after setting the simulator into operation. This initial peak is clearly caused by resuspension of dust on the road surface which was already deposited there before the experiment. After some time the concentrations decreased and leveled off on a concentration level still clearly above the ambient air concentrations. The difference between this final concentration and the ambient concentration can be interpreted as the freshly produced abrasion particles. Together with the results of the tracer gas measurements PM10 emission factors were calculated (Table 5.2.1).

Figure 5.2.3 shows a similar experiment performed on two different days with the MLS on an AC pavement in good condition. On the first day (26 May) the MLS had to be stopped after only 3 measurement cycles (15 min) due to break-down of the MLS. After fixing work on the MLS the particle measurements could be continued on 28 May when the MLS was already in operation for approx. 1 hour. After 7 APS measurement cycles (35 min) the MLS broke down again. Nevertheless important conclusions can be drawn from these few measurements. Again the initial particle concentrations (26 May) were quite high compared to ambient air, indicating again resuspension of previously deposited dust. When the measurements were resumed on 28 May (after the MLS had already been in operation for some time) only slightly higher concentrations compared to ambient air were observed. Also here PM10 emission factors were calculated (Table 5.2.1).

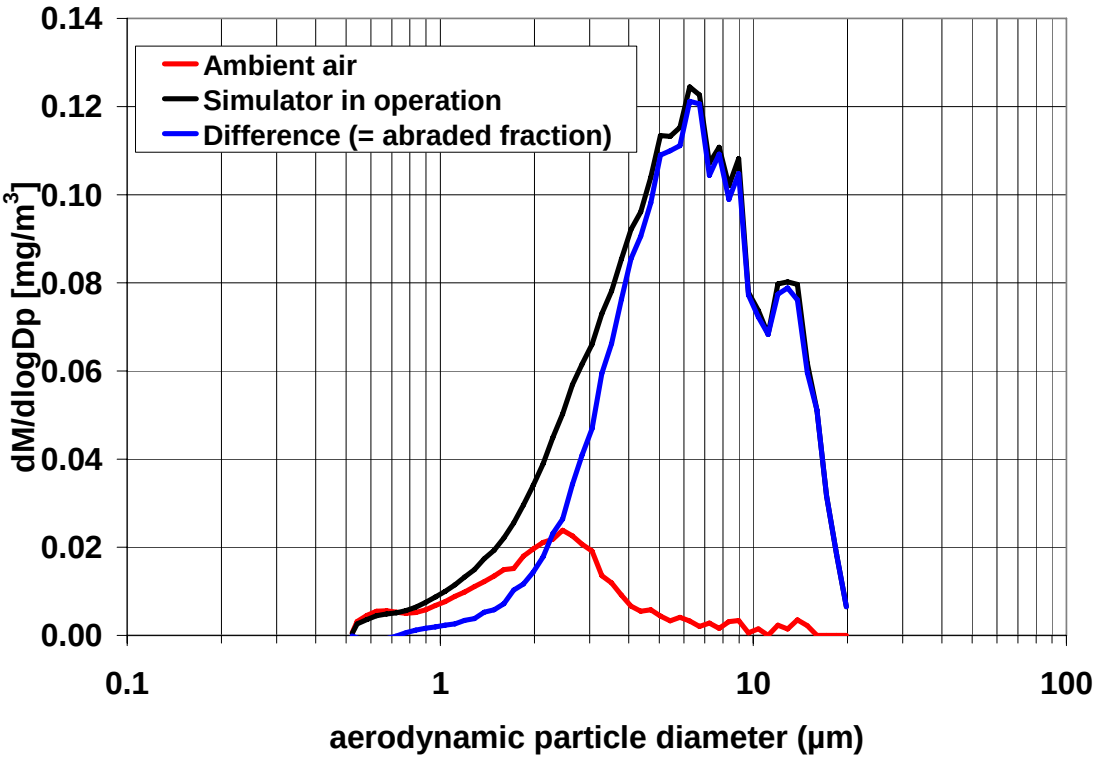

Fig. 5.2.1: Typical particle size distribution obtained from an experiment with the mobile load simulator, during a measurement period with dominating abrasion (negligible resuspension). The size distribution of the abrasion particles is clearly shifted towards the coarse side compared to the ambient size distribution.

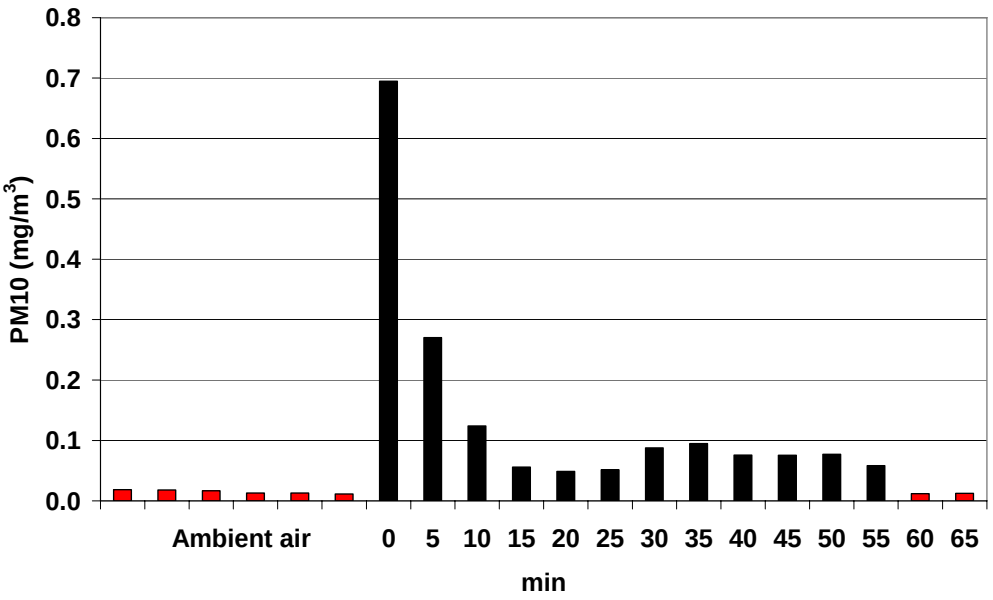

Fig. 5.2.2: Trend of resuspended and abraded particles during an experiment with the MLS (simulating HDV) on a AC pavement in relatively poor condition with an already slightly damaged surface. Every bar in the plot represents 5 min measurement with a total of 500 double wheel passages. Red bars indicate measurements of ambient air, without operation of the MLS.

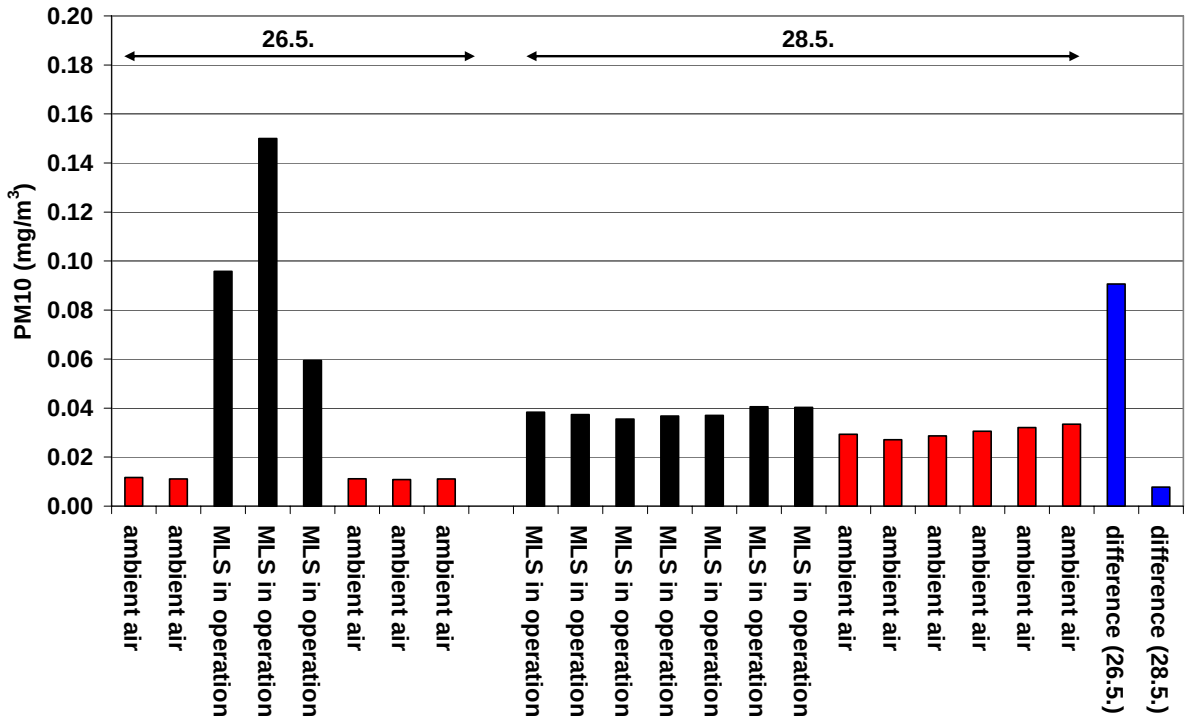

Fig. 5.2.3: MLS measurements (simulating HDV) on AC pavement in good condition (26.5. mainly resuspension, 28.5. fresh abrasion, see explanation in the text above). Every bar in the plot represents 5 min measurement with a total of 500 double wheel passages. Red bars indicate measurements of ambient air, without operation of the MLS.

Figure 5.2.4 shows the time trend of a MMLS abrasion experiment on a new AC pavement. Again the higher concentrations at the beginning of the experiment caused by resuspension of earlier deposited dust are clearly visible. The concentrations then decrease and level off only slightly above the ambient air concentration indicating only low contribution from fresh abrasion particles. In Figure 5.2.5 the same measurements on a new PA pavement are illustrated. Elevated concentrations shortly after the start of the simulator again indicate particle resuspension, however less pronounced compared to the measurement on the AC pavement. After some time PM10 concentrations were only slightly higher than the ambient air concentrations. Two measurements during this period show distinctive higher concentrations. A possible explanation for this fact could be that from time to time some grains are broken out from the porous surface of the PA pavement causing a sudden detachment of particles for a short time. Nevertheless, even considering these events, the contribution of fresh abrasion particles is quite low as were also the corresponding calculated emission factors (Table 5.2.1).

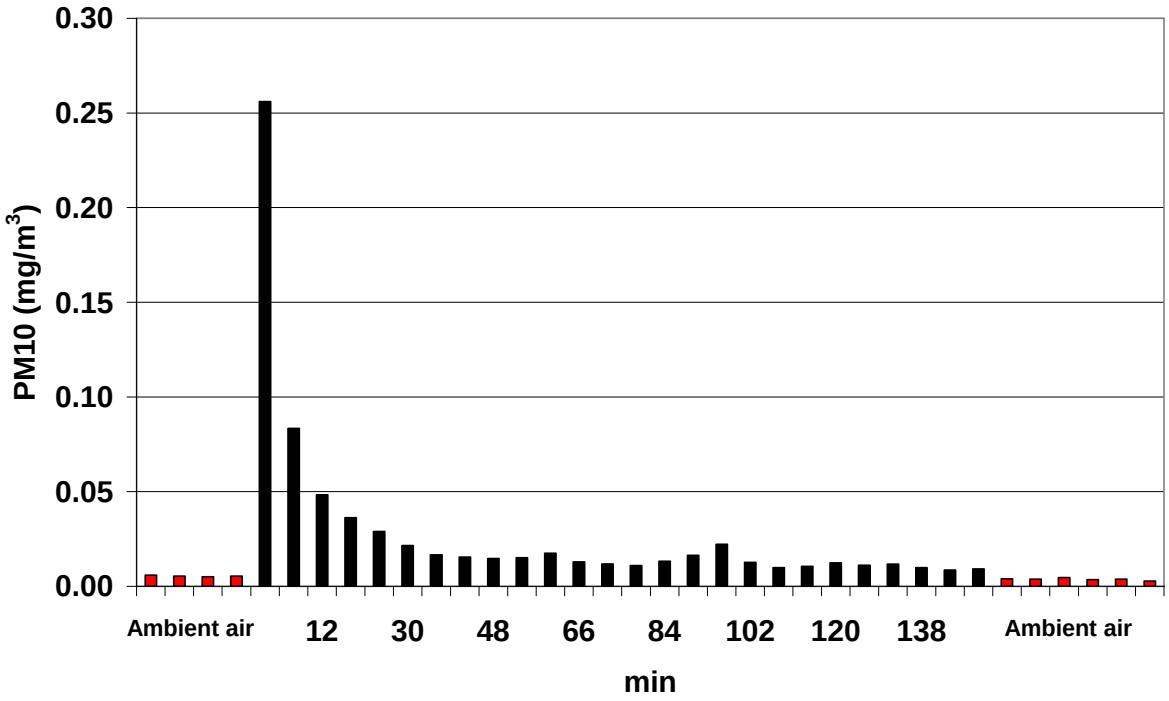

Fig. 5.2.4: MMLS (simulating LDV) abrasion experiments on a new asphalt concrete pavement. Every bar in the plot represents 6 min measurement with a total of 750 single wheel passages. Red bars indicate measurements of ambient air, without operation of the MMLS.

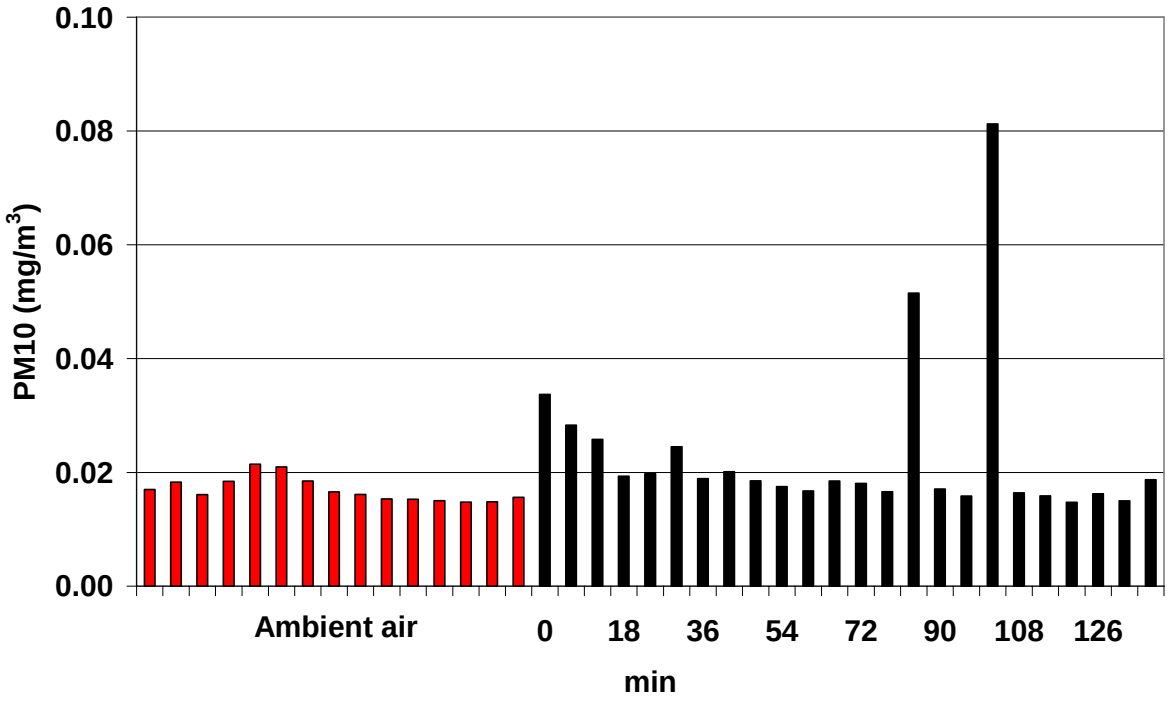

Fig. 5.2.5: MMLS (simulating LDV) abrasion experiments on a new porous asphalt pavement. Every bar in the plot represents 6 min measurement with a total of 750 single wheel passages. Red bars indicate measurements of ambient air, without operation of the MMLS.

Table 5.2.1 gives an overview of the emission factors calculated as described in the "Instrumentation and Techniques" section. The emission factors were calculated omitting the first measurement cycles dominated by resuspension thus using only the measurement cycles after a more or less stable emission was reached. The estimates for LDV and HDV were determined from the emission factors per wheel with the assumption of a linear relation between load, number of wheels/vehicle and emission, i.e.:

- EF for LDV from MMLS measurements: 12 times EF/wheel (4 wheels/vehicle, 3 times higher load/wheel)
- EF for HDV from MLS measurements: 10 times EF/wheel (10 wheels/vehicle, same load/wheel)

Table 5.2.1: PM10 emission factors for fresh particle abrasion derived from the load simulator measurements.

Type of mobile load simulator	MMLS (LDV)	MMLS (LDV)	MLS (HDV)	MLS (HDV)
Type of pavement	asphalt concrete	porous asphalt	asphalt concrete	asphalt concrete
Condition of pavement	new	new	good	poor
PM10 emission factor (mg/km/wheel)	0.25	0 – 0.2	0.7	8
PM10 emission factor (mg/km/LDV)	3	0 - 2		
PM10 emission factor (mg/km/HDV)			7	80

Emission factors for road traffic are generally expressed as mass per km per vehicle for certain traffic conditions (speed, slope etc.). This is a stringent concept if the emitted species are directly produced on-site by the traffic as it is the case for exhaust emissions as well as for freshly produced abrasion particles from brakes, tyres and road surfaces. However, resuspension is the remobilisation of previously deposited material from different sources. While the process of resuspension itself of course is caused by the traffic induced turbulence, thus depending on intensity and speed of the circulating local traffic, the amount of resuspendable dust is limited by the local deposition of dust from different sources (atmospheric deposition, dust introduced by dirty wheels or losses from truck loadings, debris from plants etc.) onto the road surface. In addition other removal processes than resuspension are possible, like wash-off by rain and wind blow-off. It is therefore difficult to describe the resuspension process with only one mass unit.

For traffic situations with low traffic and plenty of resuspendable dust on the road surface the mass unit mg/km/vehicle may be appropriate. However, for streets with high traffic frequencies the emissions from resuspension might be limited by the amount of resuspendable dust, will say the dust deposition rate. In this case the appropriate mass unit for resuspension might rather be expressed in terms of $mg/m^2/h$.

Table 5.2.2 shows emission factors calculated in mg/km/vehicle from the mean emissions during the first two measurement cycles (10 min for MLS, 12 min for MMLS). They thus represent road surface conditions with resuspendable dust. It is important to note, that the pavements were not visibly dirty at the beginning of the experiments, but just contained the dust that might have been deposited by dry or wet deposition in the

previous days and therefore represent realistic conditions. By comparison with the emission factors given in Table 5.2.1 it becomes very clear that resuspension dominates by far over fresh abrasion of particles (in particular for pavements in good condition). This finding is also supported by earlier Scandinavian investigations with different methods (Gustafsson et al. 2008; Hussein et al. 2008). Hussein et al. (2008) further showed that direct abrasion emissions from pavements were on average a factor of 2.3 higher for winter tyres compared to summer tyres. But even assuming that the tyres of the simulators were rather of summer type than winter type, the dominance of resuspension over abrasion still holds true for pavements in good condition.

The reason for the large difference between the resuspension by MMLS of porous asphalt and asphalt concrete might be caused by different dirt loads on the surfaces. Later specific experiments (described below) revealed that porous asphalt indeed tends to retain dust better than asphalt concrete, the difference, however, was only about a factor of 2.

Table 5.2.2: PM10 emission factors during the first 2 measurement cycles dominated by resuspension.

Type of mobile load simulator	MMLS (LDV)	MMLS (LDV)	MLS (HDV)	MLS (HDV)
Type of pavement	asphalt concrete	porous asphalt	asphalt concrete	asphalt concrete
Condition of pavement	new	new	good	poor
PM10 emission factor (mg/km/wheel)	6.3	0.41	11	66
PM10 emission factor (mg/km/LDV)	76	5		
PM10 emission factor (mg/km/HDV)			110	660

As clearly shown by the previous experiments resuspension of deposited dust from the road surface by vehicles seems to be an important source of PM10. Therefore, it is interesting to know whether the porosity of a road surface influences the mobilisation of deposited dust. For this purpose a defined amount of dry fine dust (10 g) collected from a near road surface was placed on the AC pavement (compact surface, low porosity) and the PA pavement (high porosity of the surface) before the MMLS was set into operation. Figure 5.2.6 shows a comparison of the PM10 emission factors for resuspension as a function of time for these two experiments. The very high values show that at least the first 30 minutes are strongly dominated by resuspension of the applied dust and fresh abrasion can be neglected. It is also clearly visible that the resuspension is higher for the AC pavement during the whole observation period of approximately one hour. It seems that a porous surface is able to retain deposited dust better than a smooth surface. Figure 5.2.7 shows a picture taken after the resuspension experiment on porous asphalt. It is clearly visible that fine dust is retained in the pores of the pavement.

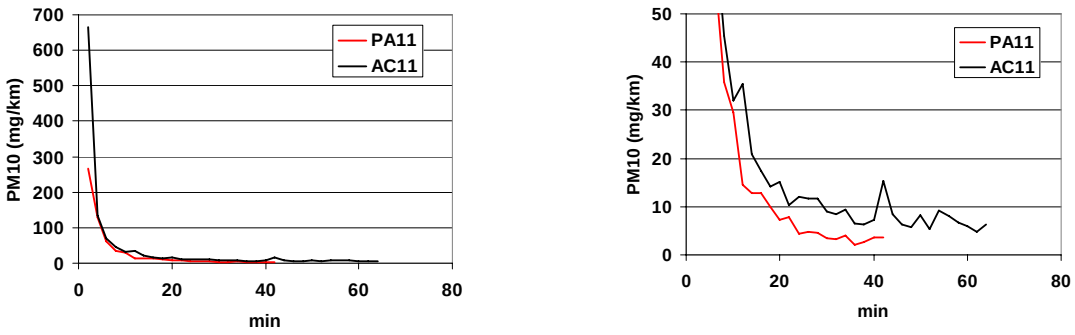

Fig. 5.2.6: Emission factors as a function of time during a MMLS (simulating LDV) abrasion experiment comparing the resuspension of fine dust from an asphalt concrete pavement (AC) and a porous asphalt pavement (PA). Left: Full scale graph. Right: Detailed view with enhanced y-axis.

Fig. 5.2.7: View of PA pavement after resuspension experiment. Pores retaining dust are clearly visible.

Possible contribution from tyres and other moving simulator parts to the emission measurements

For the evaluations and calculations presented above it was assumed that all measured particles stem either from ambient air, from road surface abrasion or from resuspension. However, two additional potential sources of particles have to be considered.

- chains and electric motors for driving the wheels of the mobile load simulators
- tyres of the wheels

In order to check for a possible influence of these sources to the measurements particle sampling in rotating drum impactors (RDI) and elemental analysis with SR-XRF was performed during some simulator experiments in addition to the APS measurements. The techniques are described in Section 3.2.

Iron (Fe) and zinc (Zn) were chosen for this purpose because abrasion particles from moving metallic simulator parts would consist more or less entirely of iron, and zinc, though by far not specific, is a useful indicator for tyre wear.

Only for the MLS experiments a quantifiable difference between ambient air and simulator emission was observed. For the MMLS no significant differences between ambient air and simulator emission occurred. In this latter case only a "worst-case" emission estimate was possible, assuming that all measured iron and zinc was emitted by the simulator and its tyres.

Tables 5.2.3 and 5.2.4 give an overview of the results. In comparison to the emissions from road surface abrasion and resuspension iron emissions from the simulators are low and can be neglected. For tyre emission a zinc content of 1% in the tyres was assumed based on earlier studies (Councell et al. 2004; Thorpe and Harrison 2008). Resulting emission factors for tyre wear were very low for MMLS despite of the "worst-case" assumptions described above. Higher values resulted for MLS operation, simulating HDV emissions. But also here tyre wear seems to be of minor importance compared to resuspension. It can, however, be comparable to the also low emissions from fresh road surface abrasion in the case of a pavement in good condition. Of course it is not possible to derive from these measurements a quantitative estimate for tyre wear in real traffic situations. But they give a strong indication that tyre wear is not to be considered a quantitatively important source of fine particle emission from road traffic.

Table 5.2.3: Emission factors of the MLS for iron and zinc and estimation of tyre wear emission.

	Fe	Zn	PM10 from tyre wear (1% Zn)
Simulator in operation (µg/m^3)	1.68	0.129	12.9
Ambient air (µg/m^3)	0.32	0.008	0.8
Difference (metal abrasion, (µg/m^3)	1.36	0.121	12.1
Emission factor (mg/km/wheel)	0.19	0.017	1.7
Emission factor (mg/km/HDV)	1.91	0.17	17

Table 5.2.4: Emission factors of the MMLS for iron and zinc and estimation of tyre wear emission.

	Fe	Zn	PM10 from tyre wear (1% Zn)
Total concentration (µg/m^3)	1	0.02	2.0
Emission factor (mg/km/wheel)	0.03	0.001	0.067
Emission factor (mg/km/LDV)	0.40	0.008	0.80

Comment to tire wear:

Reliable information for PM10 emissions from tire wear can hardly be found. Some older investigations report contributions up to 5-10% to urban PM10 concentrations. However, none of the applied methods was specific enough to be convincing. A new, still unpublished study at two urban traffic sites in Germany for the first time uses a method that seems to be really specific (analysis of pyrolysis products of tyre rubber) and find a mean contribution of tyre wear of 0.5% to urban PM10. The same work shows that the tyre wear contribution of up to 5-10% as assumed earlier really exists, but in particle fractions >10µm (TSP=total suspended particles) and not in PM10.This is also qualitatively confirmed by. Figure 5.2.8 shows a picture of dust sampled on an adhesive surface with a dedicated deposition sampler (Sigma-2, VDI 2119 Blatt 4), which is widely used in Germany for the assessment of the air quality in recreational areas (Dietze et al. 2006). Another light microscopic picture of a tire wear particle is shown in Figure 5.2.9.

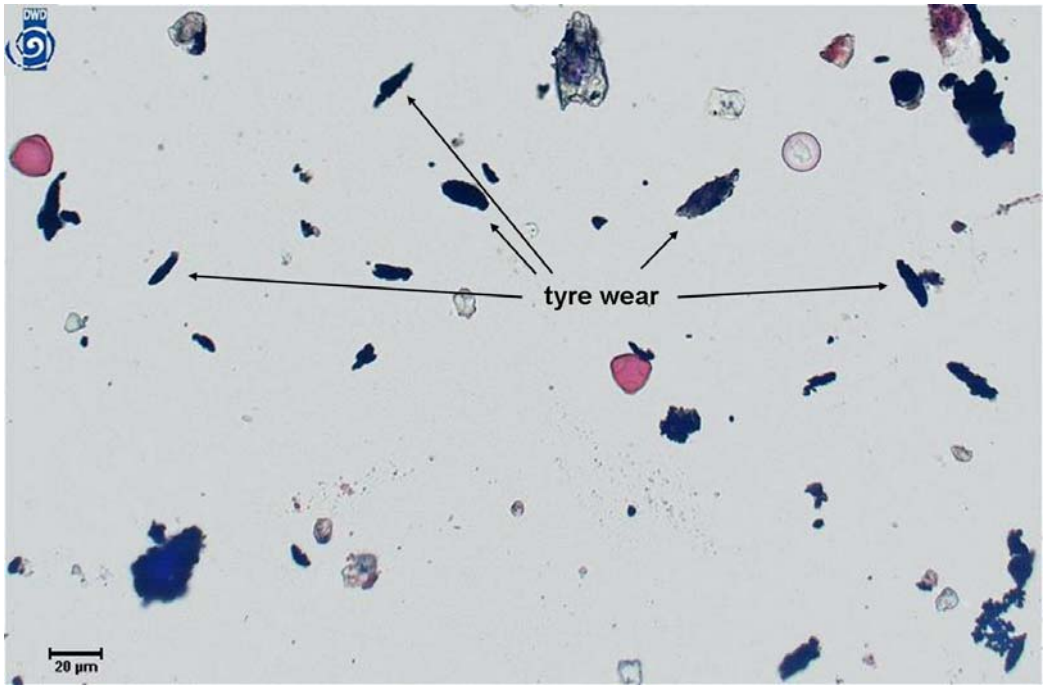

Fig. 5.2.8: Light microscopic image of a typical dust sampled at a traffic site with a deposition sampler (Sigma-2) showing large amounts of tyre wear particles (Courtesy of: V.Dietze, Deutscher Wetterdienst, Referat Lufthygiene Freiburg i.Br., Germany).

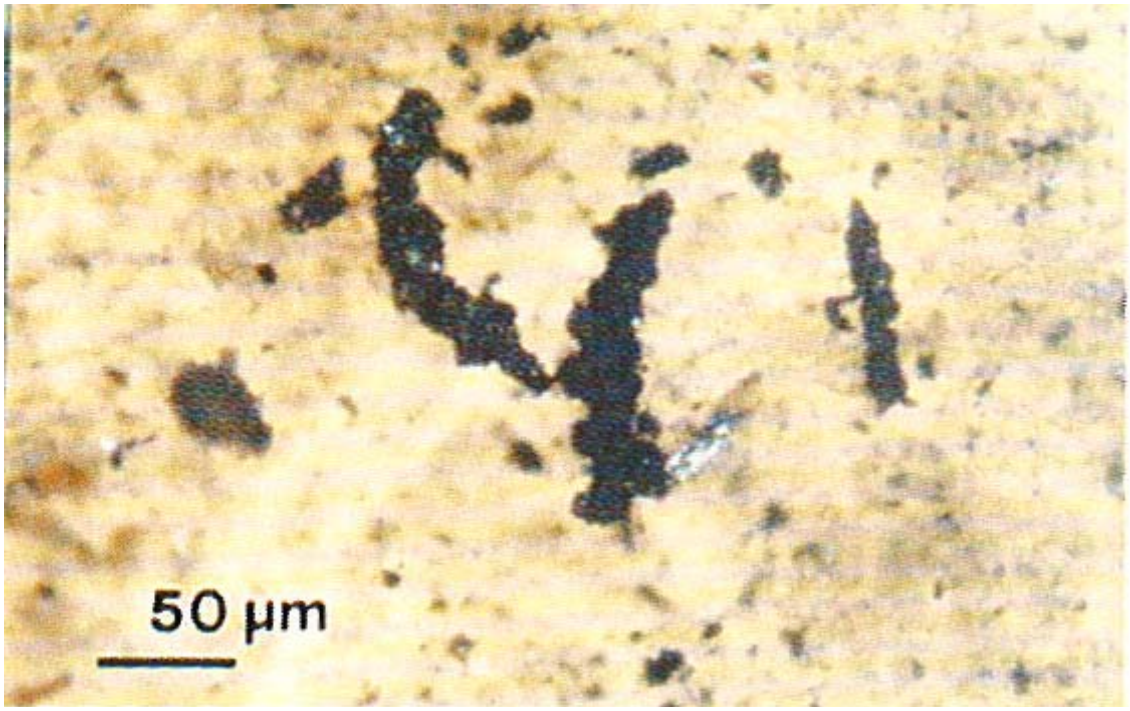

Fig. 5.2.9: Light microscopic image of a tire wear particle (Baltensperger 1985)

Conclusions

- Experiments with "Mobile Load Simulators" allow differentiating between particle emissions from abrasion and resuspension.
- "Fresh" abrasion particle emissions from pavements in good condition are quite low. Considerable abrasion emissions, however, can occur from pavements in poor condition.
- Resuspension of deposited dust can cause high particle emissions depending strongly on the dirt load of the road surface. Porous pavements seem to retain deposited dust better than compact pavements, thus leading to lower emissions due to resuspension compared to pavements with a compact surface structure (e.g. asphalt concrete).
- Tyre wear seems not to be an important source of PM10 emissions from road traffic. Results from new research in Germany find tyre wear predominantly in particle fractions > 10 µm.

5.3 Road Dust Analysis

5.3.1 General

Research focused on road dust resuspension is still scarce due to the absence of a sampling protocol, mostly if the purpose is to collect the PM10 fraction. Several studies investigated the properties of road sediments but only few studies analyzed the PM10 fraction (Han et al. 2007; Ho et al. 2003; Zhao et al. 2006). Moreover the analysis of the PM10 fraction has been generally performed in the laboratory which means inevitable losses of fine and ultrafine particles during the analysis procedure and treatments (plastic bags, pincels, sieves). In contrast the methodology employed in this study (Amato et al. 2009) allows to evaluate the exact amount of deposited PM10 and to study its variability across the city environment. Moreover, with reducing losses of fine particles, which often are hosting source specific tracers, it is possible to estimate real-world chemical profiles which are essential for Chemical Mass Balance (CMB) applications or other source attribution methods (Target shape factor analysis, Multilinear Engine).

Area deposition is reported as deposited mass per unit area, with units of, e.g., mg m^{-2}. This approach is valid for the area sampled and may be in our case extrapolated to any area with the same characteristics such as road surface, traffic density and vehicle mix, and exposure to other ambient influences like weather, transported pollution etc. It gives a direct quantification of the total mass deposited in a specified area, but leaves open during which time the material was deposited. A reasonable assumption is that most of the material has been deposited since the last precipitation, but considerable uncertainties remain, as likely not all deposited dust was washed away by the rain. In an enduring dry period, equilibrium is expected to establish between deposition and resuspension on a road surface, and the deposited mass increases more slowly and ultimately remains constant over time.

The chemical composition of deposited material is given as the ratio of the amount of each component relative to the total amount deposited. This ratio is dimensionless (% or parts per million, ppm) and is independent of the area sampled. Thus the chemical composition may be considered as representative for a wider area in a city. The chemical composition is relevant for source attribution studies.

5.3.2 Traffic counts

The sampling sites were selected to reflect different vehicle traffic characteristics, as traffic is considered to be the main reason for resuspension of road dust. Traffic counts for most of the sampling sites are given in Table 5.3.1. Pfingstweidstrasse shows the largest number of vehicles both for heavy duty and light duty vehicles and for day and night. Weststrasse shows less vehicles, which is in part a consequence of the traffic restriction during nighttime, when exclusively residential traffic is allowed. In general, light duty vehicle numbers are a factor of 10 larger than heavy duty vehicle numbers. Nighttime traffic is roughly one third to one quarter as dense as daytime traffic. Eichbühlstrasse and Kaserne counts are missing, as traffic is very low or prohibited.

5.3.3 Total PM10 deposition in Zürich

The PM10 area deposition of road dust determined for the Zürich sites in February 2008 varied within a range of 0.2 to 3.0 mg m^{-2} (Figure 5.3.2). These concentrations are related to the sampling period (February 2008 after 14 dry days), and may vary with time of year and with weather conditions. Precipitation dilutes and washes away an undetermined fraction of the deposited material. The frequency and total amount of

precipitation in Zurich (Figure 5.3.1) is such that the deposited mass observed in February is rather higher than the expected average. Total rainfall shows a constant minimum in the winter months, and higher amounts of up to a factor of 2 in the summer months. Moreover, dry periods of more than two weeks duration are quite rare events in Zurich.

The error bars in Figure 5.3.2 represent the variability of up to four samples at each site and are related not only to real-world variability of the amount of deposited dust, but also to the uncertainty of the analyses. The large error bars for Weststrasse and Milchbuck Tunnel are due to technical difficulties during the sampling and analysis procedure. Also the measurements at Kaserne were biased by onsetting rain during the measurements. Furthermore, the uncertainties also reflect the inhomogeneity of dust deposition on the road surface, which tends to accumulate at areas away from the wheels, i.e. towards the curb or the center of the road.

As the sampling was performed within three consecutive days at the end of a dry period, the observed spatial variability can be interpreted to reveal characteristics of the individual sites. Schimmelstrasse, Hardplatz and Pfingstweidstrasse were close in their range of values. In contrast, Weststrasse and Milckbuck Tunnel showed a larger average value, possibly due to a strong enrichment in the street canyon and in the tunnel, respectively. However, these average values may not be sufficiently significant due to the high experimental uncertainty for these locations. Duttweilerstrasse showed the lowest deposition, and this was likely the effect of a new road pavement (see Section 5.1 of the APART final report) and low traffic frequencies. Kaserne and Eichbühlstrasse can be considered as background sites, so their high concentrations can be related to increased deposition of mineral material. Kaserne has no traffic at all, and Eichbühlstrasse has only residential traffic, but the latter site was possibly influenced by a small construction site nearby.

Table 5.3.1: Vehicle counts at the different sampling sites in Zurich (2005). Source: Kanton Zürich (http://www.laerm.zh.ch/, http://www.gis.zh.ch/gb4/laerm/gb.asp). The traffic count at Förrlibuckstrasse corresponds to Duttweilerstrasse. Wasserwerkstrasse corresponds to Milchbucktunnel.

	Light duty vehicles / hour	Heavy duty vehicles / hour	Traffic speed daytime	Light duty vehicles / hour	Heavy duty vehicles / hour	Traffic speed nighttime	Upward slope	Downward slope
	daytime 06-22 h	daytime 06-22 h	km/h	nighttime 22-06 h	nighttime 22-06 h	km/h	%	%
Förrlibuckstrasse	635	55	45	215	10	50	0	0
Pfingstweidstrasse	2105	210	60	406	18	60	1	1
Schimmelstrasse	1306	115	45	398	12	50	0	0
Hardstrasse	1596	123	45	368	13	50	0	0
Weststrasse	1132	96	45	115	0	50	0	0
Wasserwerkstrasse	1597	65	45	379	8	50	1	1

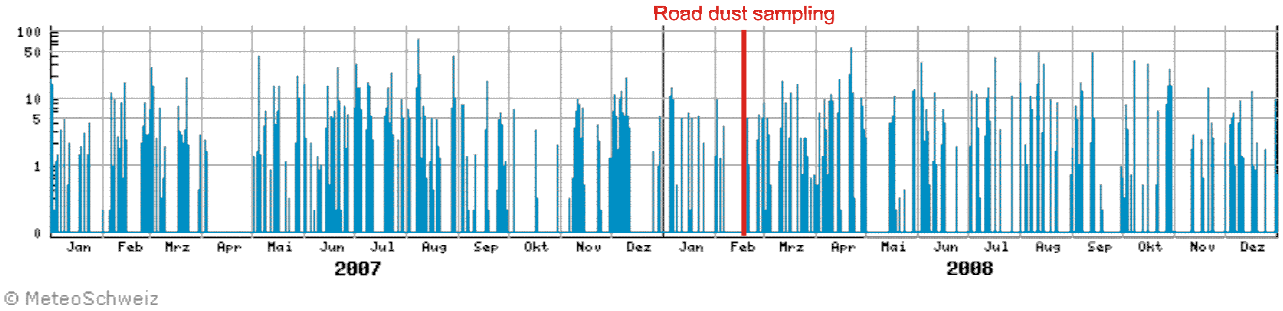

Fig. 5.3.1: Precipitation frequency and amounts (in mm per day) for Zurich-Affoltern for Jan 2007 – Dec 2008. Data: MeteoSwiss.

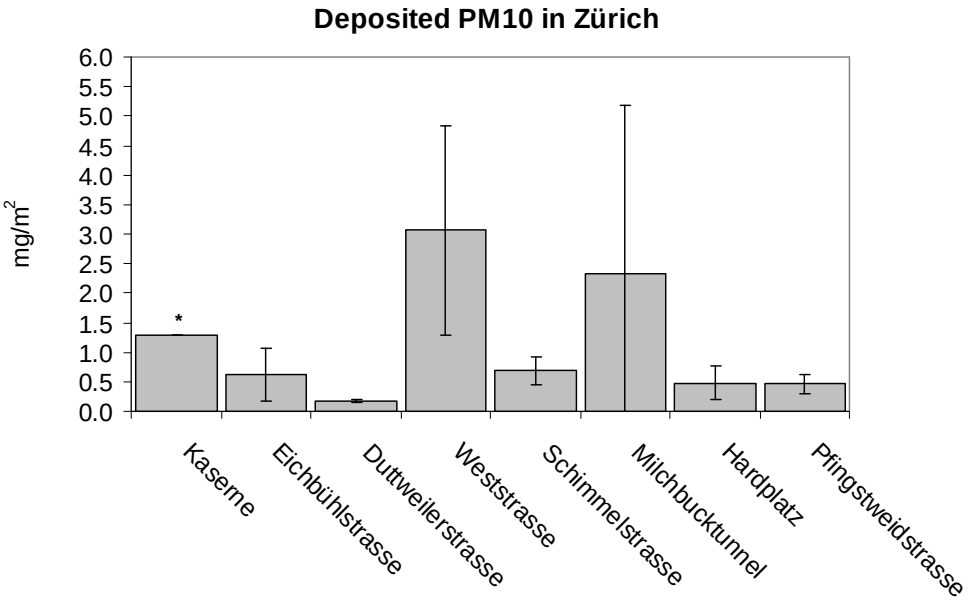

Fig. 5.3.2: Deposited total PM10 mass per m^2 for each sampling site. The black lines indicate the error bars. The sites are ordered according to increasing traffic density. Eichbühlstrasse and Kaserne are considered as background sites. See text for an explanation of the error bars. The value for Kaserne (marked with *) is based on a single filter analysis and is biased by experimental difficulties.

5.3.4 Chemical composition of deposited PM10

The PM10 deposition samples were chemically analyzed for each site to determine their composition and obtain indications on their most relevant sources (Table 5.3.2). SiO_2 and carbonaceous material (OM, and EC, with OM/OC = 1.3) make up the biggest share, followed by CaO, Fe_2O_3, Al_2O_3 and nitrate. The mean area concentrations of trace elements (Figure 5.3.3) were generally two orders of magnitude smaller than the major mass relevant compounds. The total mass was slightly overestimated by the analyzed compounds (without consideration of the experimentally biased value for Kaserne). A detailed look into the situation at the individual sampling sites reveals remarkable variation between the sites with respect to the chemical composition:

- Milchbuck tunnel shows mainly OM and EC (about two thirds) and only little SiO_2.
- Schimmelstrasse and Pfingstweidstrasse also show a high amount of OM and EC, although lower than Milchbuck tunnel. The other extreme is Eichbühlstrasse with almost no OM and EC, but rather crustal material.

- The amount of OM and EC apparently decreases with decreasing traffic numbers.
- SiO_2 occurs prominently at every site. The high amount of SiO_2 at Weststrasse may be caused by cracks in the asphalt surface where additional dust was collecting.
- Hardplatz, Milchbucktunnel and Kaserne show a large amount of undetermined material, which is at least in the last case indicating difficulties during the analysis process.

Figure 5.3.4 shows the mass contributions of the major PM10 road dust components, displayed as average of all considered locations (except Kaserne). On average, the road dust consisted mainly of two components a) roughly 50% of the mass is crustal material (SiO_2, CaO), and b) carbonaceous matter, being the sum of OM+EC and comprising also about 35% of mass. This chemical profile is useful to interpret the sources of deposited PM10.

Table 5.3.2: Deposited PM10 mass in µg m^{-2} split into key species (expressed as oxides). DL = detection limit; na = not available. The measurements at Kaserne were biased by onsetting rain.

µg/m2	**Duttweilerstrasse**	**Pfingstweidstrasse**	**Schimmelstrasse**	**Eichbühlstrasse**	**Hardplatz**	**Weststrasse**	**Milchbucktunnel**	**Kaserne**
SiO_2	72	108	309	424	116	1299	135	94
OM	47	196	294	51	122	416	517	na
EC	24	68	65	16	3	327	335	na
CaO	30.5	42.7	74.6	135.4	43.8	432.3	54.9	29.1
Fe_2O_3	14.4	13.7	113.5	47.6	23.3	127.8	48.4	18.0
Al_2O_3	7.2	5.2	28.9	40.0	7.7	96.1	14.8	9.0
NO_3^-	16.3	14.6	12.9	27.3	22.9	25.9	<DL	<DL
K_2O	<DL	<DL	<DL	13.5	<DL	22.1	<DL	<DL
MgO	3.3	4.3	9.7	14.3	4.7	60.9	6.4	3.9
SO_3	<DL	<DL	7.1	13.6	6.1	17.7	4.5	4.4
Na_2O	4.3	1.5	5.3	4.5	0.1	15.0	4.3	<DL
Cl^-	<DL	3.2	1.6	4.1	<DL	<DL	10.5	<DL
Total	175	468	691	628	481	3067	2323	1300
Determined	*219*	*458*	*922*	*790*	*349*	*2840*	*1131*	*158*
Determined %	***125***	***98***	***133***	***126***	***73***	***93***	***49***	***12***

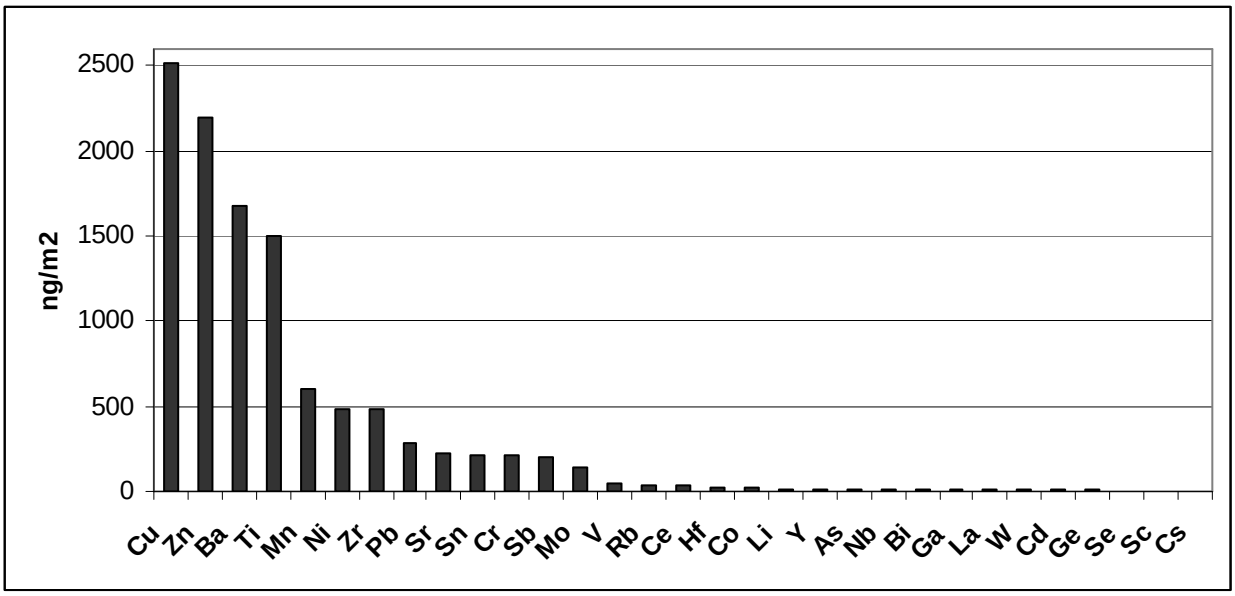

Fig. 5.3.3: Mean area concentration of deposited trace element PM10 in Zurich (averaged over all sites, including Kaserne).

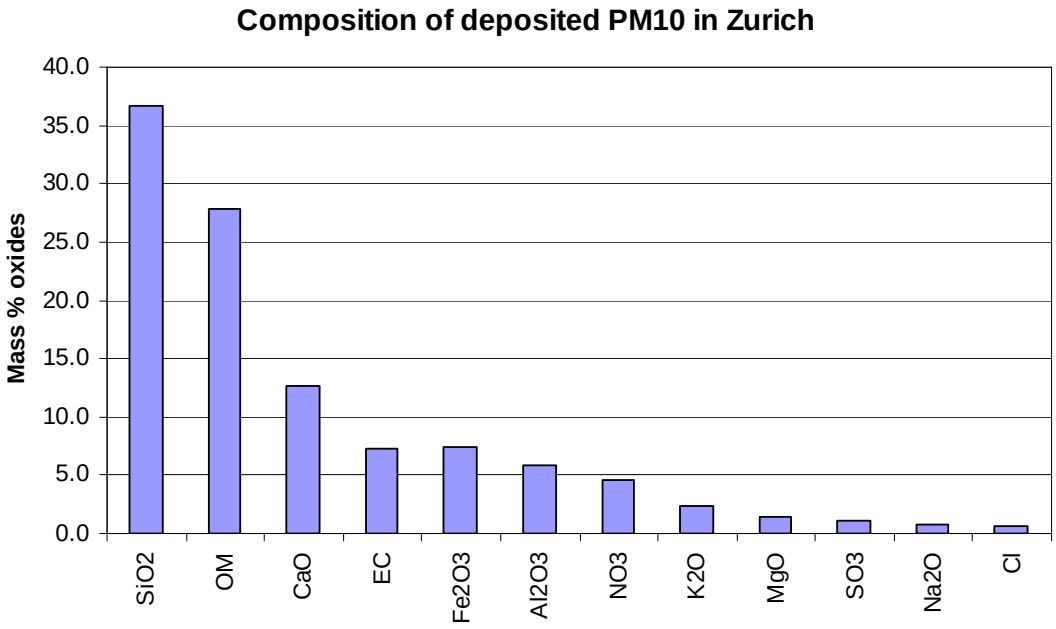

Fig. 5.3.4: Composition of deposited PM10 in Zurich (average of all considered locations except Kaserne). The compounds are displayed as oxides.

From the composition of deposited trace elements at each location (Figure 5.3.5) we can infer that:

- The chemical profile for Kaserne is biased, due to some analytical error during the weighting (it started raining during the last sampling).
- Ti, Cu, Zn and Ba are prominently present at each site.
- Other key elements for brake wear – Cr, Ni, Sn, Sb - are present at each site, even Kaserne (dispersed traffic emissions from the entire city).

- Compared to the other locations, Milchbucktunnel shows the highest fraction of Fe, Cr, Ni, Cu, Zn, Zr, Sn, Sb, which are all elements emitted by the wear of brake pads. This points to a high enrichment of brake wear in the tunnel.
- Eichbühlstrasse, which represents an urban background location, shows the highest fractions for Al, Ca, S, Li, Ti, Sr and La as well as for EC, Co, Ni and Pb.
- The Cu/Sb ratio as an indicator of brake pad wear varied between 6-8 in Schimmelstrasse, Weststrasse and Pfingstweidstrasse. A mean value of 7.0±1.9 was found in Barcelona (Amato et al. 2009).

These findings are consistent with those in Chapter 5.1.

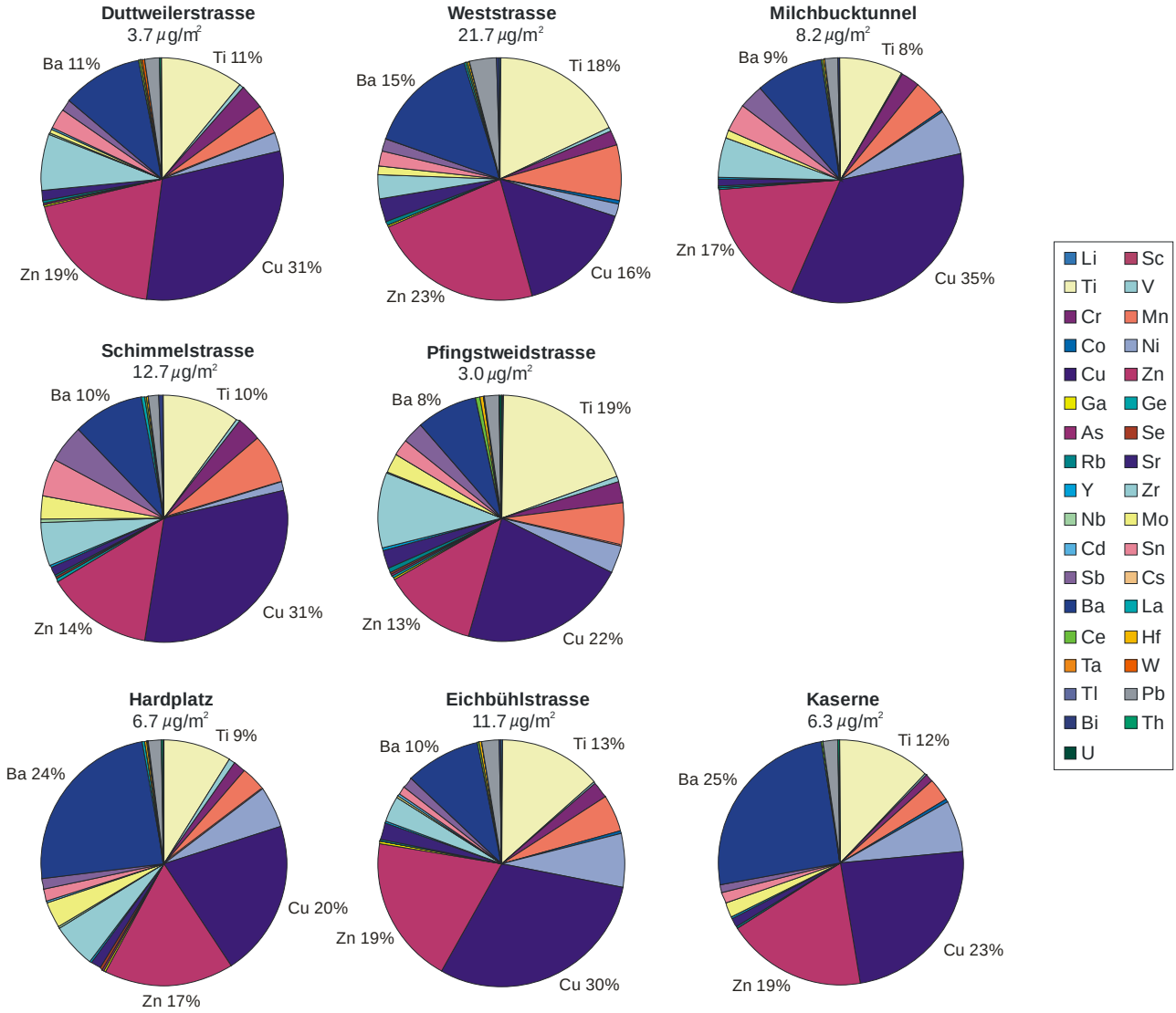

Fig. 5.3.5: Relative abundances of trace elements present in deposited PM10 in Zurich. The numbers under the site names indicate the total mass per m^2 of the considered trace elements.

5.3.5 Comparison to Barcelona

Road dust is a very complex mixture of particles, and its final composition varies depending on the local sources. The elemental composition of the deposited PM10 in Zürich was compared to the elemental crustal abundance and to results from Barcelona.

Looking at the tracer species we can draw the following conclusions for Zürich and compare them to Barcelona, where much experience with the method has been gained:

- The elements Al, Ca, Mg, P, S and Ti, are related to crustal sources and appear less enriched than in Barcelona with more construction/demolition and digging activities.
- Na, Fe, Mn, Sr, Sn, Ba and Pb were in the same concentration range as in Barcelona.
- OC, K, Cr, Zn, Sb, and Cl^- were clearly enriched in Zurich with respect to Barcelona.
- EC, Cu and Mo were between 2-3 times enriched in Zurich compared to Barcelona.
- NO_3^-, Ni and Zr were the most enriched in Zurich with respect to Barcelona.

The typical brake wear elements are thus clearly identified in Zurich and show similar or enriched concentrations when compared to Barcelona. To compare the two areas in more detail we calculate (for each element M) the [M]/[Al] ratios and plot it against the same ratios in the upper continental crust (Taylor and McLennan 1985) as shown in Figure 5.3.6. This graph shows the enrichment of each road dust element with respect to an average crustal composition, to quantify the anthropogenic enrichment of several elements, mostly Sb, Mo, Sn, Cu, Ni and Zn, which originate for example from brake wear (pads and discs). Furthermore it is possible to compare the two scenarios by the vertical bias for each element. Zr, Ni and Hf lie close to the ratio 1:1 in Barcelona, while they show significant enrichments in Zurich. Ta, Tl, Sc and P are not shown for Zurich since they were below the detection limit.

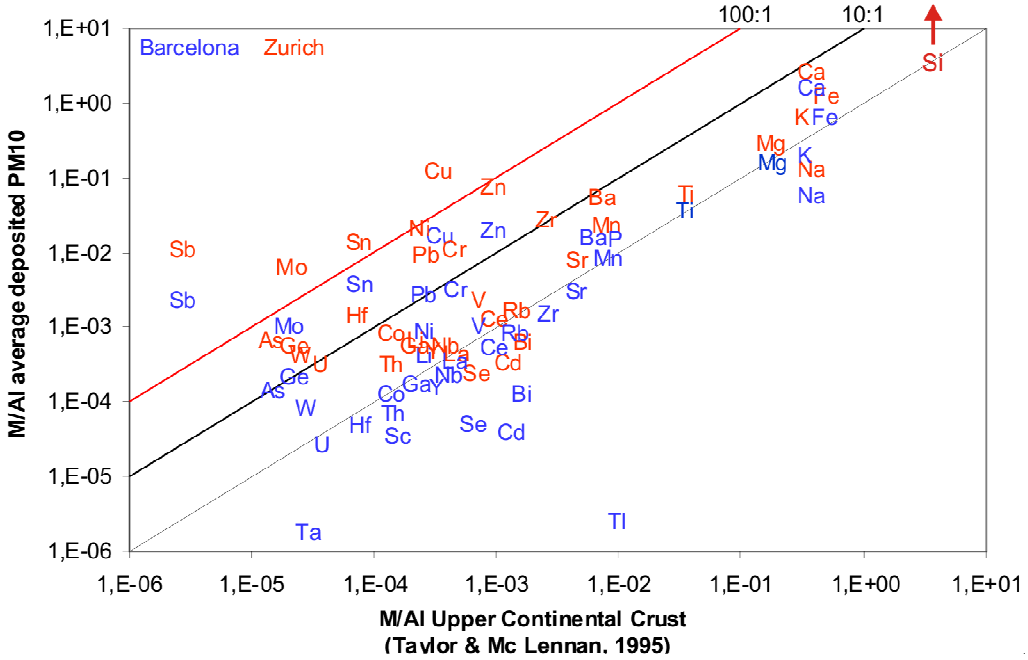

Fig. 5.3.6: Ratio of element M concentration to the Al concentration for Zurich (red) and Barcelona (blue) versus the ratio of M/Al of the upper continental crust (after Taylor and McLennan, 1985). This graph shows the relative enrichment of the elements compared to the Earth's crust.

5.3.6 Composition of PM1 in air

The high abundance of organic matter in PM10 requires attention, as it is an indicator of traffic emissions. While not directly related to abrasion processes, the spatial distribution of airborne PM1 may give additional clues to the interpretation of the PM10 composition measurements and may also be helpful for estimating the representativity of these samples. The Mosquita test run of 19 February 2008 (Figure 5.3.7) was arranged to coincide with the dust sampling campaign. The data from this test run were used to determine the chemical composition of PM1 (Figure 5.3.8).

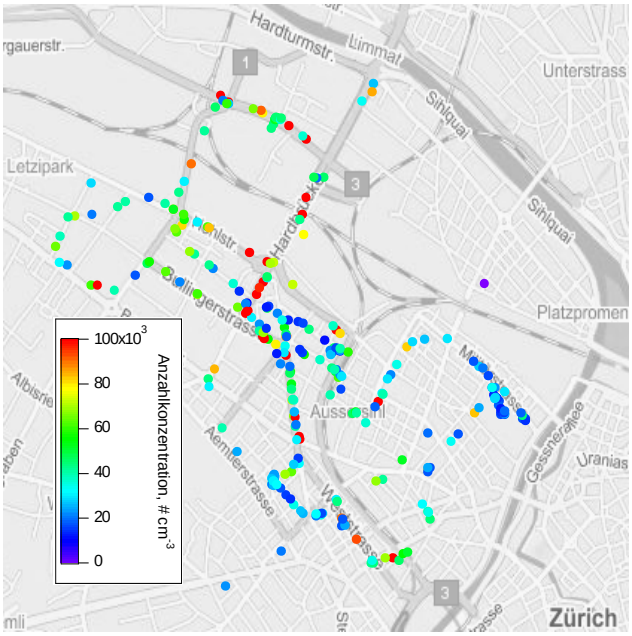

Fig. 5.3.7: Spatial distribution of the PM1 number concentrations (cm^{-3}) in Zurich on 19 February 2008.

Figure 5.3.7 shows the distribution of the PM1 number concentration. The concentration is rarely constant along a road section, but it rather shows a large variability seen in the varying colors. Eichbühlstrasse and Kaserne are blue, representing low concentrations. Hardplatz, Pfingstweidstrasse and Hohlstrasse show more red dots and thus high concentrations. Weststrasse surprisingly shows only intermediate number concentrations.

The relative composition of PM1 for individual road sections is presented in Figure 5.3.8. Nitrate (25 – 39%) and ammonium (11 – 14%) make up about half of the total mass at most places except Hardbrücke, where organic matter due to traffic is also prominent. Chloride is negligible with 1%, but secondary organic aerosol is abundant with 14 – 19%. Sulfate is quite constant throughout the city (5 – 6%). The amount of soot (black carbon) is typically larger than that of organic matter from traffic, again with the exception of Hardbrücke, where both amounts are identical with 20%. Soot as well as organic matter from traffic and wood combustion come from primary emissions, while the other components originate from secondary aerosol formation. Hence, the amount of primary PM1 aerosol varies between one quarter and one third, again with the exception of Hardbrücke, where it amounts to almost a half. This means that generally two thirds to three quarters of PM1 consists of secondary aerosol. All secondary components are distributed regionally and only the primary components have a local character.

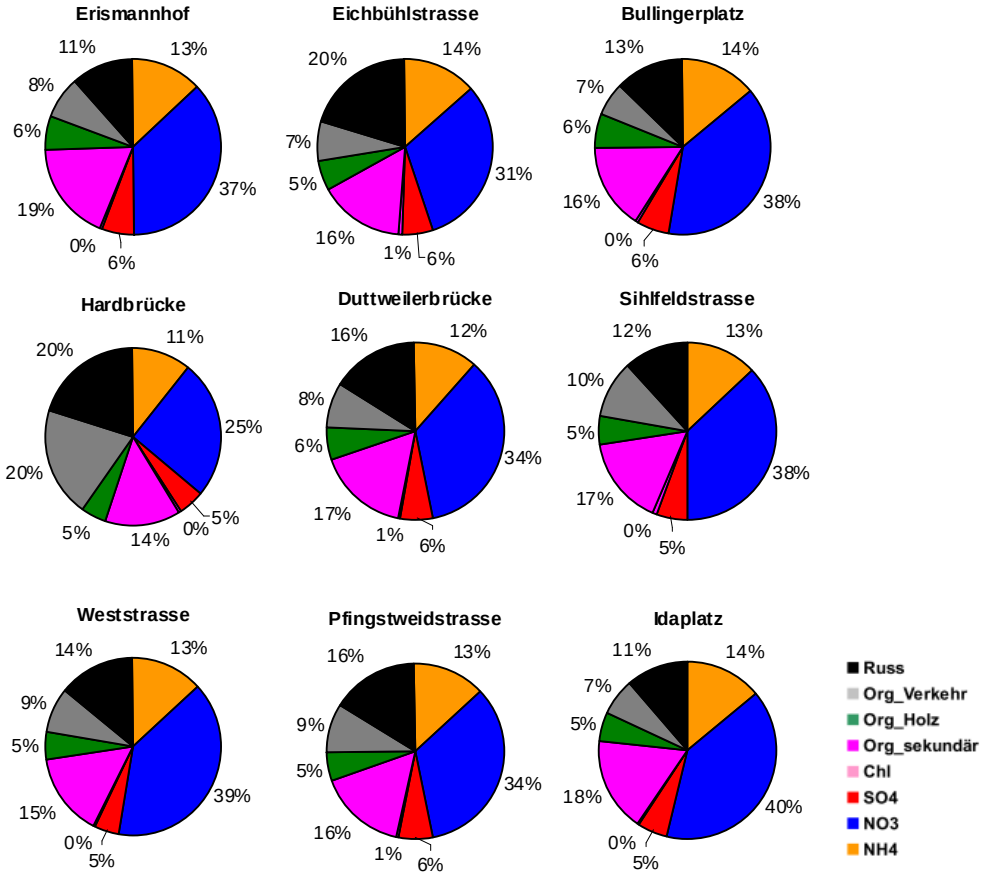

Fig. 5.3.8: The PM1 mean chemical composition in Zurich on 19 February 2008.

It has been shown for other Mosquita test runs that Kaserne reveals less traffic related and more secondary organic matter (Mohr et al. 2009), which is likely the result of the sheltering of the area from direct traffic emissions. Soot may be related mainly to traffic and wood combustion, while nitrate originates from emitted NO_x as a secondary product. The relative similarity of the PM1 composition at most of the sampling sites except Kaserne (not shown) and Eichbühlstrasse is different from the more local signature of PM10.

5.4 Distance Measurements in Härkingen

5.4.1 Goals

Distance measurements are a tool to document the size-dependent dilution of airborne particles. Some fraction may be deposited on the way from the emitting source to the sampler, but most of the particles are transported to more elevated layers in the atmosphere, such that the number of particles can be expected to decrease with increasing distance.

As non-combustion generated particles are expected in larger size fractions, an experiment with two Aerodynamic Particle Sizer (APS) spectrometers was planned and carried out at the NABEL station in Härkingen on 20 November 2008.

5.4.2 Setup

The experimental setup consisted of one APS being fixed at the hut of the NABEL station next to the A1 freeway, while a second APS was running in the mobile laboratory Mosquita II of PSI at selected distances from the freeway (and the NABEL hut, Figure 5.4.1). Six 10-min measurements were performed at each site, then the car was moved to the next place and the new measurement cycle began. Moving the car was possible within the 60 s for data storage of the APS, so no sampling time was lost for displacing the car. During the measurements, the car's engine was turned off to prevent self-contamination. Furthermore, the inlet for the APS was at approximately the same height above the car's roof as that at the NABEL station, and it was mounted on the windward side of the car.

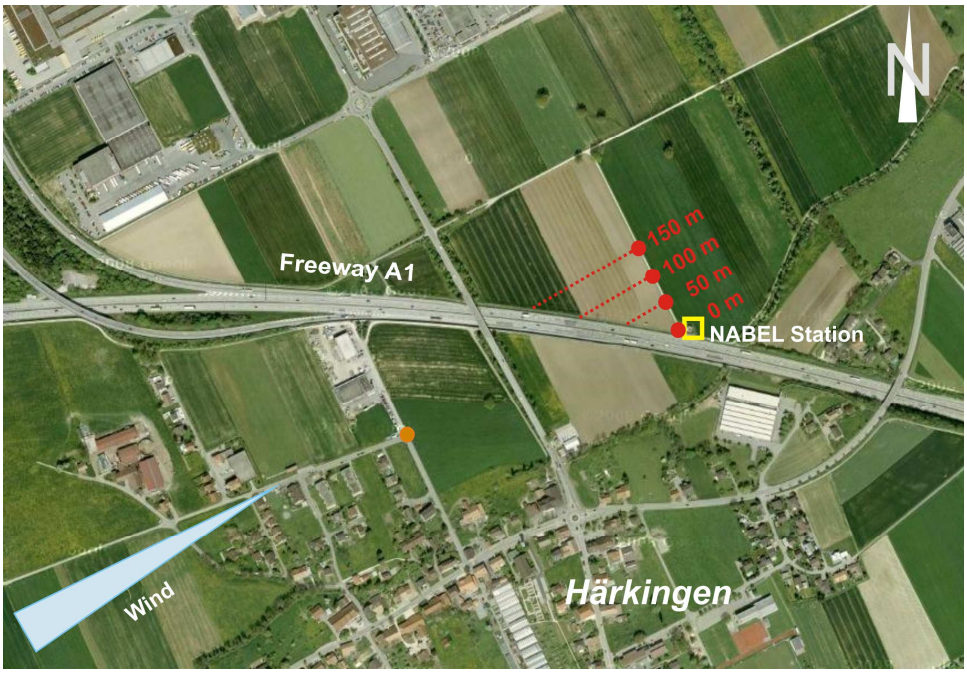

Fig. 5.4.1: Situation in Härkingen. Yellow square: NABEL station. Red dots: Positions of mobile laboratory with the PSI-APS instrument. The red dotted lines indicate the approximate distances to the freeway, with the NABEL station as a reference at 0 m. In fact, the NABEL station is located roughly 10 m besides the freeway, and this distance has to be added for each PSI-APS position. Orange dot: Position for upwind measurement. Light blue triangle: Mean wind direction.

The mobile laboratory was parked on the access road to the NABEL station at the same distance to the freeway. The distance perpendicular to the border of the freeway measures 13 m, and to the center of the freeway (between the lanes) 25 m. In the direction of the mean wind this translates to distances of 17 m and 32 m, respectively. These distances have to be added to the distance values indicated in Figure 5.4.1, i.e. 0, 50, 100 and 150 m which actually indicate the distance from a line parallel to the freeway at the distance of the NABEL station. The mobile laboratory collected air for one hour at each position. The exact position of the car was calculated under consideration of the mean wind direction. Fortunately the wind direction was quite constant during the measurements at 230°. Wind speed was moderate and increased from 3.8 to 6.7 m s^{-1} during the day. Mean temperature was 7.5 °C, and relative humidity was at 74%. In addition to the four distances from the freeway, one measurement with three 10-min cycles was taken again next to the NABEL hut, and a similar measurement was taken about 200 m on the windward side of the freeway. The latter measurement showed, however, a remarkable increase in particles with diameters smaller than 2 µm in the last 10-min sample that could not be explained. This last sample was dropped from the analysis.

Fig. 5.4.2: PSI's mobile laboratory parked next to the NABEL station at the freeway A1 in Härkingen. The inlet for the APS is the tube with inlet head emerging from the right side window of the car.

Traffic density was rather constant throughout the day, such that the emission/production of traffic related particles can be considered uniform. Two special situations occurred. During the first measurement a truck had a problem with its engine: After an explosion, a smoke cloud emerged from the engine room of the truck and passed over the NABEL station and the mobile laboratory. Due to the moderate wind speed this event was considered insignificant. In the afternoon when the mobile laboratory was again next to the NABEL station, a farmer was distributing manure on a nearby field. The wind direction was such that the plume from this activity was not reaching the NABEL station and thus did not affect the measurement.

For each distance the ratio between the PSI-APS and the NABEL-APS was calculated by a linear regression of all values in each individual size bin. The slope of this regression yielded the ratio for one size bin, and the ensemble of all ratios again yields a curve similar to a particle concentration spectrum. The spectra indicate which fraction of the particle concentration at the NABEL station can still be observed at a given distance, or how much of the original concentration has been 'lost' due to dilution with the regional background air and deposition.

The PSI APS showed consistently higher particle numbers than the NABEL APS. To remove these differences, an adjustment was performed by dividing the PSI APS counts by the ratio PSI/NABEL APS for 0 m distance (i.e. when the two instruments were collocated). The NABEL APS was taken as the (correct) reference instrument.

5.4.3 Results

The resulting size-related mass concentrations for each distance to the freeway are presented in Figure 5.4.3a. The adjustment procedure causes the two curves at 0 m to coincide. The mass spectra show two modes. The fine mode below 1 µm can be attributed to the accumulation mode of the background aerosol plus the combustion-generated particles. The coarse mode with particle diameters between 1 and 10 µm is attributed to the coarse mode of the background aerosol plus the particles that are mechanically produced (road and engine wear, brake wear, etc.). It is generally observed that with increasing distance particle mass decreases, especially for the larger particles.

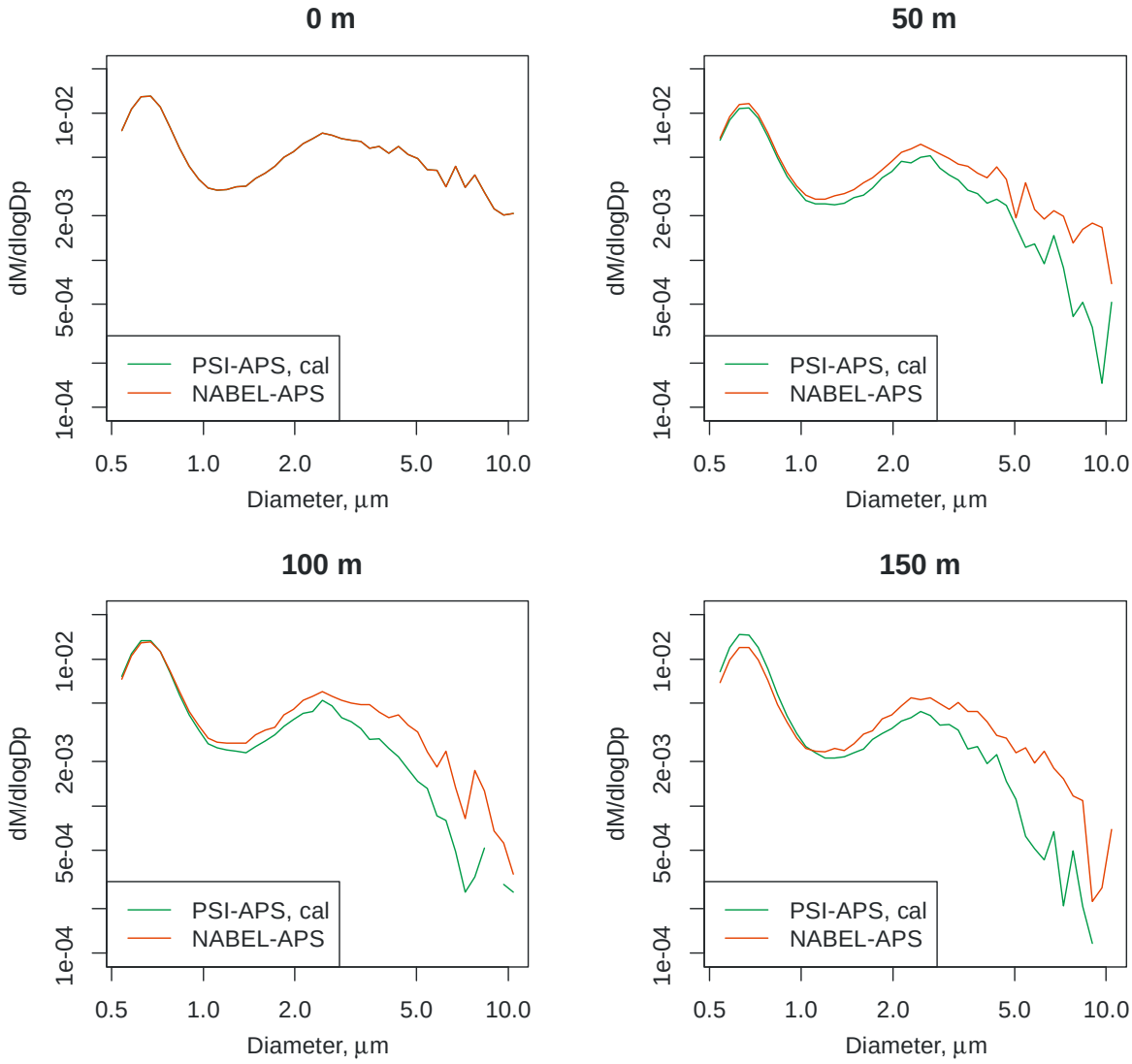

Fig. 5.4.3a: Average particle mass spectra for the different distances from the freeway. All PSI-APS spectra have been adjusted to the 0 m NABEL-APS spectrum such that both spectra for 0 m distance coincide (top left). Mass was calculated from particle volume assuming an average density of 1 kg dm^{-3}.

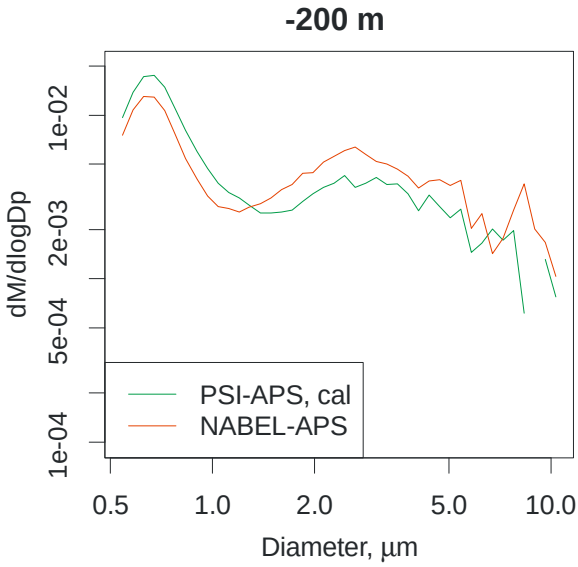

Fig. 5.4.3b: Windward mass spectrum representing the background situation (corresponding to the orange dot in the map in Figure 5.4.1). The spectrum was also adjusted to the 0 m spectrum at the NABEL station.

Figure 5.4.3b shows the windward mass spectrum based on two 10-min samples. Fine particles are more abundant at this site than at the NABEL station, while coarse particles are less abundant. This indicates that the freeway traffic is indeed a source of coarse particles. The increase in fine particles has not been studied in detail. A hypothesis is the onset of domestic heating in the houses further upwind of the station. A hint in this direction is given by the fact that the very last 10-min measurement shows this increase, but not the previous two measurements. At the time of measurement (1500 – 1510 CET), the heating cycle may have been started in the houses upwind from the mobile laboratory.

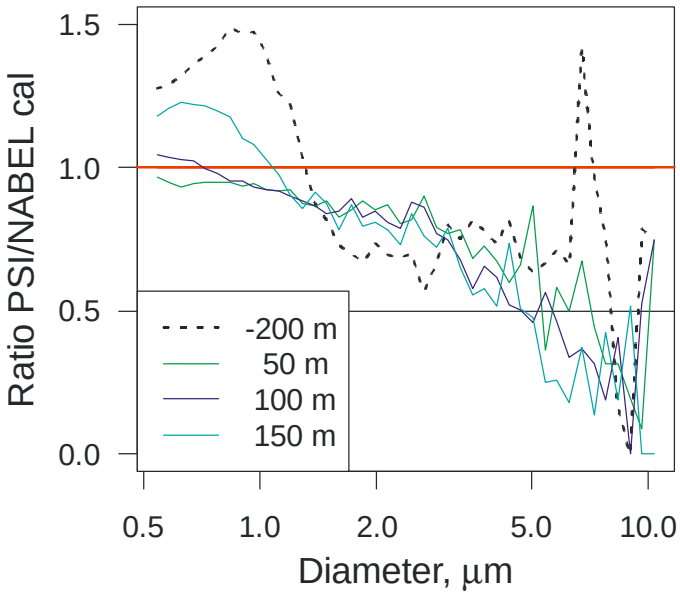

Fig. 5.4.4: Ratio PSI/NABEL of observed values for the corresponding distance. The PSI APS measurements were adjusted to the NABEL APS. -200 m indicates the measurement windward of the freeway.

The ratios between the measurements of the PSI APS and the NABEL APS for each size bin are shown in Figure 5.4.4. As expected, the ratio typically decreases with increasing particle diameter and with increasing distance from the freeway. This indicates a significant reduction of particles in the entire size range between 1 and 10 µm relative to the immediate vicinity of the freeway. The ratio is identical to 1 for 0 m distance, as this has been enforced by the adjustment of the data described above.

Although the variation of the ratio with the particle diameter was rather large, a 50% reduction in particle mass concentration of particles with a diameter of 7 µm could be estimated at 50 m. At 100 and 150 m distance, the 50% concentration decrease was reached for particles sizes of 5 µm and 3 µm, respectively.

For the windward measurement the ratio remains roughly constant at 0.7 for particle diameters larger than 2 µm. Taking this as the background value, the freeway traffic adds about 40% of mass in this size range.

Trying to eliminate the scatter of the data for larger particle diameters, a 3-modal lognormal distribution was fitted to the average mass spectrum of each distance class for each APS (Figure 5.4.5). It becomes evident that:

- particles belong to two modes, a fine mode with a peak diameter of about 0.6 µm, and a coarse mode between 2 and 3 µm.
- at the peak of the coarse mode two groups of lines can be seen, corresponding to each APS (thin lines: NABEL reference APS; thick lines: PSI downwind APS. It is evident that the distance based effect is larger than the variation within the reference spectra and downwind spectra, respectively.
- the two black curves for 0 m coincide by enforcement.
- the PSI APS curves fall off to 0 for diameters >10 µm.
- the NABEL APS curves spread for diameters >5 µm.

As these curves represent fits to observations, the uncertainties for diameters >10 µm need to be considered in the interpretations. In general the tendency that particle masses decrease with increasing distance due to meteorological dilution can be seen in the data.

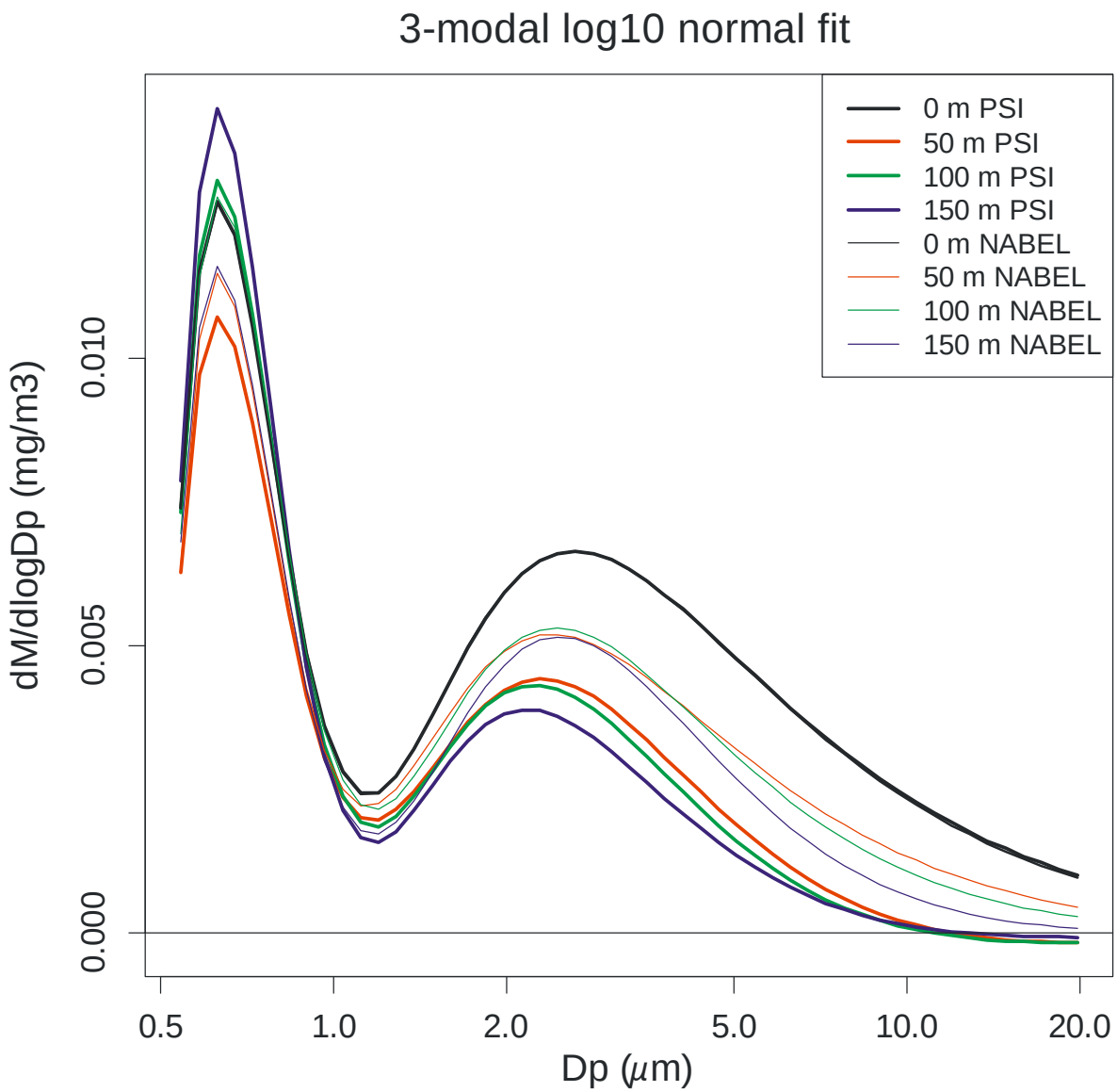

Fig. 5.4.5: APS particle mass distributions for all measured distance classes (assuming unit density). Bold lines: PSI APS data; thin lines: NABEL APS data. The NABEL APS was fixed in its location all the time, while the PSI APS was dislocated from one position to the next. Corresponding colors show the same time interval, e.g. '100 m PSI' corresponds to '100 m NABEL'. Different colors were selected for the respective distance classes, and the two instruments were distinguished with different line widths.

5.5 Mobile Measurements

5.5.1 General remark

Despite the APS calibration problems mentioned in Section 4.3 for these test runs, a comparison between APS and NABEL PM10 measurements showed acceptable agreement (Figure 5.5.1). APS data were measured at Kaserne during two or three time intervals of a couple of minutes on each pass when the mobile laboratory stopped on its route through the city of Zurich. The correct assignment of the APS measurements to the 1-h average values of the NABEL station was difficult. Due to the lack of particle collection for diameters <0.5 μm, the APS misses much of the secondary aerosol that makes up about 50% of PM10. one should expect the APS values to be lower than the NABEL values, which is not the case. As it is not possible to attribute the true reason for this good agreement of the two measurements, we conclude that the APS measurements give at least a qualitative impression of PM distributions in Zurich.

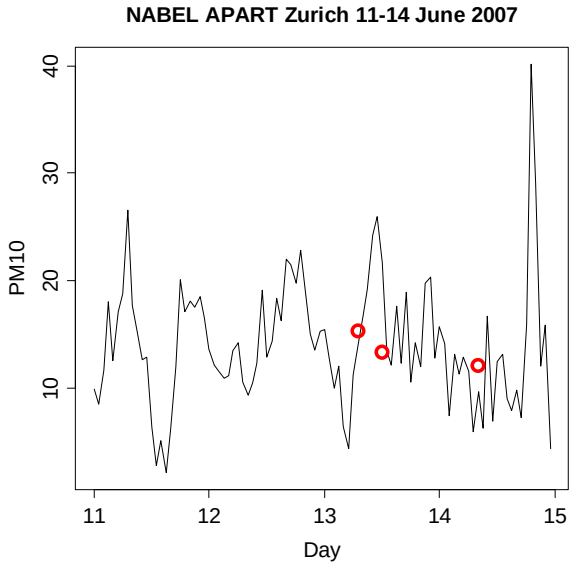

Fig. 5.5.1: Comparison between PSI APS (circles) and NABEL PM10 (line) hourly averaged measurements at Kaserne, 11 – 14 June 2007. APS data are an irregular number of 5-s measurements, depending on the dwell time of the mobile laboratory in the area. APS data are given in μg m^{-3} assuming unit density.

Various aerosol size parameters can be determined from the APS size spectra. With respect to traffic-induced particles, number and volume concentrations are the most important entities. The number concentrations typically show a maximum for the smallest particle diameters (<1 μm) and give hints towards addition of combustion generated particles to the regional background accumulation mode aerosol. In contrast, abrasion generated particles are typically larger than 1 μm. For the present measurements, large particles contribute more to the total volume (and particle mass) than small particles, despite the latter's large numbers.

In the following sections only a selection of graphics with typical or outstanding characteristics are shown and discussed. A map with the exact positions of the discussed locations is shown in Figure 4.11.

5.5.2 13 June 2007, 0731-0951 UTC

This test run showed the highest PM1 fraction of all test runs, and the maximum particle number concentration showed up at Weststrasse (Figure 5.5.2). In contrast, the area around Bullingerplatz and Eichbühlstrasse showed lower number concentrations. The difference was less so for the volume concentrations, but the two distributions were quite similar. Another typical example is the number concentration for particles in the range 2.5 – 10 µm, shown in Figure 5.5.3. The situation for this size range is different to that for PM1. High values are found in the vicinity of Hardplatz, including Hardbrücke and Hohlstrasse, and Badenerstrasse near the Letzigrund Stadium. Still larger particles show a more random distribution largely independent of traffic density and vehicle mix.

Fig. 5.5.2: Route of Mosquita on 13 June 2007 0730-0951 UTC. The PM1-PM0.5 number concentration measured with an APS is shown. Notice that some of the data points may be hidden because the mobile laboratory passed the same spot several (up to three) times during a test run.

Table 5.5.1: Mean APS particle mass concentrations (µg m^{-3}) in different size ranges assuming unit density, as well as the integrated number concentration (last column).

2007-06-13 morning 07:31 - 09:51 UTC								
Street	**Speed (km h^{-1})**	**# Samples**	**Diameter (µm)**					**Number conc (cm^{-3})**
			0.5 – 1	**0.5 -2.5**	**0.5 - 10**	**1 – 2.5**	**2.5 - 10**	
Badenerstrasse	19	30	2.8	6.6	25.2	3.9	18.6	36.2
Hardbrücke	43	10	2.8	8.1	**31.6**	**5.4**	**23.5**	37.9
Hohlstrasse	17	37	2.9	6.8	21.2	4.0	14.4	40.0
Kanonengasse	22	34	2.8	5.6	17.9	2.7	12.4	36.2
Kaserne	1	60	2.6	5.2	14.5	2.5	9.3	33.9
other roads	20	628	2.8	6.0	18.5	3.3	12.5	37.0
Pfingstweidstrasse	24	47	2.8	5.5	14.8	2.7	9.3	36.6
Weststrasse	14	100	**3.1**	6.3	15.3	3.2	9.0	**43.6**
Average			2.8	6.3	19.9	3.5	13.6	37.7

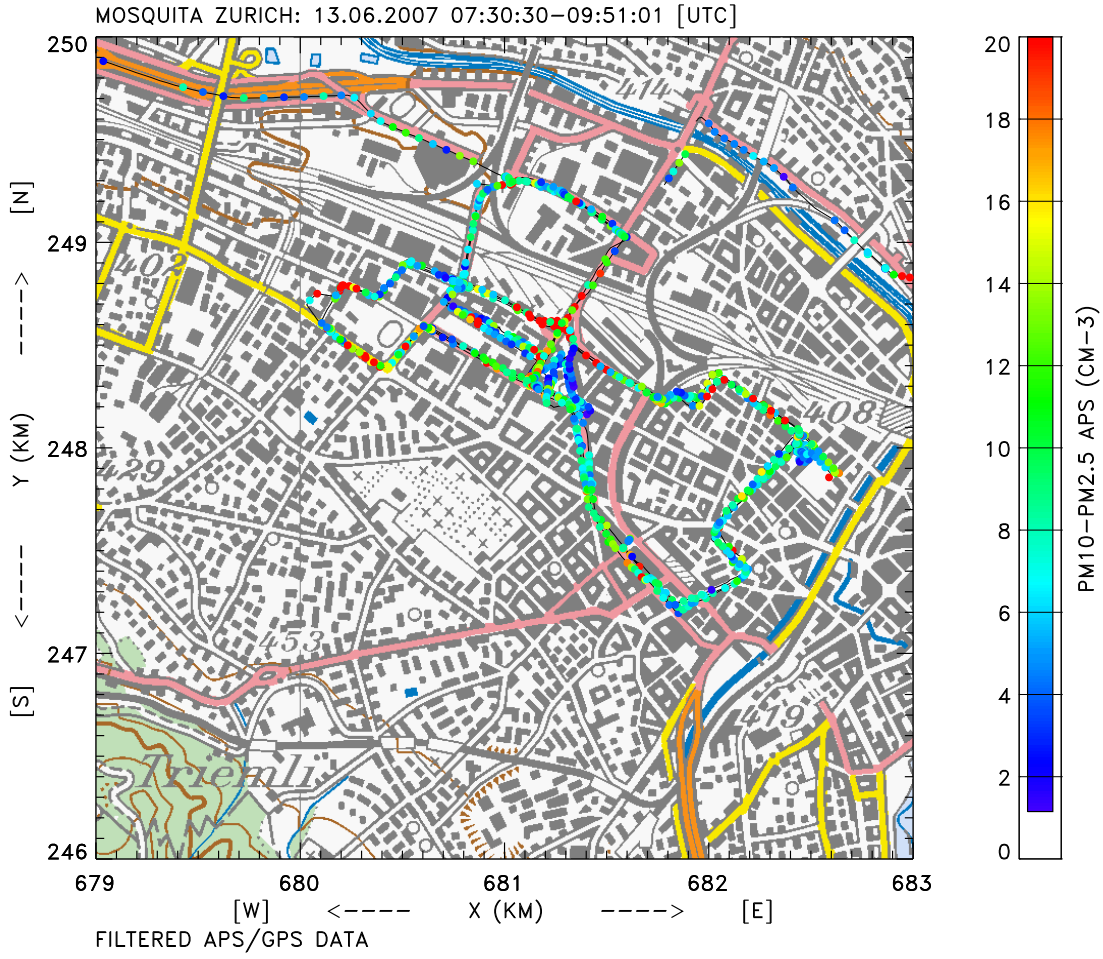

Fig. 5.5.3: Same as in Figure 5.5.2, but for PM10-PM2.5 number concentration.

Table 5.5.1 shows the mean APS particle mass concentrations in different size ranges (assuming unit density) for each individual road section. Most of these sections experienced three passes during the test run time interval, but some were tested only twice. The lowest average PM10-PM0.5 concentration of all three

test runs occurred on this morning run. In contrast, the smaller size fractions (PM2.5-PM0.5 and PM1-PM0.5) showed higher values than for the two subsequent test runs. The highest PM10-PM0.5 values were measured at Hardbrücke, while the highest PM1-PM0.5 values were observed at Weststrasse. The corresponding minima were observed at Kaserne, as expected.

In the box plots shown in Figure 5.5.4, the highest PM1-PM0.5 value was observed at Weststrasse, the lowest one at Kaserne, indicating the urban background value. The larger size fractions show the highest median values and variability at Hardbrücke (bridge), which is well exposed to influences from a larger area.

The average particle number spectra in Figure 5.5.5 show little variation for particles larger than 1 µm at this time. The volume spectra show the distribution of particle volume for different particle sizes. The scatter in the data becomes large for particle diameters >8 µm. There are two maxima in the spectra, one for particles <1 µm, the other for particles in the range 2 to 5 µm. All spectra show a similar shape, with no clear distinction with respect to traffic density. Hardbrücke shows the largest particle volume in the coarse mode.

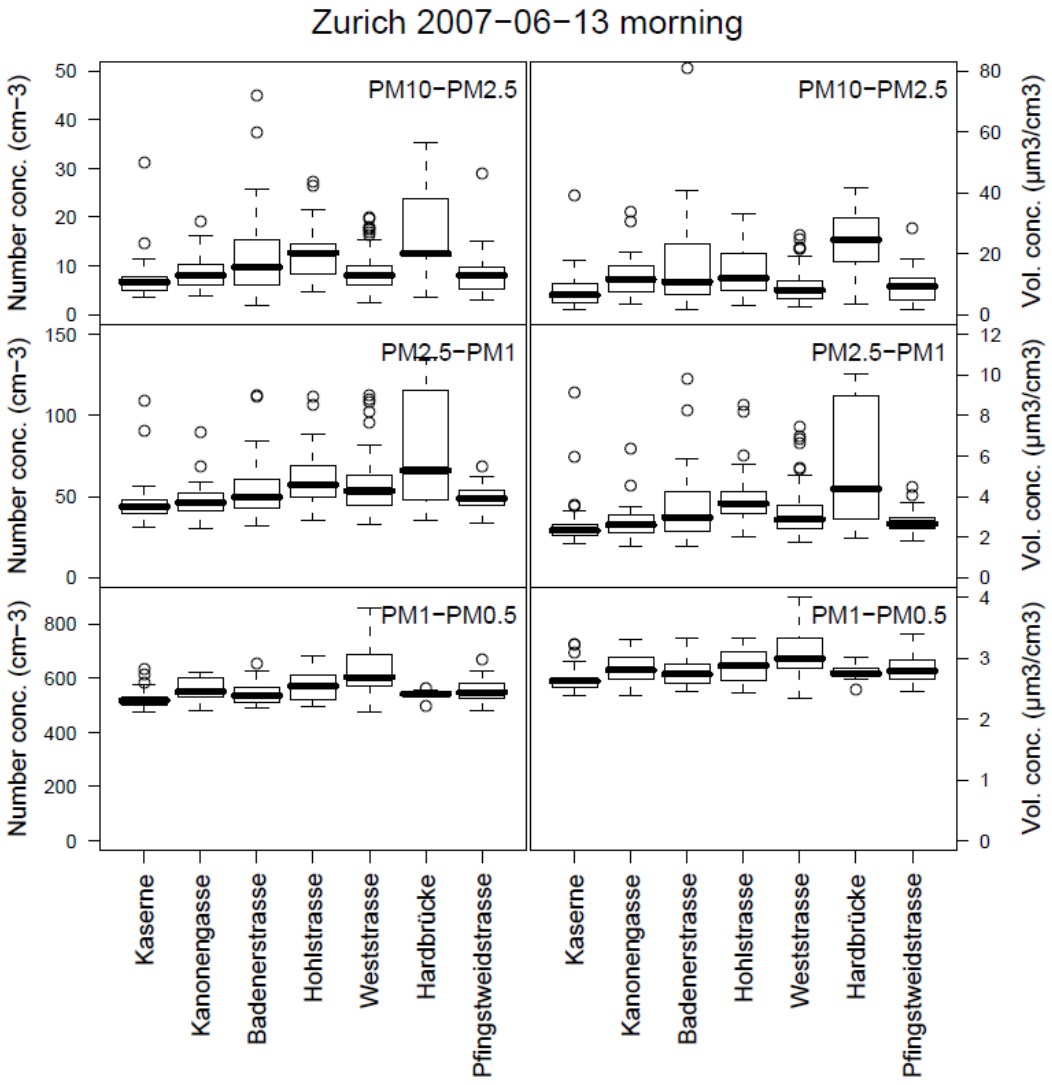

Fig. 5.5.4: Box plot of APS particle number concentrations (left) and volume concentrations (right) for individual road sections along the test run route. Locations are sorted according to increasing traffic density. The thick line in each box denotes the median value. A few extreme outliers have been cropped to improve the graphics appearance.

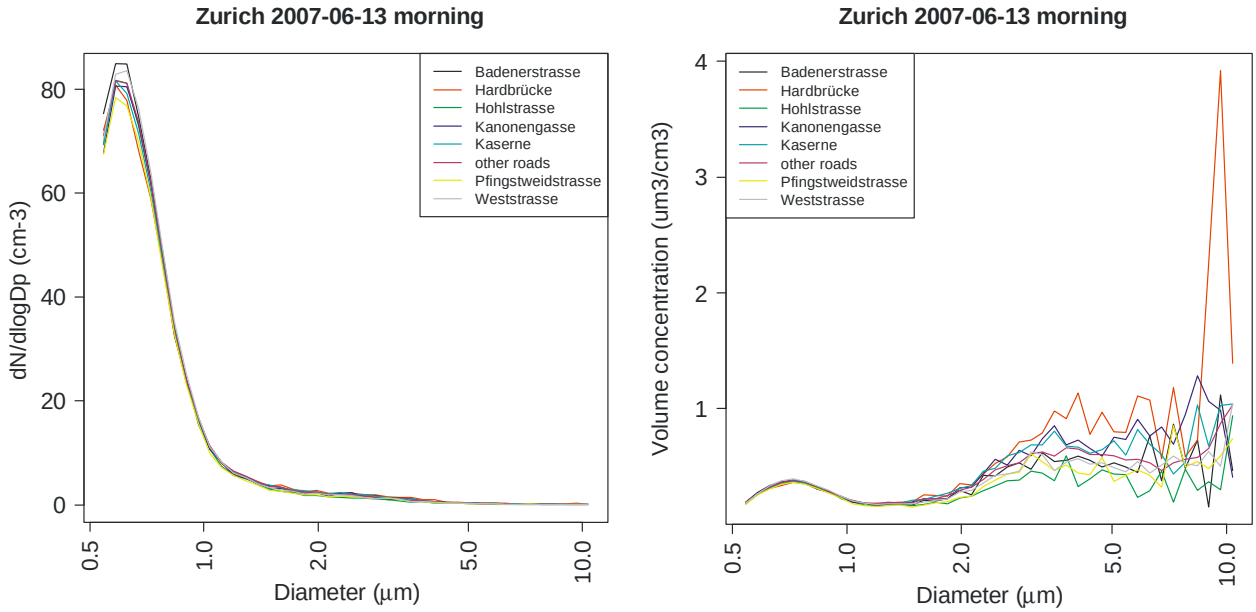

Fig. 5.5.5: APS particle number (left) and volume (right) distributions for individual road sections in Zurich, 13 June 2007 morning.

5.5.3 13 June 2007, 1135 – 1521 UTC

Compared to the morning run, the afternoon test run showed some interesting differences in the distribution pattern of PM. The highest mean volume concentrations were found at Badenerstrasse and Hohlstrasse, and Weststrasse was now among the stations with low PM concentrations, at least with respect to the larger particles (Table 5.5.2). On average, PM1-PM0.5 and PM2.5-PM0.5 were less than or about half the amount of the morning run, whereas PM10-PM0.5 was comparable to the morning run. Kaserne showed the lowest volume concentrations throughout and was now indeed an urban background station. The Mosquita test run showed less variation along the route. An example of the volume concentration of larger particles (2.5 – 10 µm) is shown in Figure 5.5.6. The most striking feature is the red dots indicating large particle volume concentrations. They are scattered randomly along the route from Badenerstrasse to Hohlstrasse and finally towards Kaserne, without clear relation to construction sites or to traffic emissions.

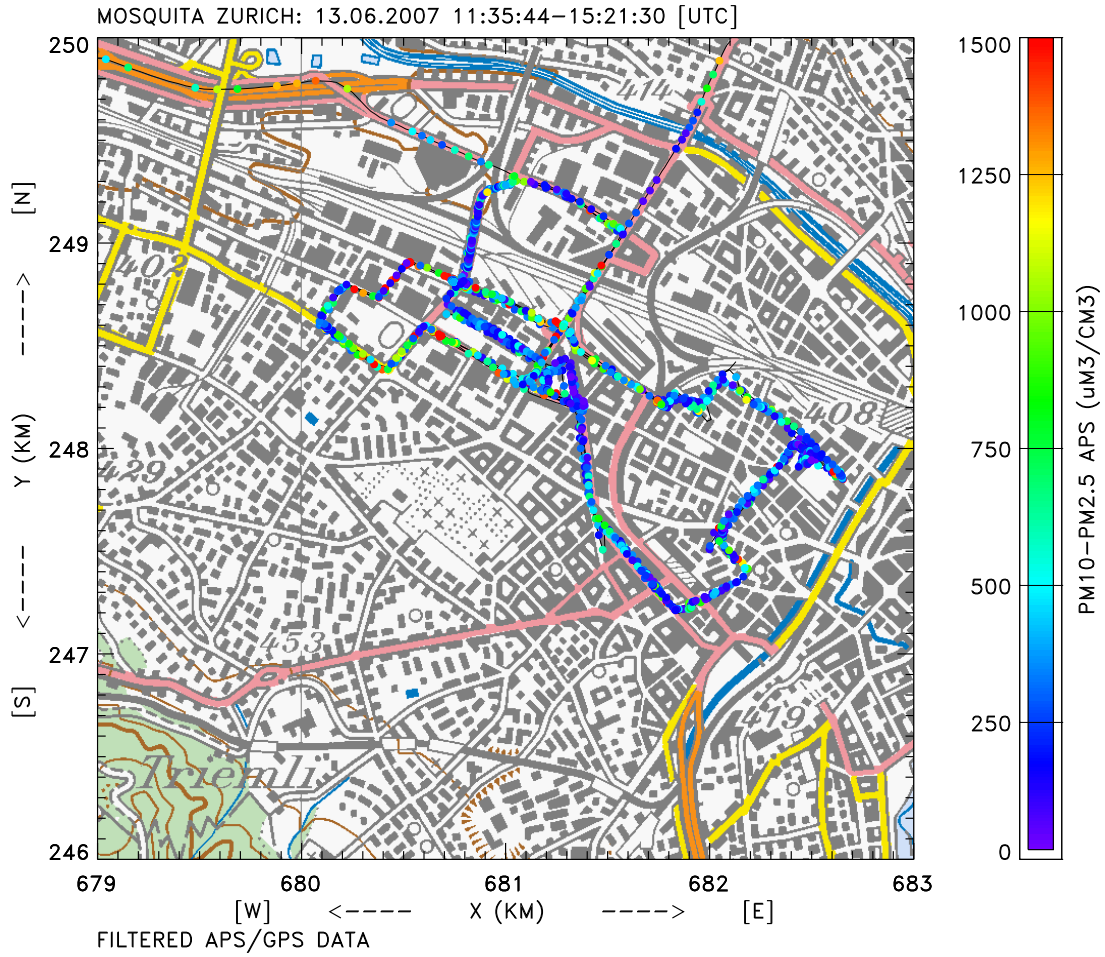

Fig. 5.5.6: Route of Mosquita on 13 June 2007 1135-1521 UTC. APS volume concentrations for particles with diameters 2.5 – 10 µm.

The box plots in Figure 5.5.7 further corroborate this view. Badenerstrasse, Hardbrücke and Hohlstrasse behaved similar for all size fractions, the other three roads and Kaserne were clearly less polluted during this run. The volume spectra (Figure 5.5.8) looked quite similar to those of the morning run, with Hardbrücke now showing the lowest values in general.

Table 5.5.2: Mean APS particle mass concentrations (µg m^{-3}) in different size ranges assuming unit density, as well as the integrated number concentration (last column).

2007-06-13 afternoon 11:35 – 15:21 UTC								
Street	**Speed (km h^{-1})**	**# Samples**	**Diameter (µm)**					**Number conc (cm^{-3})**
			0.5 – 1	**0.5 -2.5**	**0.5 - 10**	**1 – 2.5**	**2.5 - 10**	
Badenerstrasse	19	37	1.2	4.2	**25.7**	3.0	**21.6**	21.3
Hardbrücke	45	16	1.2	3.7	21.1	2.4	17.4	20.9
Hohlstrasse	17	59	**1.3**	4.5	23.7	**3.2**	19.2	**24.9**
Kanonengasse	22	37	1.1	2.8	12.8	1.7	10.0	18.7
Kaserne	1	123	1.1	2.5	11.1	1.4	8.6	18.8
other roads	16	909	1.2	3.5	18.6	2.3	15.1	20.6
Pfingstweidstrasse	23	42	1.2	3.1	15.4	1.9	12.3	21.2
Weststrasse	14	143	1.2	3.2	13.3	1.9	10.1	23.1
Average			1.2	3.4	17.7	2.2	14.3	21.2

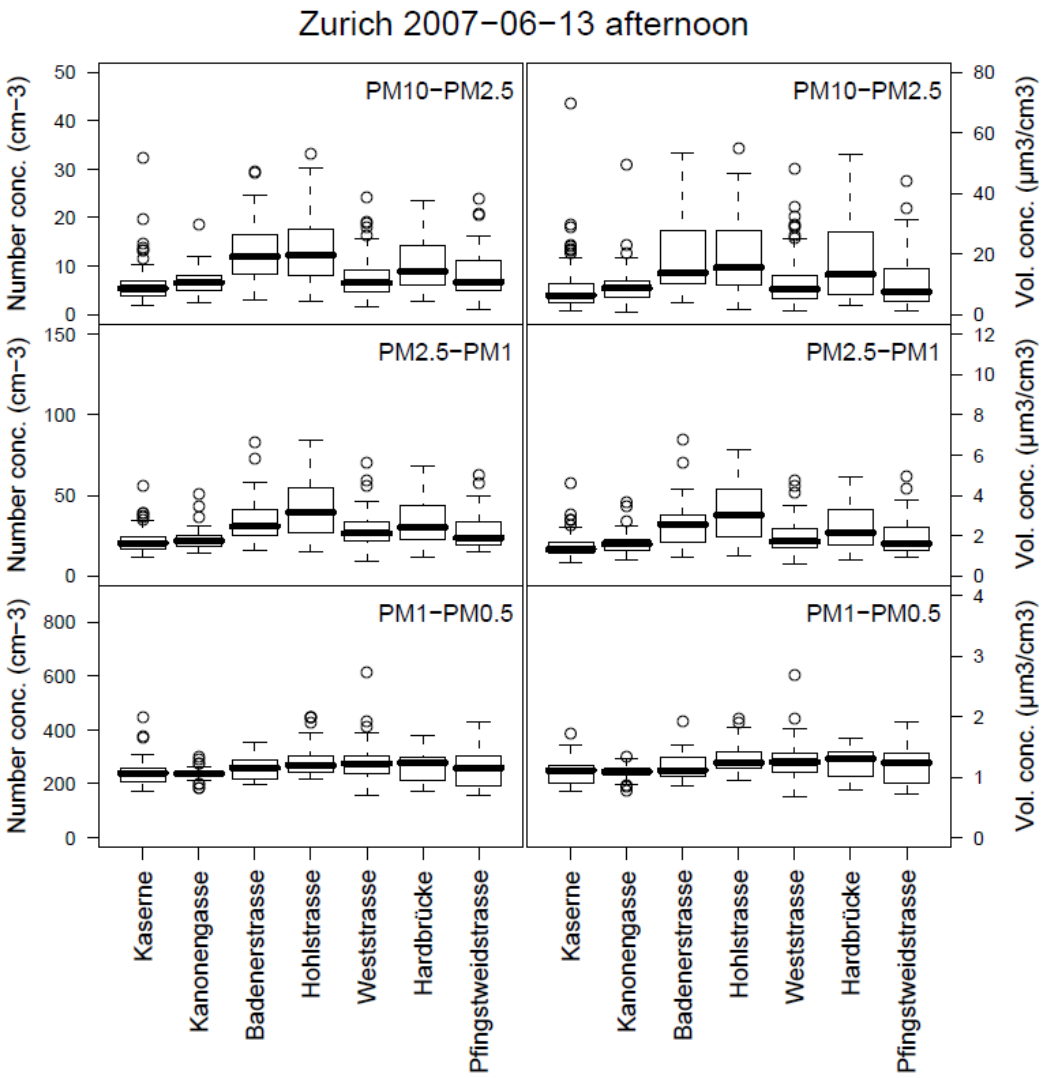

Fig. 5.5.7: Box plot of APS particle number (left) and volume (right) concentrations for individual road sections along the test run route. A few extreme outliers have been removed to improve the appearance of the graphics.

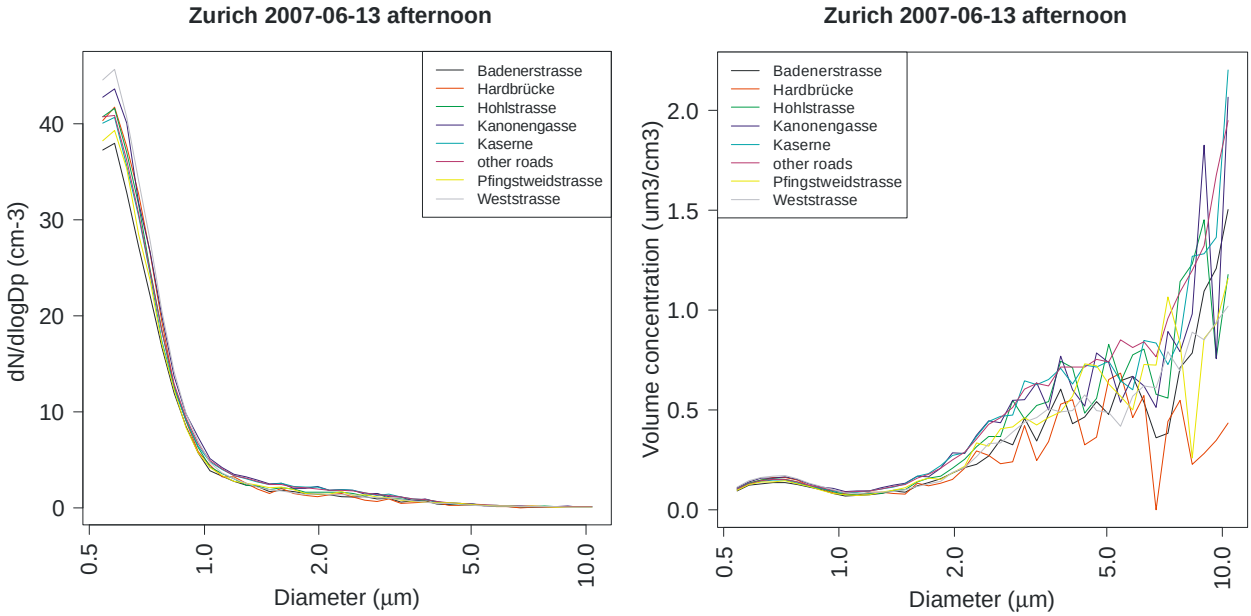

Fig. 5.5.8: APS particle number (left) and volume (right) concentration distributions for individual road sections in Zurich, 13 June 2007 afternoon.

5.5.4 14 June 2007, 0713-1044 UTC

This Mosquita run experienced the lowest PM1-PM0.5 volume concentrations, but was otherwise comparable to the other runs in the size ranges larger than PM2.5-PM0.5 (Table 5.5.3). This time, Badenerstrasse was the street with twice to three times as much PM as the other roads, while Kaserne was the least polluted site (except for PM1-PM0.5). There was construction work ongoing along Badenerstrasse, and the tendency towards larger particles supports the evidence that the measured particles were mainly dust.

Table 5.5.3: Mean APS particle mass concentrations (µg m^{-3}) in different size ranges, assuming unit density, as well as the integrated number concentration (last column).

2007-06-14 morning 07:13 - 10:44 UTC								
Street	**Speed (km h^{-1})**	**# Samples**	**Diameter (µm)**					**Number conc (cm^{-3})**
			0.5 – 1	**0.5 -2.5**	**0.5 - 10**	**1 – 2.5**	**2.5 - 10**	
Badenerstrasse	26	8	0.8	6.0	43.1	5.2	37.1	17.8
Hardbücke	42	14	1.0	4.6	28.3	3.6	23.7	24.2
Hohlstrasse	22	28	0.8	3.8	20.4	3.1	16.6	16.5
Kanonengasse	19	32	0.6	2.4	15.9	1.8	13.6	11.8
Kaserne	1	153	0.6	2.0	10.3	1.4	8.3	10.5
other roads	17	711	0.7	2.9	15.9	2.2	13.0	13.1
Pfingstweidstrasse	28	30	0.8	3.7	19.6	2.9	15.9	17.3
Weststrasse	12	119	0.8	3.0	12.0	2.1	9.1	16.5
Average			0.8	3.5	20.7	2.8	17.2	16.0

This day again identified Badenerstrasse, Hardbrücke and Hohlstrasse as more polluted than the other roads, and Weststrasse was once more mainly polluted with PM1. The high values for PM10-PM0.5 and PM20-PM0.5 were identified as being caused by individual particles. The conversion of particle number concentration to volume concentration gives them particularly much weight, but also some arbitrariness.

The spatial distribution of PM was demonstrated with the Mosquita test runs. Figure 5.5.9 shows the number concentration of particles with diameters 2.5 – 10 µm. It is evident that the largest concentrations were found in the western part of the route: Badenerstrasse, Hohlstrasse and Hardbrücke. This gross feature could be found in all particle size classes down to PM1-PM0.5.

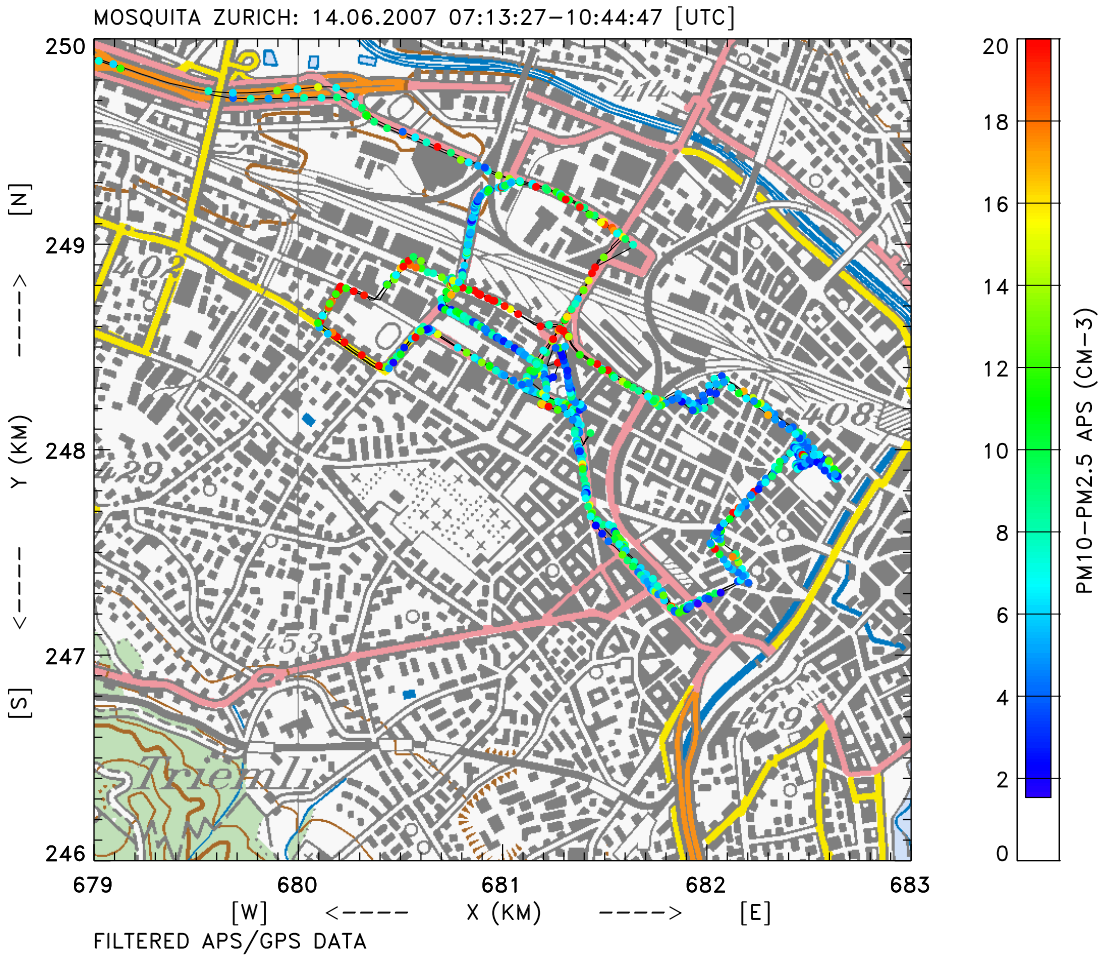

Fig. 5.5.9: Mosquita test run on 14 June 2007 0713-1045 UTC, showing number concentrations for particles with diameters 2.5 – 10 µm.

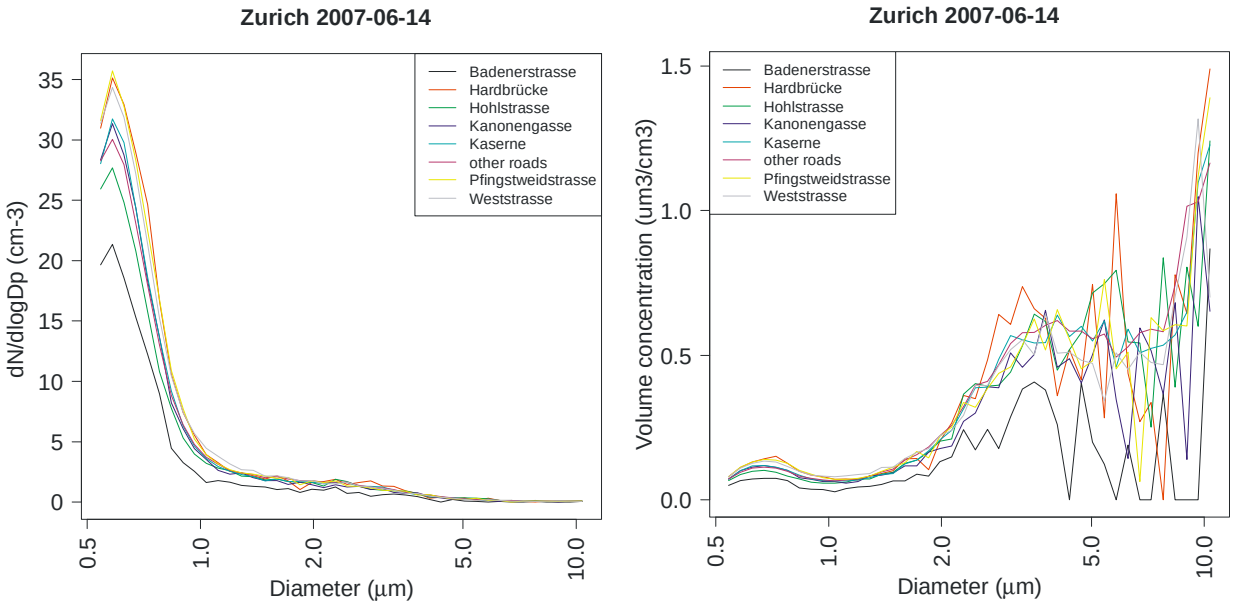

Fig. 5.5.11: APS particle number (left) and volume (right) concentration distributions for individual road sections in Zurich, 14 June 2007.

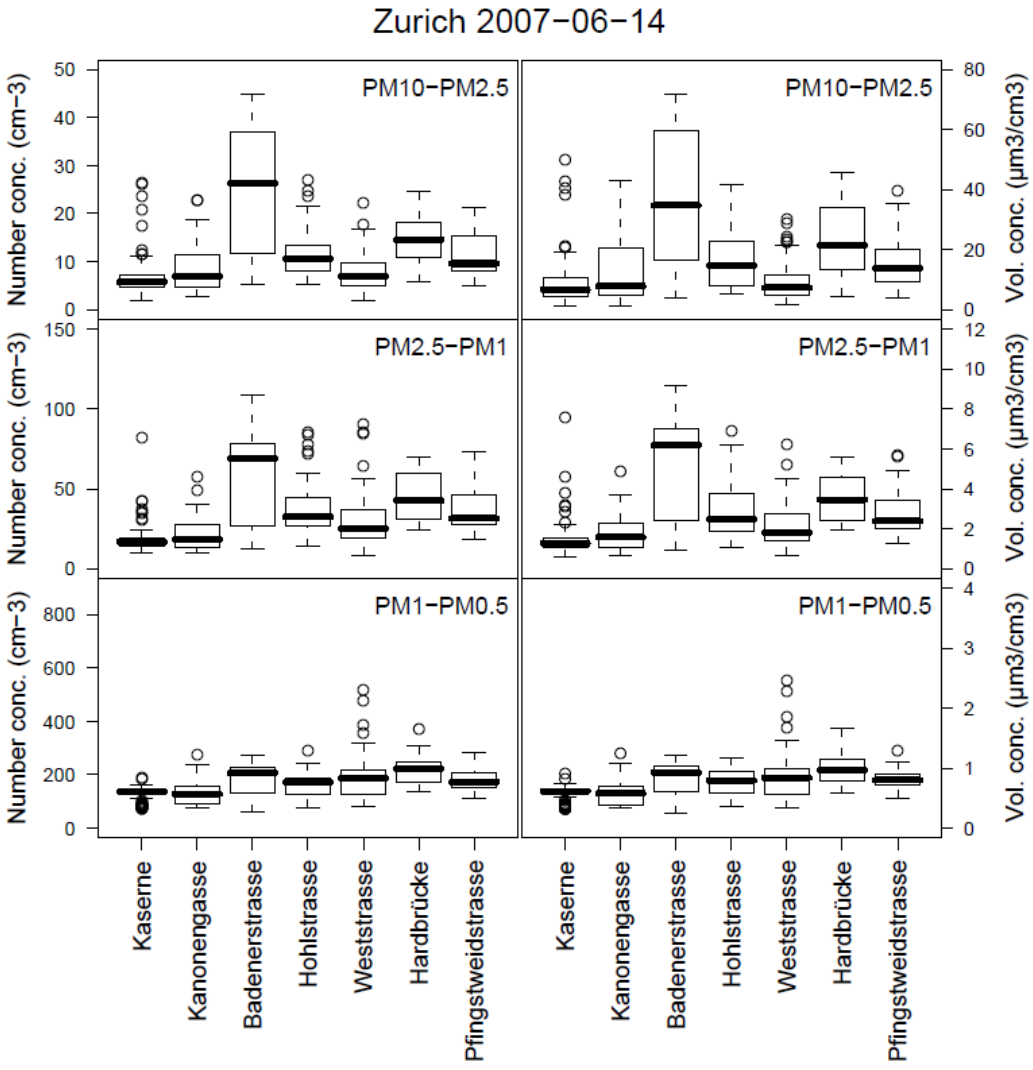

Fig. 5.5.10: Boxplot of APS particle number (left) and volume (right) concentrations for individual road sections along the test run route. The average spectra in Figure 5.5.11 exhibit a large amount of particles >10 µm (not shown).

5.5.5 Discussion

Particles originating from abrasion or resuspension processes are typically larger than 1 μm in diameter, hence an APS is a well-suited instrument to measure size spectra. During APART an APS was installed in PSI's mobile laboratory and several test runs were made with this platform. Despite a serious technical problem with the APS, its measured data agree reasonably well with data from the NABEL station Kaserne that they can be used at least qualitatively. The data were grouped into size classes and stratified according to selected road sections for statistical analysis. Individual results were discussed in the preceding sections. Here the common features to all trips shall be discussed and general conclusions shall be drawn.

The APS measurements reveal that:

- PM1-PM0.5 often behaves differently from the larger size fractions. Its geographic distribution seems more homogeneous within a considered road section than for the larger particle sizes and seems more correlated to traffic density. For PM1-PM0.5 Kaserne is at most times the cleanest site.
- The best visible tendencies for areas with consistently high concentrations (e.g. street sections) occur for the coarse size range, mainly 2.5 – 10 μm. In this size range, the area around the Letzigrund sport stadium often shows high number concentrations. Hardbrücke and the section from Hardplatz to Albisriederplatz as well as Hohlstrasse often exhibit maximum or at least elevated concentrations.
- The vicinity of Bullingerplatz shows consistently the lowest particle number concentrations. This is also valid for Eichbühlstrasse (with the exception of 13 June morning).
- The spatial distribution of particles was extremely homogeneous on the morning of 13 June.
- It is not so easy to relate the largest particles to traffic characteristics (traffic density, vehicle mix). Thus, the spatial variation of the coarse mode is likely not only influenced by traffic, but also by other sources (e.g. construction sites).
- The three case studies discussed cannot be easily related to weather characteristics.

5.6 Mass Balance and Emission Factors for Abrasion Sources

5.6.1 Introduction

For the identification and quantification of the different pollutant sources contributing to the measured PM10 mass concentrations at the individual locations, positive matrix factorization (PMF) was applied (Paatero 1995; Paatero and Tapper 1993). This statistical procedure represents a state-of-the-art method widely used in atmospheric chemistry and physics. The input to the model is a set of time series for individual PM10 constituents, along with an uncertainty value for every individual data point. While tracer species (in our case trace elements) help for the source identification, the mass dominant PM10 constituents (usually secondary aerosols etc.) contribute to a complete mass balance. The source separation capacity of the PMF method relies on the different temporal evolution of the tracer species, which allows for the distinction of an individual source. The main model assumption of PMF is that the chemical composition of the identified sources remains constant throughout time. The input species are considered to be independent, and the number of relevant sources (factors) is not determined by the model, but has to be estimated by the user. The output of the model is a set of factor profiles (source composition) and factor contribution (source time series) for every individual source, which is illustrated in Figure 5.6.1. In cases where the sum of measured input species add up to the full PM10 mass concentration at the considered location, the PMF source contributions allow for a full PM10 mass balance.

The mathematical base for PMF is a factor analysis which uses non-negativity constraints. The formal expression for the mass balance:

$$x_{ij} = \sum_{k=1}^{p} g_{ik} \cdot f_{kj} + e_{ij}$$

Where x_{ij} is the observation of species j at time i, f_{kj} the factor profile of factor k for species j and g_{ik} the factor contribution of factor k a time i. e_{ij} is the residual concentration for each observation. For each observation x_{ij}, an uncertainty s_{ij} is introduced, and the following function of the residual and uncertainty is minimized by PMF using weighted least-squares fitting:

$$Q = \sum_{i=1}^{n} \sum_{j=1}^{m} \left(\frac{x_{ij} - \sum_{k=1}^{p} g_{ik} f_{ij}}{s_{ij}} \right)$$

Choosing the best modeled number of factors for a dataset is the most critical decision to the interpretation of the PMF results. Several mathematical metrics have been used to aid determination of this value. An important criterion is the Q-value, the total sum of the squares of the scaled residuals. If all points in the matrix are fit to within their expected error, then abs (e_{ij} / s_{ij}) is ~1 and the expected Q (Q_{exp}) equals the degrees of freedom of the fitted data = mn−p(m+n) (Paatero and Hopke 2002). If the assumptions of the bilinear model are appropriate for the problem and the estimation of the errors in the input data is accurate, solutions with numbers of factors that give Q/Q_{exp} near 1 should be obtained. Values of Q/Q_{exp} >>1 indicate underestimation of the errors or variability in the factor profiles that cannot be simply modeled as the sum of the given number of components. If Q/Q_{exp} <<1, the errors of the input data have been overestimated. As

additional factors are considered, Q is expected to decrease, as each additional factor introduces more degrees of freedom that should allow more of the data to be fit. A large decrease in Q with the addition of another factor implies that the additional factor has explained significantly more of the variation in the data and has also been used as a metric for choosing a solution (Ulbrich et al. 2009).

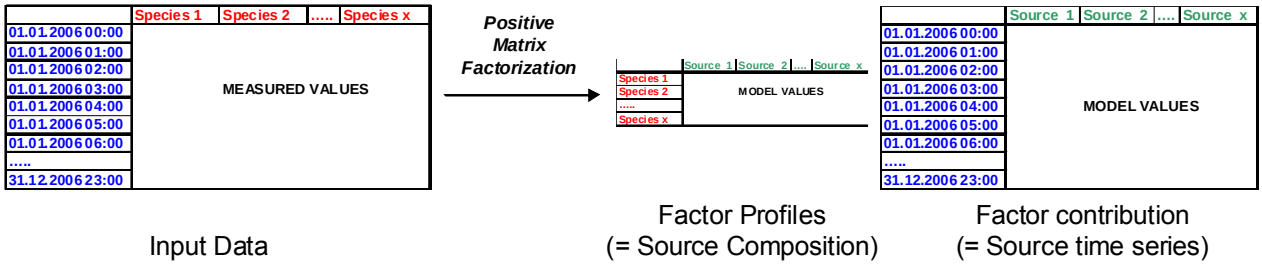

Fig. 5.6.1: Schematic illustration of PMF.

In ambient air, the temporal dynamics and the emission characteristics of most pollution sources occur within a few hours. For the trace element measurements performed within APART, the time resolution of one hour as well as the size-segregation represent a strong benefit for the source identification by PMF. The measured species covered only a fraction of total PM10. The sources identified by the PMF analysis had to be empirically extrapolated to their full mass contributions.

5.6.2 Input parameters

Table 5.6.1 lists the species included in the PMF analysis, while Table 5.6.2 presents an overview on the size of the data sets used for PMF analysis. The summed mass concentration of the detected species covered on average 15% of the total PM10 mass concentrations, which is a value found in earlier studies involving RDI-SR-XRF trace elements measurements. The input uncertainty for the individual data points were calculated based on the technical uncertainty resulting from the aerosol sampling and the uncertainty resulting from spectrometric analysis (see Tables 5.6.3, 5.6.14 and Bukowiecki et al. (2008); Bukowiecki et al. (2009b).

Table 5.6.1: Species used for PMF analysis.

Elements, Species
Si, P, S, Cl, K, Ca, Ti, Cr, Mn, Fe, Cu, Zn, Sr, Zr, Mo, Sn, Sb, Ba, Pb, BC(PM1)

Table 5.6.2: PMF data set dimensions.

Campaign	**Time of year 2007**	**Number of values**
Weststrasse*/**	February/March	314 (1-h intervals)
Kaserne*	February/March	459 (1-h intervals)
Reiden	October/November	452 (2-h intervals)

* simultaneous measurements

** reduced number of values due to missing BC(PM1) values.

According to common practice in PMF analysis (Ulbrich et al. 2009), the analysis of every individual data set included the specification of model solutions with 1 – 10 sources. Every model run was performed with 11 different starting values (fpeak = -2.5 – 2.5). To estimate the actual number of relevant sources, all model solutions were inspected and confirmed or rejected based on both model statistics evidence and chemical plausibility of the results (see following Sections).

5.6.3 PMF analysis procedure for Zürich-Weststrasse / Zürich-Kaserne

The following PMF analysis strategy was followed to obtain a robust and reliable PM10 source apportionment:

Goal: Mass balance for the traffic related PM10 fraction, including contributions for the individual abrasion sources. The traffic related PM10 fraction was considered to be the mass concentration difference between Zürich-Weststrasse and Zürich-Kaserne.

PMF boundary conditions for input data: A PMF analysis of the trace element mass concentration differences was not performed in the first place, since non-traffic related trace elements resulted in negative concentration differences during some time periods. While negative input values are *per se* allowed in PMF, the model solution is biased for these time periods. Since the non-traffic related trace elements were important for the source separation process, they were not generally omitted from the analysis. Furthermore, the size-segregated mass concentrations for the individual elements could not be treated as independent PMF parameters by default.

Data exploration model runs: Individual PMF model runs were performed for the following data sets, which fulfilled the input boundary conditions and thus were suitable for exploratory PMF analysis:

- Zürich-Weststrasse: Coarse mode particles (2.5-10 µm)
- Zürich-Weststrasse: Intermediate mode particles (1-2.5 µm)
- Zürich-Weststrasse: Submicron mode particles (0.1-1 µm)
- Zürich-Kaserne: Coarse mode particles (2.5-10 µm)
- Zürich-Kaserne: Intermediate mode particles (1-2.5 µm)
- Zürich-Kaserne: Submicron mode particles (0.1-1 µm)

The exploratory PMF analysis allowed for a reliable identification and investigation of individual traffic and background related sources, and indicated time periods with elevated background source contributions at Zürich-Kaserne. The analysis of the coarse and intermediate particle size range yielded virtually identical sources, while the analysis of the submicron identified other sources. This agrees with hypotheses made in earlier studies, which assigned abrasion and resuspension particles to particles larger than 1 µm and combustion related particles to particles smaller than 1 µm. Consequently, the elemental mass concentrations in the submicron and supermicron size range were considered as sufficiently independent parameters for a combined PMF analysis.

Refined model Runs: For a refined PMF analysis including all size ranges within the same model run, the mass concentrations in the coarse and intermediate size range were therefore consolidated into one PMF input parameter. In addition to the trace elements, black carbon within the PM1 size fraction was included into the PMF analysis for a more complete mass balance. Refined PMF runs were performed separately for

Weststrasse and Kaserne. Additionally, a PMF analysis with the elemental mass concentration differences between Weststrasse and Kaserne was performed to obtain a mass balance of the local PM10 contribution in Zürich-Weststrasse. Time periods biased by negative concentration differences were identified and taken into account during the model result interpretation. The separate PMF runs for Weststrasse, Kaserne and the concentration difference allowed for a reliable identification and separation of traffic related sources and urban background sources.

Table 5.6.3: Experimental uncertainty for the individual PMF input parameters, calculated based on the technical uncertainty resulting from the aerosol sampling and the uncertainty resulting from spectrometric analysis (Bukowiecki et al. 2009a; Bukowiecki et al. 2008). For the PMF runs, an additional value-proportional uncertainty was applied (20% for the individual runs for Weststrasse and Kaserne, 40% for the run with the concentration differences between the two sites).

Parameter	Technical / spectrometric uncertainty		Parameter	Technical / spectrometric uncertainty	
	Weststrasse, Kaserne	Difference		Weststrasse, Kaserne	Difference
	ng m^{-3}	ng m^{-3}		ng m^{-3}	ng m^{-3}
Si 1-10 µm	1.515	2.162	Cu 1-10 µm	0.867	1.228
Si <1 µm	1.054	1.496	Cu <1 µm	0.595	0.838
P 1-10 µm	0.866	1.237	Zn 1-10 µm	0.706	0.976
P <1 µm	0.733	1.033	Zn <1 µm	0.492	0.692
S 1-10 µm	0.754	1.066	Sr 1-10 µm	0.200	0.269
S <1 µm	0.519	0.734	Sr <1 µm	0.020	0.024
Cl 1-10 µm	0.534	0.756	Zr 1-10 µm	0.205	0.282
Cl <1 µm	0.367	0.519	Zr <1 µm	0.120	0.155
K 1-10 µm	0.259	0.366	Mo 1-10 µm	0.172	0.241
K <1 µm	0.178	0.252	Mo <1 µm	0.111	0.151
Ca 1-10 µm	0.175	0.247	Sn 1-10 µm	0.089	0.114
Ca <1 µm	0.120	0.170	Sn <1 µm	0.063	0.087
Ti 1-10 µm	0.064	0.091	Sb 1-10 µm	0.083	0.108
Ti <1 µm	0.044	0.063	Sb <1 µm	0.056	0.077
Cr 1-10 µm	0.025	0.036	Ba 1-10 µm	0.225	0.316
Cr <1 µm	0.017	0.025	Ba <1 µm	0.140	0.189
Mn 1-10 µm	0.021	0.030	Pb 1-10 µm	0.083	0.108
Mn <1 µm	0.015	0.021	Pb <1 µm	0.056	0.077
Fe 1-10 µm	1.747	2.470	BC <1 µm	10.0	14.1
Fe <1 µm	1.200	1.697			

5.6.4 PMF analysis procedure for Reiden (LU)

The PMF analysis of the trace element time series measured in Reiden was performed with the same input data structure as for Zürich-Weststrasse (Section 5.6.3). The input data matrix included all size ranges within the same model run. The mass concentrations in the coarse and intermediate size range were consolidated into one PMF input parameter, and black carbon within the PM1 size fraction was included into the PMF analysis for a more complete mass balance. PMF runs were performed separately for the measuring sites at both sides of the freeway. Since the definition of the upwind and downwind site depends on the prevailing wind direction, the absolute concentration difference between the two stations did not automatically correspond to the traffic related PM10 contribution. Therefore no PMF analysis with the elemental mass concentration differences could be performed, as it was performed with the concentration difference between Weststrasse and Kaserne.

To estimate the directional origin of the identified sources, a conditional probability function (CPF) was calculated for each individual source. The CPF represents a mathematical concept using wind speed and direction information, to estimate the probability of a given source contribution from a specific wind direction (Kim and Hopke 2004):

$$CPF_x = \frac{m_{>75\%,\theta,x}}{n_{tot,\theta,x}}$$

where $m_{>75\%,\theta,x}$ is the number of 2-h values of source x in wind sector θ exceeding the 75% percentile of source x, and $n_{tot,\theta,x}$ the total number of 2-h values with wind direction from sector θ. Calm winds (< 1m/s) were excluded from the analysis due to the isotropic behavior of wind vanes under calm conditions. The calculated CPF probabilities are plotted in a wind rose.

Table 5.6.4: Experimental uncertainty for the individual PMF input parameters, calculated based on the technical uncertainty resulting from the aerosol sampling and the uncertainty resulting from spectrometric analysis. For the PMF runs, an additional value-proportional uncertainty of 25% was applied.

Parameter	**Technical / spectrometric uncertainty**	**Parameter**	**Technical / spectrometric uncertainty**
	Reiden		**Reiden**
	ng m^{-3}		**ng m^{-3}**
Si 1-10 µm	1.775	Cu 1-10 µm	1.055
Si <1 µm	1.229	Cu <1 µm	0.731
P 1-10 µm	1.200	Zn 1-10 µm	0.885
P <1 µm	0.849	Zn <1 µm	0.611
S 1-10 µm	0.867	Sr 1-10 µm	0.097
S <1 µm	0.601	Sr <1 µm	0.101
Cl 1-10 µm	0.614	Zr 1-10 µm	0.248
Cl <1 µm	0.393	Zr <1 µm	0.119
K 1-10 µm	0.298	Mo 1-10 µm	0.186
K <1 µm	0.206	Mo <1 µm	0.128
Ca 1-10 µm	0.202	Sn 1-10 µm	0.112
Ca <1 µm	0.140	Sn <1 µm	0.077
Ti 1-10 µm	0.074	Sb 1-10 µm	0.105
Ti <1 µm	0.051	Sb <1 µm	0.074
Cr 1-10 µm	0.029	Ba 1-10 µm	0.248
Cr <1 µm	0.020	Ba <1 µm	0.167
Mn 1-10 µm	0.024	Pb 1-10 µm	0.083
Mn <1 µm	0.017	Pb <1 µm	0.056
Fe 1-10 µm	2.113	BC <1 µm	10.0
Fe <1 µm	1.458		

5.6.5 PMF Results Zürich-Weststrasse / Zürich-Kaserne

5.6.5.1 Overview of identified sources

Tables 5.6.5 and 5.6.6 shows the composition, the identification quality and the interpretability of the sources identified by PMF. For black carbon (BC) a high relative contribution compared to the trace elements was found for most of the sources. This was caused by the highly dominating BC mass concentrations in the PMF input data. Based on the PMF model uncertainty (unsharpness), very low amounts of BC were attributed to most sources, which were in a similar absolute mass concentration range as the trace element contributions. As it will be shown in Section 5.6.5.3, BC was however predominantly attributed to traffic and local background. Not the total PMF source mass concentration itself will be used to extrapolate the total mass concentration for the source, but rather the absolute mass concentration of individual source tracers (see Section 5.6.6.2). Therefore the bias contributions from BC will not affect the source mass balancing.

Table 5.6.5: Statistical key parameters of the selected PMF model solutions (explanation see Section 5.6.1).

Location	Value-proportional input error (%)	Number of Factors	Q/Qexp	Fpeak value
Weststrasse	20	7	1.3	0
Kaserne	20	5	2.1	0
Difference	40	3	2.5	0

Table 5.6.6: Overview of sources identified by PMF analysis.

Location	Source	Dominant Particle Size range	Dominant contributors*	Tracers/minor contributors**	Identification by PMF	Interpretability
Weststrasse only	Road traffic	Coarse, intermediate, (submicron)	Fe, BC (PM1)	Cu, Zn, Zr, Mo, Sn, Sb, Ba (brake wear tracers)	Very clear	High
	Local resuspension	Coarse, intermediate	S, Ca, Fe	Si, K, Ti, Cr, Mn and brake wear tracers	Clear	Medium-high
	Nighttime source	(Coarse), submicron	S	Cr, Mn, Ca, K (wood combustion signature)	Clear	Low
Kaserne only	Aged traffic	Coarse	S, K, Ca, Fe	Brake wear tracers	Very clear	Medium
Both locations	Resuspended road salt	Coarse	Cl	Si, P, S, K, Ca, Fe	Very clear	High
	Local mineral background	Coarse, intermediate	Si, S, Ca, Fe	K	Clear	Medium
	Secondary inorganic aerosol	Submicron	S	Si, P, K (possibly introduced by PMF)	Very clear	High
	Source with wood combustion signature	Submicron	S, Ca, K	Si, Mn, Zn, Cu	Clear	Medium

* within the analyzed species. PMF factor score >0.1

** PMF factor score < 0.1

5.6.5.2 Description of sources

Weststrasse only (Local sources):

- **Traffic:** A traffic source representing brake wear emissions and submicron black carbon emissions (exhaust) was identified at Zürich Weststrasse with a high degree of distinction. This source was clearly related to the traffic pattern found at Zürich-Weststrasse. While the PMF analysis of the mass concentration difference between the two sites was able to separate tailpipe related black carbon and brake wear, the PMF analysis of the total mass concentrations at Weststrasse was not able to separate the two sources, likely due to the high temporal synchrony of tailpipe and brake wear emissions, which could not be resolved separately against all other sources. Both analyses delivered very similar source contributions, which provided an enhanced reliability of the subsequent source extrapolation (Section 5.6.6). In the separate PMF analysis of the submicron mode the characteristic brake wear pattern was found, but direct brake wear emissions in this size range are negligible on a mass basis (see Section 5.1) and thus do not appear in the PMF analysis of the entire PM10 range. Elements that point to combustion related fuel additive emissions (Ca, S, Zn and P) were not found in significant contributions in the submicron mode of this source, indicating that the submicron emissions of these elements are more dominant from other sources.

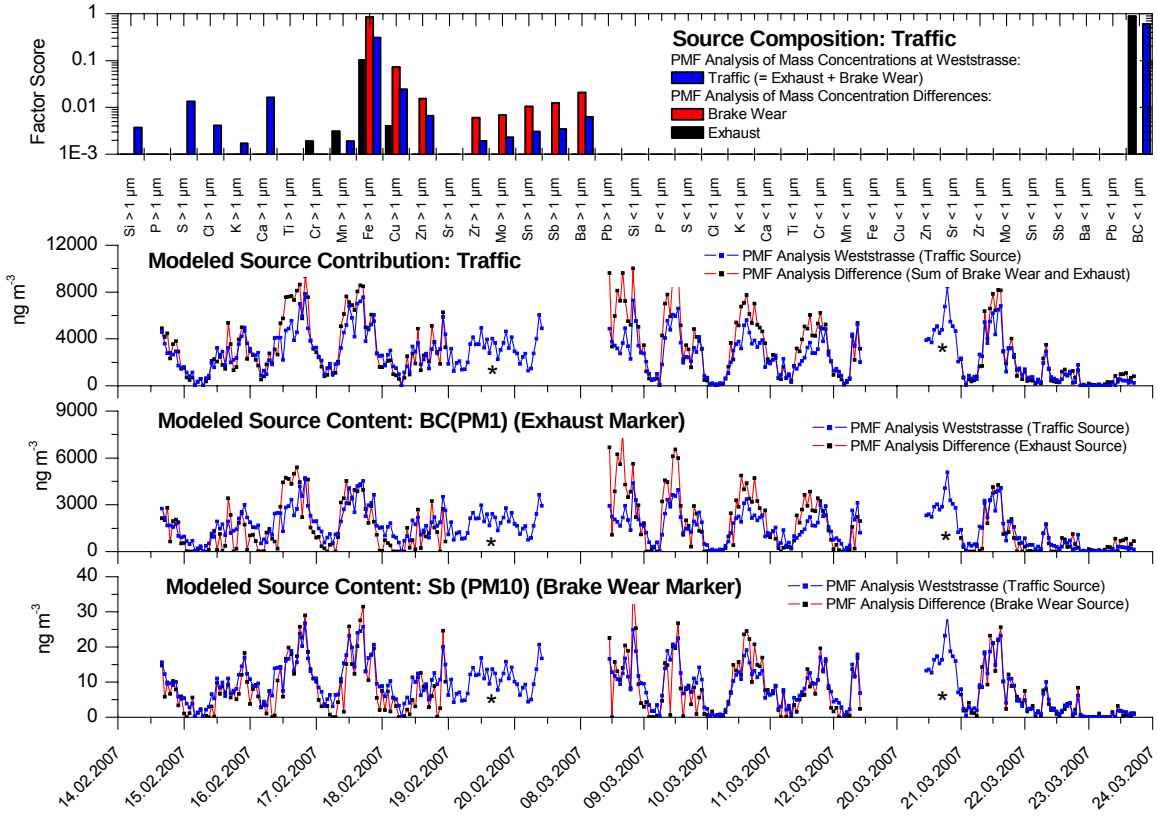

Fig. 5.6.2: Traffic: Source composition and contribution. Stars (*) indicate periods with unstable model results for the PMF analysis of the mass concentration difference Weststrasse-Kaserne.

- **Local Resuspension:** Beside direct traffic emissions, a resuspension source was identified. The daytime peaking of this source is rather regular, but there is no direct correlation to traffic frequencies (see also Section 5.1). This suggests that this source represents locally resuspended road dust at Zürich-Weststrasse. The compositional pattern agrees reasonably well with the pattern found in the road dust sampling experiments performed in Zürich one year later (Section 5.6.6.2). Again, all PMF runs delivered similar source contributions, although the agreement is less clear than for the direct traffic source.

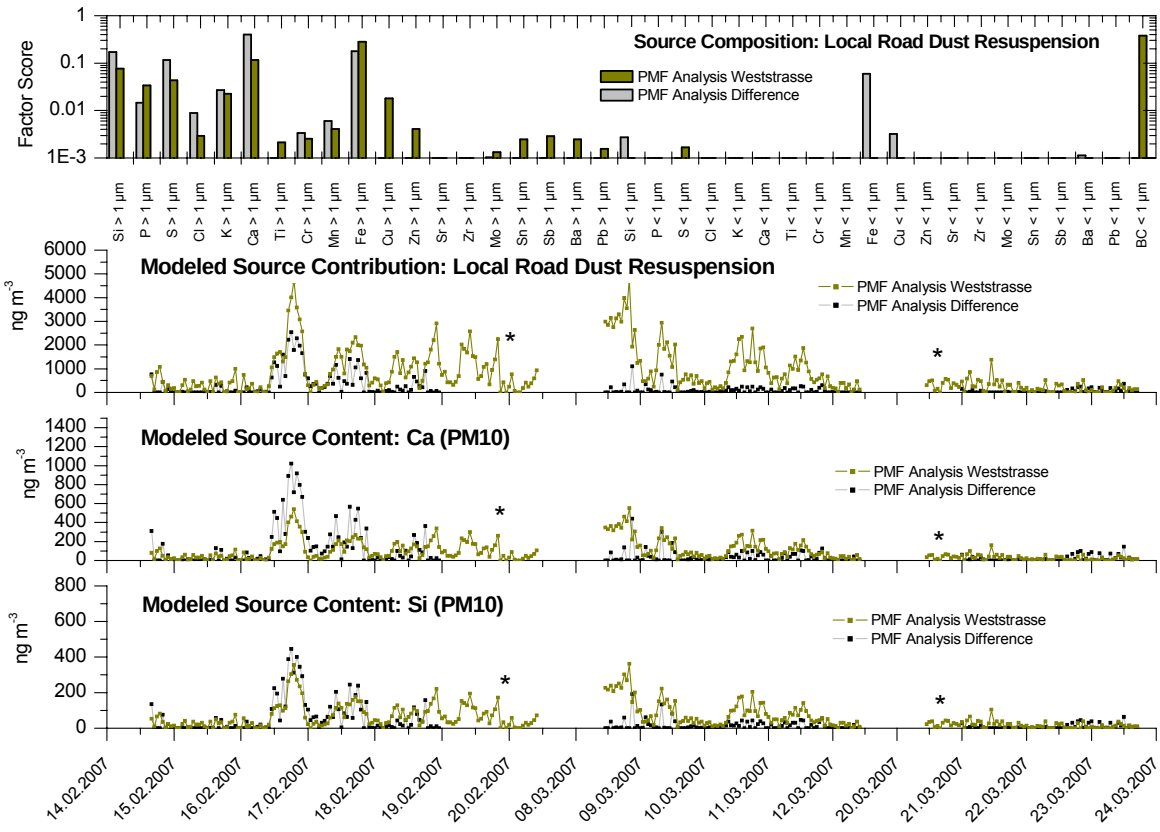

Fig. 5.6.3: Local resuspension: Source composition and contribution. Stars (*) indicate periods with unstable model results for the PMF analysis of the mass concentration difference Weststrasse-Kaserne.

- **Minor local source:** This source is clearly identified by PMF, but its mass contribution is one order of magnitude lower compared to local traffic and local resuspension. Its temporal evolution is irregular but the elevated contributions of this source occurred predominantly during nighttime. The source composition shows remarkable contributions of submicron mode tracers. The interpretation of this source remained diffuse. Since the mass contribution of this source is very low, it was omitted from further mass balance considerations (see Section 5.6.6).

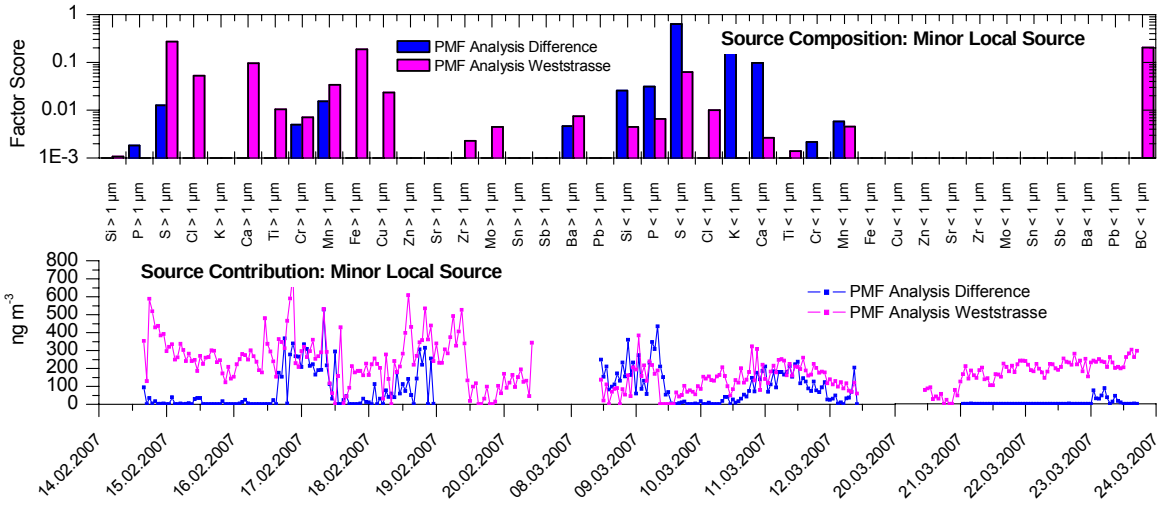

Fig. 5.6.4: Minor local source: Source composition and contribution. Stars (*) indicate periods with unstable model results for the PMF analysis of the mass concentration difference Weststrasse-Kaserne.

Kaserne only:

- **Aged traffic:** This source identified at Kaserne includes the (comparably very low) mass concentrations of brake wear related elements observed at Kaserne. The composition shows some similarity with the resuspension source found at Weststrasse, the temporal evolution is however much more diffuse.

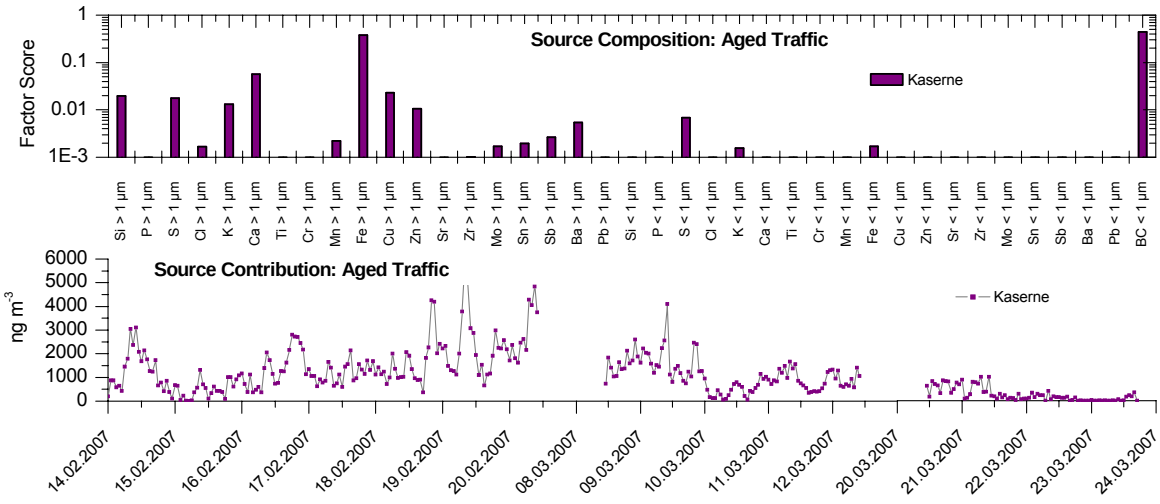

Fig. 5.6.5: Aged traffic: Source composition and contribution.

Weststrasse and Kaserne:

The temporal evolution and the characteristic source compositions of the following sources were similar for both locations. They were not identified in the PMF analysis of the concentration difference between Weststrasse and Kaserne, therefore they are considered as urban background sources. Although the temporal evolution of the individual background sources was similar for Weststrasse and Kaserne, there were distinct differences in the absolute source contributions.

- **Road salt resuspension:** This is a very characteristic coarse mode chlorine dominated source with a strongly irregular temporal pattern, depending on the road salting activities. Road salting episodes led to massive contributions also at Kaserne, where only minor de-icing activities occurred in direct proximity to the measuring containers. The drying process of resuspended salt droplets is on the order of several hours and occurs simultaneously with the meteorological dispersion of the droplets. As a result, the dried road salt aerosol particles rather represent a background source than a road-specific emission source.

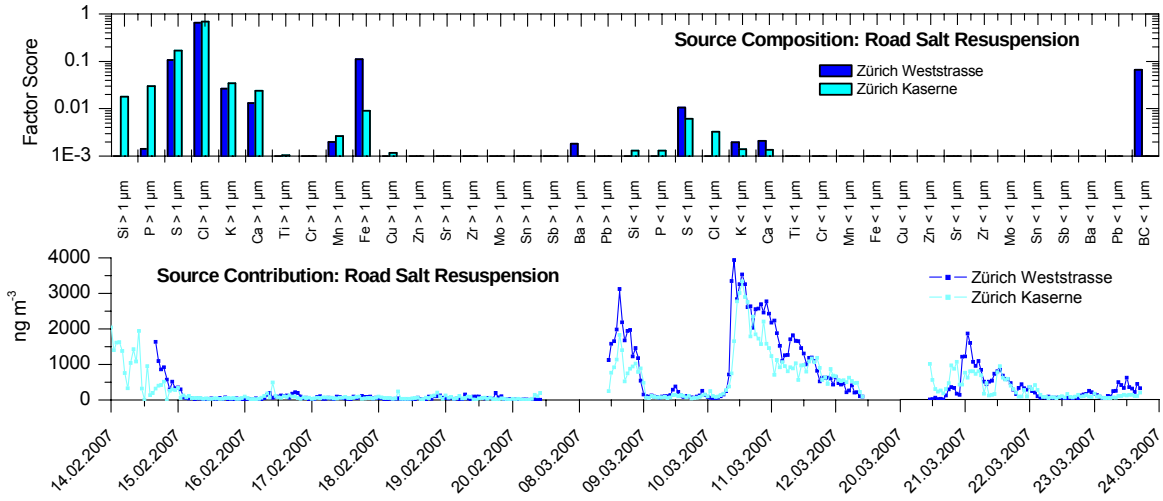

Fig. 5.6.6: Road salt resuspension: Source composition and contribution.

- **Secondary inorganic aerosol:** A very distinct source of submicron sulfur, with a characteristic and irregular temporal evolution. Submicron sulfur is attributed to ammonium sulfate, which is a dominant PM contributor formed by conversion of SO_2 to sulfate via either heterogeneous reactions in droplets (with ozone, NO_2, H_2O_2) or photochemically via OH radicals. This source is expected to have a high spatial homogeneity, which is however not reflected in the time series. A likely explanation for this discrepancy is the different contributions of BC, which will result in a bias of the absolute source mass concentrations as discussed in Section 5.6.5.1.

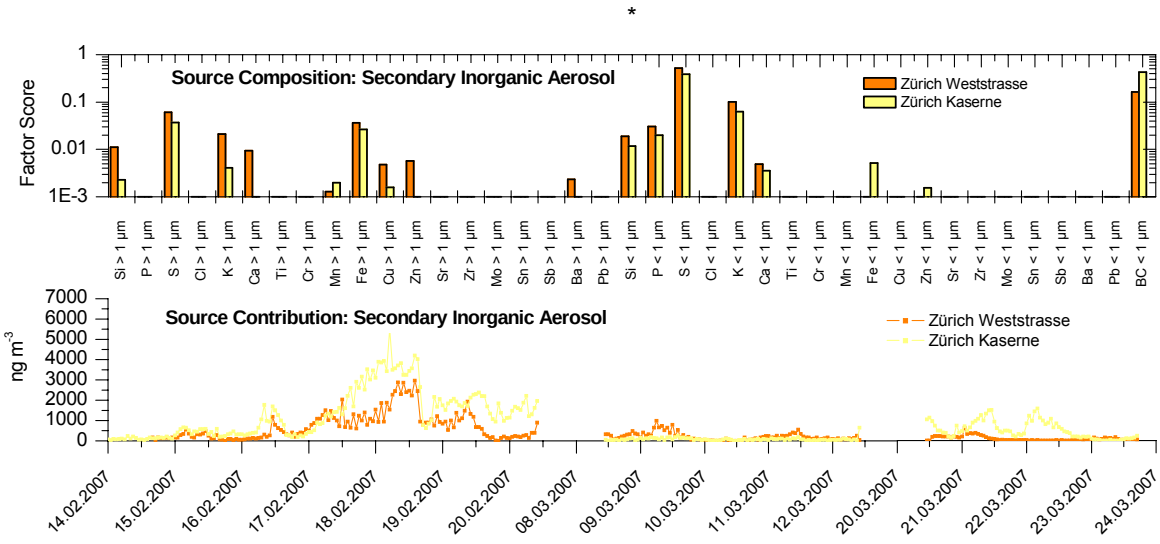

Fig. 5.6.7: Secondary inorganic aerosol: Source composition and contribution.

- **Local mineral background:** The composition of this source shows strong contributions of mineral elements, and the temporal evolution is rather irregular, indicating that this source is not traffic related and mainly influenced by meteorology. This source was identified in all size ranges and at both locations, but within the individual size ranges there are considerable variations within the composition.

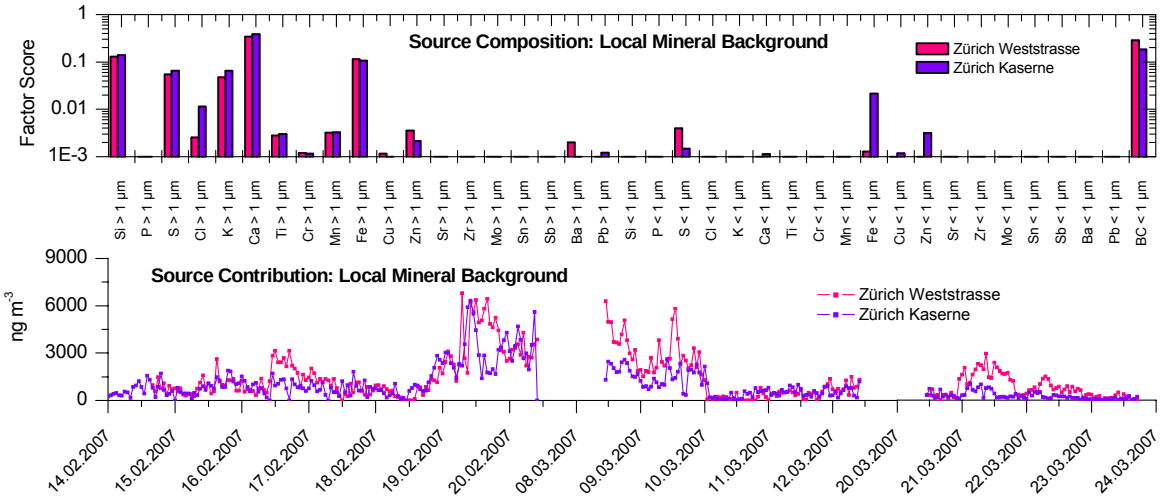

Fig. 5.6.8: Local mineral background: Source composition and contribution.

- **Wood burning signature source:** This source, including a clear wood combustion signature (submicron S, Ca, K, Zn), shows high contributions during time periods with massive total PM10 concentration (> 50 µg m^{-3}). Like the local mineral background, this source seemed mainly influenced by meteorology.

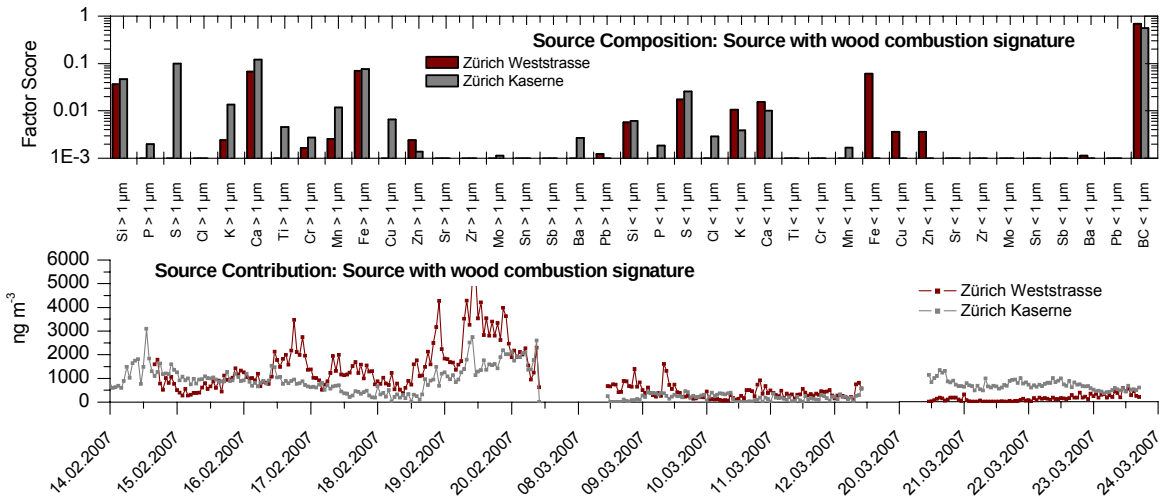

Fig. 5.6.9: Wood burning signature source: Source composition and contribution.

5.6.5.3 Attribution of trace elements to individual sources:

Table 5.6.7 and Figures 5.6.10a-c show the attribution of the measured trace elements to the sources identified via PMF at Zürich-Weststrasse.

Table 5.6.7: Major sources for a selection of trace elements detected at Zürich-Weststrasse

Parameter	Major sources
BC(PM1)	Traffic > Wood signature source > Local resuspension
Sb (1 -10 µm)	Traffic > Local resuspension
Zn (1 -10 µm)	Traffic > Local Resuspension ≈ Secondary inorganic aerosol ≈ Wood signature source
Fe (1 -10 µm)	Traffic > Local resuspension > Local mineral background
Si (1 -10 µm)	Local mineral background >> Local resuspension ≈ Wood signature source
Ca (1 -10 µm)	Local mineral background >> Wood signature source
K (1 -10 µm)	Local mineral background >> Local resuspension
S (1 -10 µm)	Local mineral background > Road Salt
K <1 µm	Secondary inorganic aerosol > Wood signature source
S <1 µm	Secondary inorganic aerosol > Wood signature source
Zn <1 µm	Wood signature source >> Local mineral background

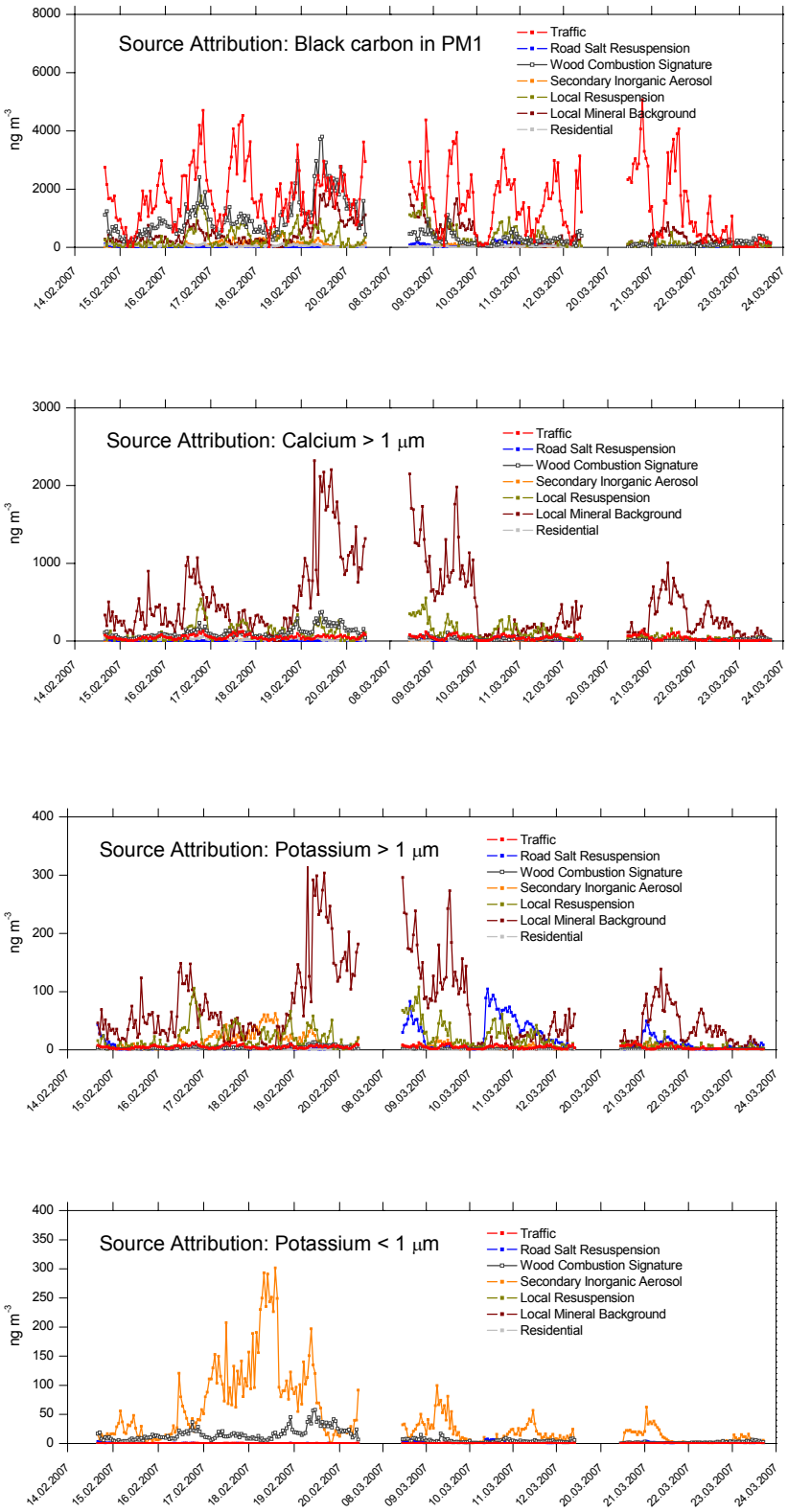

Fig. 5.6.10a: Attribution of trace elements to individual sources.

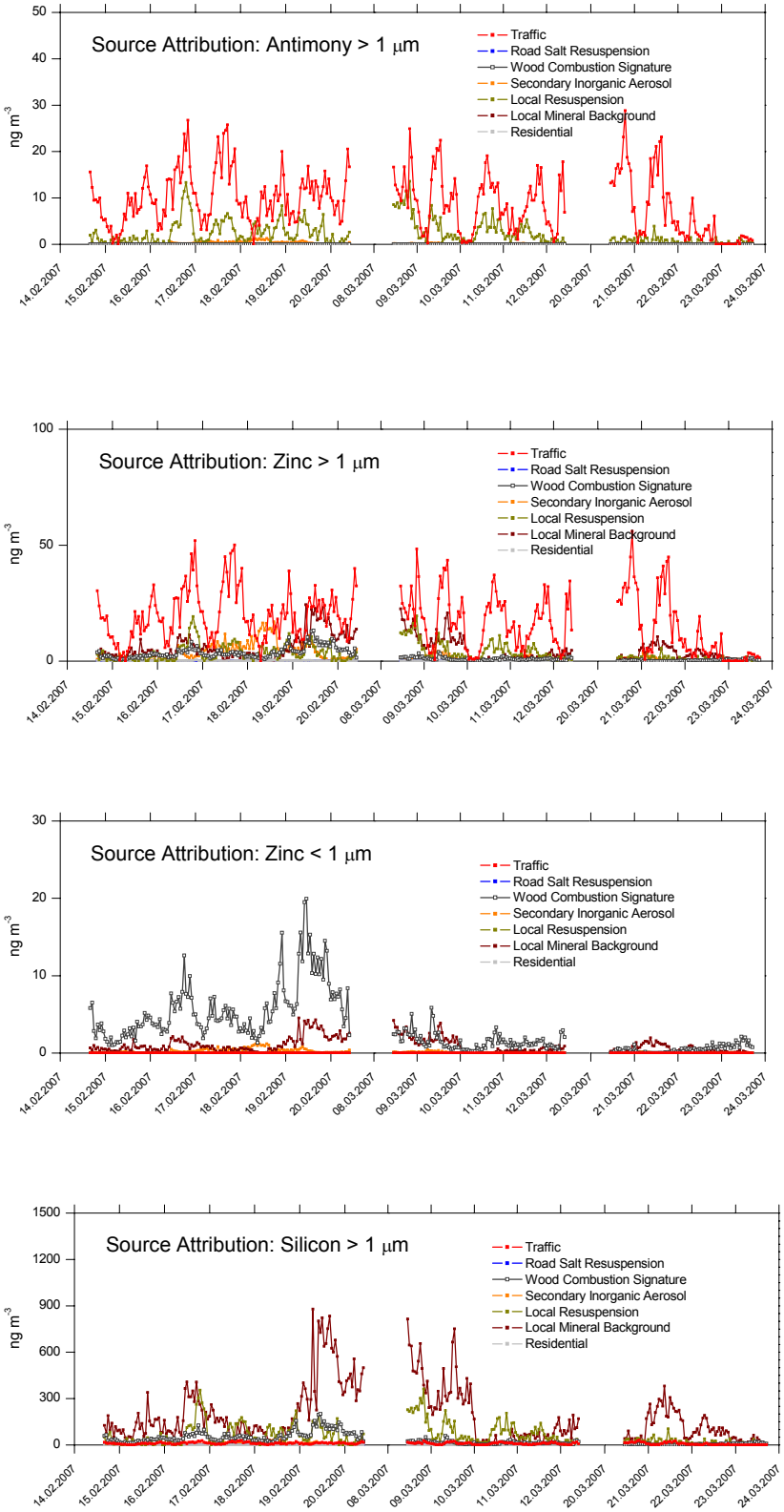

Fig. 5.6.10b: Attribution of trace elements to individual sources.

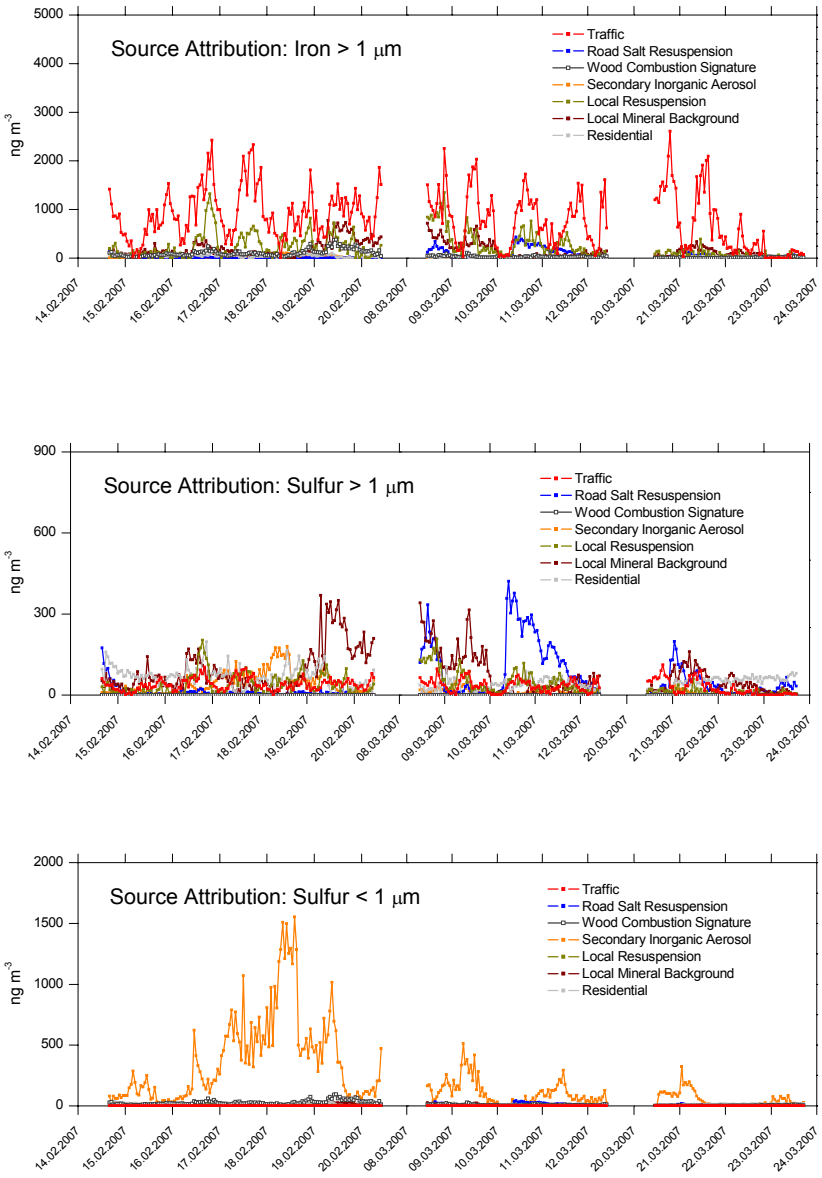

Fig. 5.6.10c: Attribution of trace elements to individual sources.

5.6.6 Zürich-Weststrasse: Source extrapolation and mass balance

5.6.6.1 Unexplained mass contributions:

Two categories of unexplained mass contributions were considered for mass balance calculations:

- *Not measured:* The measured species (considered trace elements plus black carbon) only explained ~25% (median) of the total PM10 at Weststrasse (Figure 5.6.11). In the concentration difference the explained mass fraction increased to ~50% (median), indicating the dominant contribution of black carbon. The non-measured PM10 fraction was assigned to organics, nitrates and the sum of other compounds. Since a comprehensive chemical mass balance for

PM10 was beyond scope due to the study-specific selection of measured trace elements, trace elements were not calculated as oxides to obtain the above number.

- *Measured but not modeled by PMF:* A residual fraction of the measured species were not modeled and explained by the identified sources (Figure 5.6.12). The unexplained residual was generally low but showed relevant peaks during individual episodes.

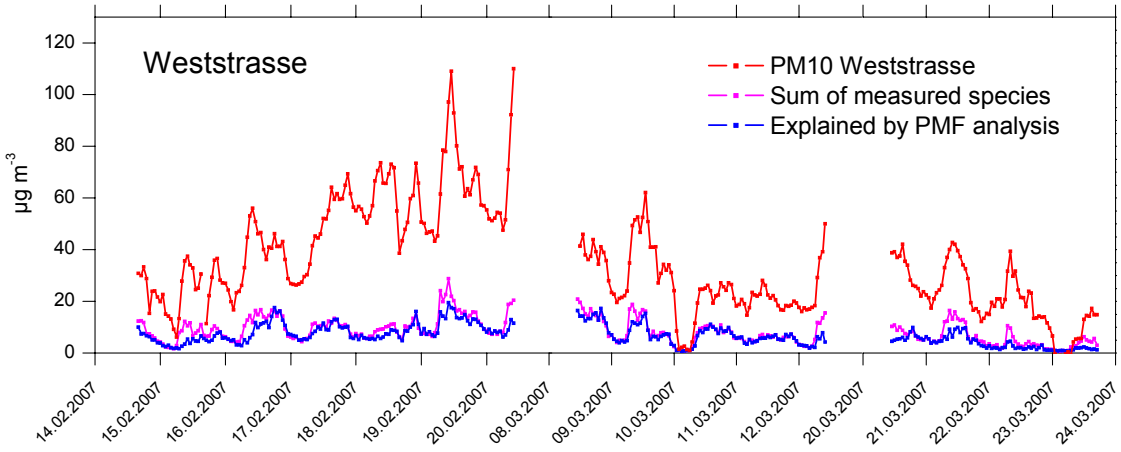

Fig. 5.6.11: Total mass contribution of the measured species (trace elements plus black carbon in PM1) at Zürich-Weststrasse.

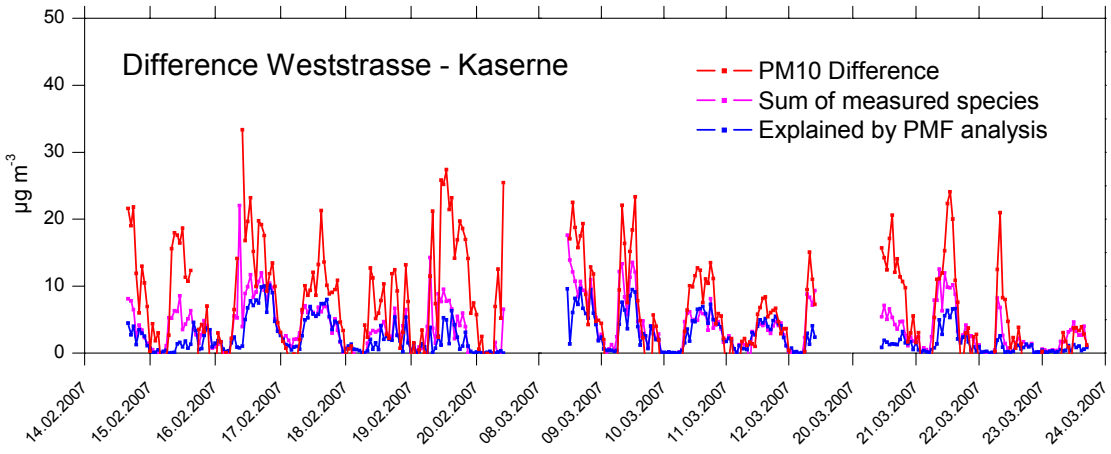

Fig. 5.6.12: Mass contribution of the measured species (trace elements plus black carbon in PM1) within the mass concentration difference Weststrasse - Kaserne.

5.6.6.2 Traffic related sources at Zürich-Weststrasse

For Zürich-Weststrasse, the following relevant traffic related sources were identified by PMF analysis of the measured species and used for mass balancing:

- Brake wear (directly traffic related emissions)
- Traffic related black carbon in PM1 (directly traffic related emissions)
- Vehicle induced resuspension of road dust (indirectly traffic related emissions)

Due to the absence of unique tracer species, separate contributions from road wear and tire wear were not identified by PMF.

For a complete mass balance, these sources were extrapolated to their full mass contributions using compositional information obtained from complementary measurements performed during APART or from literature. To establish a reliable total source contribution, more than one extrapolation hypothesis was applied where possible.

Brake Wear:

The elemental pattern for brake wear has been found to be very stable in Zürich (see Section 5.1). Table 5.6.8 presents the applied extrapolation hypotheses and Figure 5.6.13 shows the extrapolated source contribution.

Table 5.6.8 Extrapolation of brake wear.

Hypothesis	**Basis**
Mass fraction of Sb in brake dust: 1 ± 0.2%*	• Section 5.1, review of published brake dust compositions (Furuta et al. 2005; Grieshop et al. 2005; Hjortenkrans et al. 2007; Iijima et al. 2008; Johansson 2008; Sternbeck et al. 2002; von Uexkull et al. 2005)
Mass fraction of Cu in brake dust: 5 ± 2%*	
Extrapolation of Fe to Fe_2O_3 provides a largely complete brake dust mass balance.	• Other relevant mass contributions are not expected.

*Cu/Sb ratio for brake wear related Sb and Cu at Zürich-Weststrasse: 6.2 (see Section 5.1).

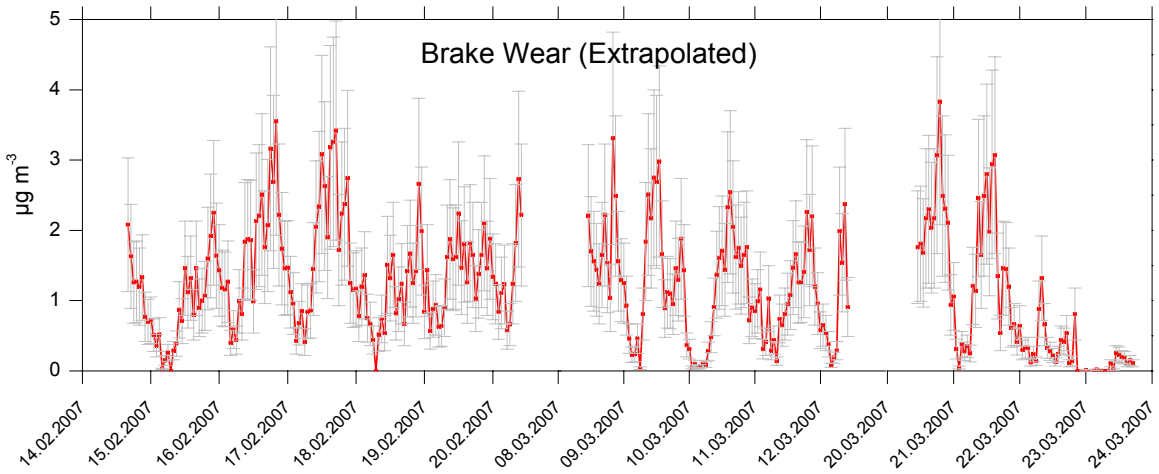

Fig.5.6.13: Brake wear: Extrapolated source contribution at Zürich-Weststrasse. The average of the three individual extrapolation scenarios is shown. The error bars show the propagated uncertainty resulting from the PMF analysis and the extrapolation.

Traffic related total carbon (exhaust):

The extrapolation from black carbon to total traffic related carbon was performed using empirical conversion factors which were gained from a) mobile measurements in Zürich and b) stationary measurements in Zürich and Dübendorf, at locations similar but not identical to Weststrasse (Table 5.6.9).

Table 5.6.9: Extrapolation for black carbon (BC: Black carbon, HOA: Hydrocarbon like traffic related organic aerosol, EC: Elemental carbon, TC: Total carbon, MAAP: Multiangle absorption photometer.

Hypothesis	**Basis**
$TC_{fossile} = EC_{fossile,EUSAAR2} + HOA_{fossile}$	EC according EUSAAR2 protocol (Cavalli et al. 2009)
$HOA/BC_{fossile,MAAP} = 0.7$	Mobile measurements in Zürich (Winter 2007/2008), see Mohr et al. (2009)
$EC_{fossile,EUSAAR2}/BC_{fossile,MAAP} = 0.75$	NABEL Station Bern Bollwerk
$BC_{fossile,MAAP}/BC_{fossile,Aethalometer}$ [*a] ~ 1	NABEL Station Dübendorf [*b]
$BC_{fossile,Aethalometer} \approx BC_{Aethalometer,PM1}$ [*a]	APART
$TC_{fossile}$ ≈ 'Exhaust' = = (1.45±0.1)*$BC_{Aethalometer,PM1}$	

[*a] BC from Aethalometer measurements at 880 nm wavelength, standard calibration.

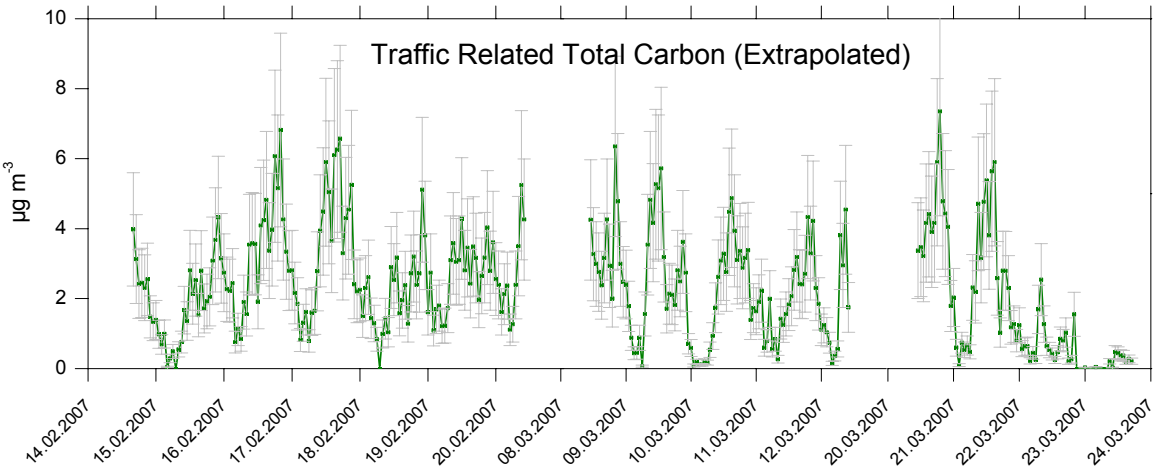

Fig. 5.6.14: Total Carbon in PM1: Extrapolated source contribution at Zürich-Weststrasse. The error bars show the propagated uncertainty resulting from the PMF analysis and the extrapolation.

Resuspension:

The road dust analysis performed during APART (Section 5.3) provided compositional information on resuspended PM10 in Zürich. Since the road dust investigations took place one year later than the stationary measurements in Zürich, a direct use of the road dust composition for the quantitative extrapolation of the PMF resuspension source introduces a considerable uncertainty. Figure 5.6.15 shows that the compositional pattern of the road dust and the PMF resuspension source is similar, but that there are large differences in

the absolute contribution of the individual elements. A relatively good agreement was found for calcium, for which the road dust analysis provided a consistent value at all stations investigated (see Section 5.3). Therefore Ca was used to estimate a quantitative contribution of resuspension. Table 5.6.10 presents the applied extrapolation hypotheses and Figure 5.6.16 shows the extrapolated source contribution. The source contribution will not be used for a quantitative calculation of emission factors for resuspension, as it will be explained in Section 5.6.6.4.

Table 5.6.10: Extrapolation of local resuspension

Hypothesis	**Basis**
Mass fraction of Ca in deposited PM10: 10.1 ± 3.7%	Road dust sampling in Zürich (Section 5.3): Value Weststrasse, uncertainty based on all roadside locations.

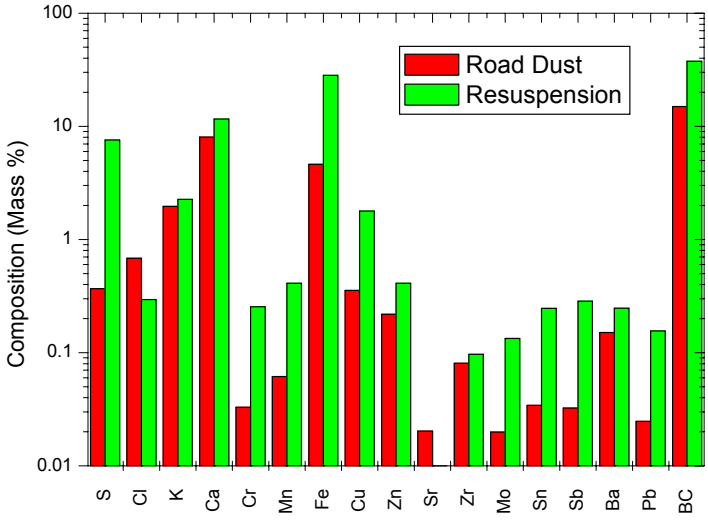

Fig. 5.6.15: Comparison of the composition of road dust (average composition of 7 locations in Zürich, see Section 5.3) and resuspended road dust in Zürich-Weststrasse (PMF analysis, see Section 5.6.5.2). The best agreement was found for Ca and thus used for extrapolation.

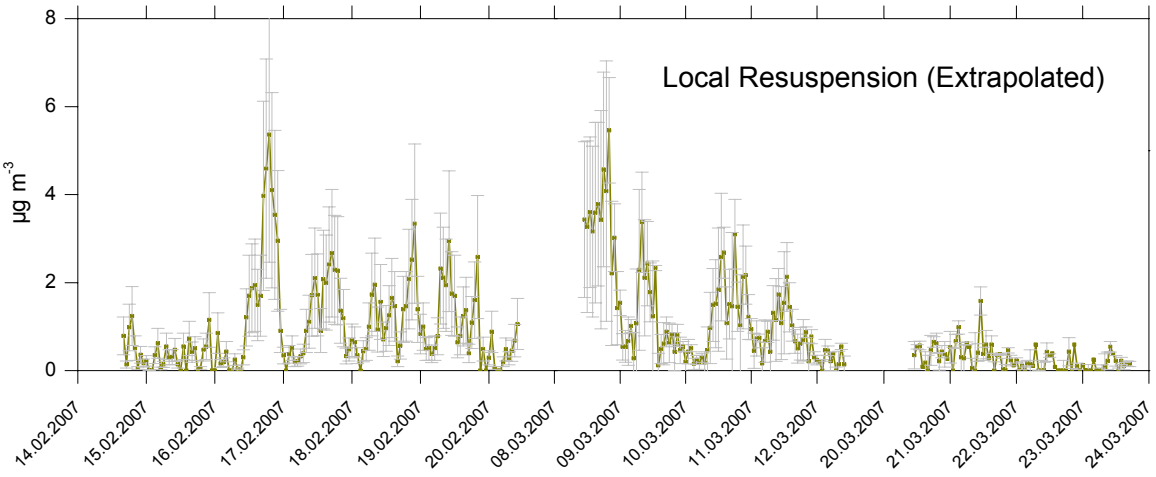

Fig. 5.6.16: Local resuspension: Extrapolated source contribution at Zürich-Weststrasse. The average of the three individual extrapolation scenarios is shown (plus standard deviation). The error bars show the propagated uncertainty resulting from the PMF analysis and the extrapolation.

5.6.6.3 Mass balance

Figure 5.6.17 shows the mass balance for the traffic related PM10 sources at Zürich-Weststrasse. During most time periods, the three considered traffic contributions (brake wear, exhaust related carbon and local resuspension) explained a major fraction of the measured PM10 difference. Two episodes with large unexplained contributions were observed, which were characterized by rainfall or a total PM10 mass concentration larger than 50 µg m^{-3} both at Weststrasse and Kaserne, respectively. During the rainfall period, the observed difference may have been caused by humidity effects. The second period represented an exceptionally high-pollution episode with possibly strong local contributions of secondary organic aerosols and ammonium nitrate.

Figure 5.6.18 shows the diurnal variation of the identified sources, along with the total traffic frequency. Also in these plots the strong correlation of brake wear and traffic related total carbon is clearly seen, while the diurnal pattern of vehicle induced resuspension is less correlated due to the reservoir effect of the street canyon and characterized by a larger statistical variation (see Section 5.3). Figure 5.6.19 shows the fractional contribution for the traffic related PM10 sources at Zürich-Weststrasse. The statistical variation indicated in the Figure represents the temporal variation of the source contributions during the considered time period in February 2007 and do not include the methodological uncertainty of the individual source quantifications.

The presented mass balance shows that with the applied source quantification for brake wear, exhaust emissions and resuspension, a considerable fraction of the traffic related PM10 remained unexplained. With the applied statistical methodology for source identification and the estimates made for the quantitative extrapolations for the source mass contributions, only approximately 60% of the experimentally measured PM10 difference was directly explained by the identified traffic related sources. While the estimates for brake wear and exhaust emissions can be considered as robust estimates, it is likely that the contribution of resuspension was underestimated using the applied assumptions for extrapolation (see above). However, for emission factor calculations the quantitative contribution of resusupension will be calculated independently.

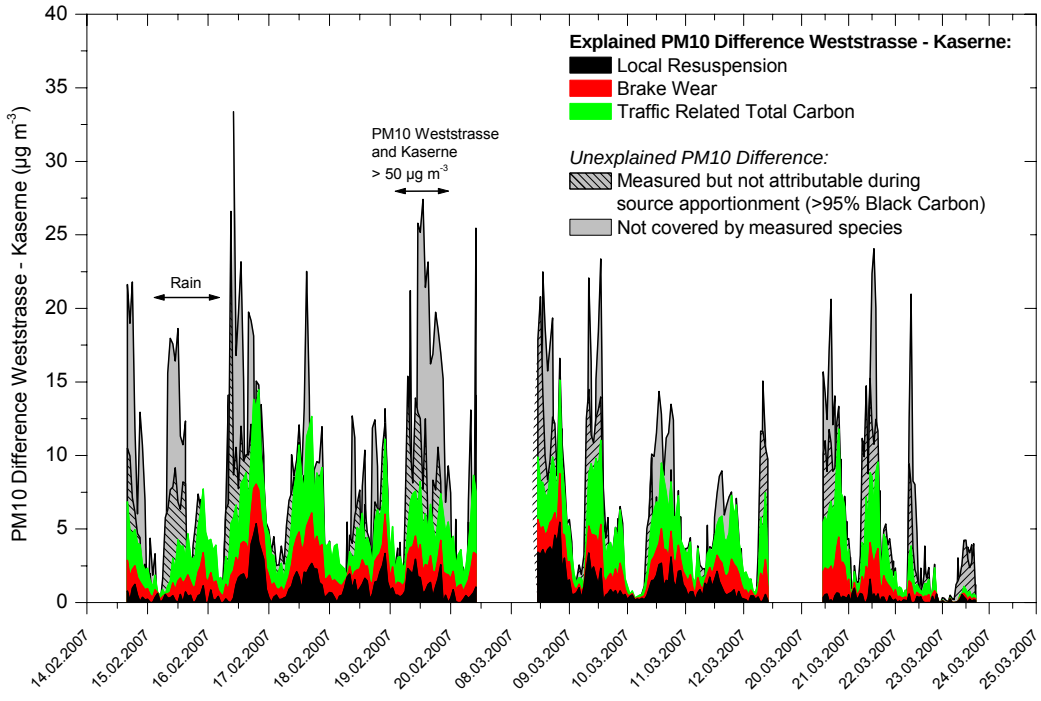

Fig. 5.6.17: Source apportionment for local PM10 at Zürich-Weststrasse (background corrected).

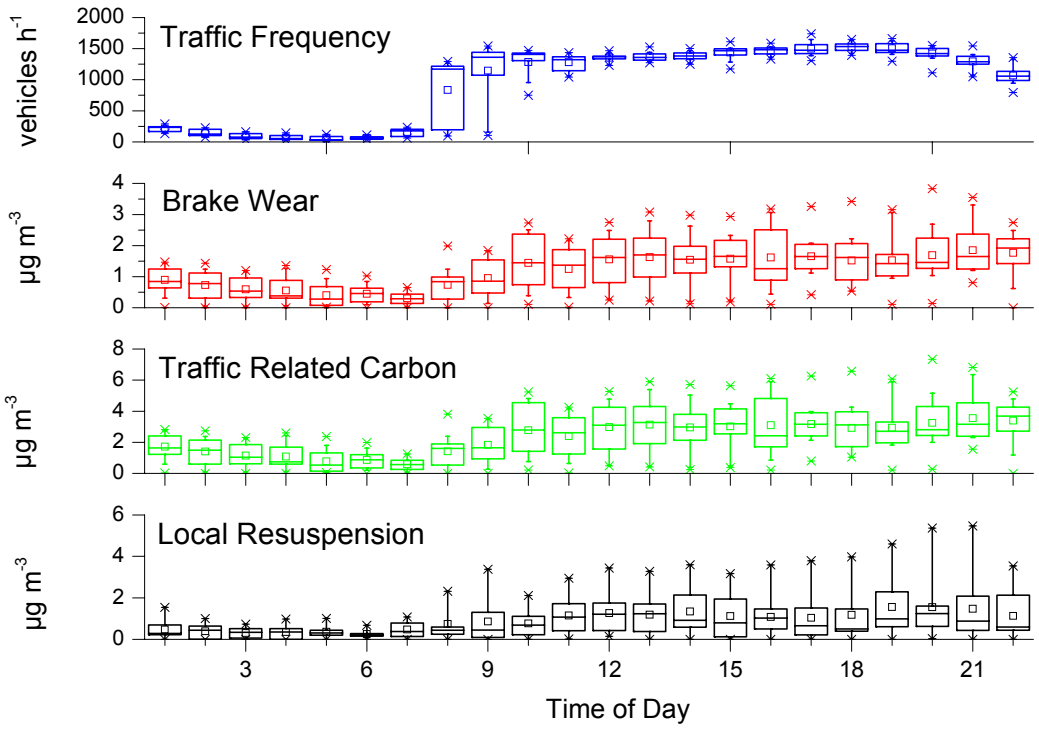

Fig. 5.6.18: Diurnal variation of the traffic related PM10 sources at Zürich-Weststrasse.

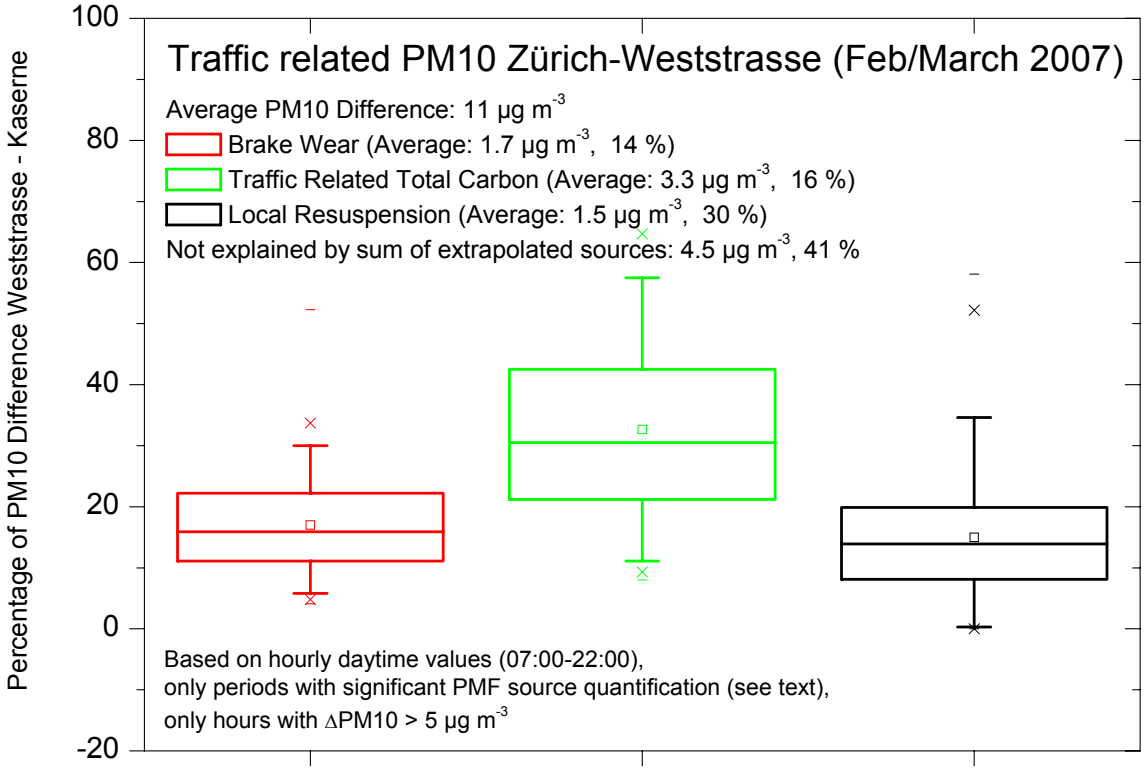

Fig. 5.6.19: Source apportionment for local (background corrected) PM10 at Zürich-Weststrasse. The statistical variation represents the temporal variability. Brake wear was quantified assuming a brake dust antimony content of 1% and a copper content of 5%. Total carbon was estimated from black carbon using an empirical conversion factor of 1.45, obtained from experimental data. Local resuspension was quantified assuming a calcium content of 10%, based on road dust analysis. (Box: First to third quartile range, plus median line. Error bars: 5-95% percentile. □: Average. x: 1-99% percentile, -: Maximum/minimum).

5.6.6.4 Source Emission Factors

The absolute mass contributions of the identified and quantified emission sources were used to calculate source emission factors for light duty vehicles (EF_{LDV}), heavy duty vehicles (EF_{HDV}), as well as the average traffic fleet (EF_{Fleet}). The same linear regression method as used for the elemental emission factors (Section 5.1) was applied, using NOx to correct for atmospheric dilution. Only hourly data from dry periods and ΔNOx > 20 µg m^{-3} were considered. The data set was checked and corrected for obvious outlier values. The following list provides conceptual information on the calculations.

Average fleet emission factors: To estimate and evaluate the total PM10 mass balance, average fleet emission factors were calculated from the experimental data for brake wear, total carbon (exhaust), resuspension and total PM10:

$$EF_{x,Fleet} = \frac{c_x \cdot d}{n_{tot}}$$

where c_x is the measured mass concentration (µg m^{-3}) assigned to the considered source or emission process *x*, n_{tot} the total vehicle frequency (vehicles h^{-1}) and d the atmospheric dilution, determined via NO_x. For brake wear, exhaust and resuspension, c_x represents the extrapolated PMF source contributions, while for PM10 c_x = Δc (Weststrasse – Kaserne). The fleet emission factor depends on the average traffic composition (6.7% HDV for the selected hourly data, 10% HDV during the entire campaign) and represents an average value for a considered time period. For PM10, the fleet emission factor includes the contribution from resuspended dust. The calculated standard deviation of the average calculated with this equation reflects the temporal variability of the traffic composition. While the quantification of brake wear and exhaust emissions was considered to be significantly robust (see Section 5.6.5.2), it is likely that the contribution of resuspension was underestimated using the applied assumptions for extrapolation.

Table 5.6.11: Experimentally determined fleet emission factors

Source	**Fleet EF (6.7% HDV) mg/km[*1]**
Brake Wear	12
Total Carbon (Exhaust)	23
Resuspension	9
PM10 inkl. Resuspension	55

LDV and HDV emission factors for brake wear and traffic related carbon: The following multilinear regression model was used to calculate vehicle specific emission factors:

$$c_x = EF_{x,LDV} \cdot \left(\frac{n_{LDV}}{d}\right) + EF_{x,HDV} \cdot \left(\frac{n_{HDV}}{d}\right) + C$$

where c_x is the measured mass concentration (µg m^{-3}) assigned to the considered source or emission process *x*, n_{LDV} and n_{LDV} are the vehicle frequencies (vehicles h^{-1}), d the atmospheric dilution, determined via NO_x and C the fitting constant. Both sources, identified by PMF and extrapolated to their full mass contributions, delivered statistically relevant results (r^2 = 0.52, related to 148 data points) and yielded a very

low fitting constant (unexplained fraction less than ± 2%). Thus, the LDV and HDV emission factors for brake wear and traffic related carbon were reasonably estimated by the multilinear regression model.

Table 5.6.12: Multilinear fit parameters

Source	EF LDV (mg/km)	EF HDV (mg/km)	C (µg m^{-3})	R2	Average difference (µg m^{-3})	Unexplained fraction (%)
Brake wear	7.8 ± 0.9	80.7 ± 11.1	-0.03 ± 0.12	0.52	1.37	-2
Traffic related carbon	14.9 ± 1.7	154.9 ± 21.3	-0.06 ± 0.24	0.52	2.42	-2

LDV and HDV emission factors for PM10 and resuspension: Resuspension is not directly related to vehicle frequencies; therefore a straightforward calculation for LDV and HDV emission factors using the above model is not possible and does not provide meaningful fitting results. Since resuspension substantially contributed to the average PM10 fleet emissions, this also applies to PM10. Two alternative calculation procedures were therefore applied to estimate vehicle specific emission factors:

- *Qualitative* multilinear regression: To account for the observed autocorrelational behavior of the pollutant time series in the Zürich-Weststrasse street canyon (due to accumulation of resuspended dust and fresh pollutants), an autoregressive term was included in the fit model (model description see also Section 5.1):

$$c_{x,t=0} = EF_{x,LDV} \cdot \left(\frac{n_{LDV}}{d} \right) + EF_{x,HDV} \cdot \left(\frac{n_{HDV}}{d} \right) + f \cdot c_{x,t-1} + C$$

  where $c_{x,t=0}$ is the measured source mass concentration at a considered hour, c_{t-1} the mass concentration measured one hour earlier and f the respective fractional coefficient (obtained by the multilinear fit). The selected time lag interval of one hour directly influences the fit results and was arbitrarily selected because it represents the maximal time resolution of the measurements. As a result, the fit results cannot be considered to be fully quantitative but nevertheless provide qualitative information on the relative ratio between LDV and HDV emission factors.

  For PM10, the fits yielded a highly negative fitting constant (C, represents non vehicle related PM10 contributions), which was explained by events with negative PM10 concentration differences (Weststrasse minus Kaserne) with simultaneous ΔNOx > 20 µg m^{-3}. The autocorrelation coefficient of the fit was 37%. For comparison, the fits were also performed without the autocorrelation term. Due to the bias inferred by the high fitting constant C the results from these multilinear fits were not used for PM10.

  The fit of the resuspension source, yielding a good fitting quality (r^2=0.7), attributed approx. 70% of the source to the autocorrelation term, indicating a strong accumulation of pollutants within the street canyon. The fit provided a very low emission factor for individual LDV (~1 mg/km/veh), while the respective value for HDV was >100 mg/km/veh. The absolute numbers themselves are biased by the model definition and the large negative fitting constant (-18% contribution to the average mass contribution). Nevertheless, the clear differentiation between LDV and HDV does not represent a model bias caused by the autoregression term and thus can be used as semiquantitative information for mass balancing purposes. Explanations of the strongly different LDV and HDV emission factors will be given in the following Sections.

Table 5.6.13: Multilinear fit parameters

Source	EF LDV (mg/km)	EF HDV (mg/km)	f	C (µg m^{-3})	R2	Average difference (µg m^{-3})	Unexplained fraction (%)
PM10	23.0 ± 5.9	918.2 ± 74.9	0.00 ± 0.00	-3.04 ± 0.83	0.56	6.10	-50
PM10	16.0 ± 5.4	614.1 ± 83.9	0.37 ± 0.06	-2.53 ± 0.75	0.65	6.10	-41
Resuspension	0.9 ± 1.7	55.0 ± 21.5	0.68 ± 0.05	-0.18 ± 0.23	0.70	1.02	-18

- *Mass balancing:* LDV and HDV emission factors for PM10 and resuspension were alternatively estimated according the following assumptions:

$$EF(PM10_{tot})_{LDV} = \sum EF_{LDV}(brake\ wear, total\ carbon, resuspension)$$

As shown above, the multilinear fit for resuspension provided a very low emission factor for individual LDV (~1 mg/km/veh). For mass balancing this value was used, flagged with a high uncertainty due to its semiquantitative nature.

$$EF(\mathrm{Re}\,suspension)_{LDV} \cong 1 \pm 5\ mg/km/veh$$

Thus (see Tables 5.6.12 and 5.6.13):

$$EF(PM10_{tot})_{LDV} = \sum EF_{LDV}(7.8 + 14.9 + 1) = 23.7\ mg/km/veh$$

Because a reliable PM10 fleet emission factor $EF(PM10_{tot})_{Fleet}$ was obtained (see Table 5.6.11), $EF(PM10_{tot})_{HDV}$ could be calculated as follows:

$$EF(PM10_{tot})_{HDV} = \frac{EF(PM10_{tot})_{Fleet} - (1-x) \cdot EF(PM10_{tot})_{LDV}}{x}$$

where x is the heavy duty vehicle fraction (6.7% for the selected set of hourly data) and $EF(PM10_{tot})_{Fleet}$ the corresponding experimental fleet emission factor for total PM10 (55 mg/km/veh).

Table 5.6.14 and Figure 5.6.20 present an overview of the calculated emission factors. Fleet emission factors for the Zürich-Weststrasse long-term average HDV fraction (10%, winter 2007/2008) were calculated from the respective HDV and LDV emission factors.

Table 5.6.14: Emission factors for the individual sources contributing to traffic related PM10, valid for Zürich-Weststrasse (urban street canyon). LDV: Light duty vehicles (including 9% delivery vans), HDV: Heavy duty vehicles (including motor coaches). Values are based on 12 days of measurements in February an March 2007, dry time periods only) and are based on NO_x emission factors estimated for Zürich-Weststrasse (Year: 2007, EF_{NOx}(LDV) = 286.8 mg km^{-1}, EF_{NOx}(HDV) = 10559 mg km^{-1}, NO_x calculated as NO_2, (INFRAS 2004)). Colors: Multilinear regression (good model performance), Multilinear regression (bad model performance), Estimated values (mass balance). The indicated uncertainties represent the propagated uncertainty from PMF analysis and source quantification (net uncertainties: brake wear 46%, exhaust 41%, resuspension 54%) and from multilinear regression (values see above). Note: The set of data used for the emission factor calculations is not completely identical to the data set used for the mass balance presented in Figure 5.6.19, which leads to slightly different fractional source contributions.

Source	**Quantification**	**Vehicle Fleet**			**LDV**	**HDV**
		Experimental value	**Calculated from LDV,HDV**			
		6.7% HDV[*1]	**6.7% HDV[*1]**	**10% HDV[*2]**		
		mg/km	**mg/km**	**mg/km**	**mg/km**	**mg/km**
Brake Wear	PMF	12	13	15	7.8 ± 3.7	80.7 ± 38.8
Total Carbon (Exhaust)	PMF	23	24	29	14.9 ± 6.3	154.9 ± 67.0
Resuspension (modeled)	PMF	9	4	6	0.9 ± 1.8	55.0 ± 36.6
PM10 incl. Resuspension (modeled)	Measured: ΔPM10 (Weststrasse-Kaserne)	55	55	76	16.0 ± 5.4	614.1 ± 83.9
PM10 without Resuspension	Sum of brake wear and TC(exhaust)	35	37	44	22.7 ± 7.3	235.7 ± 77.4
PM10 incl. Resuspension (refined estimate)	Estimated	55	55	71	23.7 ± 7.5	497.4 ± 85.7
Resuspension (refined estimate)	Estimated	18	18	27	1.0 ± 11	261.8 ± 115.0

[*1] selected time period

[*2] entire campaign (winter 2007/2008)

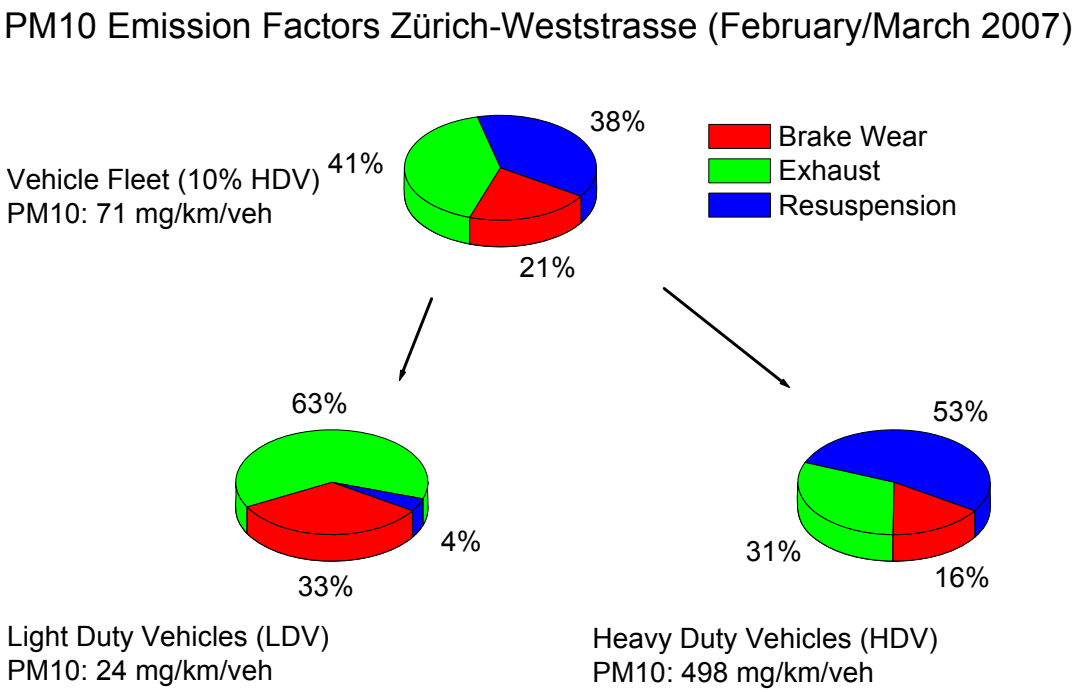

Fig. 5.6.20: PM10 emission factors determined for Zürich-Weststrasse.

The PM10 emission factors for Zürich-Weststrasse show the following characteristics:

The calculated PM10 emission factors for Zürich-Weststrasse show the following characteristics:

- Vehicle Fleet at Zürich-Weststrasse: The average PM10 emission factor, related to a HDV fraction of 10%, was mainly caused by exhaust emissions (41%) and vehicle induced resuspension of road dust (38%), followed by brake wear (21%).
- Light duty vehicles: Exhaust (63%) and brake wear (33%) were the dominant PM10 emissions. Compared to these contributions, the emissions from resuspension of road dust as well as minor contributions from road wear and tire wear, were estimated to be totally less than 5% at Zürich-Weststrasse.
- Heavy duty vehicles: Compared to light duty vehicles, the absolute emission factors for heavy duty vehicles were 15 times higher for total PM10 and 10 times higher for brake wear and the exhaust emissions. In contrast to light duty vehicles, the road dust resuspension capability of an individual heavy duty vehicle was estimated to be substantial. For Zürich-Weststrasse, more than half of the PM10 emissions of an individual heavy duty vehicle were attributed to road dust resuspension and minor contributions of road wear and tire wear.
- Comment to resuspension: Emission factors for road traffic are generally expressed as mass per km per vehicle. This concept is adequate if the emitted species are directly produced on-site by the traffic as is the case for exhaust emissions as well as for freshly produced abrasion particles from brakes, tires and road surfaces. However, resuspension is the remobilisation of previously deposited material from different sources. While the process of resuspension itself is caused by the traffic

induced turbulence, thus depending on intensity and speed of the circulating local traffic, the amount of resuspendable dust is limited by the local deposition of dust from different sources (atmospheric deposition, dust introduced by dirty wheels or losses from truck loadings, debris from plants etc.) onto the road surface. In addition other removal processes than resuspension are possible, like wash-off by rain and wind blow-off. It is therefore a simplifying approach to describe the resuspension process just in terms of "mg/km/vehicle". For traffic situations with low traffic and plenty of resuspendable dust on the road surface this mass unit may be appropriate. However, in streets with high traffic frequencies the emissions from resuspension might be limited by the amount of resuspendable dust. This is likely to be the case for Weststrasse. Here the available dust on the surface seems to be resuspended and kept in suspended state mainly by the turbulence induced by the HDV, leaving only small amounts of dust to be resuspended by the LDV. This does not imply that e.g. in a small street in a residential area with little or no HDV resuspension by LDV has not to be considered. The experiments with the mobile load simulators clearly indicate the potential also of LDV to resuspend particles. This is also confirmed by pure visual evidence from LDV driving on dirty roads. As mentioned already above, the very complex processes relevant for resuspension obviously cannot always be adequately described just in term of "mg/km/vehicle". In cases where resuspension is limited by the available deposited dust on the surface an indication in terms of "mg/m^2/h" might be more appropriate. In addition this parameter is extremely susceptible to the highly variable dirt load on road surfaces.

- Comment to road wear and tire wear: Due to the absence of unique tracer species, separate contributions from tire wear and road wear were not identified by PMF from the roadside measurements. The controlled experiments with a road wear simulator showed that direct abrasion wear from the road surface is of minor importance for pavements in good condition. In the PMF analysis, any potential trace element contributions from these sources were likely to be mixed into the other traffic related sources due to the temporal emission synchrony. Reliable information for PM10 emissions from tire wear can hardly be found in literature. Some older works report contributions up to 10% to urban PM10 concentrations. However, none of the applied methods was specific enough to be convincing. A new, still unpublished study at two urban traffic sites in Germany for the first time uses a method that seems to be really specific (analysis of pyrolysis products of tire rubber) and find a mean contribution of tire wear of 0.5% to PM10. The same work shows that the earlier assumed contribution of up to 10% tire wear assumed earlier really exists, but in particle fractions >10µm and not in PM10. This was also qualitatively confirmed by microscopic evidence. In agreement with these findings, the tire wear emissions for the simulator experiments were found to be negligible, although these emissions were considered to be only partially representative for real-world situations. Overall, there is only a low probability that the presented source apportionment is significantly biased by undetermined contributions of tire wear.

5.6.7 PMF Results for Reiden

5.6.7.1 Local wind situation

Reiden is located in a shallow river valley (Wigger river) and exhibited a regular diurnal wind direction pattern during the campaign (see Figure 5.6.21). During daytime, wind from NE was most frequent, while night time wind directions were mainly along the freeway (and valley) axes. Accordingly, time periods with highest traffic frequencies were mainly dominated by winds from NW (midday) and along the valley and freeway axis (rush hour). As a result, most distinct pollutant concentration differences were observed during midday, with the east station serving as upwind station (background) and the west station as downwind station (background and local traffic contribution).

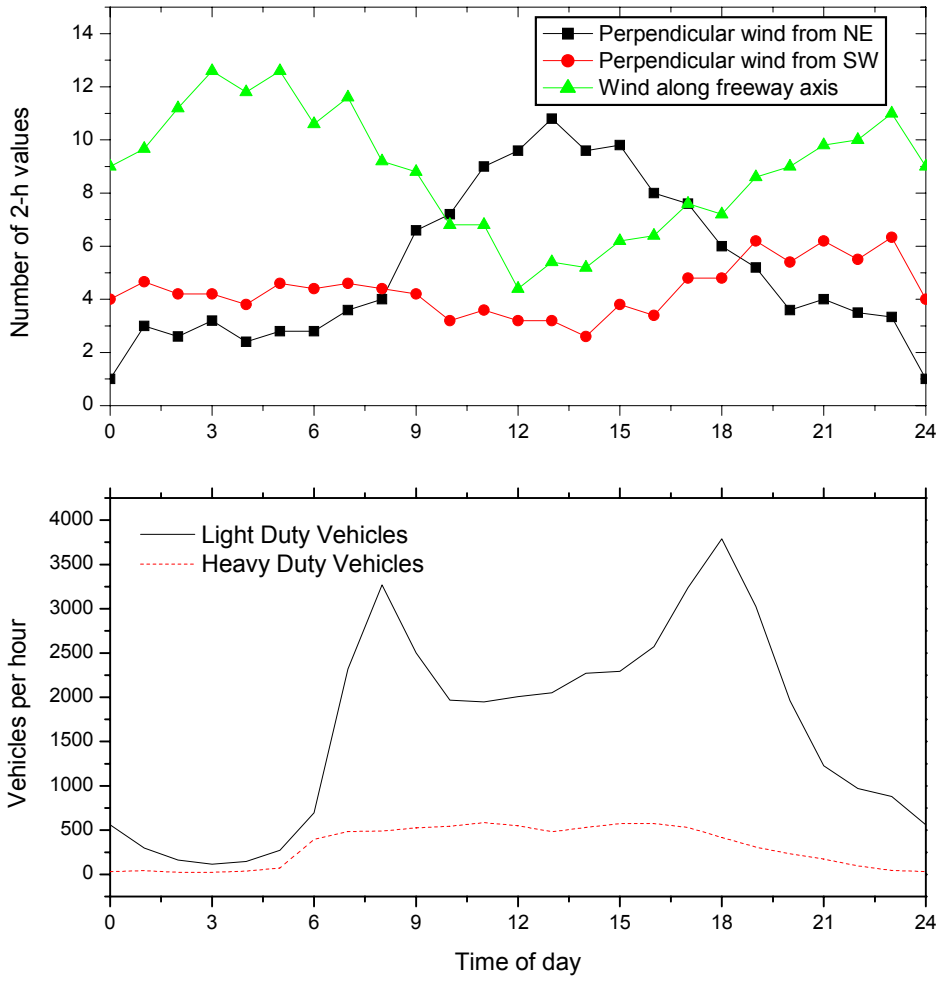

Fig. 5.6.21: Upper panel: Wind direction as a function of daytime, for the time periods considered for PMF analysis (03-12.09.07, 27.09-23.10.07 and 26.11.07-04.12.07). Lower panel: Average Traffic frequencies).

5.6.7.2 Overview of identified sources in Reiden

Tables 5.6.15 and 5.6.16 provide an overview of the sources identified with PMF. These sources were virtually identical for both the east and west stations. Differences in source strength and composition will be discussed in the subsequent Sections. For black carbon (BC) a high relative contribution compared to the trace elements was found for most of the sources. This was caused by the highly dominating BC mass concentrations in the PMF input data. Based on the PMF model uncertainty (unsharpness), very low amounts of BC were attributed to most sources, which were in a similar absolute mass concentration range as the trace element contributions. As it will be shown in Section 5.6.7.5, BC was however predominantly attributed to traffic and local background. Not the total PMF source mass concentration itself will be used to extrapolate the total mass concentration for the source, but rather the absolute mass concentration of individual source tracers (see Section 5.6.8). Therefore the bias contributions from BC will not affect the source mass balancing.

Table 5.6.15: Overview of sources identified by PMF analysis.

Source	Location	Dominant Particle Size range	Dominant contributors*	Tracers/minor contributors**	Identification by PMF	Interpretability
Road traffic	West and east	> 1µm	Ca, Fe, BC(PM1)	Cu, Zn, Zr, MO, Sn, Sb, Ba (brake wear tracers) + Si, Ca, K (resuspension tracers)	Very clear	high
Local mineral background	West and east	> 1µm	Si, S, K, Ca, Fe	Tracers see left	Very clear	high
Secondary inorganic aerosol	West and east	< 1µm	S	Si, P, K	Very clear	high
Resuspended road salt	West and east	> 1µm	Cl	S, P, S, K, Ca, Fe	Very clear	high
Source with wood combustion signature	West and east	0.1-10 µm	S, Ca, Fe, K	Si, Mn, Zn, Cu	Clear	medium
Local industry	West and east	> 1µm	S, K, Ca, Fe	P, Mn, Cu, Zn	Clear	difficult

* within the analyzed species. Score (relative mass contribution) >0.1

** score (relative mass contribution)< 0.1

Table 5.6.16: Statistical key parameters of the selected PMF model solutions ((Ulbrich et al. 2009), explanations see Section 5.6.1).

Location	Value-proportional input error (%)	Number of Factors	Q/Qexp	Fpeak value
Reiden East	25	6	1.1	0
Reiden West	25	6	1.1	0

5.6.7.3 Wind dependent traffic contribution

Figure 5.6.22 shows an extract of the time series for the traffic sources identified at both stations. As expected from the temporal dependence of the wind direction, the traffic source at the west station peaked during daytime due to the prevailing winds from NE. In contrast, the east station peaked during morning and evening rush hours, when winds from SE were more frequent (beside the frequent occurrence of axial winds). NO_x shows an almost identical behavior (see Figure 5.6.23), which is a confirmation for the traffic source identification by the PMF analysis.

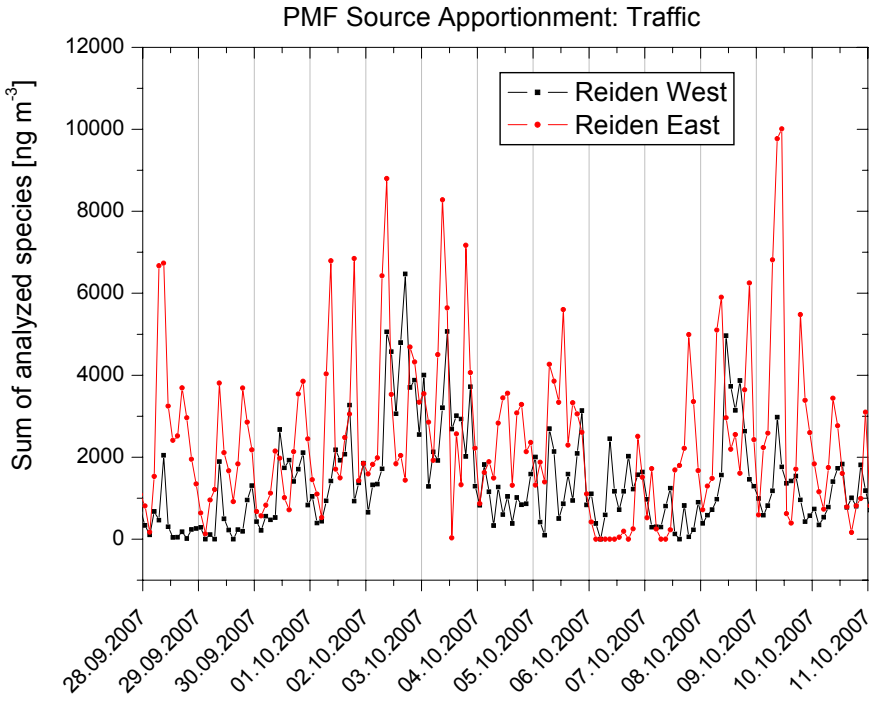

Fig. 5.6.22: Extract of time series for the traffic sources identified by PMF at both stations in Reiden.

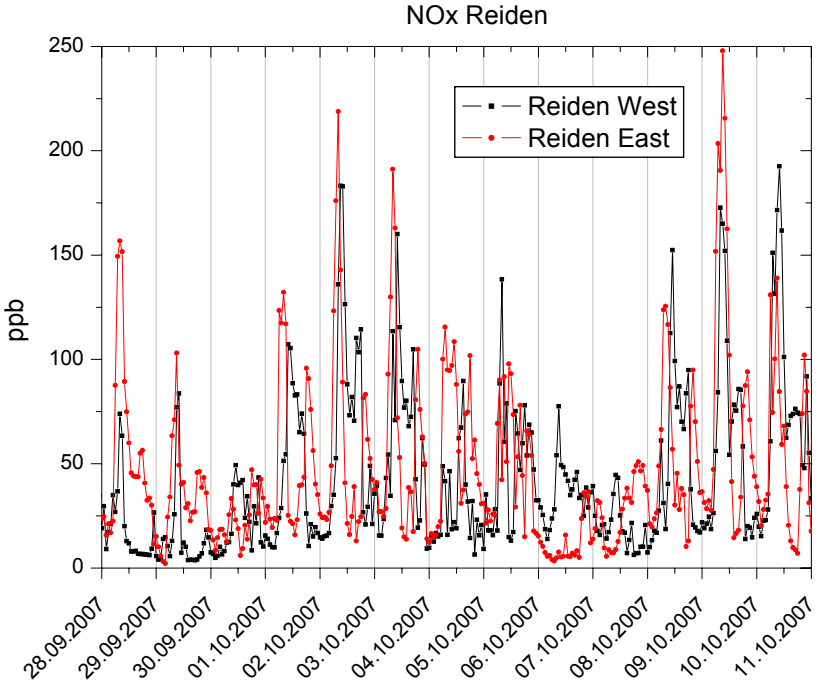

Fig. 5.6.23: Extract of time series for NO_x at both stations in Reiden.

5.6.7.4 Description of sources

- **Traffic:** A traffic source representing brake wear emissions, submicron black carbon emissions (exhaust) and additional contribution from mineral elements pointing to resuspension was identified at Reiden with a high degree of distinction. This source was clearly related to the traffic pattern and to the wind direction dependence observed for Reiden. The estimated direction of origin points towards the freeway for both stations, confirming the source identification.

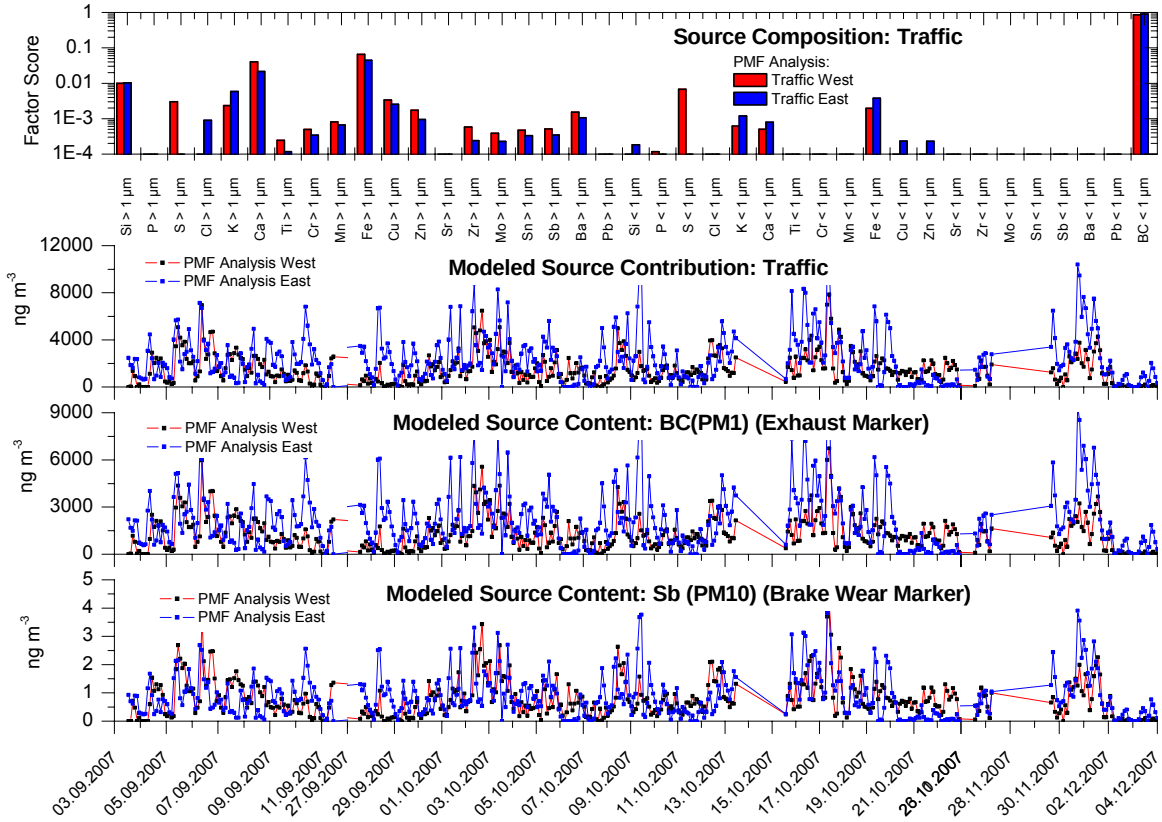

Fig. 5.6.24: Traffic: Source composition and contribution. Factor Score: Relative mass contribution to the source.

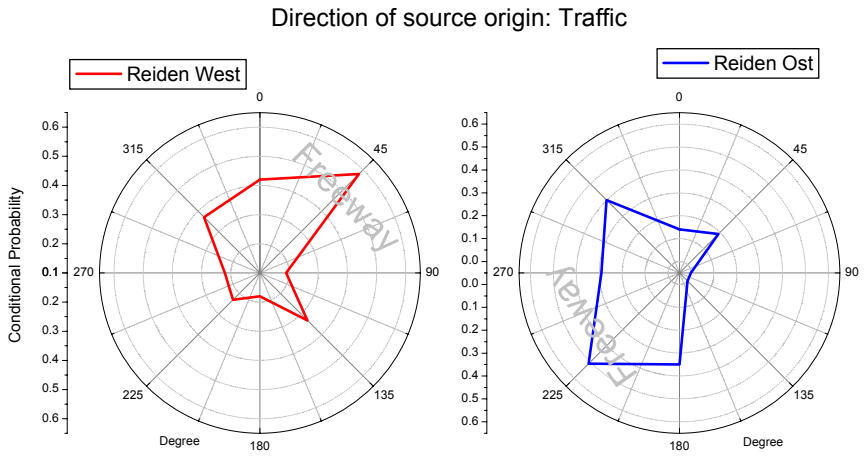

Fig. 5.6.25: Directional probability for the source origin (CPF, conditional probability function).

- **Local mineral background:** The composition of this source shows strong contributions of mineral elements, and the temporal evolution is rather irregular, indicating that this source is not traffic related and mainly influenced by meteorology. Accordingly, the source origin was virtually identical for both stations.

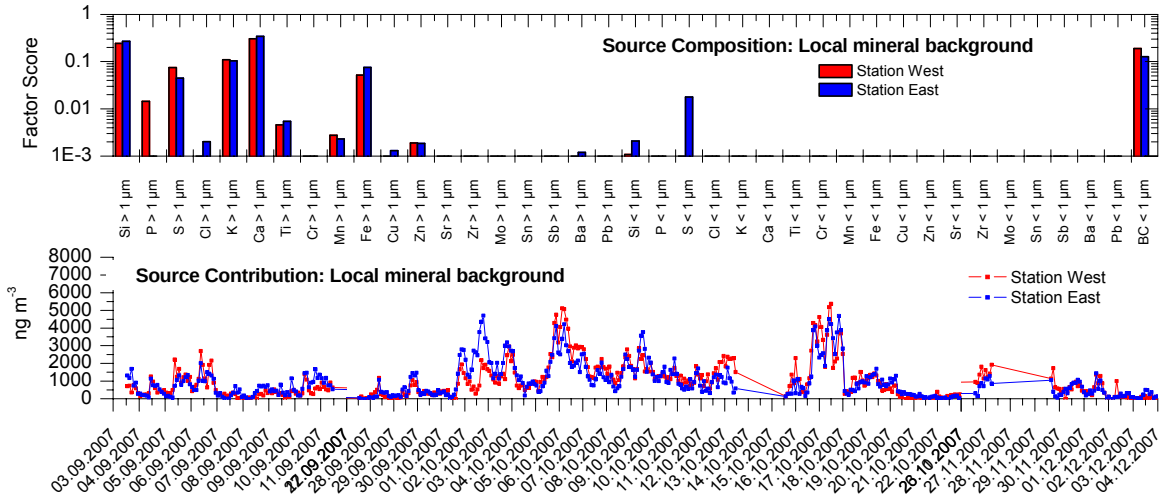

Fig. 5.6.26: Local mineral background: Source composition and contribution. Factor Score: Relative mass contribution to the source.

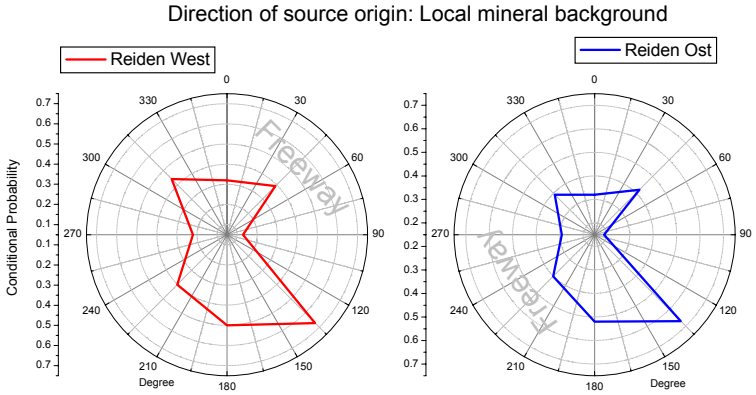

Fig. 5.6.27: Directional probability for the source origin (CPF, conditional probability function).

- **Secondary inorganic aerosol:** A very distinct source of submicron sulfur, with a characteristic and irregular temporal evolution. Submicron sulfur is attributed to ammonium sulfate, which is a dominant PM contributor formed by conversion of SO_2 to sulfate. This source is expected to have a high spatial homogeneity, which is however not reflected in the time series and the direction of origin. A likely explanation for this discrepancy is the different contributions of BC, which will result in a bias of the absolute source mass concentrations as discussed in Section 5.6.7.2.

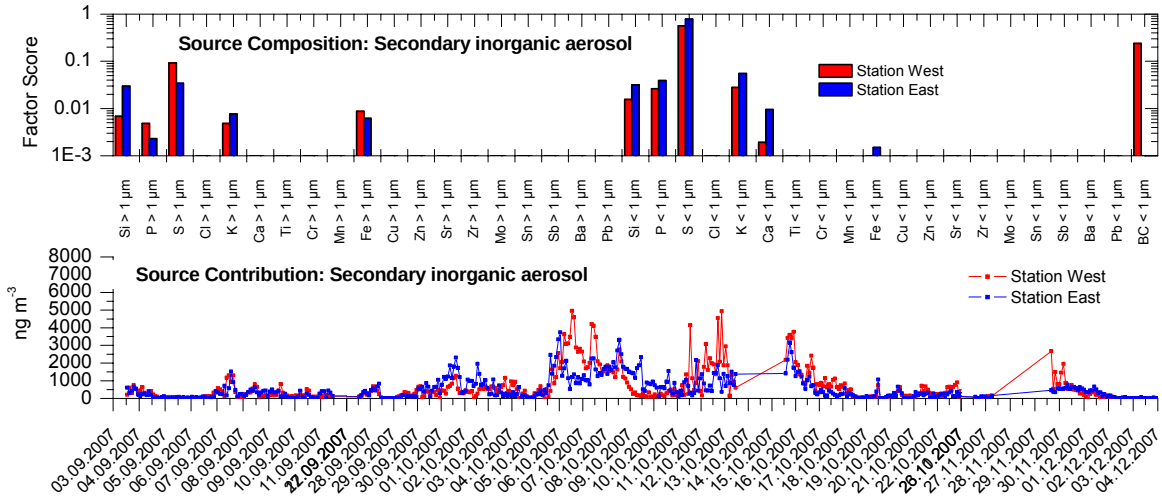

Fig. 5.6.28: Secondary inorganic aerosol: Source composition and contribution. Factor Score: Relative mass contribution to the source.

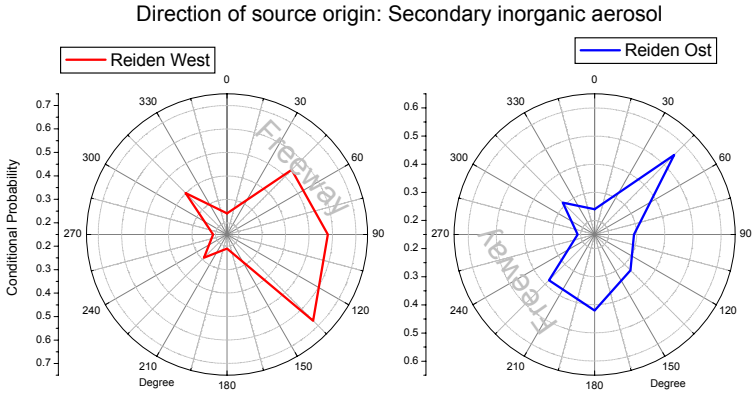

Fig. 5.6.29: Directional probability for the source origin (CPF, conditional probability function).

- **Road salt resuspension:** This is a very characteristic coarse mode chlorine dominated source with a strongly irregular temporal pattern, depending on the road salting activities. The drying process of resuspended salt droplets is on the order of several hours and occurs simultaneously with the meteorological dispersion of the droplets. As a result, the dried road salt aerosol particles rather represent a background source than a road-specific emission source. This hypothesis is supported by the similar source origin for both stations, as it is the case for the local mineral background aerosol. The source was peaking mainly end of October and beginning of December. The non-zero contributions in September were unlikely to result from road salting and could not be coherently explained.

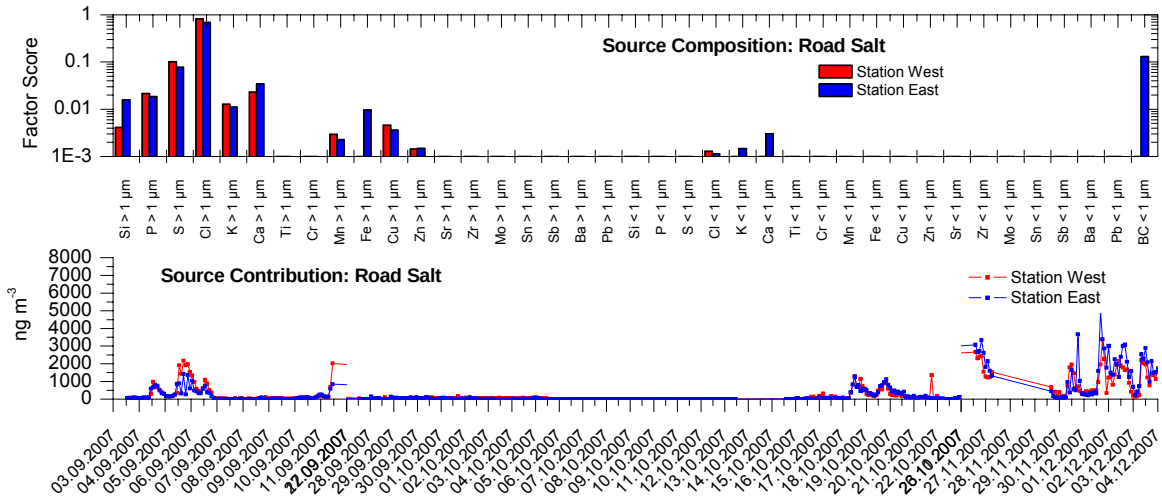

Fig. 5.6.30: Road salt resuspension: Source composition and contribution. Factor Score: Relative mass contribution to the source.

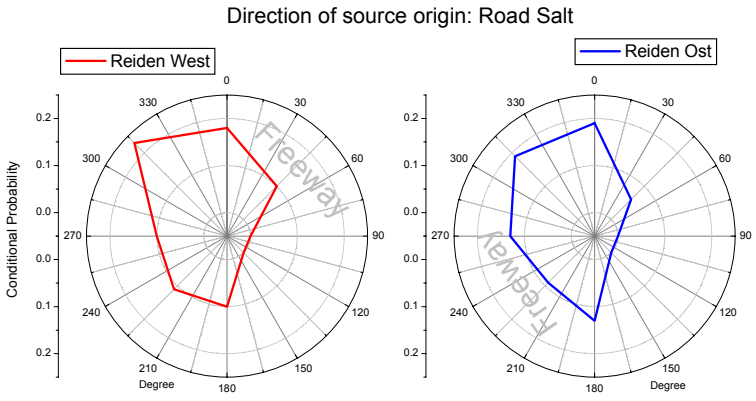

Fig. 5.6.31: Directional probability for the source origin (CPF, conditional probability function).

- **Wood burning signature source:** This source, including a clear wood combustion signature (submicron S, Ca, K, Zn), shows elevated contributions in the colder months of the year. Like the local mineral background, this source seemed mainly influenced by meteorology. The time series and the source origin suggest that the two locations were individually influenced by close-by wood burning sources (farms, town).

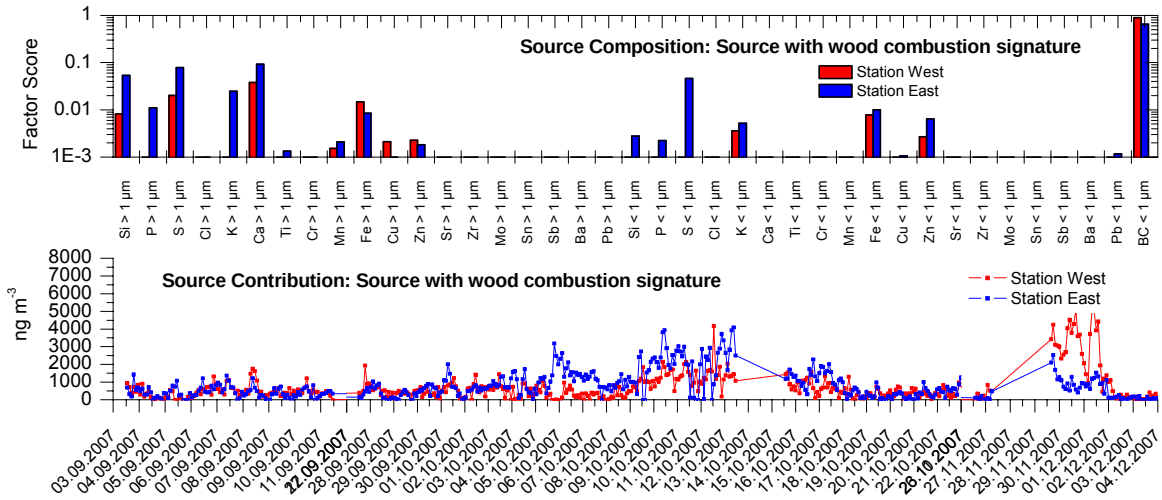

Fig. 5.6.32: Wood combustion: Source composition and contribution. Factor Score: Relative mass contribution to the source.

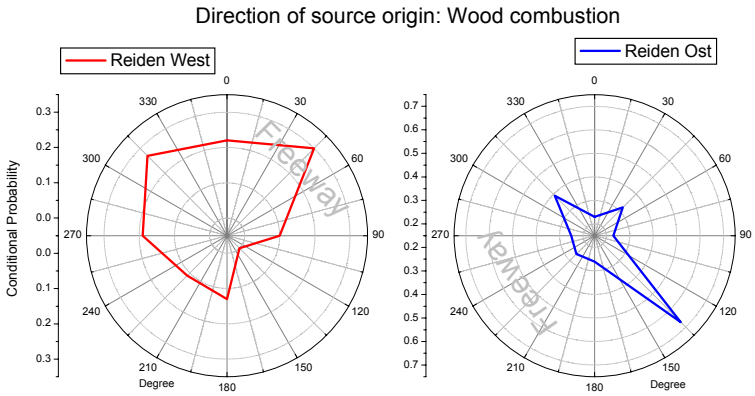

Fig. 5.6.33: Directional probability for the source origin (CPF, conditional probability function).

- Local industrial source: This source was clearly separated by PMF, but shows a very weak contribution and is difficult to interpret. The rather regular time series, the elemental pattern as well as the source origin hint to emissions from a close-by industrial area, which possibly contribute to the measured mass concentrations of the considered trace elements.

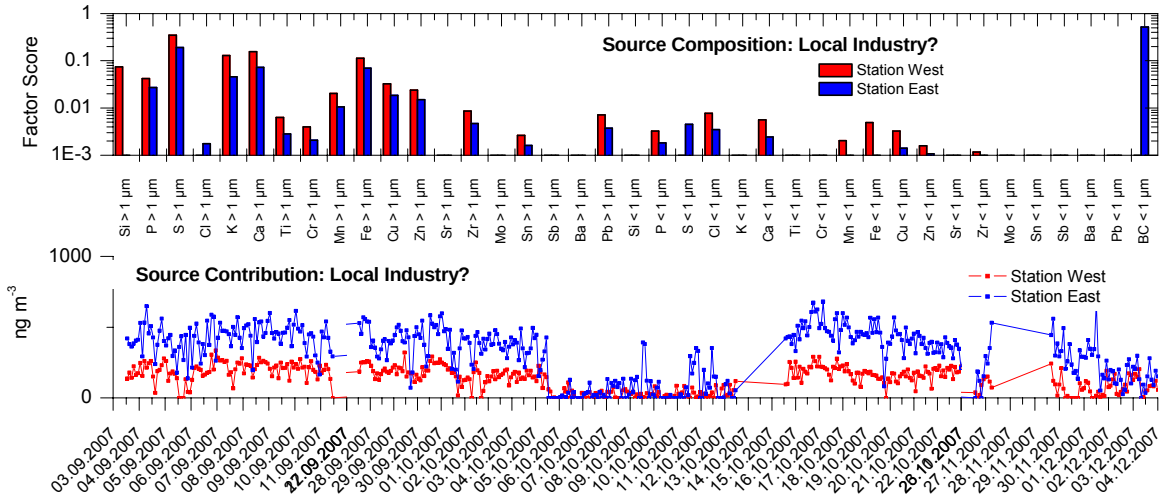

Fig. 5.6.34: Industrial source: Source composition and contribution. Factor Score: Relative mass contribution to the source.

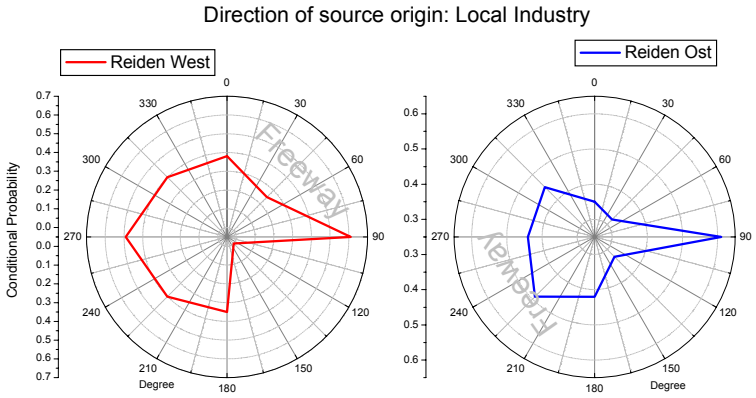

Fig. 5.6.35: Directional probability for the source origin (CPF, conditional probability function).

5.6.7.5 Attribution of species to individual sources

Table 5.6.17 and Figures 5.6.36a-c show the attribution of the measured trace elements to the sources identified via PMF at Reiden.

Table 5.6.17: Major sources for a selection of trace elements detected at Reiden (LU)

Parameter	Major sources
BC(PM1)	Traffic > Wood signature source >> Local mineral background
Sb (1 -10 µm)	Traffic
Zn (1 -10 µm)	Traffic > Local mineral background ≈ Wood signature source ≈ Local industry
Fe (1 -10 µm)	Traffic > Local mineral background
Si (1 -10 µm)	Local mineral background >> Traffic
Ca (1 -10 µm)	Local mineral background >> Traffic > Wood signature source
K (1 -10 µm)	Local mineral background >> Local Industry
S (1 -10 µm)	Local mineral background > Secondary inorganic aerosol
K <1 µm	Secondary inorganic aerosol > Wood signature source
S <1 µm	Secondary inorganic aerosol
Zn <1 µm	Wood signature source >> Local mineral background

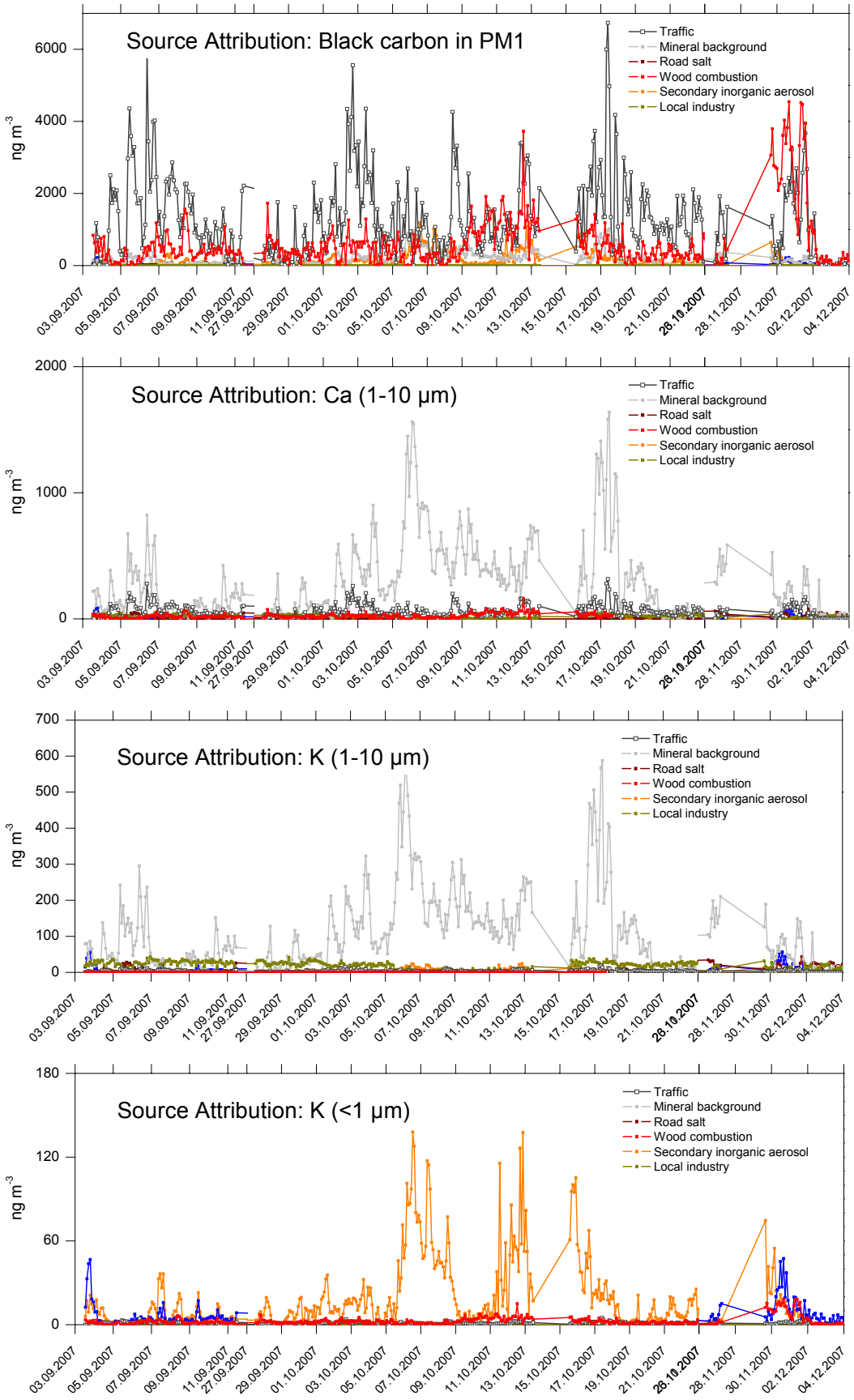

Fig. 5.6.36a: Attribution of trace elements to individual sources.

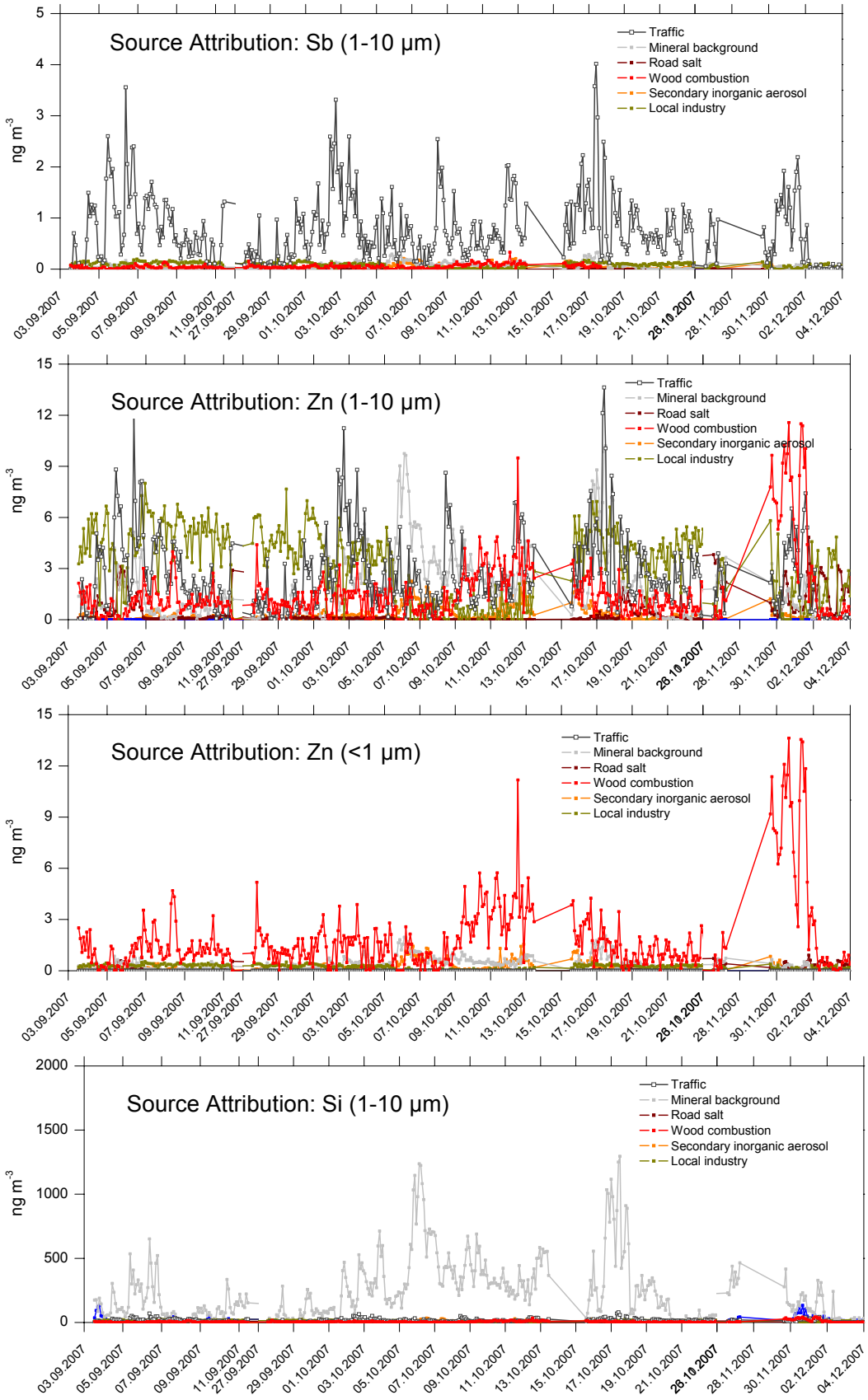

Fig. 5.6.36b: Attribution of trace elements to individual sources.

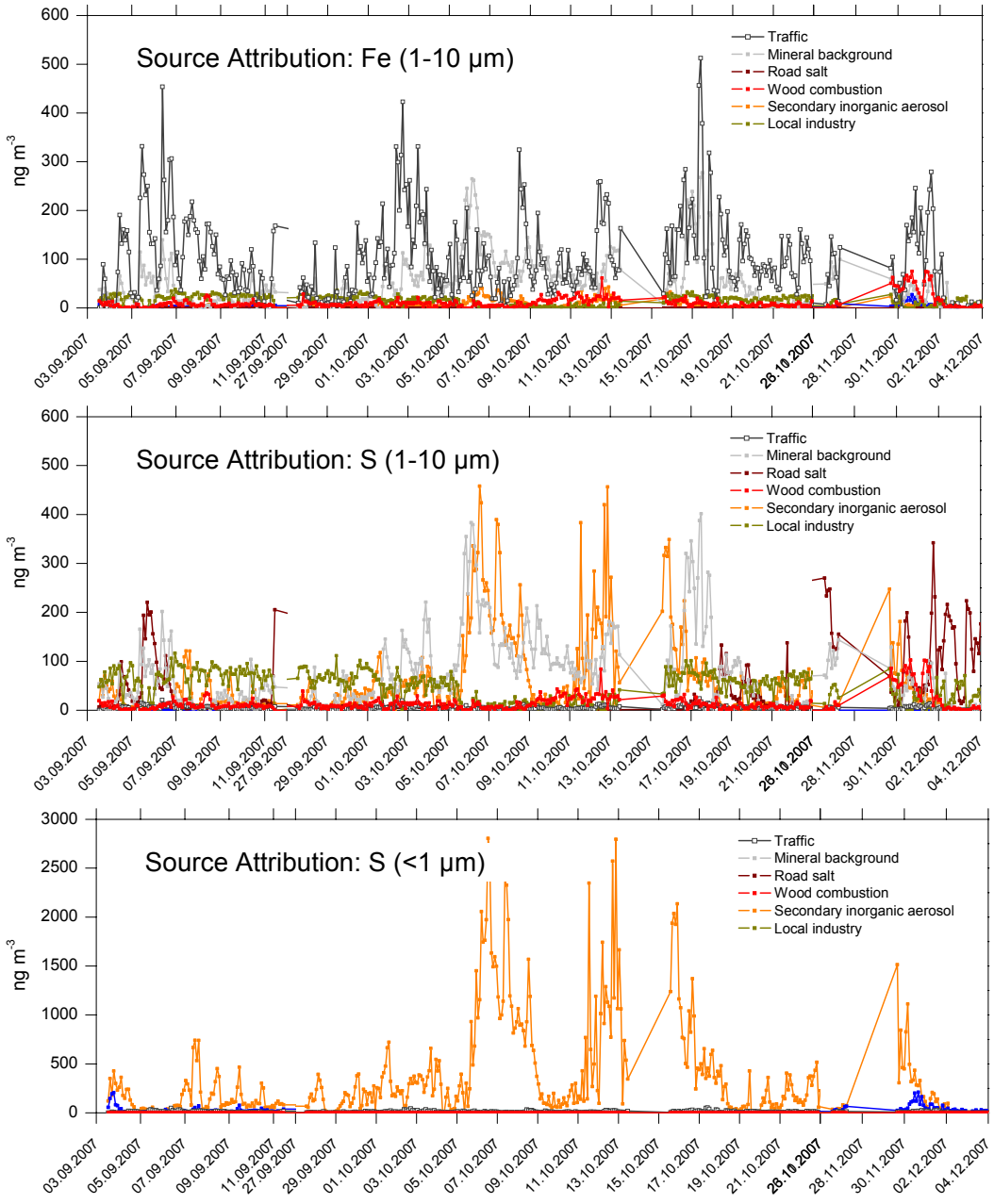

Fig. 5.6.36c: Attribution of trace elements to individual sources.

5.6.8 Reiden: Source extrapolation and mass balance

5.6.8.1 Unexplained mass contributions

A residual fraction of the measured species were not modeled and explained by the identified sources (Figure 5.6.37). The unexplained residual was generally low (<10%) and was dominated by black carbon.

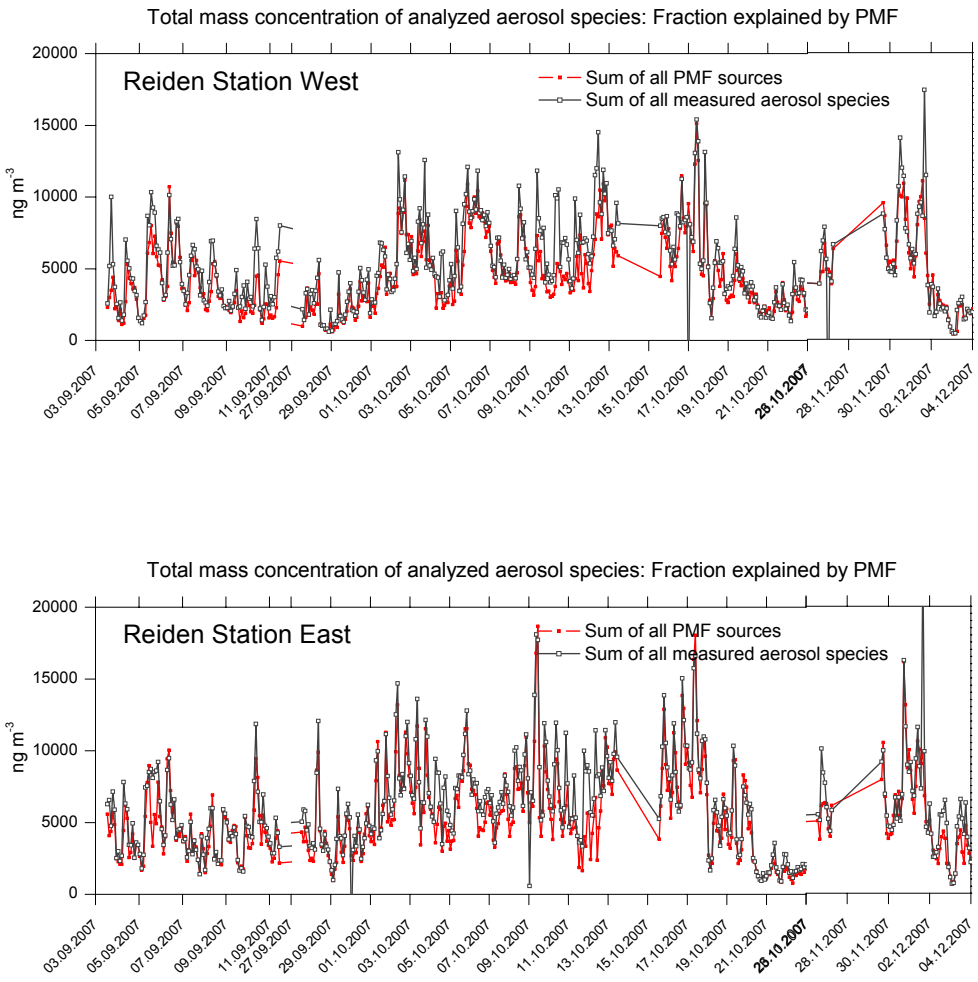

Fig. 5.6.37: Summed mass concentration of all measured species and all PMF sources.

5.6.8.2 Traffic related sources in Reiden

For Reiden, the traffic related sources identified by PMF (brake wear and traffic related black carbon) were extrapolated to their full mass contributions using the same conversion factors as for Zürich-Weststrasse (see Section 5.6.6.2). For brake wear, the brake dust composition in Reiden and Zürich-Weststrasse was assumed to be plausibly identical. Also for traffic related black carbon in PM1 (directly traffic related emissions) the same empirical conversion factor to total traffic related carbon in PM10 as for Zürich-Weststrasse was applied (factor = 1.45), because no improved estimates could be obtained for Reiden (see Section 5.6.6.2). This conversion represents an empiric estimation based on BC and traffic related organic matter (obtained by mobile measurements with an aerosol mass spectrometer from Zürich). A more detailed determination of individual conversion factors for each of the two sites was difficult.

5.6.8.3 Mass balance

For Reiden, the following traffic related PM10 sources were identified and extrapolated to their full mass contributions:

- Brake wear. Brake wear was characterized by a specific pattern of Fe, Cu, Zn, Zr, Mo, Sn, Sb and Ba. These elements are widely used constituents of brake linings and are likely to be oxidized during the brake abrasion process.
- Exhaust emissions: The exhaust emissions were predominantly composed of by carbon species. Trace elements originating from fuel additives were not specifically identified from the road side measurements, indicating that other emission sources of these elements are more relevant on a mass base.
- Contributions of mineral elements to traffic emissions were identified, pointing to road dust resuspension. A specific quantification for resuspension was however not possible due to the lack of representative road dust samples for Reiden.

Figure 5.6.38 shows the fractional contribution for the traffic related PM10 sources at the freeway site in Reiden. For the considered time period, the sum of the two identified traffic sources explained only approximately 36% of the measured PM10 difference. The remaining 64% included the non-identified contributions of road dust resuspension, road wear, tire wear. The statistical variation indicated in Figure 5.6.38 represents the temporal variability of the source contributions during the considered time period in autumn 2007. A continuous time series of the source contributions could not be obtained, since only time periods with well-defined upwind/downwind conditions were considered for the mass balance.

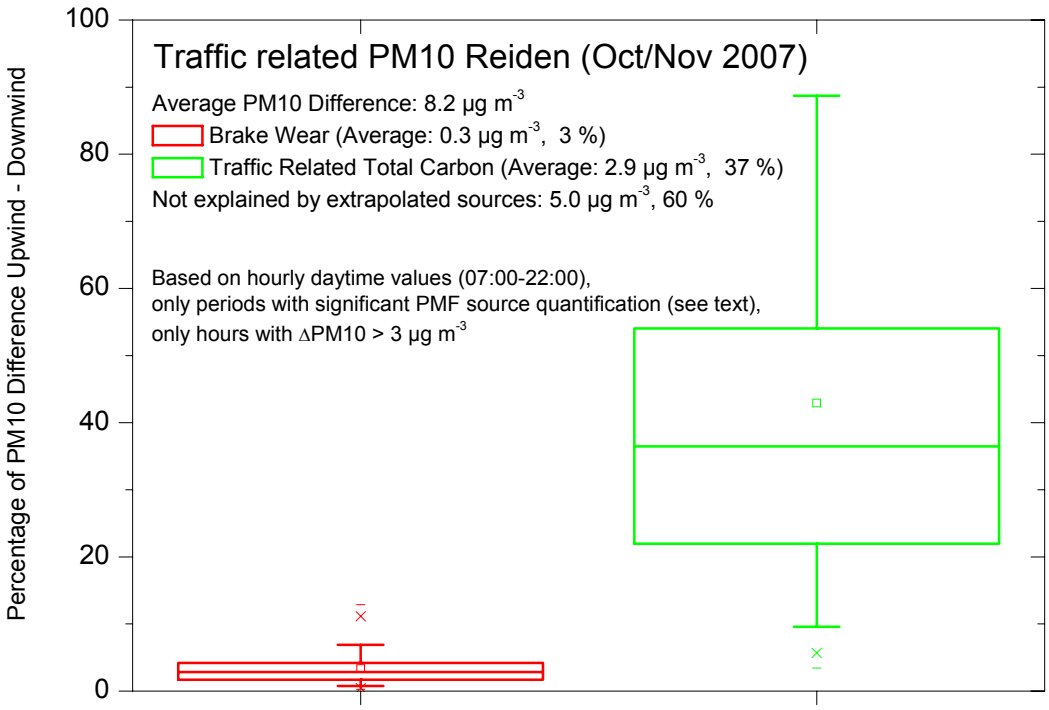

Fig. 5.6.38: Source apportionment for locally produced (background corrected) PM10 at the freeway site in Reiden (LU). The statistical variation represents the temporal variability. Brake wear was quantified assuming a brake dust antimony content of 1% and a copper content of 5%. Total carbon was estimated from black carbon using an empirical conversion factor of 1.45, obtained from experimental data. (Box: First to third quartile range, plus median line. Error bars: 5-95% percentile. □: Average. x: 1-99% percentile, -: Maximum/minimum).

5.6.8.4 Source emission factors

The absolute mass contributions of the identified and quantified emission sources were used to calculate source emission factors for light duty vehicles (EF_{LDV}), heavy duty vehicles (EF_{HDV}), as well as the average traffic fleet (EF_{Fleet}). The same linear regression method as used for the elemental emission factors (Section 5.1) was applied, using NO_x to correct for atmospheric dilution. Only hourly data from dry periods and ΔNO_x > 20 µg m^{-3} were considered (downwind minus upwind). The prevailing wind direction during traffic-rich daytime periods was from NE (see Section 5.6.7.1), therefore the traffic sources identified with PMF at the west side (downwind) station showed a stronger statistical overall correlation to traffic frequencies than at the east side (upwind) station. Consecutively, more reliable emission factors were obtained for the west side station using the multilinear regression model. The data set was checked and corrected for obvious outlier values. In contrast to Zürich-Weststrasse, the resulting amount of data was reduced, since only hours with perpendicular winds as described above were used. The following list provides conceptual information on the calculations.

Average fleet emission factors: Average fleet emission factors were calculated from the experimental data for brake wear, total carbon and total PM10:

$$EF_{x,Fleet} = \frac{c_x \cdot d}{n_{tot}}$$

where c_x is the measured mass concentration (µg m^{-3}) assigned to the considered source or emission process *x*, n_{tot} the total vehicle frequency (vehicles h^{-1}) and d the atmospheric dilution, determined via NO_x. The fleet emission factor depends on the average traffic composition (13.7% HDV for the selected hourly data, 15% HDV during the entire campaign) and represents an average value for a considered time period. For PM10, the fleet emission factor includes the contribution from resuspended dust. The calculated standard deviation of the average calculated with this equation reflects the temporal variability of the traffic composition.

Table 5.6.18: Experimentally determined fleet emission factors

Source	Fleet EF (6.7% HDV) mg/km
Brake Wear	3
Total Carbon (Exhaust)	35
PM10	88
Unexplained (resuspension)	50

LDV and HDV emission factors for brake wear and traffic related carbon and PM10: The following multilinear regression model was used to calculate vehicle specific emission factors:

$$c_x = EF_{x,LDV} \cdot \left(\frac{n_{LDV}}{d}\right) + EF_{x,HDV} \cdot \left(\frac{n_{HDV}}{d}\right)$$

where c_x is the measured mass concentration (µg m^{-3}) assigned to the considered source or emission

process x, n_{LDV} and n_{HDV} are the vehicle frequencies (vehicles h^{-1}) and d the atmospheric dilution, determined via NOx.

Brake wear and traffic related carbon were considered to be implicitly traffic related, thus their full source contributions were assumed to be caused by LDV and HDV emissions. As a consequence, the model did not include an autorcorrelation term, which is used to describe non-vehicle related source contributions. The multilinear fit quality was limited due to weak sample statistics (93 hourly values, compared to 209 for Zürich-Weststrassse). To reduce the number of fit parameters, the fitting constant (unexplained contribution) was omitted. This was based on the assumption that due to the upwind/downwind concept the entire concentration difference is entirely traffic emission related. As shown in Section 5.6.7.4, both brake wear and total traffic related carbon were extrapolated from the same PMF source related to net traffic. As a consequence, the multilinear fit quality is identical for both sources.

Table 5.6.19: Multilinear fit parameters

Source	EF LDV (mg/km)	EF HDV (mg/km)	R2	Average Difference (µg/m^3)
Brake wear	1.6 ± 0.3	9.3 ± 1.8	0.81	0.22
Total traffic related carbon	20.4 ± 4.0	118.8 ± 22.7	0.81	2.75
PM10	50.0 ± 12.6	288.0 ± 71.9	0.71	6.9
BC(PM1)	10.6 ± 1.8	101.6 ± 10.1	0.91	1.8

Table 5.6.20: Emission factors for the individual sources contributing to traffic related PM10, valid for the freeway site Reiden (national freeway A2). LDV: Light duty vehicles (including 15% delivery vans), HDV: Heavy duty vehicles (including motor coaches). Values are based on 4 days of measurements in October and November 2007, dry time periods only) and are based on NO_x emission factors estimated for Reiden (Year: 2007, EF_{NOx}(LDV) = 448 mg km^{-1}, EF_{NOx}(HDV) = 5421 mg km^{-1}, NO_x calculated as NO_2 (INFRAS 2004)). Colors: Multilinear regression (good model performance), Multilinear regression (bad model performance), Estimated values (mass balance). The indicated uncertainties represent the propagated uncertainty from PMF analysis and source quantification (net uncertainties: brake wear 70%, exhaust 26%) and from multilinear regression (values see above). Note: The set of data used for the emission factor calculations is not completely identical to the data set used for the mass balance presented in Figure 5.6.38, which leads to slightly different fractional source contributions.

Source	Quantification	Vehicle Fleet			LDV	HDV
		Experimental value	Calculated from LDV,HDV			
		13.7% HDV[*1]	13.7% HDV[*1]	15% HDV[*2]		
		mg/km	mg/km	mg/km	mg/km	mg/km
Brake Wear	PMF	3	3	3	1.6 ± 1.1	9.3 ± 6.7
Total Carbon (Exhaust)	PMF	35	34	35	20.4 ± 6.6	118.8 ± 38.4
PM10	Measured: ΔPM10 (Downwind-Upwind)	88	83	86	50.0 ± 12.6	288.0 ± 71.9
Unexplained (resuspension)	Estimated from mass balance	50	46	48	28 ± 14.3	160 ± 81.8

[*1] selected time period

[*2] entire campaign (winter 2007/2008)

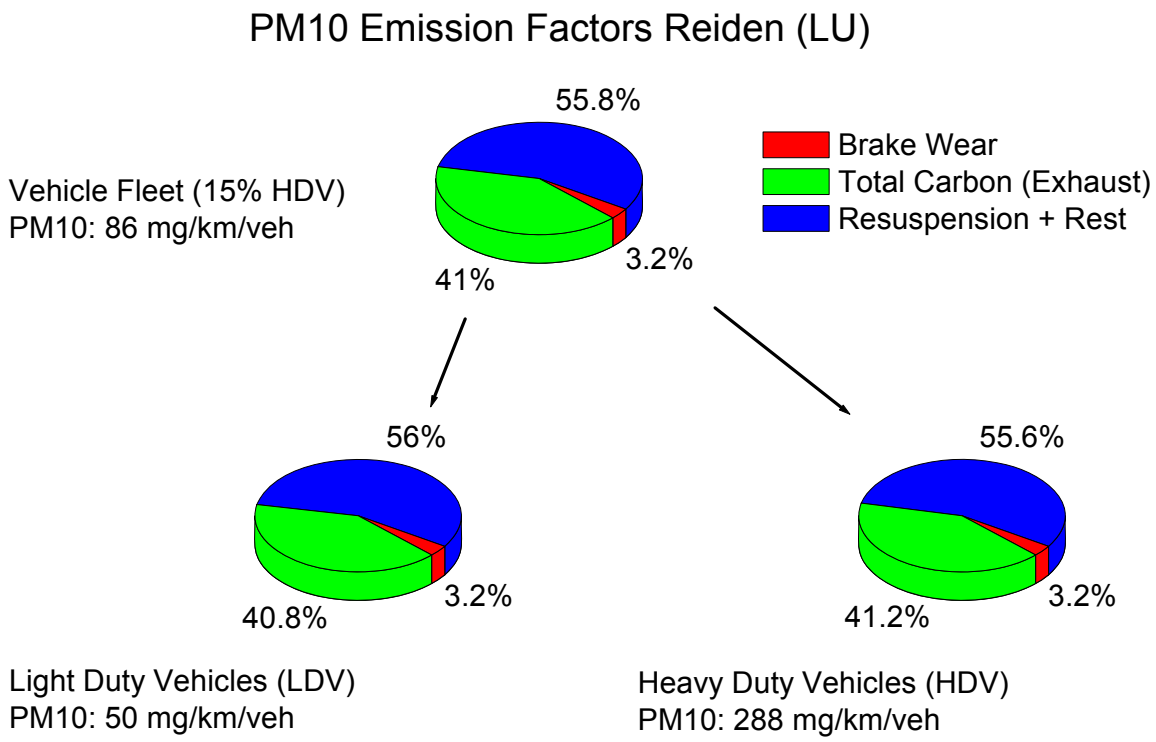

Fig. 5.6.39: PM10 emission factors determined for Reiden.

The calculated PM10 emission factors for Reiden show the following characteristics:

- Vehicle fleet at Reiden: The average PM10 emission factor for Reiden (15% HDV fraction during the entire campaign) was caused by exhaust emissions (41%) and very low contributions from brake wear emissions (3%). The remaining 56% of the traffic emissions were not directly identified, but probably represented contributions from road dust resuspension (and minor contributions from tire wear and road wear).

- LDV and HDV emission factors: The total HDV emission factor was 5.8 times higher than the total LDV emission factor. Because the mass contributions of both brake wear and traffic related carbon were extrapolated from one single net traffic source identified by PMF, the resulting LDV and HDV emission factors showed virtually identical source contributions. Accordingly, also the vehicle fleet emission factor exhibits the same source composition. An alternative calculation of LDV and HDV emission factors for brake wear and exhaust directly from measured concentration differences of specific marker species (Sb, BC) did not lead to statistically significant results. In contrast to Zürich-Weststrasse, the resuspended dust was removed laterally due to the perpendicular winds (upwind/downwind concept), rather than being kept in suspended state by the turbulence induced by heavy duty vehicles. Therefore a part of the resuspended road dust was also attributed to light duty vehicles.

6 Literature

Abu-Allaban, M., Gillies, J. A., Gertler, A. W., Clayton, R. and Proffitt, D. (2003). Tailpipe, resuspended road dust, and brake-wear emission factors from on-road vehicles. *Atmospheric Environment* 37:5283-5293.

Adachi, K. and Tainosho, Y. (2004). Characterization of heavy metal particles embedded in tire dust. *Environment International* 30:1009-1017.

Amato, F., Pandolfi, M., Viana, M., Querol, X., Alastuey, A. and Moreno, T. (2009). Spatial and chemical patterns of PM10 in road dust deposited in urban environment. *Atmospheric Environment* 43:1650-1659.

Baltensperger, U. (1985). PhD Thesis: Chemical and morphological characterization of airborne particulate matter, University of Zürich, Zürich.

Birch, M. E. and Cary, R. A. (1996). Elemental carbon-based method for monitoring occupational exposures to particulate diesel exhaust. *Aerosol Science and Technology* 25:221-241.

Bukowiecki, N., Dommen, J., Prevot, A. S. H., Richter, R., Weingartner, E. and Baltensperger, U. (2002). A mobile pollutant measurement laboratory-measuring gas phase and aerosol ambient concentrations with high spatial and temporal resolution. *Atmospheric Environment* 36:5569-5579.

Bukowiecki, N., Hill, M., Gehrig, R., Lienemann, P., Zwicky, C. N., Hegedüs, F., Falkenberg, G., Weingartner, E. and Baltensperger, U. (2005). Trace metals in ambient air: Hourly size-segregated mass concentrations detemined by Synchrotron-XRF. *Environmental Science & Technology* 39:5754-5762.

Bukowiecki, N., Lienemann, P., Hill, M., Figi, R., Richard, A., Furger, M., Rickers, K., Falkenberg, G., Zhao, Y., Steven, S. C., Baltensperger, U. and Gehrig, R. (2009a). Real-world LDV and HDV emission factors for antimony and other brake wear related trace elements. *Environmental Science & Technology* (in press).

Bukowiecki, N., Lienemann, P., Zwicky, C. N., Furger, M., Richard, A., Falkenberg, G., Rickers, K., Grolimund, D., Borca, C., Hill, M., Gehrig, R. and Baltensperger, U. (2008). X-ray fluorescence spectrometry for high throughput analysis of atmospheric aerosol samples: The benefits of synchrotron X-rays. *Spectrochimica Acta Part B: Atomic Spectroscopy* 63:929-938.

Bukowiecki, N., Richard, A., Furger, M., Weingartner, E., Aguirre, M., Huthwelker, T., Lienemann, P., Gehrig, R. and Baltensperger, U. (2009b). Deposition uniformity and particle size distribution of ambient aerosol collected with a rotating drum impactor. *Aerosol Science and Technology* 43:891-901.

BUWAL (2003). NABEL Luftbelastung 2003, in *Schriftenreihe Umwelt*, BUWAL, Bern, Nr. 370.

Camatini, M., Crosta, G. F., Dolukhanyan, T., Sung, C., Giuliani, G., Corbetta, G. M., Cencetti, S. and Regazzoni, C. (2001). Microcharacterization and identification of tire debris in heterogeneous laboratory and environmental specimens. *Materials Characterization* 46:271-283.

Cavalli, F., al, e. and al, e. (2009). *Atmospheric Measurement Techniques Discussions* in preparation.

Councell, T. B., Duckenfield, K. U., Landa, E. R. and Callender, E. (2004). Tire-wear particles as a source of zinc to the environment. *Environmental Science & Technology* 38:4206-4214.

Dietze, V., Fricker, M., Goltzsche, M., Kaminski, U. and Schultz, E. (2007). Air quality measurement in German health resorts - Part 2: Results of annual measurement series in the period of 2000 to 2004. *Gefahrstoffe Reinhaltung der Luft* 67:197-205.

Dietze, V., Fricker, M., Goltzsche, M. and Schultz, E. (2006). Air quality measurement in German health resorts - Part 1: Methodology and verification. *Gefahrstoffe Reinhaltung der Luft* 66:45-53.

Furusjo, E., Sternbeck, J. and Cousins, A. P. (2007). PM10 source characterization at urban and highway roadside locations. *Science of the Total Environment* 387:206-219.

Furuta, N., Iijima, A., Kambe, A., Sakai, K. and Sato, K. (2005). Concentrations, enrichment and predominant sources of Sb and other trace elements in size classified airborne particulate matter collected in Tokyo from 1995 to 2004. *Journal of Environmental Monitoring* 7:1155-1161.

Garg, B. D., Cadle, S. H., Mulawa, P. A., Groblicki, P. J., Laroo, C. and Parr, G. A. (2000). Brake wear particulate matter emissions. *Environmental Science & Technology* 34:4463-4469.

Gehrig, R., Hill, M., Buchmann, B., Imhof, D., Weingartner, E. and Baltensperger, U. (2004). Separate determination of PM10 emission factors of road traffic for tailpipe emissions and emissions from abrasion and resuspension processes. *International Journal Of Environment And Pollution* 22:312-325.

Gomez, D. R., Gine, M. F., Bellato, A. C. S. and Smichowski, P. (2005). Antimony: a traffic-related element in the atmosphere of Buenos Aires, Argentina. *Journal of Environmental Monitoring* 7:1162-1168.

Grieshop, A. P., Lipsky, E. M., Pekney, N. J., Takahama, S. and Robinson, A. L. (2005). Fine particle emission factors from vehicles in a highway tunnel: Effects of fleet composition and season, in *Conference on Particulate Matter Supersites Program and Related Studies*, Atlanta, GA, S287-S298.

Gustafsson, M., Blomquist, G., Gudmundsson, A., Dahl, A., Swietlicki, E., Bohyard, M., Lindbom, J. and Ljungman, A. (2008). Properties and toxicological effects of particles from the interaction between tyres, road pavement and winter traction material. *Science of the Total Environment* 393:226-240.

Gustafsson, M., Blomqvist, G., Gudmundsson, A., Dahl, A., Jonsson, P. and Swietlicki, E. (2009). Factors influencing PM10 emissions from road pavement wear. *Atmospheric Environment*:doi:10.1016/j.atmosenv.2008.1004.1028.

Han, L. H., Zhuang, G. S., Cheng, S. Y., Wang, Y. and Li, J. (2007). Characteristics of re-suspended road dust and its impact on the atmospheric environment in Beijing. *Atmospheric Environment* 41:7485-7499.

Hjortenkrans, D. S. T., Bergback, B. G. and Haggerud, A. V. (2007). Metal emissions from brake linings and tires: Case studies of Stockholm, Sweden 1995/1998 and 2005. *Environmental Science & Technology* 41:5224-5230.

Ho, K. F., Lee, S. C., Chow, J. C. and Watson, J. G. (2003). Characterization of PM10 and PM2.5 source profiles for fugitive dust in Hong Kong. *Atmospheric Environment* 37:1023-1032.

Hueglin, C., Gehrig, R., Baltensperger, U., Gysel, M., Monn, C. and Vonmont, H. (2005). Chemical characterisation of PM2.5, PM10 and coarse particles at urban, near-city and rural sites in Switzerland. *Atmospheric Environment* 39:637-651.

Hussein, T., Johansson, C., Karlsson, H. and Hansson, H. C. (2008). Factors affecting non-tailpipe aerosol particle emissions from paved roads: On-road measurements in Stockholm, Sweden. *Atmospheric Environment* 42:688-702.

Iijima, A., Sato, K., Yano, K., Kato, M., Kozawa, K. and Furuta, N. (2008). Emission factor for antimony in brake abrasion dusts as one of the major atmospheric antimony sources. *Environmental Science & Technology* 42:2937-2942.

INFRAS (2004). *Handbook of Emission Factors, http://www.hbefa.net*, Zürich.

Johansson, C. (2008). Road traffic emission factors for heavy metals. *Atmospheric Environment*:doi:10.1016/j.atmosenv.2008.1010.1024.

Ketzel, M., Omstedt, G., Johansson, C., During, I., Pohjolar, M., Oettl, D., Gidhagen, L., Wahlin, P., Lohmeyer, A., Haakana, M. and Berkowicz, R. (2007). Estimation and validation of PM2.5/PM10 exhaust and non-exhaust emission factors for practical street pollution modelling. *Atmospheric Environment* 41:9370-9385.

Kim, E. and Hopke, P. K. (2004). Comparison between conditional probability function and nonparametric regression for fine particle source directions. *Atmospheric Environment* 38:4667-4673.

Kupiainen, K., Tervahattu, H. and Raisanen, M. (2003). Experimental studies about the impact of traction sand on urban road dust composition. *Science of the Total Environment* 308:175-184.

Kupiainen, K. J., Tervahattu, H., Raisanen, M., Makela, T., Aurela, M. and Hillamo, R. (2005). Size and composition of airborne particles from pavement wear, tires, and traction sanding. *Environmental Science & Technology* 39:699-706.

Lindbom, J., Gustafsson, M., Blomqvist, G., Dahl, A., Gudmundsson, A., Swietlicki, E. and Ljungman, A. G. (2006). Exposure to wear particles generated from studded tires and pavement induces inflammatory cytokine release from human macrophages. *Chemical Research in Toxicology* 19:521-530.

Lohmeyer, A. and Düring, I. (2001). Validierung von PM10-Immissionsberechnungen im Nahbereich von Strassen und Quantifizierung der Feinstaubbildung von Strassen, Senatsverwaltung für Stadtentwicklung Berlin, Sächsisches Landesamt für Umwelt und Geologie Dresden, Radebeul, 80 pp.

Lough, G. C., Schauer, J. J., Park, J. S., Shafer, M. M., Deminter, J. T. and Weinstein, J. P. (2005). Emissions of metals associated with motor vehicle roadways. *Environmental Science & Technology* 39:826-836.

Lundgren, D. (1967). An aerosol sampler for determination of particulate concentration as a function of size and time. *Journal of Air Pollution Control Association* 17:225-229.

Mohr, C., Weimer, S., Good, C., Richter, R., Prévôt, A. and Baltensperger, U. (2009). Mobile Messungen der Partikelzusammensetzung im Rheintal und in der Stadt Zürich. Winter 2007/2008, in *PSI-Bericht 09-09*.

Moreno, T., Querol, X., Alastuey, A., Minguillon, M. C., Pey, J., Rodriguez, S., Miro, J. V., Felis, C. and Gibbons, W. (2007). Recreational atmospheric pollution episodes: Inhalable metalliferous particles from firework displays. *Atmospheric Environment* 41:913-922.

Paatero, P. (1995). Least squares formulation of robust non-negative factor analysis, in *3rd International Conference on Environmetrics and Chemometrics*, Las Vegas, NV, 23-35.

Paatero, P. and Hopke, P. K. (2002). Discarding or downweighting high-noise variables in factor analytic models, in *8th International Conference on Chemometrics in Analytical Chemistry (CAC 2002)*, Seattle, Washington, 277-289.

Paatero, P. and Tapper, U. (1993). Analysis of Different Modes of Factor-Analysis as Least-Squares Fit Problems. *Chemometrics and Intelligent Laboratory Systems* 18:183-194.

Quass, U., John, A., Beyer, M., Lindermann, J., Hirner, A. V., Sulkowki, M. M., Hippler, J. and Kuhlbusch, T. A. J. (2008). Ermittlung des Beitrages von Reifen-, Kupplungs-, Brems- und Fahrbahnabrieb an den PM10-Emissionen von Strassen. *Strassenverkehrstechnik* 5:304.

Querol, X., Alastuey, A., Rodriguez, S., Plana, F., Mantilla, E. and Ruiz, C. R. (2001). Monitoring of PM10 and PM2.5 around primary particulate anthropogenic emission sources. *Atmospheric Environment* 35:845-858.

Ropertz, A. and Suritsch, N. (2006). Einfluss von offenporigem Asphalt auf die Feinstaubbelastung an Strassen, in *4. Informationstage Geräuschmindernde Fahrbahnbeläge in der Praxis*, Berlin.

Sternbeck, J., Sjodin, A. and Andreasson, K. (2002). Metal emissions from road traffic and the influence of resuspension - results from two tunnel studies. *Atmospheric Environment* 36:4735-4744.

Szidat, S., Jenk, T. M., Gaggeler, H. W., Synal, H. A., Fisseha, R., Baltensperger, U., Kalberer, M., Samburova, V., Reimann, S., Kasper-Giebl, A. and Hajdas, I. (2004). Radiocarbon (C-14)-deduced biogenic and anthropogenic contributions to organic carbon (OC) of urban aerosols from Zurich, Switzerland. *Atmospheric Environment* 38:4035-4044.

Taylor, S. R. and McLennan, S. M. (1985). *The Continental Crust: its Composition and Evolution*. Blackwell Scientific Publications, Oxford.

Thorpe, A. and Harrison, R. M. (2008). Sources and properties of non-exhaust particulate matter from road traffic: A review. *Science of the Total Environment* 400:270-282.

Thorpe, A. J., Harrison, R. M., Boulter, P. G. and McCrae, I. S. (2007). Estimation of particle resuspension source strength on a major London Road. *Atmospheric Environment* 41:8007-8020.

Ulbrich, I. M., Canagaratna, M. R., Zhang, Q., Worsnop, D. R. and Jimenez, J. L. (2009). Interpretation of organic components from Positive Matrix Factorization of aerosol mass spectrometric data. *Atmospheric Chemistry and Physics* 9:2891-2918.

von Uexkull, O., Skerfving, S., Doyle, R. and Braungart, M. (2005). Antimony in brake pads - a carcinogenic component? *Journal of Cleaner Production* 13:19-31.

Wanner, H. and Furger, M. (1990). The Bise - Climatology of a Regional Wind North of the Alps. *Meteorology and Atmospheric Physics* 43:105-115.

Weckwerth, G. (2001). Verification of traffic emitted aerosol components in the ambient air of Cologne (Germany). *Atmospheric Environment* 35:5525-5536.

Zhao, P. S., Feng, Y. C., Zhu, T. and Wu, J. H. (2006). Characterizations of resuspended dust in six cities of North China. *Atmospheric Environment* 40:5807-5814.

Acknowledgements

- Dieses Projekt wurde durch das Schweizerische Bundesamt für Strassen (ASTRA) und das Schweizerische Bundesamt für Umwelt (BAFU) finanziell unterstützt.
- Wir danken der wissenschaftlichen Begleitkommission für die wertvollen Diskussionen und Anregungen anlässlich der halbjährlichen Begleitkommissionssitzungen.
- Die Entwicklung und Herstellung des Empa-RDI war nur möglich dank der aktiven Beteiligung folgender Personen: Daniel Rechenmacher, Slobodan Srbinovic (Konstruktion), Erwin Pieper, Alfred Mack (Werkstatt), Hugo Huber, Lukas Rotach (Elektronik) und Stefan Hösli (Gesamtkoordination).
- Bei der Probenanalyse mittels SR-XRF genossen wir stets die grossartige Unterstützung durch Karen Rickers und Gerald Falkenberg (HASYLAB at DESY Beamline L) sowie Steven S. Cliff, Yongjing Zhao, Donna Hamamoto und Al Thompson (ALS at Berkeley National Laboratory, Beamline 10.3.1).
- Die Abriebsversuche mit dem MLS und dem MMLS wurden in Zusammenarbeit mit der Abteilung Strassenbau/Abdichtungen der Empa durchgeführt, Wir danken Lily Poulikakos, Markus Erb und Simon Küntzel für die aktive Mithilfe. Zusätzliche experimentelle Unterstützung erfolgte durch Kerstin Zeyer (Empa, Abteilung Luftfremdstoffe).
- Wir danken folgenden Mitarbeitern der Empa für ihren Einsatz während der Feldkampagnen: Urs Gfeller (RDI-Probenwechsel), Christoph Zwicky (WD-XRF - Analysen), Beat Schwarzenbach (TEOM), Christoph Hüglin (fachliche und organisatorische Unterstützung) sowie Peter Honegger und Thomas Bruggisser (Transport der Messcontainer).
- Wir danken folgenden Mitarbeitern des PSI für ihren Einsatz während der Feldkampagnen, SR-XRF – Messzeiten oder Datenanalyse: René Richter, Günther Wehrle, Mari Cruz Minguillon, Michel Tinguely.
- Die Strassenstaub-Sammlung wurde von Fulvio Amato und Marco Pandolfi vom Institute of Environmental Assessment and Water Research (IDAEA) in Barcelona, Spanien, durchgeführt, wofür wir uns bedanken. Fulvio Amato war auch für die chemischen Analysen der Proben verantwortlich.
- Die Planung der Messkampagne in Reiden wurde organisatorisch durch Innet AG, Aarau unterstützt (Peter Böhler, Raffael Kaenzig). Wir danken der Innet AG ausserdem für die grosszügige Bereitstellung von Messdaten zu Qualitätssicherungszwecken.
- Wir danken der Polizei, dem Tiefbauamt sowie dem Baudepartement der Stadt Zürich für die wohlwollende Begleitung des Projekts (Bewilligung von Standplätzen, Organisation der Strassenstaub-Sammelkampagne): Daniel Vetterli, Arthur Müller, Oliver Vetter, Christian Krismer, Jürg Büchler, Kurt Friedli, Roger Hunziker, Urs Bühler, Albert Spörri, Joe Frick, Dominique Cina, Hans-Peter Huber, Willi Vonburg, Martin Horat.